Modelling, Simulation and Control of the Dyeing Process

The Textile Institute and Woodhead Publishing

The Textile Institute is a unique organisation in textiles, clothing and footwear. Incorporated in England by a Royal Charter granted in 1925, the Institute has individual and corporate members in over 90 countries. The aim of the Institute is to facilitate learning, recognise achievement, reward excellence and disseminate information within the global textiles, clothing and footwear industries.

Historically, The Textile Institute has published books of interest to its members and the textile industry. To maintain this policy, the Institute has entered into partnership with Woodhead Publishing Limited to ensure that Institute members and the textile industry continue to have access to high calibre titles on textile science and technology.

Most Woodhead titles on textiles are now published in collaboration with The Textile Institute. Through this arrangement, the Institute provides an Editorial Board which advises Woodhead on appropriate titles for future publication and suggests possible editors and authors for these books. Each book published under this arrangement carries the Institute's logo.

Woodhead books published in collaboration with The Textile Institute are offered to Textile Institute members at a substantial discount. These books, together with those published by The Textile Institute that are still in print, are offered on the Elsevier website at: http://store.elsevier.com/. Textile Institute books still in print are also available directly from the Institute's website at: www.textileinstitutebooks.com.

A list of Woodhead books on textile science and technology, most of which have been published in collaboration with The Textile Institute, can be found towards the end of the contents pages.

Woodhead Publishing Series in Textiles: Number 130

Modelling, Simulation and Control of the Dyeing Process

R. Shamey and X. Zhao

The Textile Institute

ELSEVIER

AMSTERDAM • BOSTON • CAMBRIDGE • HEIDELBERG • LONDON
NEW YORK • OXFORD • PARIS • SAN DIEGO
SAN FRANCISCO • SINGAPORE • SYDNEY • TOKYO
Woodhead Publishing is an imprint of Elsevier

Published by Woodhead Publishing Limited in association with The Textile Institute
Woodhead Publishing is an imprint of Elsevier
80 High Street, Sawston, Cambridge, CB22 3HJ, UK
225 Wyman Street, Waltham, MA 02451, USA
Langford Lane, Kidlington, OX5 1GB, UK

British Library Cataloguing-in-Publication Data
A catalogue record for this book is available from the British Library

Library of Congress Control Number: 2014940872

ISBN 978-0-85709-133-8 (print)
ISBN 978-0-85709-758-3 (online)

For information on all Woodhead Publishing publications visit our website at http://store.elsevier.com/

Typeset by RefineCatch Limited, Bungay, Suffolk

Printed and bound in the United Kingdom

To my parents, for their dedication and inspiration, and to my son, Ziyuan.

X. Zhao

To the joy of my life – my son Sean Araz Luca, and to my mom for everything!

R. Shamey

Myself when young did eagerly frequent
Doctor and Saint, and heard great argument
About it and about: but evermore
Came out by the same door as in I went
With them the seed of Wisdom did I sow,
And with my own hand wrought to make it grow;
And this was all the Harvest that I reap'd-
"I came like Water, and like Wind I go."

Omar Khayyam

Rendered into English verse by Edward Fitzgerald

Woodhead Publishing Series in Textiles

1 **Watson's textile design and colour Seventh edition**
Edited by Z. Grosicki
2 **Watson's advanced textile design**
Edited by Z. Grosicki
3 **Weaving Second edition**
P. R. Lord and M. H. Mohamed
4 **Handbook of textile fibres Volume 1: Natural fibres**
J. Gordon Cook
5 **Handbook of textile fibres Volume 2: Man-made fibres**
J. Gordon Cook
6 **Recycling textile and plastic waste**
Edited by A. R. Horrocks
7 **New fibers Second edition**
T. Hongu and G. O. Phillips
8 **Atlas of fibre fracture and damage to textiles Second edition**
J. W. S. Hearle, B. Lomas and W. D. Cooke
9 **Ecotextile '98**
Edited by A. R. Horrocks
10 **Physical testing of textiles**
B. P. Saville
11 **Geometric symmetry in patterns and tilings**
C. E. Horne
12 **Handbook of technical textiles**
Edited by A. R. Horrocks and S. C. Anand
13 **Textiles in automotive engineering**
W. Fung and J. M. Hardcastle
14 **Handbook of textile design**
J. Wilson
15 **High-performance fibres**
Edited by J. W. S. Hearle
16 **Knitting technology Third edition**
D. J. Spencer
17 **Medical textiles**
Edited by S. C. Anand
18 **Regenerated cellulose fibres**
Edited by C. Woodings
19 **Silk, mohair, cashmere and other luxury fibres**
Edited by R. R. Franck

20 **Smart fibres, fabrics and clothing**
Edited by X. M. Tao
21 **Yarn texturing technology**
J. W. S. Hearle, L. Hollick and D. K. Wilson
22 **Encyclopedia of textile finishing**
H-K. Rouette
23 **Coated and laminated textiles**
W. Fung
24 **Fancy yarns**
R. H. Gong and R. M. Wright
25 **Wool: Science and technology**
Edited by W. S. Simpson and G. Crawshaw
26 **Dictionary of textile finishing**
H-K. Rouette
27 **Environmental impact of textiles**
K. Slater
28 **Handbook of yarn production**
P. R. Lord
29 **Textile processing with enzymes**
Edited by A. Cavaco-Paulo and G. Gübitz
30 **The China and Hong Kong denim industry**
Y. Li, L. Yao and K. W. Yeung
31 **The World Trade Organization and international denim trading**
Y. Li, Y. Shen, L. Yao and E. Newton
32 **Chemical finishing of textiles**
W. D. Schindler and P. J. Hauser
33 **Clothing appearance and fit**
J. Fan, W. Yu and L. Hunter
34 **Handbook of fibre rope technology**
H. A. McKenna, J. W. S. Hearle and N. O'Hear
35 **Structure and mechanics of woven fabrics**
J. Hu
36 **Synthetic fibres: Nylon, polyester, acrylic, polyolefin**
Edited by J. E. McIntyre
37 **Woollen and worsted woven fabric design**
E. G. Gilligan
38 **Analytical electrochemistry in textiles**
P. Westbroek, G. Priniotakis and P. Kiekens
39 **Bast and other plant fibres**
R. R. Franck
40 **Chemical testing of textiles**
Edited by Q. Fan
41 **Design and manufacture of textile composites**
Edited by A. C. Long
42 **Effect of mechanical and physical properties on fabric hand**
Edited by H. M. Behery
43 **New millennium fibers**
T. Hongu, M. Takigami and G. O. Phillips

44 **Textiles for protection**
Edited by R. A. Scott
45 **Textiles in sport**
Edited by R. Shishoo
46 **Wearable electronics and photonics**
Edited by X. M. Tao
47 **Biodegradable and sustainable fibres**
Edited by R. S. Blackburn
48 **Medical textiles and biomaterials for healthcare**
Edited by S. C. Anand, M. Miraftab, S. Rajendran and J. F. Kennedy
49 **Total colour management in textiles**
Edited by J. Xin
50 **Recycling in textiles**
Edited by Y. Wang
51 **Clothing biosensory engineering**
Y. Li and A. S. W. Wong
52 **Biomechanical engineering of textiles and clothing**
Edited by Y. Li and D. X-Q. Dai
53 **Digital printing of textiles**
Edited by H. Ujiie
54 **Intelligent textiles and clothing**
Edited by H. R. Mattila
55 **Innovation and technology of women's intimate apparel**
W. Yu, J. Fan, S. C. Harlock and S. P. Ng
56 **Thermal and moisture transport in fibrous materials**
Edited by N. Pan and P. Gibson
57 **Geosynthetics in civil engineering**
Edited by R. W. Sarsby
58 **Handbook of nonwovens**
Edited by S. Russell
59 **Cotton: Science and technology**
Edited by S. Gordon and Y-L. Hsieh
60 **Ecotextiles**
Edited by M. Miraftab and A. R. Horrocks
61 **Composite forming technologies**
Edited by A. C. Long
62 **Plasma technology for textiles**
Edited by R. Shishoo
63 **Smart textiles for medicine and healthcare**
Edited by L. Van Langenhove
64 **Sizing in clothing**
Edited by S. Ashdown
65 **Shape memory polymers and textiles**
J. Hu
66 **Environmental aspects of textile dyeing**
Edited by R. Christie
67 **Nanofibers and nanotechnology in textiles**
Edited by P. Brown and K. Stevens

68 **Physical properties of textile fibres Fourth edition**
W. E. Morton and J. W. S. Hearle
69 **Advances in apparel production**
Edited by C. Fairhurst
70 **Advances in fire retardant materials**
Edited by A. R. Horrocks and D. Price
71 **Polyesters and polyamides**
Edited by B. L. Deopura, R. Alagirusamy, M. Joshi and B. S. Gupta
72 **Advances in wool technology**
Edited by N. A. G. Johnson and I. Russell
73 **Military textiles**
Edited by E. Wilusz
74 **3D fibrous assemblies: Properties, applications and modelling of three-dimensional textile structures**
J. Hu
75 **Medical and healthcare textiles**
Edited by S. C. Anand, J. F. Kennedy, M. Miraftab and S. Rajendran
76 **Fabric testing**
Edited by J. Hu
77 **Biologically inspired textiles**
Edited by A. Abbott and M. Ellison
78 **Friction in textile materials**
Edited by B. S. Gupta
79 **Textile advances in the automotive industry**
Edited by R. Shishoo
80 **Structure and mechanics of textile fibre assemblies**
Edited by P. Schwartz
81 **Engineering textiles: Integrating the design and manufacture of textile products**
Edited by Y. E. El-Mogahzy
82 **Polyolefin fibres: Industrial and medical applications**
Edited by S. C. O. Ugbolue
83 **Smart clothes and wearable technology**
Edited by J. McCann and D. Bryson
84 **Identification of textile fibres**
Edited by M. Houck
85 **Advanced textiles for wound care**
Edited by S. Rajendran
86 **Fatigue failure of textile fibres**
Edited by M. Miraftab
87 **Advances in carpet technology**
Edited by K. Goswami
88 **Handbook of textile fibre structure Volume 1 and Volume 2**
Edited by S. J. Eichhorn, J. W. S. Hearle, M. Jaffe and T. Kikutani
89 **Advances in knitting technology**
Edited by K-F. Au
90 **Smart textile coatings and laminates**
Edited by W. C. Smith
91 **Handbook of tensile properties of textile and technical fibres**
Edited by A. R. Bunsell

92 **Interior textiles: Design and developments**
Edited by T. Rowe
93 **Textiles for cold weather apparel**
Edited by J. T. Williams
94 **Modelling and predicting textile behaviour**
Edited by X. Chen
95 **Textiles, polymers and composites for buildings**
Edited by G. Pohl
96 **Engineering apparel fabrics and garments**
J. Fan and L. Hunter
97 **Surface modification of textiles**
Edited by Q. Wei
98 **Sustainable textiles**
Edited by R. S. Blackburn
99 **Advances in yarn spinning technology**
Edited by C. A. Lawrence
100 **Handbook of medical textiles**
Edited by V. T. Bartels
101 **Technical textile yarns**
Edited by R. Alagirusamy and A. Das
102 **Applications of nonwovens in technical textiles**
Edited by R. A. Chapman
103 **Colour measurement: Principles, advances and industrial applications**
Edited by M. L. Gulrajani
104 **Fibrous and composite materials for civil engineering applications**
Edited by R. Fangueiro
105 **New product development in textiles: Innovation and production**
Edited by L. Horne
106 **Improving comfort in clothing**
Edited by G. Song
107 **Advances in textile biotechnology**
Edited by V. A. Nierstrasz and A. Cavaco-Paulo
108 **Textiles for hygiene and infection control**
Edited by B. McCarthy
109 **Nanofunctional textiles**
Edited by Y. Li
110 **Joining textiles: Principles and applications**
Edited by I. Jones and G. Stylios
111 **Soft computing in textile engineering**
Edited by A. Majumdar
112 **Textile design**
Edited by A. Briggs-Goode and K. Townsend
113 **Biotextiles as medical implants**
Edited by M. W. King, B. S. Gupta and R. Guidoin
114 **Textile thermal bioengineering**
Edited by Y. Li
115 **Woven textile structure**
B. K. Behera and P. K. Hari

116 **Handbook of textile and industrial dyeing. Volume 1: Principles, processes and types of dyes**
Edited by M. Clark
117 **Handbook of textile and industrial dyeing. Volume 2: Applications of dyes**
Edited by M. Clark
118 **Handbook of natural fibres. Volume 1: Types, properties and factors affecting breeding and cultivation**
Edited by R. Kozłowski
119 **Handbook of natural fibres. Volume 2: Processing and applications**
Edited by R. Kozłowski
120 **Functional textiles for improved performance, protection and health**
Edited by N. Pan and G. Sun
121 **Computer technology for textiles and apparel**
Edited by J. Hu
122 **Advances in military textiles and personal equipment**
Edited by E. Sparks
123 **Specialist yarn and fabric structures**
Edited by R. H. Gong
124 **Handbook of sustainable textile production**
M. I. Tobler-Rohr
125 **Woven textiles: Principles, developments and applications**
Edited by K. Gandhi
126 **Textiles and fashion: Materials design and technology**
Edited by R. Sinclair
127 **Industrial cutting of textile materials**
I. Viļumsone-Nemes
128 **Colour design: Theories and applications**
Edited by J. Best
129 **False twist textured yarns**
C. Atkinson
130 **Modelling, simulation and control of the dyeing process**
R. Shamey and X. Zhao
131 **Process control in textile manufacturing**
Edited by A. Majumdar, A. Das, R. Alagirusamy and V. K. Kothari
132 **Understanding and improving the durability of textiles**
Edited by P. A. Annis
133 **Smart textiles for protection**
Edited by R. A. Chapman
134 **Functional nanofibers and applications**
Edited by Q. Wei
135 **The global textile and clothing industry: Technological advances and future challenges**
Edited by R. Shishoo
136 **Simulation in textile technology: Theory and applications**
Edited by D. Veit
137 **Pattern cutting for clothing using CAD: How to use Lectra Modaris pattern cutting software**
M. Stott

138 **Advances in the dyeing and finishing of technical textiles**
M. L. Gulrajani
139 **Multidisciplinary know-how for smart textiles developers**
Edited by T. Kirstein
140 **Handbook of fire resistant textiles**
Edited by F. Selcen Kilinc
141 **Handbook of footwear design and manufacture**
Edited by A. Luximon
142 **Textile-led design for the active ageing population**
Edited by J. McCann and D. Bryson
143 **Optimizing decision making in the apparel supply chain using artificial intelligence (AI): From production to retail**
Edited by W. K. Wong, Z. X. Guo and S. Y. S. Leung
144 **Mechanisms of flat weaving technology**
V. V. Choogin, P. Bandara and E. V. Chepelyuk
145 **Innovative jacquard textile design using digital technologies**
F. Ng and J. Zhou
146 **Advances in shape memory polymers**
J. Hu
147 **Design of clothing manufacturing processes: A systematic approach to planning, scheduling and control**
J. Gersak
148 **Anthropometry, apparel sizing and design**
D. Gupta and N. Zakaria
149 **Silk: Processing, properties and applications**
Edited by K. Murugesh Babu
150 **Advances in filament yarn spinning of textiles and polymers**
Edited by D. Zhang
151 **Designing apparel for consumers: The impact of body shape and size**
Edited by M-E. Faust and S. Carrier
152 **Fashion supply chain management using radio frequency identification (RFID) technologies**
Edited by W. K. Wong and Z. X. Guo
153 **High performance textiles and their applications**
Edited by C. A. Lawrence
154 **Protective clothing: Managing thermal stress**
Edited by F. Wang and C. Gao
155 **Composite nonwoven materials**
Edited by D. Das and B. Pourdeyhimi
156 **Functional finishes for textiles: Improving comfort, performance and protection**
Edited by R. Paul
157 **Assessing the environmental impact of textiles and the clothing supply chain**
S. S. Muthu
158 **Braiding technology for textiles**
Y. Kyosev
159 **Principles of colour appearance and measurement**
A. K. R. Choudhury

Preface

Colour is one of the most important criteria in the production and retail of textiles. It significantly affects sales volumes, and is also directly related to consumer satisfaction. Fashion and market demands require that textile dyers be able to respond to shade changes in a relatively short time period. The need to minimise the time of dyeing while ensuring the standards are maintained necessitates the use of sophisticated control strategies. This requires a careful monitoring and control of parameters that affect the interaction of dye with fibres in the dyebath and is therefore one of the most important aspects of production in the textile supply chain. This book aims to introduce the development and application of reliable monitoring and control systems for the dyeing of textile fibres, with a view to obtaining dyeing processes that are both economical and environmentally sound. Various influential parameters, including temperature, fluid flow and direction, pH and dye concentration in the dyebath, in the pre-set and real-time exhaustion control of conventional (all in) as well as step-wise addition of dyebath components such as dyes and auxiliaries, are discussed, and their role in controlling dye exhaustion and levelness of dyes is elucidated. The modelling aspect of the book mainly concentrates on batch dyeings, specifically package or beam dyeing processes, since they allow chemical engineering principles, applied to packed-bed reactors, to be emulated in textile dyeing. Such models can, relatively easily, be modified for application to other types of machinery or processes.

The application of pre-set exhaustion profiles – linear, quadratic or exponential in shape – in the dyeing of textile fibres, and the advantages and disadvantages associated with the use of these methods, are also examined. Calculation of the rate of dye exhaustion in these processes based on various mathematical models is explained. Feed-forward control algorithms are introduced and their application to determining the desired rates of dye exhaustion in the dyebath based on dyebath conditions is described. Modelling of dyebath control in the portion-wise addition of dye or chemicals to the dyebath, integration dyeing methods, is also investigated. A major impediment to the commercialisation of this approach has been the capital cost and the potential need to redesign dyeing machinery. However, with the significant reductions in the cost of components, including spectrophotometers

and increased computational power available at low cost, this approach is gaining momentum. Indeed, a number of companies in the United States and the Far East (China, Taiwan, Korea, etc.) are already utilising state-of-the-art technology to improve their right-every-time production dyeing rates.

With this in mind, this book is divided into eight chapters. Chapter 1 introduces the concept of textile dyeing, based on a brief review of various types of dyes and fibres and the interaction that takes place between dyes and fibrous assemblies. The mode of controlling dyeing processes based on conventional time-temperature profiles, as well as those based on controlling the rate of dye exhaustion in real time, is introduced. Package dyeing processes and parameters influencing the adsorption and diffusion of dyes within packages are then described. Various adsorption isotherms and factors that affect the dyeing of fibres are examined. Different control strategies based on assessing the amount of dye in the dyebath are then briefly assessed.

Chapter 2 presents the basic principles underlying the dyeing process. Some of the more quantitative aspects of dyeing equilibrium and kinetics, including standard affinity of dyes and dyeing rates, are then examined. The change in chemical potential of dye at the standard state from the solution to the fibre due to the presence of electrolytes is explained. Transport of dye in the dyebath involving sorption is described and various adsorption isotherms are examined. A general dynamic expression of dye sorption by textile fibres is introduced. Diffusion phenomena and models describing the diffusion of dye into textile fibres are then evaluated.

In Chapter 3 the theoretical background for the mechanistic description of flow phenomena in open channel and porous media is elucidated. Relevant works are described and the equations governing flow are explained. Fundamental concepts of dispersion, convection and diffusion are clarified and models that describe these processes are evaluated. The role of bulk and dispersive flow in dye transfer within a packed-bed medium and the effect of including flow parameters on modelling dye dispersion and diffusion are then evaluated, and various models incorporating flow properties are examined.

Chapter 4 develops theoretical models to simulate the dyeing process, starting from brief critical conclusions based on convective dispersion and fluid mechanics models as well as those that describe both the dye transfer and flow phenomena during dyeing. Using the theoretical concepts discussed in the previous chapters, the system is described by a set of partial differential equations. Darcy's law and the Navier–Stokes and Brinkman equations are examined. The boundary and initial conditions are also defined and discussed. The solutions of these models, which describe the dynamic behaviour of the system under given conditions of flow rate and given dyeing parameters, are also compared.

Chapter 5 provides an examination of the numerical solutions of the dyeing models that can be applied to different conditions. The application of analytical software applications to solve systems of highly non-linear simultaneous coupled

partial differential equations is described. The finite difference and finite element methods are introduced. The partition of the fibrous assembly geometry into small units of a simple shape, or mesh, is examined. Different polygonal shapes used to define the element are briefly described. The defined geometries, boundary conditions and mesh of the system are used to determine solutions to the equations of flow or mass transfer models.

In Chapter 6 the results of the simulation of the package dyeing process based on various models are presented. In this section it is explained that, while Darcy's law assumes that the only driving force for flow in a porous medium is the pressure gradient, and the global transport of momentum by shear stress in the fluid is ignored, Brinkman's equations can be used to extend Darcy's law to include the viscous transport in the momentum balance and the velocities in the spatial directions as dependent variables. These models, as well as the effect of flow velocity and direction, package permeability and dye dosing profiles on dye distribution, are described and their validity examined.

The first part of Chapter 7 introduces the main types of control strategies. The mathematical methods of controlling different dyeing parameters, specifically pH measurement, the effect of various parameters on pH and the development of pH control strategies, are then examined. The performance of different control strategies on the outcome of dyeing, using a pilot package dyeing machine, is also briefly investigated. The control of the dyeing process according to pre-set exhaustion and other profiles is also described. The control strategies shown in this chapter take advantage of basic digital and analog controllers, and readers are advised to consider other sophisticated controllers currently available, as well as more advanced software applications, to facilitate this process.

It is with pleasure that we include Chapter 8, written by Professor Warren Jasper of North Carolina State University and Dr Melih Günay, who cover the implementation of real-time dyebath monitoring in various types of dyeing machinery. They discuss the principles of a dyebath monitoring technology that allows analysis and control of the dyeing process, and use Beer's law to determine the amount of dye in the dyebath, even in a mixture. The principles of spectral additivity and spectral morphing are then examined, and their application to the calculation of the rate and degree of dye exhaustion in the dyebath is described. They conclude that such measurement technology can aid in troubleshooting root causes in shade reproducibility that can occur from variability in dye strength, the fabric or the dyeing process.

The production of work and the ensuing documentation leading to the writing of this book has taken over two decades. This book would not have been possible without the initial research conducted under the supervision of Dr J.H. Nobbs at the Colour Chemistry Department of Leeds University, UK, in the early 1990s. Dr Nobbs developed a Quick Basic 4.5-based software application to control a pilot-scale dyeing machine in Leeds in the late 1980s. The work was extended over a period of 10 years by a number of researchers, including one of the authors of this

book. The software incorporated some of the models discussed in certain sections of this book. We have received help from a large number of graduate students, colleagues and friends, who are duly acknowledged. We are also grateful to Dr Juan Lin for assistance in generating some of the figures and Mr M. Zubair for assistance with collection of references.

We believe this book should be a good source of information, not only for academics and researchers but also for coloration professionals, experts and technologists, engineers, textile dyeing machinery designers and allied industries.

Renzo Shamey
North Carolina State University

Xiaoming Zhao
Tianjin Polytechnic University

Definition of terms

Affinity: The quantitative expression of substantivity. It is the difference between the chemical potential of the dye in its standard state in the fibre and the corresponding potential in the dyebath. Note: Affinity is usually expressed in units of calories (joules) per mole. Use of this term in a qualitative sense, synonymous with substantivity, is frowned on.

Batchwise processing: Processing of material as lots or batches in which the whole of each batch is subjected to one stage of the process at a time. It is the opposite of continuous processing.

Beam dyeing: Dyeing of textile material wound onto a hollow perforated roller (beam), through the perforations of which dye-liquor is circulated.

Beck/winch: An open vessel, formerly made of wood or iron, nowadays of stainless steel, for the wet processing of textile materials.

Colour yield: The depth of colour obtained when a standard weight of colorant is applied to a substrate under specified conditions.

Diffusion: Movement of the dye molecules from the surface of the fibre to the interior of the fibre.

Equilibrium time t_e: is the time when exhaustion of dye slows down and begins to level off as it reaches its ultimate exhaustion, $E(t_e)$.

Exhaustion: The percentage of dye that has migrated onto the substrate. *%Exhaustion* is a function of the initial concentration, $C(0)$, and current concentration, $C(t)$ (if no liquid is added during a dyeing) and is calculated as follows:

$$\%\text{Exhaustion} = 1 - C(t)/C(0) \times 100$$

Final exhaustion is the value of the exhaustion at the end of a dyeing.

Exhaustion Rate ΔE/Δt is determined by calculating the average exhaustion rate between the strike and equilibrium times as follows:

$$\%\,Rate\,of\;Exhaustion = \frac{E(t_e) - E(t_s)}{t_e - t_s}$$

Exhaustion, Maximum % rate: The value of the maximum rate of % exhaustion. This is a critical value which often affects the levelness of the dyeing.

Exhaustion, Temperature for maximum exhaustion % rate: The temperature at which the maximum rate of % exhaustion occurs. Near this temperature the exhaustion rate decreases, affecting levelness.

Fastness: The property of resistance to exposure to various conditions (e.g. washing, light, rubbing, chemicals, gas fumes). Note: On the standard scale, five grades are usually recognised, from 5, signifying unaffected, to 1, grossly changed. For lightness, eight grades are used, 8 representing the highest degree of fastness.

Fixation: Immobilisation of the dye molecules inside the fibre. Note: Different methods include 'insolubilisation' (e.g. for vat and sulfur dyes in cotton; polymeric binders with pigments), 'chemical bonds' (e.g. hydrogen bonding for direct dyes in cotton), 'ionic bonding' (e.g. acid dyes in wool and nylon, and basic dyes in acrylic), covalent bonding (e.g. reactive dyes in cotton) and solubility in the fibre (e.g. disperse dyes in polyester, nylon and acetate).

Grey (greige): Woven or knitted fabrics as they leave the loom or knitting machine, i.e. before any bleaching, dyeing or finishing treatment has been given to them. Some of these fabrics, however, may contain dyed or finished yarns. Note: In some countries, particularly in the North American continent, the term 'greige' is used. For woven goods, the term 'loomstate' is frequently used as an alternative. In the linen and lace trades, the term 'brown goods' is used.

Jet-dyeing machine: (a) A machine for dyeing fabric in rope form, in which the fabric is carried through a narrow throat by dye-liquor circulated at a high velocity. (b) A machine for dyeing garments in which the garments are circulated by jets of liquid rather than by mechanical means.

Mercerisation: The treatment of cellulosic textiles in yarns or fabric form with a concentrated solution of caustic alkali, whereby the fibres swell, the strength and dye affinity of the materials are increased, and the handle is modified. The process takes its name from its discoverer, John Mercer (1884).

Package dyeing: A method of dyeing in which the liquor is circulated radially through a wound package. Note: Wound packages include slubbing in top form and cheeses or cones of yarn.

Piece-dyeing: Dyeing in fabric form.

Scouring: The treatment of textile materials in aqueous or other solutions in order to remove natural fats, waxes, proteins and other constituents, as well as dirt, oil and other impurities.

Sequestering agent: A chemical capable of reacting with metallic ions so that they become part of a complex anion. The principle is used to extract calcium ions from hard water, iron (II) and copper ions from peroxide bleach liquors and various metallic ions from dyebaths, by forming a water-soluble complex in which the metal is held in a non-ionisable form.

Shade: (a) A common term loosely employed to broadly describe a particular colour or depth, e.g. pale shade, 2% shade, mode shade and fashion shade. (b) To bring about relatively small modifications in the colour of a substrate in dyeing by adding further small amounts of dye, especially with the object of matching a given pattern more accurately.

Strike time t_s and temperature $T(t_s)$: The time and the corresponding dyeing temperature at which the dye starts to go onto fabric at an increasing rate. Especially in synthetic fibres at the glass transition temperature, the fibre relaxes and expands, and eventually allows dye molecules to penetrate into the amorphous regions. Knowing the time and temperature of this point may permit fibre manufacturers to compare different fibres for blending and quality control purposes. It may also provide data on the comparative information on fibre morphologies and crystallinity.

Stripping: Destroying or removing the dye or finish from a fibre.

Substantivity: The attraction between a substrate and a dye or other substrate under the precise conditions of testing, whereby the latter is selectively extracted from the application medium by the substrate.

Surfactant/surface active agent: An agent, soluble or dispersible in a liquid, which reduces the surface tension of the liquid.

Nomenclature

Adsorption, diffusion and dispersion-related variables	
Adsorption coefficient	K
Diffusion coefficient	D, D_{dif}
Dispersion coefficient	D, D_{dis}
Dispersivity	α
Rate of diffusion	R_d
The adsorptive coefficient	λ_i
The rate constant for adsorption	k_1, K_a
The rate constant for desorption	k_{-1}, K_d
Time of sorption	t_m
Dosing-related variables	
Dosing time	t_p
Differential control volume	CV
Exhaustion %	$E\%$
General control parameter for all exhaustion profiles	Q
Temperature of dyebath at time t_j	$T(t_j)$
The absorbance of the dyebath at time t	$A(t)$
The adjusted target rate	*Knxt*
The calculated concentration derivative	*cdrv*
The current temperature	*Tave*
The desired exhaustion rate (fraction/min)	*ExhRate*
The dissociation constants of acids and bases	K_a, K_b
The desired rate constant	*Kset*
The desired temperature	*Tset*
The first-order current rate constant	*Kave*
The rate of dosage at any time t	V_{dos}
The rate of temperature rise	*Trmp*
The total volume of the solution to be dosed	V
Vectors of the spectral components of the individual dyes	$\mathbf{f}_i$
Volume at temperature T	V_T
Volume at temperature 0 Celsius	V_0

Fibrous assembly-related variables

Fibre density	s_F
Package density	s_p
Porosity or voidage of the porous medium	ε, ξ
The area of the solid phase in a cross-section of area	A_{solid}
The area of the void phase in a cross-section of area	A_{voids}
The Darcy permeability	k_D
The fibre denier	d
The height of the package	h, L
The inner radius of the package	r_i
The outer radius of the package	r_o
The permeability	k
The shape factor	S
The specific permeability	K_s
The specific surface, or surface area of the material that makes up the porous body	S_0
Total pressure inside the package	p_i
Total pressure outside the package	p_o

Fluid flow-related variables

Dispersive flux	j_{dis}
Flow rate	Q
Hydrodynamic pressure	P
The actual velocity within the pores or voids (interstitial velocity)	V_i, v_x
The average velocity of the bulk flow	v
The bulk velocity	U
The constant of proportionality	k_D
The convective flux due to the bulk flow	J_c
The convective coefficient	V_i
The cross-flow velocity	U (u, v, w)
The density of the fluid	ρ
The dispersive coefficient	D_i
The displacement of a plate due to force	U_x
The dye flux at the inflow face	$J_{x,\,in}$
The dye flux at the outflow face	$J_{x,\,out}$
The hydraulic diameter	D_h
The Kozeny constant	K_0
The pipe diameter	d
The shear strain	γ
The shear stress	τ
The shear viscosity	η
The superficial velocity of the fluid	V_s
The total force on a plate	F_x

The velocity (or velocity vector) of the flow	u
The velocity vector in the porous medium (yarn assembly)	u_1
The viscosity of the fluid	μ, η
The volume of flow per time and area of the package	q
Total flux	J
Velocity field components	V_r, $V\theta$
Volumetric flow rate	F
General controller-related variables	
Controller output	P
Controller output with no error	P_0
Error signal	E
Measured value	C_M
Pre-set controller output	P_i
Setpoint (desired) value	C_{SP}
The derivative gain constant	K_D
The set error value	E_i
The proportional constant between error and controller output	K_P
General variables	
Absorbance	A
Area	A
Constants	$A_0, A_1, \ldots, B_0, B_1$
Distance	x, r
Distance between nodes	h
Gravity	g
Order of interpolation polynomial	n
Pathlength of light travelling through solution	l
Pressure	p
Space index	j
Temperature	T
Temperature (in Kelvin)	T_k
The Arrhenius constant	A
The condition number of a matrix	$\kappa(F)$
The extinction coefficient of dye, absorptivity	ε
The initial light intensity or photon flux entering the flow cell	I_0
The light intensity exiting the flow cell	I
The Reynolds number	Re
The unit normal vector	n
The universal gas constant	R
Time	t
Time index	n
Volume	V

Kinetics and thermodynamics-related variables

The activation energy of dyeing	E_a
The standard affinity associated with sorption	$-\Delta\mu^\circ$
The standard enthalpy change	ΔH°
The standard entropy change	ΔS°
The chemical potential	μ
The chemical potential of the dye in the solution	μ_s
The chemical potential of the dye in the fibre	μ_f
The chemical activity of the dye in the solution	a_s
The chemical activity of the dye in the fibre	a_f
The standard chemical potential for the dye in its standard state in the solution	μ_s^0
The standard chemical potential for the dye in its standard state in the fibre	μ_f^0
The internal fibre phase	F
The external aqueous solution phase	S
The internal accessible volume of fibre	V
The amount by which the energy of an activated molecule exceeds the average energy of the solute molecule	E

Potential and pH-related variables

Observed potential	E
pH at time *t*	pH_t
pH at the start of the process	pH_0
Standard potential	E_0
Target pH at the end of the process	pH_f
The activity of hydrogen ions in solution	a_{H^+}
The concentration of chlorine ions in solution	$[Cl^-]_S$
The concentration of sodium ions in solution	$[Na^+]_S$
The dielectric constant	ε
The dissociation constant for water	K_w
The ion charge, the valence of the ion *i*	Z_i
The ionic strength	u, I
The ion-size parameter (in angstroms)	$\mathring{A}$
The molal concentration of hydrogen ion in solution	C_{H^+}
The molarity of the original solution	M_0
The stable fixed potential including reference internal potential	$E^{0'}$

Variables related to the amount of dye in solution and fibre

Adsorbed dye concentration	C_f, ν, Q, A
Amount of dye absorbed by the fibre at the end of sorption	C_m
Concentration	C
Concentration of dye in solution	C_s, $[D^{z-}]_S$, C

Concentration of dye in the dyebath at time t	C_t
Concentration of dye in the mixing tank at the beginning of dyeing	C_{ini}
Concentration of dye in the mixing tank at time t	C_1
Initial concentration of dye in the dyebath	C_0
Mass of dye on fibre	M
Mass of dye on fibre within the differential control volume over the time δt	M_p
Mass of dye in liquid within the differential control volume over the time δt	M_f
Maximum number of adsorption sites occupied by dye molecules	C_{max}, ν^*
The amount of adsorbate on the absorbent	F
The concentration of dye i in admixture	C_i
The concentration of dye on fibre at equilibrium	$[D^{z-}]_F$
The current concentration	*cnow*
The desired concentration	*cset*
The dye concentration measured at time t	$C'(t)$
The mass of the dye taken up per mass of the fibre, at time t and plane x	M_F
The target concentration	*cnxt*
The true starting concentration	*cstart*
The value of the liquor concentration just before entry into the packed bed	C_{in}
The values of the liquor concentration just after exit from the packed bed	C_{out}
The volume concentration in the dye-liquor at time t at the plane x inside the package	C_L

1

Introduction to dyeing and dyehouse automation

DOI: 10.1533/9780857097583.1

Abstract: This chapter introduces the concept of textile dyeing, based on a brief review of various types of dyes and fibres and the interaction between dyes and fibres, and the mode of controlling dyeing processes based on conventional time-temperature profiles as well as those based on controlling the rate of dye exhaustion. The package dyeing process and parameters influencing the adsorption and diffusion of dyes within packages are then introduced. Various adsorption isotherms are briefly examined and factors that affect the dyeing of fibres are discussed. Different control strategies based on assessing the amount of dye in the dyebath are then briefly examined.

Key words: dyeing, dyes, textile fibres, dyeing quality, dyeing rate, levelness, dyeing vessels, package dyeing, dyeing automation, exhaustion profiles.

1.1 Introduction

Dyeing is a very complicated process with many different phenomena occurring simultaneously. It covers different areas of science including chemistry, physics, mechanics, physical chemistry, fluid mechanics, thermodynamics and others.[1] Devising the most efficient dyeing process typically involves the following concerns: machinery design, pre-selection of dyes of compatible properties, use of pH versus time profiles, selection of liquor ratio, flow rate and flow direction reversal times, and design of temperature versus time profiles.[2]

1.1.1 Textile fibres

A fibre is characterised by its high ratio of length to thickness, and by its strength and flexibility. Fibres may be of natural origin, or formed from natural or synthetic polymers. They are available in a variety of forms. Staple fibres are short, with length-to-thickness ratios around 10^3 to 10^4, whereas this ratio for continuous filaments is at least several million.[3] The form and properties of a natural fibre such as cotton are fixed, but for artificially made fibres a wide choice of properties is available by design. The many variations include staple fibres of any length, single continuous filaments (monofilaments), or yarns constituted of many filaments (multi-filaments). The fibres or filaments may be lustrous, dull or semi-dull, coarse, fine or ultra-fine, circular or of any other cross-section, straight or crimped, regular or chemically modified, and solid or hollow.

Natural fibres have a number of inherent disadvantages. They exhibit large variations in staple length, fineness, shape, crimp and other physical properties,

depending upon the location and conditions of growth. Animal and vegetable fibres also contain considerable and variable amounts of impurities, whose removal before dyeing is essential, and entails much processing. Artificially made fibres are much more uniform in their physical characteristics. Their only contaminants are small amounts of slightly soluble low molecular weight polymer and some surface lubricants and other chemicals added to facilitate processing. These are relatively easy to remove compared with the difficulty of purifying natural fibres.[4]

Water absorption is one of the key properties of a textile fibre. Protein or cellulosic fibres are hydrophilic and absorb large amounts of water, which causes radial swelling. Hydrophobic synthetic fibres such as polyester, however, absorb almost no water and do not swell. The hydrophilic or hydrophobic character of a fibre influences the types of dyes that it will absorb.[5] The ability to be dyed to a wide range of hues and depths is a key requirement for almost all textile materials.

An important property of a textile fibre is its regain, which is the weight of water absorbed per unit weight of completely dry fibre, when it is in equilibrium with the surrounding air, at a given temperature and relative humidity. The regain increases with increase in the relative humidity but diminishes with increase in the air temperature. Water absorption by a fibre liberates heat (exothermic) and will therefore be less favourable at higher temperatures. The heat released is often a consequence of the formation of hydrogen bonds between water molecules and appropriate groups in the fibre.[6] When the final regain is approached by drying wet, swollen fibres, rather than by water absorption by dry fibres, the regain is higher. The fibres at present available may be classified as shown in Fig. 1.1.

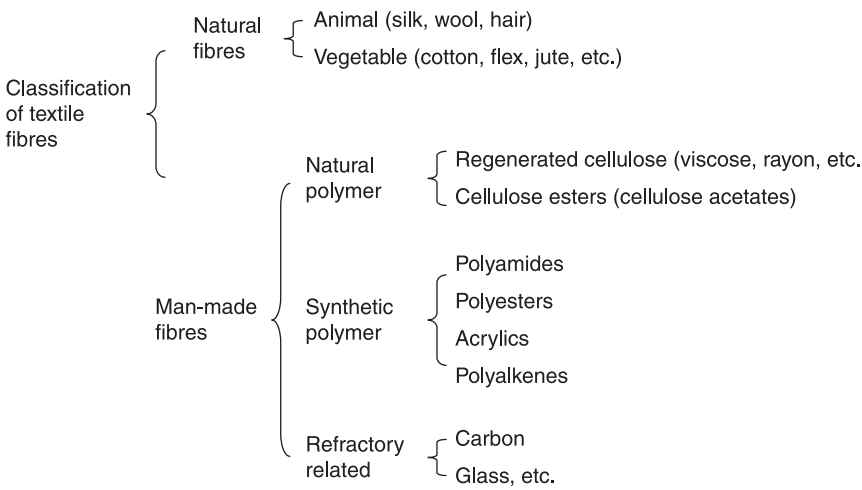

1.1 Classifications of fibres.

For hydrophilic fibres such as wool, cotton and viscose, the relatively high regain values significantly influence the gross weight of a given amount of fibre. This is significant in dyeing. Amounts of dyes used are usually expressed as a percentage of the weight of material to be coloured. Thus, a 1.0% dyeing corresponds to 1.0 g of dye for every 100 g of fibre, usually weighed under ambient conditions. For hydrophilic fibres, the variation of fibre weight with varying atmospheric conditions is therefore an important factor influencing colour reproducibility in repeat dyeings.

1.1.2 Dyes

A dye is a substance capable of imparting its colour to a given substrate, such as wool. A dye must be soluble in the application medium, usually water, at some point during the coloration process. It must also exhibit some substantivity for the material being dyed and be absorbed from the aqueous solution.[7]

For diffusion into a fibre, dyes must be present in the water in the form of individual molecules. These are often coloured anions; for example, sodium salts of sulphonic acids. They may also be cations such as Mauveine, or neutral molecules with slight solubility in water, such as disperse dyes. The dye must have some attraction for the fibre under the dyeing conditions so that the solution gradually becomes depleted. In dyeing terminology, the dye has substantivity for the fibre and the dyebath becomes exhausted.[8]

The four major characteristics of dyes are:

- intense colour
- solubility in water at some point during the dyeing cycle
- substantivity for the fibre being dyed
- reasonable fastness properties of the dyeing produced.

The structures of dye molecules are complex in comparison with those of most common organic compounds. Despite their complexity, dye structures have a number of common features. Most dye molecules contain a number of aromatic rings, such as those of benzene or naphthalene, linked in a fully conjugated system. This means that there is a long sequence of alternating single and double bonds between the carbon and other atoms throughout most of the structure. This type of arrangement is often called the chromophore or colour-donating unit. The conjugated system allows extensive delocalisation of the π electrons from the double bonds and results in smaller differences in energy between the occupied and unoccupied molecular orbitals for these electrons. At least five or six conjugated double bonds are required in the molecular structure for a compound to be coloured.[9]

Table 1.1 shows partial classifications of dyes as presented in the Colour Index. In order to gain an optimum result, the appropriate dye class for the fibre must be used, along with specific dyeing conditions. The ten major dye classes involve

Table 1.1 Classification of dyes according to chemical constitution and usage

Classification of dyes according to chemical constitution	Classification of dyes according to textile usage
Azo dyes	Acid dyes
Anthraquinone dyes	Azoic dyes
Heterocyclic dyes	Basic dyes
Indigoid dyes	Direct dyes
Nitro dyes	Disperse dyes
Phthalocyanine dyes	Mordant dyes
Polymethine dyes	Pigment
Stilbene dyes	Reactive dyes
Sulphur dyes	Sulphur dyes
Triphenylmethane	Vat dyes

acid, metal complex, mordant, direct, vat, sulphur, reactive, basic, disperse and azoic dyes. Some of the ten major dye classes shown in Table 1.1 can be used to dye the same fibre type, but varying conditions are required. For example, acid, metal complex, mordant and reactive dyes can all be used to dye wool. However, there may be one type of dye that is preferred for a certain dyeing process, for example, disperse dyes for polyester fibres.

There are numerous factors involved in the selection of dyes for colouring textile materials in a particular shade.[10] Some of these are:

- the type of fibres to be dyed
- the form of the textile material and the degree of levelness required – level dyeing is less critical for loose fibres, which are subsequently blended, than it is for fabric
- the fastness properties required for any subsequent manufacturing processes and for the particular end-use
- the dyeing method to be used, the overall cost and the machinery available
- the actual colour requested by the customer.

Figure 1.2 illustrates the approximate relative annual consumption of the major types of fibres and dyes estimated for the year 2000. The inner pie chart shows the data for fibres, and the lengths of the outer doughnut indicate the relative proportions of the various kinds of dyes used.

1.1.3 Dyeing

When a textile fibre is immersed in a solution of dye under suitable conditions, the fibre becomes coloured, the colour of the solution decreases and dyeing has occurred.[9] True dyeing occurs when the dye is absorbed with a decrease in

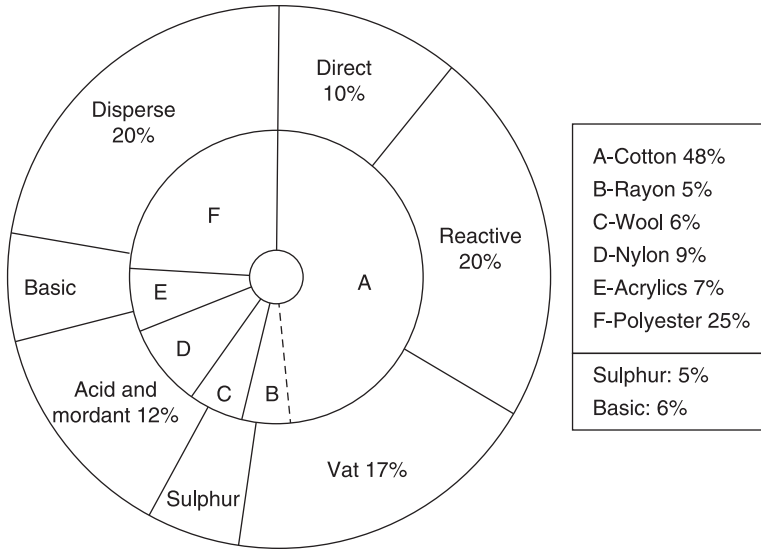

1.2 Relative annual global consumption of fibres and dyes estimated for the year 2009 (fibre production 7.5×10^{10} kg/year, dye consumption 9×10^{8} kg/year).

concentration of dye in the dyebath and when the resulting dyed material possesses some resistance to the removal of dye by water washing.[11]

It is not just the simple impregnation of the textile fibre with the dye that occurs during the dyeing process. A dye is taken up by a fibre as a result of the chemical interactions between them. Many dyes for textiles are water soluble and their molecules ionise into positively and negatively charged ions. The uptake of the dye by the fibre will depend on the nature of the dye and its chemical constitution. The strongest dye–fibre attachment is that of a covalent bond, with another important interaction being electrostatic attraction, which occurs when the dye ion and the fibre have opposite charges. In all dyeing processes van der Waals forces, hydrogen bonds and hydrophobic interactions are also involved. The combined strength of the molecular interactions is referred to as the affinity of the dye for the substrate. The substantivity of the dye is a less specific term and is often used to indicate the level of exhaustion. It is the attraction between the substrate and a dye under precise conditions where the dye is selectively extracted from the medium by the substrate. Different types of textile fibre require different kinds of dyes, and in general dyes which are suitable for one type of fibre will not dye other types effectively.[5]

Most textile dyeing processes initially involve transfer of the coloured chemical, or its precursor, from the aqueous solution onto the fibre surface: a process called adsorption. From there, the dye may slowly diffuse into the fibre. This occurs

down pores, or between fibre polymer molecules, depending on the internal structure of the fibre. The overall process of adsorption and penetration of the dye into the fibre is called absorption. Absorption is a reversible process. The dye can therefore return to the aqueous medium from the dyed material during washing, a process called desorption. Besides direct absorption, coloration of a fibre may also involve precipitation of a dye inside the fibre, or its chemical reaction with the fibre. These two types of process result in better fastness to washing, because they are essentially irreversible processes.

Levelness is the uniformity of dye distribution (and hence colour) on textiles. Two fundamental mechanisms contribute to a level batch dyeing.[12] One is the initial sorption of dye during the dyeing; the other is the migration of dye after initial sorption on the fibre. An initial level sorption will lead to a level dyeing. An unlevel sorption may be corrected if sufficient migration takes place.[13] The mechanisms are controlled by adding dyes and chemicals, textile substrate, and parameters of the dyeing process such as dyebath pH, liquor ratio, flow rate and temperature.[14]

Dyeing is not a purely physical process like painting or other colouring processes involving the physical application of pigments. There are difficulties encountered in controlling the physiochemical changes that occur during dyeing, in order to maximise factors such as colour yield, level dyeing, penetration, colour fastness, etc. Therefore there is a vast sub-technology of speciality chemical auxiliaries used in preparation for dyeing and in the dyeing process itself, such as additives and after-treatments.[15]

1.1.4 Various stages for dyeing textile materials

Textile fibres can be dyed at various stages, such as loose fibre, top, tow, yarn, fabric or garments during processing. The levelness requirements for dyeing loose fibre are less strict than for dyeing at the yarn stage or at later stages, since the further processing of the loose fibre produces some mixing of the dyed fibres, e.g. during carding or gilling, which improves the levelness of the resultant colour. For yarn dyeing levelness is much more critical, because, whether the yarn will be made into fabric, either by knitting or weaving, or into carpet, any unevenness in the dyeing of the yarn will show in the finished goods.[16]

1.2 Factors affecting dyeing quality

The aim of successful dyeing is to ‘achieve the desired shade, at the right price, with sufficient levelness, whether dyeing loose fibre, yarn or piece goods, with sufficient colour fastness to withstand both processing and consumer demands, but without adversely affecting the fibre quality’.[17] Of these, an acceptable level of uniform dye uptake at all parts of the substrate may be the most important criterion.[18]

A typical dyeing process may be divided into several steps, as follows:

- establishment of equilibrium between associated molecular dye and single molecules of dye in solution
- diffusion of monomolecular dye to the diffusional boundary layer at the fibre surface
- diffusion of dye through the boundary layer at the fibre surface
- adsorption of dye at the fibre surface
- diffusion of the dye into the fibre interior
- desorption and readsorption of dyes (migration).

These steps form a reversible equilibrium system. Each of the six steps can influence the levelness of dyeings.[19] A complete quantitative analysis of the effects of many factors which influence the levelness of dyeing would require the development of a mathematical model involving a significant number of parameters. This is, however, a very difficult task.[20] For practical applications, one may initially try to identify a few variables that are thought to have a larger impact on levelness and restrict the development of the model to the effects of these few most important variables.

The Donnan equation involves nine factors:[19] concentration of dye in fibre, concentration of dye applied, liquor ratio, distribution of ions between solution and fibre, the ionic charge on the dyestuff molecule, the internal volume of the fibre, the affinity of the dye, the gas constant and the dyeing temperature. All together, these terms describe the dyebath conditions.

Harvey and Park[21] suggested that to obtain reproducible dyeings, whether this is on a laboratory, pilot-plant or bulk scale, the following factors in the dyeing process must be controlled or measured:

- quality of water supply
- preparation of substrate
- dyeability of substrate
- weight of substrate
- weighing of dyes and chemicals
- dispensing method for dyes and chemicals
- selection of dyes
- standardisation of dyes
- moisture content of dyes
- moisture content of substrate at weighing
- dyebath additives
- liquor ratio
- pH of dyebath
- machine flow and reversal sequence
- time/temperature profile.

Heane[22] has suggested that, for a given dye–fibre combination, the important factors influencing the degree of levelness in package dyeing include:

- the rate of dye liquor circulation and its reversal
- the package density and the shape of the package
- the rate of dye uptake in relation to temperature, time, pH and other factors.

Vosoughi[23] concluded that the most important parameters affecting levelness of dyeing in a package dyeing operation could be listed as follows:

- package construction and shape
- package density and porosity
- flow rate (circulation rate) of dye liquor
- flow direction of dye liquor in packages
- rate and manner of dye bath exhaustion
- rate of temperature rise
- pH of dye bath
- presence of retarding, levelling or other chemical agents.

It can be seen that there is not complete agreement among authors who have studied the subject as to the significance of each of the factors affecting the levelness of dyeing. Various workers have placed different degrees of emphasis on each of the above factors and also on factors that are not listed above. There may also be disagreement on the mechanism by which any one of these factors operates. Furthermore, it should be noted that the parameters in this list are not quite independent, and in some cases the effect of two of these factors may be considered as one effect.

1.3 Practical difficulties involved in dyeing process control

There are some practical difficulties in achieving a quality dyeing when considering dyeing process control.

1.3.1 Dyeing rate

Dyeing rates are of greater practical significance than the exhaustion at equilibrium because continuation of dyeing to equilibrium is uneconomical. Long dyeing times increase the risk of fibre damage and dye decomposition, particularly at higher dyeing temperatures. On the other hand, very rapid dyeing will usually result in the colour being unlevel.[10] This implies that dyeing should be neither too slow nor too fast. In order that dyes are used economically and as little as possible is wasted in the dyehouse effluent, the dyer prefers a high degree of exhaustion in a relatively short dyeing time. However, dyeing must be controlled so that it is not so rapid that it is difficult to produce a level dyeing.

The slope of the exhaustion curve gives information on the rate of dyeing. The determination of these curves, however, requires much work and they are dependent on the dyeing conditions and the nature of the goods. The dyeing rate is influenced by the temperature and by chemicals such as salts and acids, all of which also influence the final exhaustion. A clear distinction of the effects of process variables on the dyeing rate and on the final exhaustion at equilibrium is essential.

1.3.2 Flow rate

During the dyeing process, the supply of dye through the solution to the surface of the fibres/yarns can occur in two ways, either by aqueous diffusion of dye through the liquor, or by convective movements of the fluid which replace the depleted solution by fresh solution.[24] Diffusion is a much slower process than the convective transport of dye, except at very low velocities of liquor flow.

However, an exact solution to the problem of convective diffusion to a solid surface requires first the solution of the hydrodynamic equations of motion of the fluid (the Navier–Stokes equations) for boundary conditions appropriate to the mainstream velocity of flow and the geometry of the system. This solution specifies the velocity of the fluid at any point and at any time in both tube and yarn assembly. It is then necessary to substitute the appropriate values for the local fluid velocities in the convective diffusion equation, which must be solved for boundary conditions related to the shape of the package, the mainstream concentration of dye and the adsorptions at the solid surface. This is a very difficult procedure even for steady flow through a package of simple shape.[24]

1.3.3 Initial stage of dyeing

The initial rate of dyeing (the initial slope of exhaustion versus time) is called the strike. Rapid strike by a dye often results in initial unlevelness and must be avoided for those dyes that cannot subsequently migrate from heavily to lightly dyed areas of the fabric. For dyes of rapid strike, the dyeing conditions must limit the initial rate of exhaustion, and therefore improve the levelness of the dyeing. The strike depends on the dyeing temperature, the dyeing pH and the presence of any auxiliaries.

Even for dyes of moderate and low strike, the objective of uniform dyeing of the fibre mass is rarely achieved during the initial stages of the operation. This is because of irregularities in the material's construction, in the fibre packing and in the distribution of residual impurities, as well as differences in temperature and flow rate of the solution in contact with the fibres.

1.3.4 Dye/fibre types and dye migration

Different types of textile fibre require different kinds of dyes, and in general dyes which are suitable for one type of fibre will not dye other types effectively.[11] The

greater the substantivity of the dye for the fibre being dyed, the higher the degree of exhaustion of a dye at equilibrium. Often, a very substantive dye will give a high initial rate of absorption, or strike. Substantivity is the 'attraction' between dye and fibre whereby the dye is selectively absorbed by the fibre and the bath becomes less concentrated.

The ability of a dye to migrate and produce a level colour, under the given dyeing conditions, is obviously an important characteristic. It can overcome any initial unlevelness resulting from a rapid strike. Migration of the dye demonstrates that the dye can be desorbed from more heavily dyed fibres and reabsorbed on more lightly dyed ones. This is important in package dyeing, where uniform colour of the yarn throughout the package is essential. While migration is important for level dyeing, it has two major drawbacks. First, dyes with greater ability to desorb from dyed fibres during migration usually mean that the dyeings will have lower fastness to washing. Dyes of very high washing fastness are essentially non-migrating dyes, for which level dyeing depends upon very careful control of the rate of dye uptake by the material. The second problem with migrating dyes is that good migration may result in lower exhaustion, again because of their ability to desorb from the fibres.

1.3.5 Factors affecting levelness of dyeing

As has been indicated, dyeing is a very complicated process, with very different phenomena occurring simultaneously. Unlevelness can arise in many forms, such as the unlevelness between sides, ends and layers of a package. The causes are as numerous as the effects. To analyse quantitatively the effects of many factors which influence the levelness of dyeing is a very difficult task, since it would require the development of a mathematical model involving a significant number of parameters. Also, to investigate the dye transfer through the package will involve the solution of non-linear partial differential equations. Little work has been done on this aspect, according to the literature.

1.3.6 Measurement of levelness

Measurement of levelness and its causes is difficult, although objective measurements have been proposed. The levelling ability of dyes is routinely tested under a fixed set of circumstances, but the effect of changing circumstances is less often reported. Similarly, a distinction between levelness of strike and levelness from migration is not usually studied.

1.4 Package dyeing machinery

Package dyeing is the process of choice in this book, mainly because the yarn dyeing process requires a great degree of process control to enable production of

material with high degrees of dye uniformity. In addition, yarn package dyeing can meet the fast response demands of the market, as well as avoiding the storage of large quantities of dyed material, which would not be economical.

The process is carried out in either hank or package form. Compared with hank dyeing, package dyeing enjoys various advantages, such as lower production costs as well as higher standards of levelness achieved. A high degree of reproducibility can be obtained using package dyeing. In general, these advantages may be summarised as follows:[25]

- reduced quantities of waste, including dye and chemicals
- higher speeds of back winding and elimination of hank reeling
- savings in energy, water, dye, chemicals, labour and space
- possibility of high-temperature dyeing
- rapid drying is possible
- better controllability and better levelness
- process can be readily automated.

However, a major disadvantage of yarn package dyeing is the introduction of two further winding stages into the overall production, which increases the time, as well as the cost of the process.

Automation in the dyeing industry has witnessed a rapid growth. Several fully automated systems have been introduced to the market. Some of these machines are capable of loading and unloading the dyeing vessel with the package material at a very high speed. These systems are reviewed by Thornton.[26]

1.4.1 Package dyeing requirements for a level dyeing

Achieving a successful level dyeing in a package dyeing system is highly dependent on the care taken during the preparation stage. The density of the package and its uniformity are therefore among the most influential factors in the outcome of the dyeing process. The yarn needs to be wound into a suitable form, for instance, cheese, cake, cone or rockets. Both metal and plastic formers have found use in the dyeing industry.

The first yarn dyeing machine was built in 1882 by Otto Bermaier, who used an open bath with fluid flow only from the inside to the outside of the package.[27] Later in the design of the machinery, the reversal of the pump was used to change the direction of the fluid flow and the dyebath was enclosed. Uniform circulation of the liquor, the rate of the fluid flow and a change in the fluid flow direction are also important factors in the levelness of the material obtained. The circulation is achieved by forcing the liquor through the perforated spindle and the package. The two-way direction of the fluid flow has been thought to increase the levelness of the dyeing obtained.[28]

Yarn package dyeing machinery requires a few essential parts. These have been considered by various authors.[28,29] Wyles[28] has summarised these as:

- the dye vessel
- the package carrier
- pumps (circulation and secondary)
- heating devices
- liquor flow and flow reversal devices.

Sampling tanks and expansion tanks are also considered by some authors as other important parts of the dyeing machine. Each of these is briefly reviewed below.

1.4.2 The dyeing vessel

Since virtually all modern dyeing machines are pressurised, the dyeing vessel, or kier, should be capable of operating at temperatures of up to 140 °C. This requires the kier to withstand pressures of up to 4.5 bar. Stainless steel is normally used in the design of the machinery. The weight of the package as well as water also necessitates the kier to withstand up to 5 tonnes in weight. The height and diameter of the biggest package dyeing vessels are up to 2 m.

The lid is very heavy and operated pneumatically. Loading and unloading of the package in some factories is now automated, and therefore in some layouts machinery is placed below the floor level and a monorail is used to carry the robots for loading and unloading of the machine.

Other designs for the vessel have attracted some attention. One of these designs introduces a horizontal dyeing vessel by OBEM.[25]

A typical schematic representation of a package dyeing vessel can be seen in Fig. 1.3.

1.4.3 The package carrier

After the winding of the yarn onto formers to form the packages, these are placed on perforated spindles that allow the passage of liquid to the fibre. An end cap is used to prevent the flow of the liquid from the top of the spindle and to compress the packages together to ensure as uniform permeability as possible.

Total number of spindles per carrier is determined by the overall diameter of the package to be dyed. The number of packages per spindle varies, but is usually around eight to ten.

1.4.4 Pumps

Dyeing machines may have more than one pump. One of these is the main circulation pump, which is normally located at the base of the kier, as close to the centre as possible to reduce frictional flow losses. These may be centrifugal or axial.

In a review of pumps by Horn,[30] it is stressed that, whatever the type of pump used, the pressure generated should be constant for a moderate change in the volume of flow. This is normally a result of leaks from the columns of

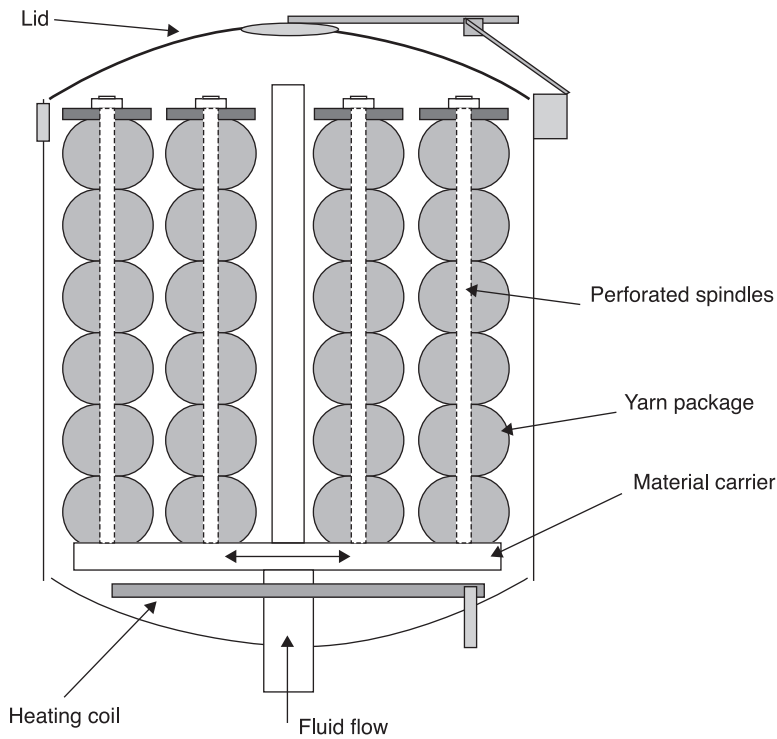

1.3 A schematic view of the dyeing vessel.

the spindles and is also observed when long spindles together with high liquor ratios are used.

Secondary pumps are normally centrifugal and are used to pressurise the whole system by sucking the liquid from the bottom of the kier and feeding it to the main pump. Cavitation, which is a result of steam bubbles forming at high temperatures on the low-pressure side of the pump, may also be avoided if the whole system is pressurised even when dyeing at 100 °C.

Other pumps for injecting dye and chemicals are also used in package dyeing machinery. The number of auxiliary pumps on a machine depends on the number of inlets for injecting various chemicals throughout the course of dyeing.

1.4.5 Heating devices

Various methods of heating have been used in the design of dyeing machinery. The earliest models used injection of hot steam inside the dyeing vessel. These systems had many drawbacks, such as the yellowing effect on the packages (as a result of rust being carried with the steam towards the machine), the change in the overall liquor ratio and channelling of the packages most adjacent to the inlet of

the steam. Therefore, in the new design the steam was passed through a closed coil, which was placed at the bottom of the kier. This system is still in use, and in many cases cooling water is also pumped in to the same coil when it is required to reduce the temperature of the dyeing vessel.

A number of methods have been used to control the heating and cooling of the system. The most advanced methods make use of a microprocessor. Examples of these have been marketed by various manufacturers.[31,32]

1.4.6 Liquor flow and flow reversal devices

In order for the dyeing to take place, the liquor should reach the package. This is carried out by forcing the liquor through the perforated spindles and formers and then through the yarn package. This method is called in-to-out fluid flow. A high dye uptake at surfaces most available to the flowing liquor can cause an unlevel dyeing, resulting in overdyeing in some regions, removal of which is usually a long process and in some cases almost impossible.

The reversal of the direction of the fluid flow has been discussed by many authors. This has been made possible by using either axial flow type pumps, in which the entire system of the pumping is reversed, or by using four-way valves when centrifugal pumps are employed. Figure 1.4 shows a schematic view of the type of fluid flow through the package of the material.

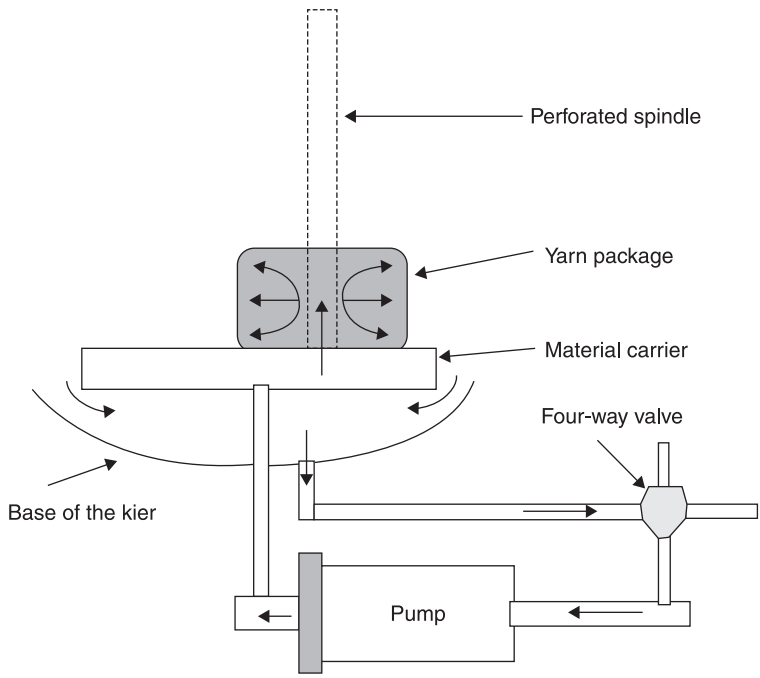

1.4 A schematic view of the fluid flow in the dyeing machine.

In axial pumps the reversal of the fluid flow direction may cause significant down times when several reversals are used. In a novel system discussed by Cegarra,[33] a piston-like device inside the kier is used that allows frequent and efficient flow reversals.

1.4.7 Sampling and expansion tanks

Some package dyeing machines are fitted with an external sampling tank. This is used to identify the problems that may occur during the dyeing. However, despite the care taken, it is extremely difficult to reproduce the exact conditions of the dyeing vessel, and therefore the diagnostics are not necessarily correct. Other methods have also been used, which are described elsewhere.[28]

The expansion tank is used for the dual purpose of addition of dye and other chemicals into the dyebath and to accommodate the expanded volume of the liquor in the dyebath at high temperatures.

1.5 Difficulties in package dyeing

Levelness is one of the most crucial factors for the success of any dyeing procedure. In the case of yarn package dyeing, as a result of a high dye uptake at surfaces most available to the flowing liquor overdyeing in some regions is observed, removal of which is usually a long and costly process and in some cases almost impossible.

In order to overcome this problem, the addition of levelling agents as well as flow reversal has been considered. However, in some cases, such as the dyeing of cellulosic fibres with reactive dyes or acrylic fibres with cationic dyes, unlevelness is still beyond the tolerance limit even with the addition of cationic retarders for cationic fibres or other auxiliaries for cellulose. Meanwhile, the question of the overall cost, which is increased by the addition of these materials into the dyebath, still remains. Moreover, these materials are not always environmentally friendly.

For a given dye–fibre combination, the important factors influencing the degree of an unlevel dyeing can be shown as:[22]

- the rate of dye liquor circulation and its reversal
- the package density and the shape of the package
- the rate of dye uptake in relation to temperature, time, pH and other factors.

A different classification based on two sets of factors is presented by Bauer.[34] These are described as either ‘formula side factors’ such as dye recipe, type of fibre, etc., or ‘production side factors’ such as liquor circulation rate, the package dyeing machine and the form of the textile material. Some other factors, such as the compatibility ratio of dyes and so on, could also be considered. These factors are not examined in detail in this study.

1.5.1 The effect of liquor circulation in dyeing

Various authors have studied the effect of the rate of liquor circulation in dyeing. Vickerstaff pointed out[4] that, because of a lower concentration of the dye in the liquor near the surface of the fibre or trapped in the spaces of the yarn compared with the external dyebath, the rate of dyeing is dependent upon the efficiency with which the dye is transported to the material being dyed, either by liquor circulation through the material or by the material's movement with respect to the dyebath.

McGregor and Peters[35] examined the mass transport process and defined two boundary layers. The hydrodynamic boundary layer is defined as a layer within which the velocity of liquor rises from zero to 99% of the main stream velocity. The layer within which the concentration of the dye rises from that at the fibre surface to 99% of the main stream is termed the diffusion boundary layer. The latter was regarded as a layer of liquid which hindered the passage of dye from the bulk of the dyebath to the fibre surface. They showed that an increase in the main velocity stream or in the efficiency of liquor circulation decreased the thickness of the diffusion boundary layer and hence increased the rate of dyeing. They found a main stream above which the dyeing rate no longer increased with an increase in velocity and where the thickness of the diffusion boundary layer could be considered zero.

Beckmann and Hoffmann[36] studied the relationship between the rate of liquor flow and the rate of exhaustion. They showed that the relative dye concentration in the liquor within the package changed with the rate at which the liquor flowed through. The difference in liquor concentration across the package was related to that at the surface of the fibre by the adsorption isotherm involved, while the rate of exhaustion at a particular position inside the package was proportional to the local liquor concentration at the surface of the fibre. Thus, the overall rate of exhaustion and the levelness of the dyeing were related to the rate of exhaustion within the package. For a given overall rate of flow, there was a maximum permissible rate of exhaustion beyond which the degree of unlevelness would no longer be acceptable. It was also stated that the difference in a local rate of liquor flow caused by factors such as the structure of the material being dyed would lead to a degree of unlevelness.

Hasler[37] found that levelness depends on the frequency of contact between the dye liquor and the material. Bolton and Crank[38] developed a relationship between the rate of exhaustion and the flow rate and concluded that, provided the package of the fibre is not damaged or distorted, the higher the flow rate, the better the resulting dyeing. Heane *et al.*[22] also came to similar conclusions.

Whittaker[39] concluded that in a one-directional fluid flow the out-to-in flow direction is preferable, since the radius of the package is decreasing and therefore the liquor passes through a smaller surface area. However, for unstable packages, because of shrinkage and distortion, the in-to-out flow is preferred.

The effect of the reversal of fluid flow on the quality of the resulting dyeing has also been discussed by various authors. Clifford[40] studied the effect of high fluid flow on levelness and distortion of the package and concluded that especially soft packages in a one-directional flow are more likely to be deformed. He also stated that a reversal of flow on each circulation results in a better levelness being achieved. Carbonell[41] further studied the effects of the frequency of reversal, and highlighted that more frequent reversals than circulations result in poor levelness being achieved, since the centre of the package is never thoroughly flooded with the dye liquor.

Hasler[37] claimed that, if flow was reversed at the end of each complete circulation, a fourfold increase in the exhaustion rate could be observed. Beckman and Hoffmann,[36] however, concluded that one reversal per four to eight circulations provides optimum levelness. Ren[42] and Illett[43] suggested that levelness may have an inverse relationship with the frequency of the fluid flow reversals. They have also attempted to model the effect of fluid flow rate and flow reversal on the resulting levelness. Discussions by Bohrer[44] point out that flow in one direction does not necessarily result in negative effects on the quality of the dyeing.

Some attention has also been paid to the effect of bulk and dispersive flow. When fluid flows in a packed bed, two flow phenomena come into play: these are known as bulk and dispersive flow. These flows create rate-determining steps in the sequence that determines the overall rate of transfer of dye to a given point on the fibre surface at a particular time. Burley[45–47] developed a model of the dyeing process which included these effects. The nature of these flows is explained in detail below.

1.5.2 Bulk flow

When fluid is pumped through a cylindrical package from entrance to exit, the main physical process that contributes to the fluid transport is bulk flow. In the simplest case, the fluid moves uniformly along the radius of the package by bulk flow.

1.5.3 Dispersive flow

Dispersive flow arises due to a non-uniform flow passage within a package. This allows neighbouring fluid elements to separate continually and mix as the fluid passes in bulk between the fibres and through the package. These flows are superimposed on the main (bulk) flow of fluid.

In order to include the effect of the dispersive flow in a model of the dyeing process, Fick's law can be used. In a similar way to a molecular diffusion coefficient, D, dispersive flows can be described by a dispersion coefficient, D_{dis},[45] i.e.:

$$R_d = -D_{dis}.\ (dC/dr) \qquad [1.1]$$

where R_d is the overall rate of diffusion (dispersive transport)

dC/dr is the local concentration gradient.

The dispersion process is a combination of physical mixing due to the flows through the randomly oriented passages in the package with other contributions from eddy diffusion* in the jets and wakes behind sudden contractions and expansions in the kier.

1.5.4 The effect of bulk and dispersive flow

Burley[45–47] showed in his model that an optimum void velocity of liquor flow, which is the minimum velocity at which even dye distribution in the liquor around the individual yarns occurs, could be achieved. Because of the non-linear nature of the equations in the model and their complexity, it has not been yet used in a practical process control system.

1.5.5 The effect of the shape and density of the package in level dyeing

Packages are subject to various mechanical, hydrostatic and hydraulic forces. Therefore, they should be capable of withstanding the handling forces as well as flow of the hot dye liquor. The density of the package should be as uniform as possible, as this has a direct relationship with the quality of the dyeing. The density of the package needs to be optimum to obtain an appropriate flow of dye liquor and prevent channelling at the same time. The permeability of the packages on the same load should be identical to ensure the uniform treatment of yarn across the dyeing vessel. McGregor[48] studied the physical chemistry of dye package permeability and presented equations that enable an estimate to be made of the amount of fluid flow that passed through the yarn, as opposed to the amount that passed around it. Vosoughi[23] studied the influence of the permeability of the package and included these effects in the Burley model of the dyeing process.

The effect of package density on the degree of unlevelness was also studied by Heane *et al.*[22] He stressed that the degree of unlevelness has a direct linear relationship with the density of the package.

Denton[49] has investigated the effect of the shape of the wound package on the flow pattern inside individual packages. He advocated that cylindrical shaped packages have better flow characteristics than cones. This is a result of the shape of the flow in conical packages, which contains both axial and radial vectors. This can be seen in Fig. 1.5. He showed[50,51] that the ratio of the rates of fluid flow

* Eddy diffusion: the migration and interchange of portions of a fluid as a result of their turbulent motion, occurring in high Reynolds numbers.

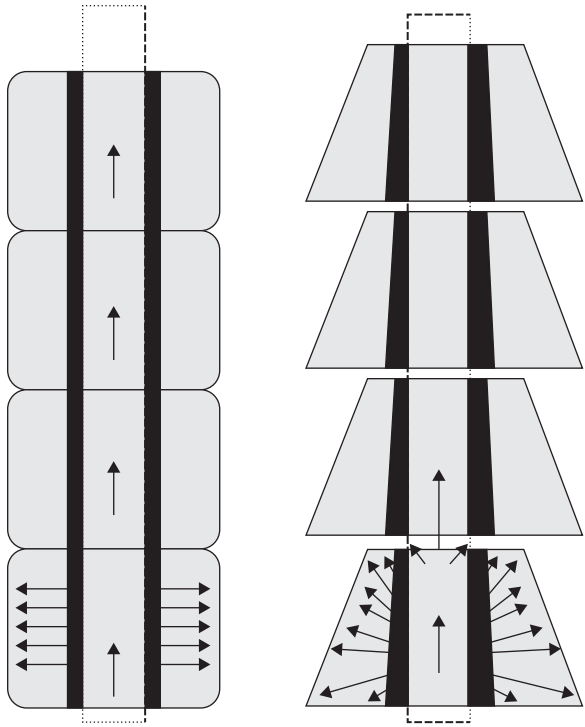

1.5 Fluid flow across conical and cylindrical packages (taken from Denton[51]).

in the areas where the flow was the highest to that in the areas where the flow was the lowest was 22:1, and in some cases 40:1. Thus, he concluded that the first step to avoid such differences is to use the cylindrical shaped packages which are compressed together at the base and top.

When the packages are wound onto compressible springs, the density variation can be minimised. However, it is important to point out that even small local variations in the density of the package directly influence the final levelness achieved in any dyeing system.

1.5.6 The effect of rate of uptake of dye from the liquor

A dyeing cycle in a conventional exhaust procedure can be divided into:

- the exhaustion;
- the diffusion; and
- the migration phase.

In the exhaustion phase, dye moves from the liquor to the fibre surface, where it disperses more or less evenly. In the diffusion phase, the dye exhausted onto the fibre surface and peripheral zones penetrates into the interior of the fibre and distributes itself evenly. In the migration phase, dye molecules move from sites with high concentration to sites with lower concentration. Therefore, it was suggested[52] that a level dyeing can be achieved by utilising one of the following methods:

- simpler control at the beginning of the dyeing and allowing a longer time for the migration
- precise control of dyeing during the exhaust phase by controlling temperature, pH, auxiliaries and electrolytes.

The first method has some limitations, since a level dyeing can only be achieved when the migration of dye molecules in the system is possible. This may be considered for the dyeing of wool with 'acid levelling' dyes or acrylic with Maxilon M dyes.[53] The second method is of wider use, since most dyeing systems do not permit unlevelness correction by migration to be made towards the end of the dyeing cycle. This is the case when there is a high affinity between dye and fibre, for example in the case of dyeing wool with acid milling or acrylic with basic dyes or cotton with reactive dyes.

The concept of the optimum exhaustion curve was investigated by several groups following the definition of a 'critical dyeing rate', which must not be exceeded for level dyeing.

Boulton and Crank[38] advocated a slow rate of initial exhaustion and thereafter an increasing rate of dyebath exhaustion. Carbonell *et al.*[41] tried to relate dyeing machinery conditions to the behaviour of individual dyes and used mathematically defined values that are dependent on concentration, auxiliaries and fibre affinity. The method was found applicable only for the disperse dye system.

Cegarra[54] suggested that a linear exhaustion curve results in a level dyeing. He defined 'isoreactive dyeing' as one with a constant sorption rate, where over a small change in time (dt) there would be a proportional change of concentration in the dyebath (dCt); i.e.:

$$dCt / dt = C_m / t_m \qquad [1.2]$$

where C_m is the amount of dye absorbed by the fibre at the end of a sorption process time (t_m).

A modified Cegarra–Puente[54] equation, with the inclusion of the Arrhenius equation, resulted in a method to calculate a target exhaustion rate at any given time t_i. Ruttiger *et al.* and Siegrist[55–57] showed that there is a significant dyeing parameter, *Vsig*, also known as the critical rate of dyeing, for each machine/goods system. They concluded that this occurs at a particular time at which results turn out just level, irrespective of the dyeing mechanisms and the heating rate. So it appeared that, for a level dyeing, the dyeing rate should always be lower than the critical rate and, if the shortest possible time is desired, then the optimum

exhaustion profile is a linear function of the dyeing time. They claimed that *Vsig* roughly increases with an increase in the flow rate of the liquor. Hasler[37] proposed that an even rate of absorption will result in an even dyeing, and to achieve this the quantity of dye extracted per circulation must remain constant, thus also deriving a linear exhaustion profile. It was mentioned that the ratio of the difference in concentration between the inlet and outlet of the package to the mean concentration of the liquor should be controlled to less than a limiting value if level dyeing was to be achieved.

Beckmann and Hoffmann[36] recognised that the greater the ratio of the rate of the exhaustion to that of liquor circulation, the greater the concentration difference between the different positions within the package. They pointed out that for a constant rate of circulation, in order to minimise the concentration difference, the exhaustion should be linear with time.

Research was carried out by a number of groups on how to achieve a linear exhaustion curve by a predicted time–temperature variation.

Brooks[58] showed that, for a given flow direction within a package, the difference in concentration across the radius was found to be proportional to the overall rate of exhaustion of the dye used. For a constant rate of depletion of dye, this difference must be constant throughout the dyeing. This has cast serious doubts on the linear function being the optimum exhaustion profile. He stated that neither linear exhaustion curves nor the time–temperature profile recommended by dye manufacturers result in best level dyeing. He showed that exponential curves and exhaustion curves proportional to the square root of time t give superior levelness compared with previous models.

Medley and Holdstock[59] developed the 'simple depletion theory', which suggests that a non-linear profile, in which the rate of dye uptake by a layer in the package is proportional to the concentration of dye in the liquor at that position, gives the most level dyeing.

Ren[42] studied the exhaustion profiles and concluded both theoretically and experimentally that the quadratic exhaustion profile is more likely to result in better levelness than any other profile. The control of the exhaustion of a dyeing process to achieve the various profiles will be discussed in Chapter 7.

1.6 Automation in the dyehouse

The control of dyeing processes has come a long way since the manual regulation of a steam valve, the only method of temperature control available at the beginning of the 1950s. Since then, the technology of dyeing process control has evolved relatively rapidly, from simple manual operations to sophisticated computer-controlled machines, in the following decades. As the use of such equipment has increased, the scope of application has widened, to include functions such as filling, draining, and addition of chemicals and dyes to the dyeing machine as well as time/temperature programming.[2,60]

Developments in equipment have resulted in the real cost of control systems decreasing. The availability of more sophisticated and powerful equipment at no major increase in purchase price makes it affordable to control a large number of parameters in the dyeing process.

The advantages of automation and control have been well documented,[61] but they can be catalogued to include the following benefits:[62]

- increase in productivity
- improvement in quality with reduced loss of material
- improved reproducibility
- increased flexibility
- savings in dyes, chemicals and labour
- general reduction in processing costs.

1.6.1 Temperature control

In practice, temperature control is still the most commonly used method for controlling the rate in the dyeing industry. Rate of dyeing is greatly dependent on temperature, increasing in all cases with an increase in temperature, but the final exhaustion may increase or decrease depending upon the particular dyeing system.[4] Also, the rate at which the temperature is raised is known to be one of the most important factors which determine levelness of dyeing. Time/temperature schemes for dye application to appropriate substrates are usually set in pattern cards provided by dye manufacturers as guidance to dyers. In this commonly practised state of affairs, the recommended scheme for temperature variation of the dyebath usually comprises a number of steps, each specified by a rate of temperature variation in °C/min. Such a scheme is commonly referred to as a time/temperature programme or profile, and is largely based on the dye manufacturer's empirical knowledge for a given fibre.

The time/temperature control, however, does not necessarily represent control of the dyeing process, since the parameter is checked without any reference to the condition of the material being processed at that point in time, and the incorrect assumption is made that dyeing conditions are dependent merely on the time/temperature function.[37] Temperature control in dyeing is an indirect method of controlling the rate of exhaustion of dyes onto the fibre; without information about the actual rate of exhaustion during a particular dyeing, the process cannot be optimised. Ideally, the temperature of the liquor should be adjusted according to the actual rate of exhaustion occurring during a dyeing process.

1.6.2 Exhaustion control

Dyeing is carried out either as a batch exhaustion process, or as a continuous impregnation and fixation process. In exhaust dyeing, all the material is in contact with all the dye liquor from which the fibres absorb the dyes. The dye

concentration in the bath, therefore, gradually decreases. The degree of dyebath exhaustion as a function of time describes the rate and extent of the dyeing process. For a single dye, the exhaustion is defined as the mass of dye taken up by the material, divided by the total initial mass of dye in the bath. For a bath of constant volume:

$$\% \text{ Exhaustion} = (C_0 - C_t)/C_0 \qquad [1.3]$$

where C_0 and C_t are the concentrations of dye in the dyebath initially and at some time, t, during the process, respectively.

Exhaustion curves, such as that shown in Fig. 1.6, may be determined at a constant dyeing temperature, or under conditions where the temperature and other dyeing variables are changing. For many dyeings, a gradual increase of the dyeing temperature controls the rate of exhaustion, aided possibly by the addition of chemicals such as acids or salts. In cases where the dyes in the deeply dyed fibres are not able to desorb into the bath and then be redistributed onto paler fibres, such control is essential to ensure that the final colour is as uniform as possible.[5] Such redistribution of dyes is called migration.

The slope of a dyeing exhaustion curve (Fig. 1.6) defines the rate of dyeing at any instant during the process. The rate of dyeing gradually decreases until, if dyeing is continued long enough, an equilibrium is reached where no more dye is

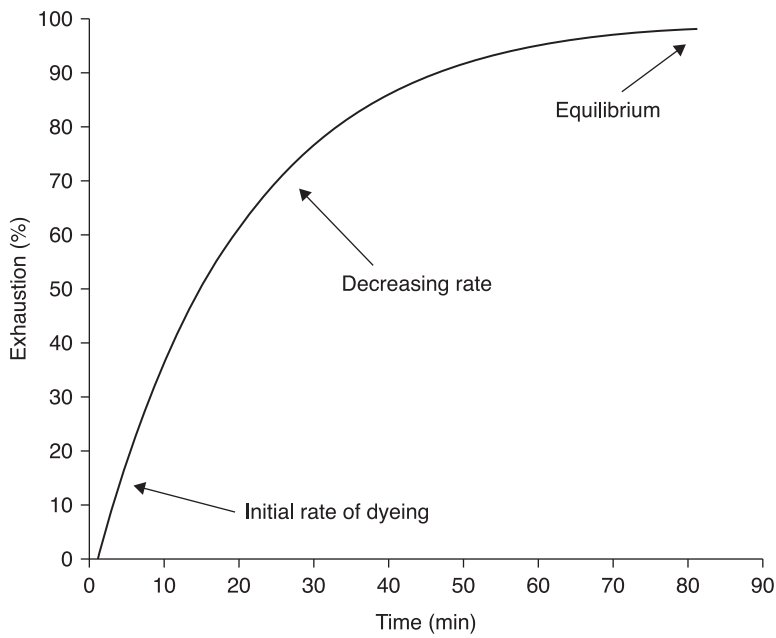

1.6 Dyebath exhaustion as a function of time.

taken up by the fibres. There is now a balance between the rates of absorption and desorption of the dye. The equilibrium exhaustion is the maximum possible exhaustion under the given conditions. The lack of any further increase in exhaustion does not necessarily mean that a true equilibrium exists. It is possible for the dye in solution to be in equilibrium with dye located on the outer surfaces of the fibres. True equilibrium only exists when the dye in solution is in equilibrium with dye that has fully penetrated into the centre of the fibres. Dyeings rarely continue to this point, since it may take a relatively long time to attain. In fact, many commercial dyeings barely reach the point of constant exhaustion.[15]

There are two basic methods of achieving a level exhaustion dyeing in any dye/fibre system; the first is by dye migration, and the second is by controlled dye exhaustion.[58] The first method involves exhausting all of the dye onto the fibre and then allowing it to migrate between the fibres in order to 'level out' the dyeing. These are dyes which are able to migrate from the fibre back into the liquor and then transfer back to the fibre. This redistribution of dye improves the levelness of the dyeing and normally takes place when the dye liquor is at the boil. In this method the dye is not completely exhausted onto the substrate, which can lead to poor reproducibility of colour, and hence additions of dye to correct the final shade are often necessary.

The second method is to ensure that the dye is exhausted in a level manner from the start of the dyeing. In this method, the dyeing rate is controlled by changing the parameters of the dyebath at a controlled rate so that the dye is deposited on the yarn in a uniform manner throughout the package. Careful control of these parameters, such as dyeing temperature, pH or amount of electrolyte and flow rate, etc., is often necessary to obtain level, well-penetrated dyeings. This is essential if the dye initially absorbed is unable to migrate from heavily dyed to poorly dyed areas during the process.

1.6.3 Exhaustion profiles

Variation of the concentration of dye in the dyebath during the dyeing is referred to as the exhaustion profile, and the shape of this profile has been believed by many researchers to be the greatest determining factor in levelness of dyeing.[58,59,63]

Exhaustion control has been developed theoretically and in the laboratory by several workers. The earlier workers used knowledge of the dyeing kinetics to devise a time/temperature profile to give a particular exhaustion profile; later workers attempted direct control of the exhaustion rate.

Studies of the theoretical basis of the relationship between levelness of dyeing and the rate of dye uptake by textile substrates were initiated by Boulton and Crank[38] in 1952 and were followed in the 1960s by Cegarra *et al.*[63] and Carbonell *et al.*[64] Since then there have been many investigations into methods of controlling the exhaustion of the dyebath in order to improve levelness.[23,64–67] This has been an area of much disagreement among researchers.

Linear exhaustion profile

Carbonell *et al.* developed a mathematical representation of various exhaustion profiles and went on to calculate practical time/temperature profiles that would result in linear exhaustion profiles.[41] Cegarra *et al.* carried out more work aimed at establishing detailed kinetic relationships in order to carry out 'isoreactive' dyeings, in which the dyeings have a linear exhaustion profile.[54,68]

Cegarra *et al.* later modified this approach to apply it to dyeings that used continuous addition (or integration) of dye into the dyebath.[69–72] These dyeings were carried out at constant temperature, using a predetermined dye addition profile to achieve linear exhaustion. This method was defined as integration dyeing, which can be used to control the dye absorption during the integration, so as to avoid the possibly initially fast and anomalous absorption, which may cause unlevel dyeings. In practice, this method is often used to improve the levelness when all the dyes are added at the beginning of the process. Hasler[37] believed that linear exhaustion is most likely to give a level result, and developed a control strategy for automation of a dyeing machine such that the percentage exhaustion per circulation never rises above the critical value for levelness.

Other exhaustion profiles

Brooks[58] questioned the use of linear exhaustion profiles. He put forward the view that a rapid uptake at the start of the process, with a gradual slowing of the exhaustion thereafter, should give a better result than a linear profile. His argument was that the critical part of the exhaustion phase is the final phase, when the amount removed from the bath is large compared to that remaining, leading to a greater risk of unlevelness. He examined two profiles of this type: an exponential curve and one with the exhaustion proportional to square root time.

Brooks' experimental work showed that both exponential and square root profiles give a clear improvement over both a linear profile and a standard constant temperature ramp dyeing. He also recommended that efforts be made to devise a reliable concentration monitoring system and exhaustion control system. Beckmann and Hoffmann supported Brooks' ideas concerning a high exhaustion rate at the start of dyeing and slowing down thereafter. Nevertheless, they recommended aiming at a linear exhaustion profile due to limitations imposed by an imperfect knowledge of the precise conditions of the material being dyed.[73]

Medley and Holdstock[59] developed a mathematical model of the dyeing process, defined as 'simple depletion theory'. Using this theory, they were able to show that an exponential exhaustion profile should give the optimum levelness for the same reasons as Brooks' empirical argument – that at the end of the exhaustion phase the risk of unlevelness is greatest. Their work also involved the development of a commercial dyebath monitoring system in order to apply their theoretical work to a real dyehouse situation.[74]

Ren,[42] in collaboration with Nobbs, developed a theoretical model of the package dyeing process, which can be used to quantify the difference between the amount of dye inside and outside of the package over the whole of a dyeing cycle, which leads to the proposal of a new type of optimum exhaustion profile, the quadratic profile.

Experimental work on dyebath exhaustion control was also carried out using a pilot-scale radial flow package dyeing machine,[43] and the results supported the findings of the theoretical model. In particular, it was found that a quadratic profile was preferable to an exponential profile, which in turn was preferable to a linear profile. All controlled exhaustion dyeings gave better levelness than a standard (constant temperature ramp) dyeing method. This work was continued by Illett,[43] who improved the mathematical solution of the Nobbs–Ren model and applied it to axial flow machines.

Although a great deal of theoretical work has been carried out in this area, no consensus has yet been reached on the optimum exhaustion profile, or even whether solely controlling the rate of exhaustion is, in fact, an optimisation of the overall process. As Beckmann and Hoffman[36] point out, there is little point in developing complex monitoring and control strategies if the target profile is not clearly defined. Also, however closely the exhaustion rate is controlled, unlevelness may still occur due to other problems with the processing machinery, such as poor agitation or differences in temperature between different parts of the machine. In these cases, acceptable levelness may only be achieved by use of chemical levelling agents to allow improved migration of the dye.

1.6.4 Chemical engineering approach analysis

Wai[75] and Burley *et al.*[76] developed a complex mathematical model using principles well known in chemical engineering. They considered the package as a packed bed chemical reactor. The processes of convection, dispersion, absorption and desorption of dye to and from the packed bed of fibres are modelled, while account is also taken of the addition of dye to, and the possible removal of liquor from, the mixing tank.[66] They further developed the model of a packed bed reactor and defined two equations for axial and radial flow processes.[76] Example simulations showed that advantages include a decreased time to reach a level dyeing and faster attainment of equilibrium.

Vosoughi[23] continued the work of Burley *et al.* His equations were developed to describe the diffusion of dye into the fibre interior. These equations were solved numerically using appropriate boundary conditions to result in dimensionless relationships for both axial and radial flows.

Telegin[77] presented a mathematical description of convective mass transfer in the processes of solution flow round a single fibre and through a layer of fibres, which provides a theoretical estimation of the rate of convective mass transfer in the liquid processes of textile treatment.

The above-mentioned works, which describe the influence of the dyeing conditions on the kinetics of dye uptake, either ignore the dispersion or adsorption factor, or fail to define the flow velocity within the package. The details will be discussed in the next chapter.

1.7 References

1. Shamey R., Nobbs J.H. (2000), 'The Application of Feedforward profiles in the Control of Dyeing Machinery' *Textile Chemist and Colorist*, **32**, 2, 47–52.
2. Nobbs J.H. (1997), 'Control Parameters in Dyeing Machinery Operation' *Journal of the Society of Dyers and Colourists*, **107**, 430–3.
3. Johnson A. (1989), *Theory of Coloration of Textiles*, SDC, Bradford.
4. Vickerstaff T. (1968), *The Physical Chemistry of Dyeing*, 2nd edn, Oliver and Boyd.
5. Broadbent A. (2002), *Basic Principles of Textile Coloration*, SDC, Bradford.
6. Shore J. (1990), *Colorants and Auxiliaries*, SDC, Bradford.
7. Aspland J.R. (1993), 'The Application of Ionic Dyes to Ionic Fibers: Nylon, Silk and Wool and Their Sorption of Anions' *Textile Chemist and Colorist*, **25**, 3, 55–9.
8. Hoffmann F. (1990), 'Levelness in Yarn Dyeing: Advances in Theory and Practice' *Textile Chemist and Colorist*, **22**, 11–16.
9. Welham A. (2000) 'The Theory of Dyeing (and the Secret of Life)' *Journal of the Society of Dyers and Colourists*, **116**, 140–3.
10. Warnet S.B. (1995), *Fiber Science*, Prentice Hall.
11. Hearle J. (1993), *Physical Properties of Textile Fibers*, 3rd edn, The Textile Institute.
12. Lewin M. (1983), *Handbook of Fibre Science and Technology*, Volume 1, Prescott Inc.
13. Nettles J. (1983), *Handbook of Chemical Specialties*, Prescott Inc.
14. Kulkarni S.V. (1986), *Textile Dyeing Operations*, Noyes Publications.
15. Bird C., Boston W. (1972), *The Theory of Coloration of Textiles*, SDC, Bradford.
16. Parton K. (1997), 'The Dyeing of Wool: Past, Present and Future' *Journal of the Society of Dyers and Colourists*, **113**, 341–3.
17. Brooks J.H. (1972), 'Levelness in the Dyeing of Wool Yarn and Fabric' *Journal of the Society of Dyers and Colourists*, **88**, 184–6.
18. Yuan C.Q., Bide M. (1998), 'Textiles and the Environment from AATCC' *Textile Chemist and Colorist*, **30**, 62–5.
19. Huang C., Yu W. (1999), 'Control of Dye Concentration, pH, and Temperature in Dyeing Processes' *Textile Research Journal*, **69**, 914–18.
20. Gailey I. (1989), *International Dyer and Textile Printer*, **5**, 31.
21. Harvey H.N, Park J. (1989), 'Automation in the Dyeing Laboratory and Its Influence on Accuracy in Batch Dyeing' *Journal of the Society of Dyers and Colourists*, **105**, 207–11.
22. Heane D.G., Hill T.C., Park J., Shore J. (1979), 'Package Dyeing of Acrylic Fibre Yarn: Important Parameters which Influence Level Dyeing' *Journal of the Society of Dyers and Colourists*, **95**, 125–42.
23. Vosoughi M. (1985), 'Numerical Simulation of Packed Bed Adsorption applied to a Package Dyeing Machine' PhD Thesis, Heriot-Watt University, UK.
24. Chen H.L, Noel C.J. (1995), 'Experimental Methods for the Analysis of Dye Desorption' *Textile Chemist and Colorist*, **95**, 27, 2, 23–7.

25. Park J. (1981), *A Practical Introduction to Yarn Dyeing*, SDC, Bradford.
26. Thornton A. (1994), 'Fully automated yet versatile systems' *International Dyer*, **5**, 25.
27. Obermaier O., German Patent 23, 117 (6.10.1882).
28. Wyles D.H. in Duckworth C. (ed.) (1983), *Engineering in Textile Coloration*, Dyers Company Publications Trust.
29. Fleming R., Gaunt J.F. (1977), 'Developments in Package Dyeing' *Rev. Prog. Coloration and Related Topics*, **8**, 47–59.
30. Horn P.J. (1965), 'Specific Problems in the Dyeing of Cellulosic Fibres in Circulating–liquor Machines' *Journal of the Society of Dyers and Colourists*, **81**, 262–8.
31. Beacon Controls Ltd, Technical Pamphlet, 14–18 Campus Road, Bradford, West Yorkshire, BD7 1HR.
32. Zella Instrumentation & Control Ltd, Technical Pamphlet, Brunel Drive, Northern Road Industrial Estate, Newark-on-Trent, Nottinghamshire, NG24 2EQ.
33. Cegarra J. (1973), 'A New Package Dyeing Apparatus' *Melliand Textilberichte*, **54**, 394; *Melliand Textilberichte* English Edition, **2**, 4, 306–8.
34. Bauer K.H., Boxhammer J., Kockett D., Toldrian P. (1979), 'Verfahren und Gerät zur Optimierung und Regelung des Farbauszugs bei Badfärbungen; Technik und praktische Erfahrungen in der PAC-Färberei. 1. Teil' *Textilveredlung*, **14**, 183.
35. McGregor R., Peters R.H. (1965), 'The Effect of Rate of Flow on Rate of Dyeing I – The Diffusional Boundary Layer in Dyeing' *Journal of the Society of Dyers and Colourists*, **81**, 393–400.
36. Beckmann W., Hoffmann F. (1977), 'The Relationship Between Liquor Flow and Levelness in Package and Beam Dyeing', *Textile Chemist and Colorist*, **9**, 10, 22–7.
37. Hasler R. (1975), 'Optimizing Package, Beck and Jet Dyeing' *Textile Chemist and Colorist*, **7**, 36–9.
38. Boulton J., Crank J. (1952), 'Package Dyeing I—A Theoretical Model and its Relation to Technical Practice' *Journal of the Society of Dyers and Colourists*, **68**, 109–16.
39. Whittaker J. (1961), 'Practical Problems in Preparation and Dyeing of Cross-wound Packages' *Journal of the Society of Dyers and Colourists*, **77**, 690–9.
40. Clifford F. (1972), 'Rapid Reversal-A Technique for Increasing Quality of Dyestuff Application' *American Dyestuff Reporter*, **61**, 40.
41. Carbonell J., Hasler R., Walliser R., Knober W. (1973), 'Mathematical Relationship between Dyeing Kinetics and Liquor Throughput and Their Effect on the Homogeneity of Dye Distribution of the Fiber' *Melliand Textilberichte*, **54**, 68; *Melliand Textilberichte* English Edition, **2**, 1, 62–7.
42. Ren J. (1985), 'A Thesis on the Development of a Mathematical Model of the Batch Dyeing Process and its Application to the Simulation and Computer Control of A Dyeing Machine' PhD Thesis, Dept. of Colour Chemistry, Leeds University.
43. Ilett S.J. (1990), 'Investigation of the Package Dyeing Process Using a Fixed Bed Reactor as a Model System' PhD Thesis, Dept. of Colour Chemistry, Leeds University.
44. Bohrer E.S. (1991), 'The Importance of Short Liquor Technology and Synchronised Dyeing in the Batchwise Dyeing of Fabric and Yarn' *Journal of the Society of Dyers and Colourists*, **107**, 212–15.
45. Burley R. (1990), Pollution Seminar 'Engineer Your Way Out', Edinburgh, Heriot-Watt University.
46. Burley R., Wai P.C., McGuire G.R. (1987), 'Modelling the Dynamic Behaviour of a Packed-bed Adsorber' *Journal of the Textile Institute*, **19**, 164–88.

47. Burley R.W., Rattee I.D., Flower J.R. (1969), 'Mass-transfer Processes in Hank-dyeing Machines I—Theory and Experimental Studies' *Journal of the Society of Dyers and Colourists*, **85**, 187–92.
48. McGregor R., Peters R.H. (1965), 'The Effect of Rate of Flow on Rate of Dyeing I– The Diffusional Boundary Layer in Dyeing' *Journal of the Society of Dyers and Colourists*, **81**, 393–400.
49. Denton M.J. (1959), 'An Electrolytic Tank for the Investigation of Fluid Flow Patterns in Yarn Packages' *Journal of the Textile Institute*, **50**, T521–T527.
50. Denton M.J. (1963), 'Flow Patterns In Package Dyeing' *J. Text Institute*, **54**, T406–T408.
51. Denton M. (1964), 'The Permeability of Cross-Wound Cotton Yarn Packages' *Journal of the Textile Institute*, **55**, T228–T242.
52. Carbonell J., Hasler R., Walliser R., 'Chem. Phys. Chem. Anwenungstech. Grenzflachenaktiver Stoff' Ber. Inst. 6 Kongr. (11–25. 9. 1972), Band 3, 383–403.
53. Giles C.H. (1974), 'A Laboratory Course in Dyeing', 3rd edn. S.D.C., Bradford.
54. Cegarra J., Puente P., Valldeperas J. (1976), 'Isoreactive Dyeing Systems' *Journal of the Society of Dyers and Colourists*, **92**, 327–31.
55. Ruttiger W., Ehlert J. (1972), 'The Critical Dyeing Speed – an Identification Value of Processing Technique for the Time Saving and Even Dyeing on the Apparatus' *Textil-Praxis*, **27**, 10, 609–16.
56. Ruttiger W., Wolf H. (1974), 'Possibilities and Limitations of Rapid Dyeing Techniques' *Melliand Textilberichte*, **55**, 10, 876–9; *Melliand Textilberichte* English Edition, **3**, 10, 762–5.
57. Siegrist G. (1977), 'Developments in Rapid-dyeing Methods and Machinery' *Review of Progress in Coloration and Related Topics*, **8**, 24–35.
58. Brooks J.H. (1975), 'The Effect of the Shape of the Exhaustion Curve on Levelness of Dyeing' *Journal of the Society of Dyers and Colourists*, **91**, 394–8.
59. Medley J.A., Holdstock C.R. (1980), 'The Choice of Optimum Dye Exhaustion Profiles in the Direct Control of Dyeing' *Journal of the Society of Dyers and Colourists*, **96**, 286–92.
60. Lewis D. (1992), *Wool Dyeing*, SDC, Bradford.
61. Bialik Z., Park J., Walker D.C. (1979), 'Control Engineering in the Dyeing and Finishing Industry' *Review of Progress in Coloration and Related Topics*, **10,** 55–60.
62. Park J. (1985), 'Developments in Dyeing Process Control' *Review of Progress in Coloration and Related Topics*, **15**, 1–5.
63. Cegarra P., Puente P. (1967), 'Considerations on the Kinetics of the Dyeing Process of Polyester Fibers with Dispersed Dyes' *Textile Research Journal*, **37**, 343–50.
64. Carbonell J., Haster R., Walliser R. (1974), 'Circulating Liquor Dyeing in a New Light' *Melliand Textilberichte*, **55**, 149; *Melliand Textilberichte* English Edition, **3**, 2, 110–13.
65. Hoffmann F., Mueller F. (1979), 'Model Calculations on Levelness in Package Dyeing' *Journal of the Society of Dyers and Colourists*, **95**, 178–86.
66. Burley R., Wai P.C., McGuire G.R. (1985), 'Numerical Simulation of an Axial Flow Package Dyeing Machine' *Appl. Math. Modelling*, **9**, 1, 33–9.
67. Nobbs J.H., Ren J. (1985), Proceedings of 29th Hungarian Textile Conference, Budapest.
68. Cegarra J., Puente P., Valldeperas J. (1974), 'Characteristics of Acrylic Fibers and Kinetics of Dyeing with Cationic Dyes' *Textile Chemist and Colorist*, **6**, 8, 23–7.

69. Cegarra J., Puente P., Valldeperas J., Pepió M. (1988), 'Dyeing by Integration' *Textile Research Journal*, **58**, 645–53.
70. Cegarra J., Puente P., Valldeperas J., Pepió M. (1989), 'Kinetic Aspects of Dye Addition in Continuous Integration Dyeing' *Journal of the Society of Dyers and Colourists*, **105**, 349–55.
71. Cegarra J., Puente P., Valldeperas J. (1992), 'Dyeing Wool Packages with Continuous Dosage of Dye' *Journal of the Society of Dyers and Colourists*, **108**, 86–9.
72. Cegarra J., Enrich F., Pepió M., Puente P. (1999), 'Modelling of integration dyeing of a wool package with acid dyes' *Journal of the Society of Dyers and Colourists*, **115**, 92–4.
73. Beckmann W., Hoffmann F. (1988), 'Sistemi colorimetrici per la realizzazione dei procedimenti di tintura' *Tinctoria*, **85**, 70.
74. Holdstock C.R. (1988), 'The Measurement and Control of Dyebath Exhaustion' PhD Thesis, University of Leeds, UK.
75. Wai P.P.C. (1984), 'Dynamic Behaviour of a Reactive Packed Bed Adsorption System' PhD Thesis, Heriot-Watt University, UK.
76. Burley R., Wai P.C., McGuire G.R. (1987), 'Process Engineering Approach to Dyeing Machinery—A Study of Package Dyeing Machine Dynamics' *Chem. Eng. Res. Des*, **65**, 505–13.
77. Telegin F.Y. (1988), 'Convective Mass Transfer in Liquid Treatment Processes' *Journal of the Society of Dyers and Colourists*, **114**, 49–55.

2

Principles underlying the dyeing process

DOI: 10.1533/9780857097583.31

Abstract: Chapter 2 presents the basic principles underlying the dyeing process; it is concerned mainly with some of the more quantitative aspects of dyeing equilibrium and kinetics, including standard affinity of dyes. The change in chemical potential of dye at the standard state from the solution to the fibre due to the presence of electrolytes is examined. Transport of dye in the dyebath involving sorption is described and various adsorption isotherms are examined. A general dynamic expression of dye sorption by textile fibres is then introduced. Diffusion phenomena and models describing the diffusion of dye into textile fibres are then evaluated.

Key words: dye transport, sorption, adsorption, adsorption isotherms, standard affinity of dyes, diffusion, diffusional boundary layer, Fick's laws.

2.1 Introduction

The theory of dyeing covers a wide range of subjects, mainly in the area of physical chemistry. Some of the subjects included in dyeing theory are:[1]

- the state of dyes in solution and in the fibre during and after dyeing
- the rates of dyeing processes and how these are influenced by mass transfer of dye from the dyebath solution to the dye–fibre interface, and by diffusion of the dye from the interface into the fibre
- the phenomena occurring at the dye–fibre interface, such as dye molecule adsorption and the effects of surface potentials
- the nature of the interactions between dye and fibre molecules, which are the origin of substantivity
- the treatment of dyeing as a thermodynamic equilibrium and its description in terms of thermodynamic variables
- the theory of fibre structure and how this influences dyeing rates and equilibrium.

The fundamental concepts of these subjects have been extensively discussed in a series of publications.[2–4] Concerning the main objective of the present work, this chapter will introduce some of the more quantitative aspects of dyeing equilibrium and kinetics.

2.2 Dye transport from the bulk solution to the fibre surface

Dyeing is a process that takes time. The transfer of a dye molecule from the dye solution into a fibre is usually considered to involve the initial mass transfer from

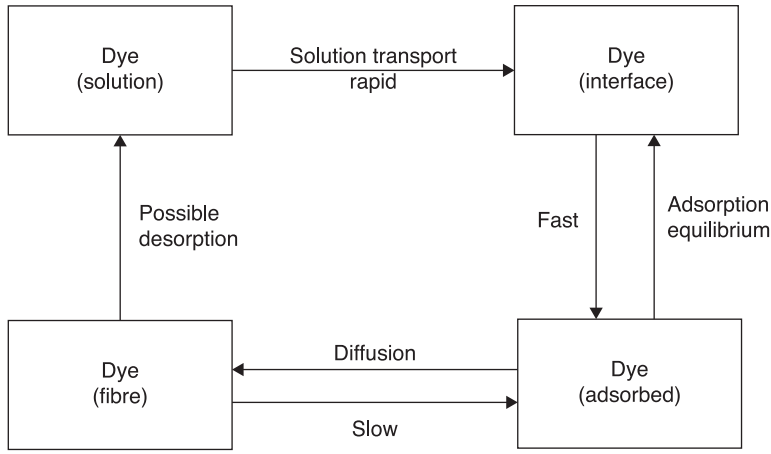

2.1 Dye transfer from the solution into a fibre.

the bulk dye solution to the fibre surface, adsorption of the dye on the fibre surface, followed by diffusion of the dye into the fibre, as shown in Fig. 2.1. Diffused dye may desorb and re-enter the dyebath. This process will continue until equilibrium is achieved.

The transfer of dye from the bulk of the solution to the fibre surface is fast; the rate generally increases with increasing flow rate; the adsorption equilibrium is rapid, so it is usually assumed that the overall rate of dyeing depends on the rate of diffusion of the dye into the fibre. Inadequate control of the rate of dye adsorption will result in unlevel dyeings unless the dye can subsequently migrate from deeply dyed to lightly dyed regions of the package.[3] Therefore, the control of the first two stages of the process, namely the initial mass transfer from the bulk solution to the fibre surface and adsorption of the dye on the surface, is important for a level dye distribution throughout the substrate to be achieved.

When a fibre, yarn or piece of cloth is immersed in a dye solution, the rate at which the dye is taken up is generally dependent upon the extent to which the liquor is agitated, and tends to approach a maximum value when the stirring is vigorous.[5] The effect of stirring on the rate of dyeing of fibres with various dyes has been examined by a number of researchers. In the dyeing of wool with acid dyes and cotton with direct dyes it has been shown that, as agitation is increased, the rate of dyeing increases and tends to become independent of speed at the higher rates of circulation.

A fundamental concern in dyeing of textiles is to ensure that the dye liquor penetrates to all parts of the substrate, and that it is distributed as evenly as possible within the material. In the case of package dyeing, this applies to any one package and equally between one package and another. In package dyeing, ideally

identical packages are subjected to a common pressure head and each package receives the same flow of liquor and undergoes identical processing. In practice, however, packages vary to a greater or lesser extent in hardness and size because of variations in tension and other factors in winding. These variations are of major importance, since, in wet processes, denser packages are less easily penetrated by the liquor than softer ones, and differences in flow rate can lead to shade differences in dyeing. In open width dyeing of the substrate, uniformity across the width of the package as well as the inner and outer layers of the roll should be ensured. Temperature variations within the machine that result in variations in diffusion of dyes across the roll as well as inner and outer layers of the substrate should be carefully controlled. In rope dyeing, such as batch dyeing of substrates in jet or winch, movement of the substrate within the machine and dwelling time and temperature must be carefully controlled, as these parameters influence the uptake of dye by the substrate. In addition, the dye liquor should be uniformly agitated to ensure uniform presentation of dye to the substrate throughout the dyeing process.

The influence of agitation in increasing the rate of uptake is dependent in large measure on the hydrodynamic complexity of the system. Unfortunately, however, flow through the fibrous assemblies cannot be described in any simple fashion, due to the extreme complexity of defining the flow of liquor through a mat of fibres, or through yarns or cloth.[5]

In spite of the complications of real systems, some of the principles governing the process may be elucidated by consideration of simpler systems, e.g. a plane sheet or film of material immersed in dye liquor whose direction of flow is parallel to the sheet. On making contact with the dye liquor, dye is adsorbed by the film, so that the neighbouring liquor becomes deficient in dye; dye is transported to the surface by dispersion from the bulk, but the quantity transferred is modified by the speed at which the liquor flows past the film.

Calculations of the rate at which the fibres can take up dye require knowledge of the flow pattern of the liquor before analysis of diffusion may be attempted. Experimental investigations of flow of dye liquor through masses of fibre lead to the conclusion that, at the rates commonly used in dyeing, the flow is streamline rather than turbulent, so attention may be confined to streamline conditions.[6,7]

Several papers have been published concerning the influence of flow rate on dyeing in both the practical and theoretical aspects. It is known that higher rates of flow of dye liquor through a package result in better levelness of the dyeings. Boulton and Crank[8] described a theoretical model of a yarn package and discussed the level absorption of dye in a yarn package. They showed the importance of the effects of flow velocity and the rate of strike and levelling properties of the dyestuff. The results from practical experiments were examined in the light of the theoretical model.[9]

Another important factor, the diffusional boundary layer, the layer over which the resistance to passage of dye from the bulk of the dyebath occurs, has been the

subject of numerous publications[10,11] and is discussed in detail by McGregor and Peters.[12] Dye liquor that is flowing past the surface of textile fibre develops velocity gradients. In the region approaching the fibre's surface, the velocity of the dye liquor decreases from that which exists in the mainstream to that which exists at the fibre surface. The region of velocity change is referred to as a hydrodynamic layer.

The importance of the diffusional boundary layer is found in the layer's influence on sorption and desorption rates. Diffusional boundary layers act to impede or decrease rates of sorption or desorption of dye by the fibre, the effect increasing with increasing thickness of the layer. When dyebath flow velocity is not uniform throughout the textile mass, the rate of dye uptake will not be uniform, leading to dyeing unlevelness.[13] The influence of the diffusional boundary layer on sorption of dye increases with increasing equilibrium exhaustion of the dyebath. This fact is consistent with the observed behaviour of commercial dyeing systems. For example, it is widely known that dyes of high affinity result in high equilibrium exhaustion and are difficult to apply uniformly. It is found that the thickness of the diffusional boundary layer decreases with increase in flow velocity so that the mass transfer to the surface is increased. It is believed that a very large proportion of the observed unlevelness is caused by flow rate differences in various regions of the textile material. Cellulose fibres acquire negative charges on their surface in an aqueous solution, where a diffuse electrical double layer is formed.[14] The sorption of anionic dyes on cellulose can be influenced by the addition of electrolytes, which offsets the electrical potential on the fibre surface. In addition, the added electrolytes can facilitate the dye sorption process by disrupting the H-bonded structure of water, which can hydrate anionic dyes and ionic sites on the fibre surface.[15]

The physical structure of fibres, such as cellulose, greatly influences the dye sorption process. The accessible volume of fibre to dye is generally termed the internal accessible volume (V), which represents the internal void space, or pores, within a fibre. In thermodynamics of sorption, V is referred to as the volume of the internal phase per kilogram of dry fibre ($\mathrm{L\,kg^{-1}}$).[16] Determination of the internal volume of fibre greatly influences the calculation of standard affinity associated with sorption ($-\Delta\mu^{\circ}$). It has been shown that V can be determined based on a two-phase dye sorption model, expressed in a linear logarithmic form, according to a trial-and-error procedure.[17–24] The uniform presentation of dye liquor to the textile material is of obvious importance.

Denton[25] examined the difficulty of removing trapped air inside a package during the wetting-out process. Hadfield and Lemin[26] also described the effect of air, present because of foaming, on the permeability of packages.

Whittaker[27] reviewed the types of package in general use and called attention to the care needed in their preparation. Fox[28] summarized the major factors contributing to the production of high-quality dyed yarn, and in particular discussed some of the faults that can arise from the use of unsatisfactory packages.

It is critical that, during the dye transfer stage from the dye solution to the fibre surface, efforts should be made to ensure that the rate of dyebath flow is uniform throughout the textile mass in exhaustion dyeing processes. However, even with the best of efforts, uniformity of dyebath flow cannot be guaranteed in all cases, since the question of flow through packages is very complicated, and this is discussed in detail elsewhere.[29] The dyer must thus employ methods that will tend to level out the inevitable unevenness that occurs in the early stages of the dyeing process. As previously noted, perhaps the most effective method is to raise the 'energy level' of the system by the use of higher dyeing temperatures and/or suitable chemical auxiliaries that promote migration of dye.

2.3 Adsorption of dyes by textile fibres

2.3.1 Adsorption from solution

Adsorption from solution is important in many practical situations. In dyeing processes, it is necessary to distinguish between adsorption and absorption. Adsorption refers to an excess concentration at the surface, while absorption implies a more or less uniform distribution of the solute in the solid. In these processes the solid phase is known as the 'adsorbent' or 'absorbent', and the solute (or other species) as the 'adsorbate' or 'absorbate', respectively. In some cases it may be difficult to distinguish between adsorption and absorption, or, because of lack of data, it may not be known which process is occurring; the term 'sorption' is then used.[2] It is probable that adsorption occurs at all surfaces.

If a molecular species completely saturates the adsorbent surface with a single layer of molecules (or ions), the adsorption is known as unimolecular or monomolecular. On the other hand, the formation of multi-layers can occur, referred to as multimolecular adsorption. The latter, no doubt, occurs in the dyeing of nylon fibres with mono-sulphonated acid dyes, where dye aggregation is believed to take place within the fibre.

In practice, there are two kinds of adsorption.[2] Interaction of the adsorbate with the surface may take place simply through forces of physical attraction, i.e. intermolecular forces, and this type of adsorption is known as physical adsorption. It occurs on surfaces where the valency requirements of the atoms in the surface have already been satisfied by bonding with neighbouring atoms. If, on the other hand, a surface is unsaturated, that is, the atoms in the surface are not fully satisfied by bonding with neighbouring atoms, chemical adsorption or chemisorption occurs. Here, chemical bonds form between the adsorbate and the surface.

Physical adsorption occurs rapidly, because no activation energy is required. For the same reason it is temperature-independent.[3] Chemisorption, being a chemical reaction, may require an appreciable activation energy, in which case it will proceed at a reasonable rate only above a certain temperature. In many instances of adsorption it is difficult to distinguish between the two types by the rate of the process. For a surface that is so unsaturated that the activation energy

is zero or very small, chemisorption can be rapid even at low temperatures. Thus, a rapid adsorption does not necessarily imply physical adsorption.

2.3.2 Adsorption isotherms

An adsorption isotherm gives the concentration of a substance adsorbed on a solid surface in relation to its concentration in the surrounding fluid when the system is at equilibrium at a constant temperature.[30] The graph representing a dyeing adsorption isotherm has the adsorbed dye concentration (C_f in $g\,kg^{-1}$ or $mol\,kg^{-1}$), plotted against the solution concentration (C_s in $g\,l^{-1}$ or $mol\,l^{-1}$). Adsorption isotherms are useful for the information they provide on the dyeing mechanism. There are three main types of dyeing adsorption isotherm, usually referred to as the Nernst, Langmuir and Freundlich isotherms. Most dyeing systems involving only adsorption are completely reversible.[31] Equilibrium isotherms, established by adsorption of dye from solution onto initially undyed fibres, are identical to those obtained by desorption of dye from dyed fibres into an initially blank dyebath.

The Nernst isotherm is the simplest and is given by Eq. 2.1:[32]

$$C_f = kC_s \qquad [2.1]$$

where k is a constant. This is also the equation describing the distribution or partition of a solute between two immiscible solvents. The graph of C_f against C_s is linear up to the point corresponding to the dye saturating the fibre.

The Langmuir isotherm applies to adsorption on specific sites in the solid, of which there are often only a limited number.[3] Such a situation exists in the dyeing of nylon, wool and silk with simple acid dyes by an ion exchange mechanism.[33] The Langmuir adsorption isotherm is easily derived. The rate of desorption depends only on the fraction of occupied sites (C_f/C_{max}). The rate of adsorption of dye onto the fibre from solution depends upon the fraction of unoccupied sites ($1-C_f/C_{max}$) and the concentration of dye in the solution (C_s). At equilibrium, the two opposing rates are equal and can be represented by Eq. 2.2:[1]

$$k_1\left(1-\frac{C_f}{C_{max}}\right)C_s = k_{-1}\frac{C_f}{C_{max}} \qquad [2.2]$$

where k_1 and k_{-1} are the rate constants for adsorption and desorption respectively, and C_{max} is the maximum number of adsorption sites that dye molecules can occupy in the fibre. The rearrangement of this relationship leads to Eq. 2.3:

$$\frac{C_f}{C_{max}} = \frac{KC_s}{1+KC_s} \qquad [2.3]$$

where K is the value of k_1/k_{-1}. The graph of C_f versus C_s for the Langmuir isotherm, as shown in Fig. 2.2, clearly shows that the fibre becomes saturated with dye when

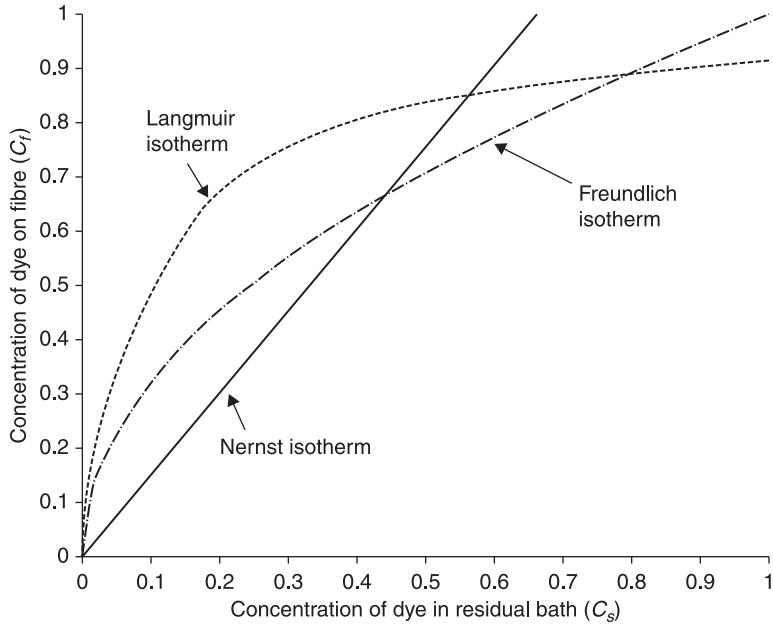

2.2 Adsorption isotherm.

all the available adsorption sites are occupied. The maximum number of sites in the fibre can be determined from the slope of the linear graph of C_s/C_f versus C_s according to Eq. 2.4:

$$\frac{C_s}{C_f} = \frac{C_s}{C_{max}} + \frac{1}{KC_{max}} \qquad [2.4]$$

The Nernst isotherm (shown in Eq. 2.1) can be seen as a special case of the Langmuir isotherm for the condition where KC_s is very small compared with unity. For this condition, the initial portion of the plot of the Langmuir isotherm is linear, as required for the Nernst isotherm.

The Freundlich isotherm applies to the situation where dye adsorption onto the fibre is not limited by a number of specific adsorption sites and the fibre does not become saturated with dye. A typical system is one for which the dye ion and the fibre surface have the same type of electrical charge. The empirical equation describing this isotherm is shown in Eqs 2.5a or 2.5b:[34]

$$C_f = kC_s^{\alpha} \qquad [2.5a]$$

or:

$$log(C_f) = log(k) + \alpha\, log(C_s) \qquad [2.5b]$$

where k is a constant, and the exponent α often has a value around 0.5 for the adsorption of anionic dyes on cellulosic fibres.[1] The amount of dye adsorbed by the cotton fibres depends upon the available pore surface area. Initially, the dye molecules adsorb on the surfaces of the most accessible pores, but increasingly the dye must penetrate into the less accessible areas, so adsorption becomes more difficult. The dye molecules may even adsorb onto a layer of dye molecules already adsorbed on the pore surfaces, creating multilayers of dye on the fibre. The derivation of the Freundlich isotherm does not follow a simple method such as that shown for the Langmuir isotherm.

It is assumed that any system to which the simulation model is to be applied can be represented by one of the three isotherms, Nernst, Freundlich and Langmuir isotherms, or by a combination of them.[35] For example, the dyeing of many synthetic fibres with disperse dyes follows the Nernst isotherm.[36,37] The dye transfers to fibre, in which it is soluble, from the aqueous bath, in which it is only slightly soluble.

It is generally true that the dye absorption isotherm is linear at low dye concentrations.[38] In this situation the dye molecules behave as though they were in a solution inside the fibre and are partitioned between the fibre and the dyebath so that, at any temperature, the ratio of dye in the fibre to dye in solution is constant. Deviations commonly occur at relatively high concentrations, but ideal linear behaviour is observed with disperse dyes over a wide range of concentration. On the other hand, high concentrations of direct and vat dyes on cellulosic fibres commonly exhibit Freundlich type isotherms;[39] this occurs apparently as a consequence of aggregation of dye molecules inside the fibres.

Langmuir type absorption isotherms are observed when only a limited number of dye sites are available inside the fibre. In this case the concentration of dye in the polymer reaches a maximum limiting level as the concentration of dye in the dyebath is increased. This behaviour is typical of acid levelling dyes on wool and silk.[40,41]

2.3.3 General dynamic expression of dye sorption by fibres

During the dyeing processes, the concentrations of dye in the liquor and on the fibre surface at a particular point at any time may not be at equilibrium with each other; a dynamic model is therefore required which represents the time dependency of the concentrations of the dye on the fibre surface. To simulate the textile dyeing processes of various systems it is desirable to build a general expression describing the relationship between the amount of dye adsorbed on the surface of the fibres and the amount of dye remaining in the liquor.

The sorption behaviour of dye molecules on a substrate is generally described using isothermal models. The standard affinity associated with sorption ($-\Delta\mu^{\circ}$) is used to explain the behaviour of different dyes in a particular system or the same dye on different substrates.

Sorption is a complex process, which is controlled by dye–substrate interactions involving various types of intermolecular forces, such as electrostatic (ionic),[42–44] van der Waals (London),[45–46] polar (hydrogen bonding)[47–50] and hydrophobic (cooperative binding) interactions.[51–54] The interaction forces involved in a sorption system depend on the physical and chemical properties of dyes and substrates. In general the adsorption of dye into the fibres can be represented by the following mechanism:[55]

$$Fibre + Dye \leftrightarrow Fibre \cdot Dye$$

This leads to a reversible rate expression shown in Eq. 2.6a:

$$\frac{d[Fibre \cdot Dye]}{dt} = K_a[Fibre][Dye] - K_d[Fibre \cdot Dye] \quad [2.6a]$$

where *Fibre* represents the unadsorbed surface, which can be expressed by subtracting the concentration of dye on fibres (v) from the total adsorbent capacity (v^*), *Dye* represents the concentration of dye in liquor (C), $Fibre \cdot Dye$ denotes the concentration of dye on fibres (v), K_a is the adsorption rate constant, and K_d is the desorption rate constant. Therefore, the rate can be expressed by Eq. 2.6b:

$$\frac{dv}{dt} = K_a C(v^* - v) - K_d v \quad [2.6b]$$

In terms of scaled quantity f, this will take the form shown in Eq. 2.7a:[56]

$$\frac{df}{dt} = K_a C^a(1 - bf) - K_d f \quad [2.7a]$$

where a and b are constants. Equation 2.7a is the general dynamic expression relating the concentration of dye on fibres and that in the dye liquor. It can be reduced to the general equilibrium expression shown in Eq. 2.7b by setting $df/dt = 0$:

$$f = \frac{KC^a}{1 + bKC^a} \quad [2.7b]$$

where $K = K_a/K_d$ is the adsorption coefficient. This general equilibrium expression (Eq. 2.7b) can be reduced to the following simpler forms:

Nernst isotherm when $a = 1$ and $b = 0$,
Freundlich isotherm when $0 < a < 1$ and $b = 0$, and
Langmuir isotherm when $a = 1$ and $b = 1$.

It should be emphasised that although Eq. 2.7 is a complex form of the adsorption isotherms and involves more parameters, it is convenient for the numerical study of the adsorption phenomena, since it uses a single mathematical expression for

the description of various adsorption systems. Here we use such a general expression as a component of the simulation model described for the package dyeing process.

2.3.4 Standard affinity of a dye

Dyeing equilibrium is usually discussed in terms of the chemical potential. The chemical potential is defined as the change in free energy of a system that occurs when the composition of a phase changes by a unit molar amount of substance, all other variables such as the temperature, pressure and the amounts of other components remaining constant. The chemical potential of a system is a property related to certain parameters such as temperature or voltage. These determine the direction and rate of heat transfer, or the direction and size of charge transfer (current), respectively.[2]

A transformation, at constant temperature and pressure, occurs so that the substance transfers from the state of higher to lower chemical potential until equilibrium is attained. In the case of dyeing, if the chemical potential of the dye in solution is higher than that in the fibre, the dye will transfer to the fibre. As the chemical potential in the solution falls, that in the fibre increases. At equilibrium, the chemical potential of the dye in the fibre is equal to the chemical potential of the dye in the solution,[1] leading to the relationships shown in Eq. 2.8:

$$\begin{aligned} \mu_s &= \mu_s^0 + RT\ln(a_s) \\ \mu_f &= \mu_f^0 + RT\ln(a_f) \end{aligned} \qquad [2.8]$$

In these equations, μ_s and μ_f are the chemical potentials of the dye in the solution and in the fibre, respectively, and a_s and a_f are the respective activities or effective concentrations. μ_s^0 and μ_f^0 are the standard chemical potentials for the dye in its standard state in the solution and in the fibre, respectively. The standard states are those for which the dye activity in either phase is unity. R is the universal gas constant and T represents the absolute temperature. At equilibrium, $\mu_s = \mu_f$, and thus Eqs 2.9a and 2.9b can be derived:

$$\mu_f - \mu_s = 0 = \mu_f^0 - \mu_s^0 + \mathrm{RT}\ln\left(\frac{a_f}{a_s}\right) \qquad [2.9a]$$

therefore:

$$-\Delta\mu^0 = \mu_f^0 - \mu_s^0 = -\mathrm{RT}\ln\left(\frac{a_f}{a_s}\right) \qquad [2.9b]$$

The standard affinity of a dye for a fibre ($-\Delta\mu^0$) is defined as the difference of the standard chemical potentials of the dye in the two phases, as shown in Eq. 2.10a:[3]

$$-\Delta\mu^0 = -(\mu_f^0 - \mu_s^0) = RT\ln\left(\frac{a_f}{a_s}\right) = RT\ln(K) \qquad [2.10a]$$

where K is the equilibrium constant for dyeing.

The standard affinity is a measure of the tendency of the dye to move from its standard state in solution to its standard state in the fibre, both at unit activity. For dyeing to have a large equilibrium constant, the standard chemical potential in the solution must be larger than that in the fibre, and the value of the standard affinity ($-\Delta\mu^0$) is thus positive when $K > 1$.[1]

The problem in determining affinities in dyeing is to find suitable expressions for the activities, or effective concentrations, of the dye in the fibre (a_f) and in solution (a_s). This is difficult, and usually molar concentrations must be substituted. For example, in dyeing a synthetic fibre with a pure non-ionic disperse dye at equilibrium, Eq. 2.10b may be employed:

$$-\Delta\mu^0 = RT\ln\left(\frac{C_f}{C_s}\right) \qquad [2.10b]$$

The equilibrium constant for dyeing with a dye of given affinity is given by $K = C_f/C_s$ and depends only on the temperature. This is exactly the situation described by the Nernst isotherm, from which the affinity can be calculated directly with the assumption that the term C_f/C_s is a correct approximation to satisfy the activity quotient a_f/a_s.[57]

The equation for the standard affinity shows that the dyeing equilibrium constant decreases with increasing temperature if ($-\Delta\mu^0$) is positive. In other words, more dye adsorbs at lower temperatures, although reaching equilibrium at lower temperatures takes longer. It can be assumed that, over a small temperature range, the standard affinity is independent of the temperature, although temperature variations must be considered in more precise studies.[1]

The activity of the dye in the fibre cannot be directly determined, and there is no choice but to substitute activity with the concentrations of dye derived from isotherms. For different types of dyes, different standard states are usually involved, so that affinities of a dye for different types of fibres often cannot be compared directly. Although this thermodynamic approach is academically satisfying, it is based on some questionable assumptions.[31]

As an example, the two-phase sorption model used to describe the process assumes that a sorption system of anionic dyes on cellulose has two phases, the internal cellulose fibre (F) phase and the external aqueous solution (S) phase, and that any adsorbed ion on the fibre surface is considered to be dissolved in the internal phase.[3] Figure 2.3 shows the distribution of ions at equilibrium in the two-phase sorption system containing an anionic dye (Na_ZD) and sodium chloride ($NaCl$).[58–59] The chemical potential (μ) of Na_ZD can be expressed in terms of its

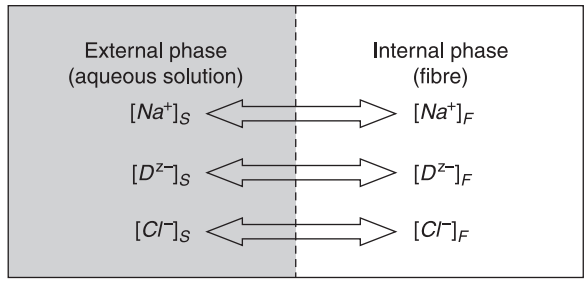

2.3 Distribution of ions in the two-phase equilibrium sorption system.

activity (α), as shown in Eq. 2.8.

Since a difference exists between the chemical potentials of the dye on fibre (μ_F) and in aqueous solution (μ_S), the dye anions tend to move from aqueous solution onto fibre until the chemical potentials of Na_ZD are the same on each side of the fibre boundary (vertical line in Fig. 2.2), where a sorption equilibrium is reached, as expressed in Eq. 2.9.

The change in chemical potential of dye at the standard state from the aqueous solution to the fibre is known as the standard affinity of dye sorption ($-\Delta\mu^0$), as shown in Eq. (2.9b).

Although it is possible to calculate the dye activity in aqueous solution using the Debye–Hückel equation, its accuracy assumes application to small spherical ions in solutions of low total ionic strength.[60] Extending the system to account for the radii of the dye ions may not be strictly accurate or applicable due to the structure of dye molecules. In addition, many dyebaths would not be considered to be of low ionic strength. Despite this, the most challenging issue is that no direct method has been reported to enable calculation of dye activity in fibre.

In Eq. 2.9b $-\Delta\mu^\circ$ is a measure of the tendency of the dye to move from aqueous solution to fibre when it is in its standard state in each phase. Therefore, it can be regarded as the driving force in the kinetics of the sorption process. Since the dye activities in Eq. 2.9b involve the freely moving sodium ions as well as dye anions, the concentration of *NaCl* can influence the sorption equilibrium. $-\Delta\mu^\circ$ can be determined experimentally providing concentrations of sodium ions in the fibre $[Na^+]_F$ and in the aqueous solution $[Na^+]_S$ are known.

Since Na_ZD and *NaCl* are strong electrolytes and completely dissociate in aqueous solution, dye activity is generally approximated using Eq. 2.11:

$$\alpha_S = [D^{z-}]_S [Na^+]_S^z \qquad [2.11]$$

where $[D^{z-}]_S$ and $[Na^+]_S$ are the concentrations of dye and sodium ions in solution, and z is the ionic charge of the dye.

Providing the volume of aqueous solution is significantly in excess of the

internal accessible volume of fibre, $[Na^+]_S$ can be considered to be equivalent to the sum of all counter ions in aqueous solution, including the dye and chloride ions, as shown in Eq. 2.12:

$$[Na^+]_S = z[D^{z-}]_S + [Cl^-]_S \quad [2.12]$$

The determination of α_F, unlike α_S, is complex. Commonly, the concentration of dye on fibre $[D^{z-}]_F$ at equilibrium, conveniently expressed in moles per kilogram of dry fibre, is approximated based on either the depletion of dye in the aqueous solution or extraction from the fibre. In Eq. 2.9b all concentration terms are expressed in moles per litre, and as such the factor V is given in litres per kilogram to convert $[D^{z-}]_F$ and $[Na^+]_F$ to a volume base. Dye activity in fibre is thus approximated using Eq. 2.13:

$$\alpha_F = \frac{[D^{z-}]_F [Na^+]_F^z}{V^{z+1}} \quad [2.13]$$

where the factor V is the internal accessible volume of fibre, representing the sum of internal pores or the void space within the fibre. The factor V is commonly used to compare and contrast different fibre structures.[18–24]

The solution of Eq. 2.13 requires the determination of the factor V and $[Na^+]_F$, which cannot be measured directly. Generally $[Na^+]_F$ is determined using the electrical neutrality condition in fibre (Eq. 2.14) and applying the Donnan equilibrium between fibre and aqueous solution (Eq. 2.15, as expressed in Eq. 2.16).

$$[Na^+]_F = z[D^{z-}]_F + [Cl^-]_F \quad [2.14]$$

$$\frac{[Na^+]_F [Cl^-]_F}{V^2} = [Na^+]_S [Cl^-]_S \quad [2.15]$$

$$[Na^+]_F = 0.5\left\{z[D^{z-}]_F + (z^2[D^{z-}]_F^2 + 4V^2[Na^+]_s[Cl^-]_S)^{0.5}\right\} \quad [2.16]$$

In order to determine V, Eq. 2.9b is usually expanded in a logarithmic form, shown in Eq. 2.17. By adjusting V, a linear relationship between $\ln(\alpha_F)$ and $\ln(\alpha_S)$ can be obtained. However, care should be exercised to ensure not only that the best-fit straight line has a unit slope but also that $-\Delta\mu°$, obtained from Eq. 2.18, remains constant for all data points. The best fits are routinely obtained by trial and error and assigning an arbitrary value to the factor V, and often involve complex mathematical calculations; in addition, the log-log plot of sorption data is not very sensitive to changes in V.

$$\ln\alpha_F = \ln\alpha_S + \frac{-\Delta\mu°}{RT} \quad [2.17]$$

$$-\Delta\mu\infty = \mathrm{RT}\ln\left(\frac{[D^{z-}]_F [Na^+]_F^z}{V^{z+1}[D^{z-}]_S [Na^+]_S^z}\right) \quad [2.18]$$

In order to simplify the determination of V and $-\Delta\mu^\circ$, a model can be developed by rearranging Eq. 2.18 into Eq. 2.19 and substituting Eq. 2.16 into Eq. 2.19 to obtain Eq. 2.20.

$$[D^{z-}]_S = \frac{[Na^+]_F^z}{[Na^+]_S^z V^{z+1} e^{\left(\frac{-\Delta\mu^\circ}{RT}\right)}}[D^{z-}]_F \qquad [2.19]$$

$$[D^{z-}]_S = \frac{[D^{z-}]_F \left\{z[D^{z-}]_F + (z^2[D^{z-}]_F^2 + 4V^2[Na^+]_S[Cl^-]_S)^{0.5}\right\}^z}{2^z[Na^+]_S^z V^{z+1} e^{\left(\frac{-\Delta\mu^\circ}{RT}\right)}} \qquad [2.20]$$

Equation 2.20 can be used to describe equilibrium sorption of anionic dyes on cellulose in the presence of an infinite concentration of electrolyte, approximated by employing a relatively high concentration of sodium chloride in a dyebath, which is common in practice. In Eq. 2.20, $[D^{z-}]_S$ is only a function of $[D^{z-}]_F$ because z and $[Cl^-]_S$ are known, $[Na^+]_S$ can be calculated from Eq. 2.12, and V and $-\Delta\mu^\circ$ are constant. In this non-linear model, V and $-\Delta\mu^\circ$ are two model parameters which can be estimated by fitting the model to sorption data.

An important aspect of equilibrium sorption of dyes on fibres is to investigate the thermodynamics of dyeing. The $-\Delta\mu^\circ$ values are usually used to calculate the standard enthalpy change (ΔH°) and the standard entropy change (ΔS°) from the linear thermodynamic relationship given in Eq. 2.21. A linear plot of $-\Delta\mu^\circ/T$ versus $1/T$ can thus be used to validate the performance of such a non-linear model.

$$\frac{-\Delta\mu^\circ}{T} = \frac{-\Delta H^\circ}{T} + \Delta S^\circ \qquad [2.21]$$

2.4 Diffusion of the dye into the interior of the fibre

2.4.1 Diffusion phenomena

In spite of the influence which liquor agitation has on the rate of dyeing, earlier workers have accumulated a considerable body of information concerning the kinetics of dyeing in which the effects of agitation have been ignored. Workers were motivated by the desire to obtain data in a concise form on the relative dyeing properties of ranges of dyes, in order to enable the practical dyer to determine the quantities of dyes which are adsorbed at equilibrium and the relative rates at which the dyes are taken up. In particular, it was considered that if, the dyer wished to dye two or more dyes in admixture, he could obtain compatible mixtures by choosing dyes with the same rate of dyeing characteristics. In earlier works, it was thought adequate to assume that, since the diffusion coefficients of the dyes in the fibres were several thousand times less than those in the liquor, the rates of dyeing could be considered to be governed by diffusion in the fibre.[57]

Diffusion is the process by which matter is transported from one part of a system to another as a result of random molecular motion. The mechanical process of diffusion involves movement of the molecules of concern through voids and interstitial spaces between molecules in the medium through which they are moving. The movement of molecules occurs along a concentration gradient, i.e. from areas of high concentration to a low concentration. This eventually leads to an equalisation of chemical potential and concentration throughout the system.[2] The more complex and larger the molecules undergoing diffusion, the longer the process takes until there is an equal concentration in both environments.

Where there is more than one phase, the chemical potential of the diffusant is constant throughout the system only when true dynamic equilibrium has been achieved, even though the concentrations in each phase may differ considerably. In dyeing processes one phase consists initially of the fibre or filament and the other is usually a dye solution in which the undyed fibre is immersed. Although apparently a simple transfer process of dye passing from solution to the interior of the fibre, the mechanism of dyeing in its entirety is more complex.

It is necessary to study diffusion in terms of simple models before any advances can be made in dealing with real or experimental investigations of actual dyeing processes. In view of the complexity of the diffusion process, real dyeing systems are studied on the basis of simpler idealised situations, but these simpler models have considerable restrictions or conditions imposed on them to make them amenable to mathematical treatment.

Two models are generally used to describe the diffusion of dyes into fibres. The first is the pore model, in which the movement of dissolved dyes is described as diffusion into the pores of fibres that are filled with water. In this model, the diffusion coefficients strongly depend on the number and size of pores in the fibre at fixed dyeing conditions. The assumption for the applicability of this model is that the pores of the substrate are large in comparison to the molecular dimensions of the dye molecules, and that the pore network is accessible to the dyes.[2]

The second model is called the free volume model, where dye diffusion takes place in the void volume in the non-crystalline regions of the fibres. This void volume is formed by the segmental motion of polymer chains, a process that commences at the glass transition temperature of the fibre. The shift in the free volume in the non-crystalline regions promotes the diffusion of molecules that are sufficiently small.[1]

The pore model is mainly adopted for the diffusion of dyes into hydrophilic fibres from an aqueous solution in which fibres swell markedly. Therefore it is presumed that water-filled channels of the fibres provide a transfer route for dye molecules to reach their adsorption sites.[61] However, Peters and Ingamells[62] concluded that the pore model in its entirety cannot be accepted. The free volume mechanism mainly dominates when hydrophobic fibres are dyed.

Hori and Zollinger[63] summarised discussions on the two models in relation to dyeing wool and cellulosic fibres. The dyeing of cellulosics is considered to be

best understood in terms of the porous matrix model, while the behaviour of wool and silk most nearly approximates the free volume model. Rohner,[64] however, pointed out that there was insufficient evidence for the validation of either the pore or the free volume model, and in general these models represent an oversimplified version of the real situation.

Diffusion has been studied most extensively with relatively simple dyes such as anionic sulphonated azo dyes from the levelling acid and direct classes. Also a considerable amount of work has been carried out with reactive dyes, despite the fact that they eventually become immobilised by chemical reactions with the fibre. Other types of reactions, particularly those involving large increases in the relative molecular mass of dyes, make studies of diffusion behaviour even more complicated. As a consequence, little work has been carried out with chrome, vat, sulphur and azoic dyes.[38]

2.4.2 Fick's laws of diffusion

In theoretical treatments of diffusion, it is usual to characterise the migration of dyes in terms of a diffusion coefficient D (m^2/s). Diffusion coefficients are most usually determined by the application of Fick's laws. Direct measurement of diffusion coefficients can be carried out by measuring the rate of disappearance of dye from solution or by direct observation of dye migration within various substrates. Diffusion coefficients that have been measured by indirect methods (such as changes in dyebath concentration with time) are sometimes referred to as 'apparent' diffusion coefficients. Such diffusion coefficients may not necessarily indicate the rates at which primary diffusion processes occur at the molecular level inside fibres.

The theory and application of Fick's laws have been widely discussed in the literature and in a considerable number of standard texts.[1–3,31,65] Fick's first law asserts that, under steady-state conditions, the quantity dS of a substance that diffuses through unit area of a plane located at x in a time interval dt is proportional to the concentration gradient (dc/dx) and the diffusion coefficient D, as shown in Eq. 2.22:

$$\frac{dS}{dt} = -D\frac{dC}{dx} \qquad [2.22]$$

Fick's second law expresses the rate of change of the concentration of dye at a point x with time, as shown in Eq. 2.23:

$$\frac{dC}{dt} = D\frac{d^2C}{dx^2} \qquad [2.23]$$

Fick's equations can be integrated by various methods to enable diffusion coefficients to be evaluated from experimental data. Complete solutions to Fick's equations present considerable computational problems because of the number of

variables involved. It is usual to simplify the calculations by making a number of assumptions.

Although fibres can have a range of shapes and cross-sections, they are usually considered to be circular in cross-section and infinitely long to simplify calculations. Other common assumptions are as follows:

- The diffusion coefficient varies only with temperature.
- There is an instantaneous equilibrium between the dye in solution and in the fibre.
- The uptake of dye is controlled only by diffusion.
- The absorption isotherm of the dye has a linear shape.[66]

Despite the obvious departures from the ideal behaviour in natural fibres, it has been common in theoretical treatments of diffusion behaviour to use the same simplifying assumptions that have been employed with synthetic fibres. While the results provide qualitative estimates of diffusion coefficients, some caution must be exercised in detailed interpretation of their meaning. Etters[66] pointed out that a lack of appreciation of the prerequisites for mathematical applicability of diffusion equations derived from Fick's laws probably has led to the publication of diffusion coefficients that are less than precise. However, it is likely that the values are useful for characterising the relative diffusion properties of dyes.

2.4.3 Factors influencing the diffusion

It has been observed, with many types of fibres, that the most even dyeings are usually obtained with dyes that diffuse most rapidly inside the fibres.[31,67] On the other hand, rapidly diffusing dyes generally have wet-fastness properties that are poorer than those which diffuse more slowly. Compromises between evenness and wet fastness must thus be struck for many practical purposes.

Diffusion rate is a characteristic property of a dye, independent of fibre structure, rate of liquor flow and dyebath volume, and largely independent of dye and electrolyte concentration. Since diffusion of dye in the fibre plays a very important role in the successful completion of the dyeing operation, where thorough penetration of the filaments is attained and where migration of colour, involving diffusion of dye in and out of filaments, is such a key consideration, the diffusion rates of individual dyes may be used as a guide to their dyeing behaviour.[5] Dyes that diffuse rapidly will, in general, show good levelling and penetrating properties and will be easy to apply, while slowly diffusing dyes will show the reverse characteristics.

Basic information from the measurement of diffusion has provided useful insights into the mechanisms of dyeing and the properties of dyed material. However, because of the complicated structures of fibres, especially in natural fibres, detailed theoretical treatments to describe the uptake of dyes have been difficult to develop. Dye diffusion has been observed and described in

phenomenological terms, but is not yet completely understood at the molecular level. The best fit between theory and experiment has been obtained with viscose rayon, as a natural polymer that most closely resembles synthetic polymers.[38] New methods are being developed for the direct determination of diffusion pathways, particularly in keratin fibres, that have the potential to provide further explicit information on how colorants actually enter natural fibres and where they are finally located within the fibres.

Present research assumes that there is an instantaneous equilibrium between the dyes in solution and in the fibre. For a level dyeing, the uniformity of dye distribution throughout the fibrous assembly during the dyeing is, therefore, the main concern.

2.5 Rate of dyeing

Although the rate of diffusion of a dye inside a fibre is of great interest, the overall rate of dyeing under conditions similar to those used in practice is often considered to assume equal or even greater importance to the dyer.[3] The rate of dyeing can be described as the measured rate at which dye leaves the dyebath, which is the main factor determining the magnitude of the inequalities in dye distribution throughout the fibre mass which are always present in the initial stages of dyeing. In order to gain an idea of the dyeing rate to be expected in practice, many attempts have been made to follow the adsorption of dye under conditions similar to those used in practice.

The general principles of such measurements are well established. A dyeing process is carried out under suitable conditions and the amount of dye on the fibre or remaining in solution is estimated at intervals or continuously by colorimetric methods. The results are commonly expressed in terms of the percentage exhaustion of the bath (E%), which is the percentage of the ratio of the dye adsorbed on the fibre at a given time (C_f) to that originally present in the bath (C_0). In practice the temperature of dyeing often varies with time, but for rate measurements it is generally kept constant to obtain a time/adsorption isotherm.

Observations show that, if dyeing rates measured under practical conditions are compared with the rates of diffusion of the same dyes inside the fibre, very little correlation would be apparent. The relationship between affinity, rate of diffusion and rate of dyeing was investigated by Vickerstaff.[3] He concluded that, in the calculation of the rate of dyeing, if the affinity between dye and fibre is high, the dyeing rate should depend on the affinity and the efficiency of liquor circulation, or on the aqueous diffusion coefficient in a stagnant bath. If the affinity is low, however, the dyeing rate should be related to the rate of diffusion of dye inside the fibre.

The dyeing rate is significantly affected by the temperature of the dyebath, increasing in all cases with an increase in temperature.[3,5] The effect of temperature on dyeing rate may be expressed in a quantitative manner by determining the

activation energy of the process. For this purpose it is preferable to consider the rate of diffusion in the fibre rather than the overall dyeing rate, since the diffusion of the dye through a fibre has a greater temperature coefficient than the diffusion through the aqueous phase. The number of molecules able to diffuse into the fibrous assembly at any moment is proportional to the concentration of solute and to an exponential term $e^{-E/RT}$, where E is the amount by which the energy of an activated molecule exceeds the average energy of the solute molecule.

Leaving the temperature factor aside, the rate of dyeing is governed by a number of other parameters including, when appropriate, mechanical factors such as the structure of the material: whether it is loose fibre, yarn or cloth; the dyebath volume or liquor to goods ratio; the rate of agitation or circulation; the affinity of the dye to the fibre, together with the dye concentration; pH; and electrolyte content of the dyebath. Naturally, in any investigation of the relative properties of a series of dyes, measurements will be made under carefully standardised conditions, but it cannot be assumed that variations in any one of these factors will affect each dye in the series to the same extent. This is particularly the case with variations in pH and concentration factors.[68]

It is well accepted that the rate of dyeing in practice is markedly dependent on the efficiency with which the dyebath is circulated through the material being dyed.[2] The influence of agitation in increasing the rate of uptake is, however, dependent in a large measure on the hydrodynamic complexity of the system, which was discussed in the first section of this chapter.

The rate of dyeing, as distinct from the diffusion coefficient, is proportional to the surface area of the fibres presented to the dyebath. The surface area of a filament is proportional to the square root of the fibre denier, $d^{1/2}$. The rates of dyeing are also dependent on the physical structure of the fibres, e.g. orientation and crystallinity, and hence such a relationship only applies to fibres which are almost identical in these respects.

In practice, dyeing is carried out in different machines in which the ratio of the volume of dye liquor to mass of the substrate, i.e. liquor to goods ratio, may vary widely from about 1:1 to 40:1. Generally, when the liquor ratio is reduced, the dyeing rate is increased.[5]

The charge on a fibre can also influence the rate at which dyes are taken up at the fibre surface. For example, wool and silk fibres assume a positive charge at low pH, and this greatly facilitates uptake of negatively charged dyes at the fibre surface. On the other hand, cotton rapidly assumes a negative charge in water, so, when dyed with anionic dyes, there is a further barrier to dye absorption.[1] The repulsive effects generated are reduced by the addition of neutral electrolyte in the dyebath.

Several workers have examined the influence of dyeing conditions, such as flow rate, concentration of dye in the dye bath, and temperature, on dyeing rate and attempted to express the process quantitatively.[56,69–71] The basic assumptions used in such works include the following:

- The dye-liquor is well stirred so that the concentration of dye throughout the liquor is taken to be uniform.
- Density and flow velocity inside the fibrous assemblies are assumed to be uniform and independent of time.
- The transport of dye across the medium is according to a dispersed flow.

Some of the proposed models deal with the physical chemistry of dye convection, diffusion and adsorption in dyeing. These models define the relationship between the dyeing parameters and the resulting quality of dyed material, and are discussed in detail in Chapter 3.

2.6 References

1. Broadbent A. (2002), *Basic Principles of Textile Coloration*, SDC, Bradford.
2. Johnson A. (1989), *Theory of Coloration of Textiles*, SDC, Bradford.
3. Vickerstaff T. (1954) 'Cellulose-dyeing Equilibria with Direct Dyes' *The Physical Chemistry of Dyeing*, 2nd edn, Oliver and Boyd, London, pp. 191–256.
4. Lewis D. (1992), *Wool Dyeing*, SDC, Bradford.
5. Crank J., Park G. (1968), *Diffusion in Polymers*, Academic Press.
6. Crank J. (1964), 'The Permeability of Cross-Wound Cotton Yarn Packages' *Journal of the Textile Institute*, **55**, T228.
7. Fretland W. (1997), 'Controlling Fiber and Flow in Yarn Dyeing' *American Dyestuff Reporter*, **86**, 9, 42–6.
8. Boulton J., Crank J. (1952), 'Package Dyeing I – A Theoretical Model and its Relation to Technical Practice' *Journal of the Society of Dyers and Colourists*, **68**, 109–16.
9. Armfield W., Boulton J., Crank J. (1956), 'II – The Effect of Liquor Ratio on Direct Dyeing' *Journal of the Society of Dyers and Colourists*, **72**, 278–86.
10. Etters J.N. (1981), 'The Diffusional Boundary Layer: Some Implications for the Dyeing Technologist' *Journal of the Society of Dyers and Colourists*, **97**, 170–9.
11. Etters J.N. (1991), 'The Influence of the Diffusional Boundary Layer on Dye Sorption from Finite Baths' *Journal of the Society of Dyers and Colourists*, **107**, 114–16.
12. McGregor R., Peters R.H. (1965), 'The Effect of Rate of Flow on Rate of Dyeing I – The Diffusional Boundary Layer in Dyeing' *Journal of the Society of Dyers and Colourists*, **81**, 393–400.
13. Etters J.N. (1995), 'Kinetics of Dye Sorption: Effect of Dyebath Flow on Dyeing Uniformity' *American Dyestuff Reporter*, January **84**, 1, 38.
14. Schmickler W. (1996), 'Electronic Effects in the Electric Double Layer' *Chemical Reviews*, **96**, 8, 3177–200.
15. Rattee I.D. (1974), 'The Role of Water in Dyeing' *Journal of the Society of Dyers and Colourists*, **90**, 10, 367–72.
16. Sumner H.H. (1989), 'Thermodynamics of Dye Sorption' in: Johnson A., editor, *The Theory of Coloration of Textiles*, 2nd edn, Society of Dyers and Colourists, Bradford, pp. 255–372.
17. Willis H.F., Warwicker J.O., Standing H.A., Urquhart A.R. (1945), 'The Dyeing of Cellulose with Direct Dyes, Part II: The Absorption of Chrysophenine by Cellulose Sheet' *Transactions of the Faraday Society*, **41**, 506–41.

18. Marshall W.J., Peters R.H. (1947), 'The Heats of Reaction and Affinities of Direct Dyes for Cuprammonium Rayon, Viscose Rayon and Cotton' *Journal of the Society of Dyers and Colourists* **63**, 12, 446–61.
19. Peters R.H., Vickerstaff T. (1948), 'The Adsorption of Direct Dyes on Cellulose' *Proceedings of the Royal Society (London)* A192, 292–308.
20. Standing H.A. (1954), 'The Direct Dyeing of Cellulose: a Method for the Analysis of Equilibrium Absorption Data in terms of Current Quantitative Theories' *Journal of the Textile Institute*, **45**, 1, T21–9.
21. Holmes F.H. (1958), 'The Absorption of Chrysophenine G by Cotton: A Test of Quantitative Theories of Direct Dyeing' *Transactions of the Faraday Society*, **54**, 1172–8.
22. Carrillo F., Lis M.J., Valldeperas J. (2002), 'Sorption Isotherms and Behaviour of Direct Dyes on Lyocell Fibres' *Dyes and Pigments*, **53**, 2, 129–36.
23. Ibbett R.N., Phillips D.A.S., Kaenthong S. (2006), 'Evaluation of a Dye Isotherm Method for Characterisation of the Wet-state Structure and Properties of Lyocell Fibre' *Dyes and Pigments*, **71**, 3, 168–77.
24. Ibbett R.N., Phillips D.A.S., Kaenthong S. (2007), 'A Dye-adsorption and Water NMR-relaxation Study of the Effect of Resin Cross-linking on the Porosity Characteristics of Lyocell Solvent-spun Cellulosic Fibre' *Dyes and Pigments*, **75**, 3, 624–32.
25. Denton M.J. (1962), 'The Wetting-Out of Yarn Packages' *J. Text Institute*, **53**, T477–T488.
26. Hadfield H., Lemin D. (1961), 'Foam, Flow, and Level Dyeing' *Journal of the Society of Dyers and Colourists*, **77**, 198–205.
27. Whittaker J. (1961), 'Practical Problems in Preparation and Dyeing of Cross-wound Packages' *Journal of the Society of Dyers and Colourists*, **77**, 690–9.
28. Fox M.R. (1962), 'Practical Aspects of Vat Dyeing of Cotton Yarn Packages' *Journal of the Society of Dyers and Colourists*, **78**, 393–404.
29. McGregor R. (1965), 'The Effect of Rate of Flow on Rate of Dyeing II – The Mechanism of Fluid Flow through Textiles and its Significance in Dyeing' *Journal of the Society of Dyers and Colourists*, 81, 429–38.
30. Trotman E. (1975), *Dyeing and Chemical Technology of Textile Fibres*, 5th edn, Charles Griffin Co. Ltd.
31. Bird C.L. (1972), *The Theory and Practice of Wool Dyeing*, SDC, Bradford.
32. Bird C.L., Partovi H.K., Tabbron G. (1959), 'The Dyeing of Cellulose Acetate with Disperse Dyes VIII – Determination of Fibre Saturation Values' *Journal of the Society of Dyers and Colourists*, **75**, 600–4.
33. Aspland J.R. (1993), 'The Application of Ionic Dyes to Ionic Fibers: Nylon, Silk and Wool and Their Sorption of Anions' *Textile Chemist and Colorist*, **25**, 3, 55–9.
34. Giles C.H. (1973), 'The History and Use of the Freundlich Adsorption Isotherm' *Journal of the Society of Dyers and Colourists*, **89**, 287–91.
35. Schuler M.J. (1982), 'The Physical Chemistry of Dyeing: Enigma and Understanding' *Textile Chemist and Colorist*, **14**, 13–21.
36. Etters J.N. (1994), 'Sorption of Disperse Dye by Polyester Fibers: Boundary Layer Transitional Kinetics' *Textile Research Journal*, **64**, 406–13.
37. White H.J. Jr (1960), 'Some Theoretical Considerations of the Dyeing of Cellulose Acetate with Disperse Dyes' *Textile Research Journal*, **30**, 5, 329–38.
38. Brady P.R. (1992), 'Diffusion of dyes in natural fibres' *Rev. Prog. Coloration*, **22**, 58.
39. Aspland J.R. (1992), 'A series on dyeing. Chapter 3/Part 1. Vat dyes and their application' *Textile Chemist and Colorist*, **1**, 22–4.

40. Sivaraja Iyer S.R., Srinivasan D. (1984), 'The Influence of Temperature on the Thermodynamics of Acid Dye Adsorption on Wool Fibres' *Journal of the Society of Dyers and Colourists*, **100**, 63–6.
41. Mitsuishi M., Yaqi T., Jian X., Hamada K., Ishiwatari T. (1992), 'Silk Dyeing in Acid Dyes: Results of Equilibrium and Kinetic Studies for the Mixture Dyeing of Silk with Acid Dyes' *Textile Asia* **23**, 4, 92–5.
42. Sevim A.M., Hojiyev R., Gül A., Çelik M.S. (2011), 'An Investigation of the Kinetics and Thermodynamics of the Adsorption of a Cationic Cobalt Porphyrazine onto Sepiolite' *Dyes and Pigments*, **88**, 1, 25–38.
43. D'Ilario L., Francolini I., Martinelli A., Piozzi A. (2009), 'Insight into the Heparin-Toluidine Blue (C.I. Basic Blue 17) Interaction' *Dyes and Pigments*, **80**, 3, 343–8.
44. Auxilio A.R., Andrews P.C., Junk P.C., Spiccia L. (2009), 'The Adsorption Behavior of CI Acid Blue 9 onto Calcined Mg-Al Layered Double Hydroxides' *Dyes and Pigments*, 81, **2**, 103–12.
45. Yue Y., Chen X., Qin J., Yao X. (2009), 'Characterization of Interaction between C.I. Acid Green 1 and Human Serum Albumin: Spectroscopic and Molecular Modeling Method' *Dyes and Pigments*, **83**, 2, 148–54.
46. Ding F., Huang J., Lin J., Li Z., Liu F., Jiang Z., Sun Y. (2009), 'A Study of the Binding of C.I. Mordant Red 3 with Bovine Serum Albumin Using Fluorescence Spectroscopy' *Dyes and Pigments*, **82**, 1, 65–70.
47. Bird J., Brough N., Dixon S., Batchelor S.N. (2006), 'Understanding Adsorption Phenomena: Investigation of the Dye-Cellulose Interaction' *Journal of Physical Chemistry B*, **110**, 39, 19557–61.
48. Ding F., Li N., Han B., Liu F., Zhang L., Sun Y. (2009), 'The Binding of C.I. Acid Red 2 to Human Serum Albumin: Determination of Binding Mechanism and Binding Site Using Fluorescence Spectroscopy' *Dyes and Pigments*, **83**, 2, 249–57.
49. Yamaki S.B., Barros D.S., Garcia C.M., Socoloski P., Oliveira O.N., Atvars T.D.Z. (2005), 'Spectroscopic Studies of the Intermolecular Interactions of Congo Red and Tinopal CBS with Modified Cellulose Fibers' *Langmuir*, **21**, 12, 5414–20.
50. De Clerck K., Rahier H., Van Mele B., Westbroek P., Kiekens P. (2007), 'Dye–Fiber Interactions in PET Fibers: Hydrogen Bonding Studied by IR-Spectroscopy' *Journal of Applied Polymer Science*, **106**, 3, 1648–58.
51. An W., Jiao Y., Dong C., Yang C., Inoue Y., Shuang S. (2009), 'Spectroscopic and Molecular Modeling of the Binding of Meso-tetrakis(4-hydroxyphenyl)porphyrin to Human Serum Albumin' *Dyes and Pigments*, **81**, 1, 1–9.
52. Nemethy G., Scheraga H.A. (1962), 'Structure of Water and Hydrophobic Bonding in Protein, Part III: the Thermodynamic Properties of Hydrophobic Bonds in Proteins' *Journal of Physical Chemistry*, **66**, 10, 1773–89.
53. Maruthamuthu M., Sobhana M. (1979), 'Hydrophobic Interactions in the Binding of Polyvinylpyrrolidone' *Journal of Polymer Science: Polymer Chemistry Edition*, **17**, 10, 3159–67.
54. Yang Y., Ladisch C.M. (1993), 'Hydrophobic Interaction and its Effect on Cationic Dyeing of Acrylic Fabric' *Textile Research Journal*, **63**, 5, 283–9.
55. Wai P.P.C. (1984), 'Dynamic Behaviour of a Reactive Packed Bed Adsorption System' PhD Thesis, Heriot-Watt University, UK.
56. Vosoughi M. (1993), 'Numerical Simulation of Packed Bed Adsorption Applied to a Package Dyeing Machine' PhD Thesis, Heriot-Watt University, UK.
57. Alberghina G., Longo M.L., Torreet M. (1983), 'Adsorption Thermodynamics and Diffusion of Disperse Anthraquinone Dyes in Acetate Fibre' *Dyes and Pigments* **4**, 49–58.

58. Xu C., Shamey R. 'Nonlinear Modeling of Equilibrium Sorption of Selected Anionic Adsorbates from Aqueous Solutions on Cellulosic Substrates: Part 1: Model Development' *Cellulose*, **19**, 3 (08/2013) 615–25.
59. Xu C., Shamey R., 'Nonlinear Modeling of Equilibrium Sorption of Selected Anionic Adsorbates from Aqueous Solutions on Cellulosic Substrates: Part 2: Experimental Validation' *Cellulose*, **19**, 3 (08/2013) 627–33.
60. Debye P., Hückel E. (1923), 'The Theory of Electrolytes. I. Lowering of Freezing Point and Related Phenomena' *Physikalische Zeitschrift*, **24**, 185–206.
61. Hori T., Kamon N., Kojima H., Rohner R.M. Zollinger H. (1987), 'Structure Correlation between Diffusion Coefficients of Simple Organic Compounds and of Anionic and Cationic Dyes in Water' *Journal of the Society of Dyers and Colourists*, **103**, 265–70.
62. Peters R.H., Ingamells W. (1973), 'Theoretical Aspects of the Role of Fibre Structure in Dyeing' *Journal of the Society of Dyers and Colourists*, **89**, 397–405.
63. Hori T., Zollinger H. (1986), 'Role of Water in the Dyeing Process' *Textile Chemist and Colorist*, **18**, 10, 19–25.
64. Rohner R.M., Zollinger H. (1986), 'Porosity versus Segment Mobility in Dye Diffusion Kinetics—A Differential Treatment: Dyeing of Acrylic Fibers' *Textile Research Journal*, **56**, 1–13.
65. McGregor R. (1974), *Diffusion and Sorption in Fibres and Films*, vol. 1, London Academic Press.
66. Etters J.N. (1980), 'Diffusion equation made easy' *Textile Chemist and Colorist*, **12**, 140–5.
67. Boulton J. (1938), 'A Classified List of Direct Dyes for Use with Viscose Rayon' *Journal of the Society of Dyers and Colourists*, **54**, 268–73.
68. Bird C. and Boston W. (1975), *The Theory and Practice of Wool Dyeing*, SDC, Bradford.
69. Ren J. (1985), 'A Thesis on the Development of a Mathematical Model of the Batch Dyeing Process and its Application to the Simulation and Computer Control of a Dyeing Machine' PhD Thesis, Dept. of Colour Chemistry, Leeds University.
70. Burley R., Wai P.C., McGuire G.R. (1985), 'Numerical Simulation of an Axial Flow Package Dyeing Machine' *Appl. Math. Modelling*, **9**, 1, 33–9.
71. Telegin F.Y. (1998), 'Convective Mass Transfer in Liquid Treatment Processes' *Journal of the Society of Dyers and Colourists*, **114**, 49–55.

3

Dye transport in fluid systems

DOI: 10.1533/9780857097583.54

Abstract: The theoretical background for the mechanistic description of flow phenomena in open channels and porous media is elucidated. Relevant works are described and the equations governing flow are explained. Fundamental concepts of dispersion, convection and diffusion are clarified and models that describe these processes are evaluated. The role of bulk and dispersive flow in dye transfer within a packed bed medium and the effect of including flow parameters on modelling dye dispersion and diffusion are then evaluated, and various models incorporating flow properties are examined.

Key words: laminar flow, dispersive flow, bulk flow, porous media, permeability, convective dispersion, diffusion, dispersion, Taylor dispersion, convection, momentum balance, Darcy's law, Navier–Stokes model, packed bed reactor, CDE, STM, MIM.

3.1 Introduction

As mentioned in Chapter 2, when textile materials are immersed in the dye solution, the rate at which the dye is taken up is dependent upon the extent to which the liquor is agitated, and tends to approach a maximum value when the stirring is vigorous. This phenomenon, unfortunately, cannot be described in any simple fashion within fibrous assemblies, because of the extreme complexity of defining the flow of liquor through the textile materials. The dyeing of fibres, yarns or cloth can be treated as mass transfer in a porous medium, defined by convective dispersion equation.[1]

The theories that have been employed to derive the macroscopic differential equations that describe solute transport through porous media may be grouped into different classes.[2] The most widely used theory for convection-dispersion of chemicals in porous media is that based on fluid mechanics.[3] In this section we introduce the relevant concepts on fluid mechanics, porous media, and mass transfer in both fluid systems and porous media. These concepts provide the theoretical fundamentals for the modelling of the dyeing process.

3.2 Fluid properties in perspective

3.2.1 The mechanical behaviour of a fluid

The mechanical behaviour and properties of a material may be defined in terms of shear stress (τ) (force per unit area, Pa) and the shear strain (γ) (dimensionless term, which is a relative displacement). These are related to the total force (F_x) on the plate and the displacement (U_x) of the plate, as shown in Fig. 3.1 and Eqs 3.1and 3.2[4]:

$$\tau = \frac{F_x}{A_y} \quad [3.1]$$

$$\gamma = \frac{U_x}{h_y} = \frac{dU_x}{dy} \quad [3.2]$$

The response of the material, in terms of the relationship between the shear stress and shear strain, defines the mechanical properties by which the material may be classified. If the material between the plates is a perfectly rigid solid, it will not move at all no matter how much force is applied (unless it breaks). Thus, Eq. 3.3 can be used to define this material:

$$\gamma = 0 \quad [3.3]$$

At the other extreme, if the molecules of the material are so far apart that they exert negligible influence on each other (e.g. a low-pressure gas), the plate can be moved by the application of a negligible force, and Eq. 3.4 can be used to describe this material:

$$\tau = 0 \quad [3.4]$$

This material is called an inviscid (Pascalian) fluid. However, if the molecules do exhibit significant attraction as they move past one another, such that the relative rate of movement (e.g. the velocity gradient) is proportional to the applied force (e.g. shear stress), the material is called a Newtonian fluid[4] and is described by Eq. 3.5.

$$\tau = \eta\dot{\gamma} \quad [3.5]$$

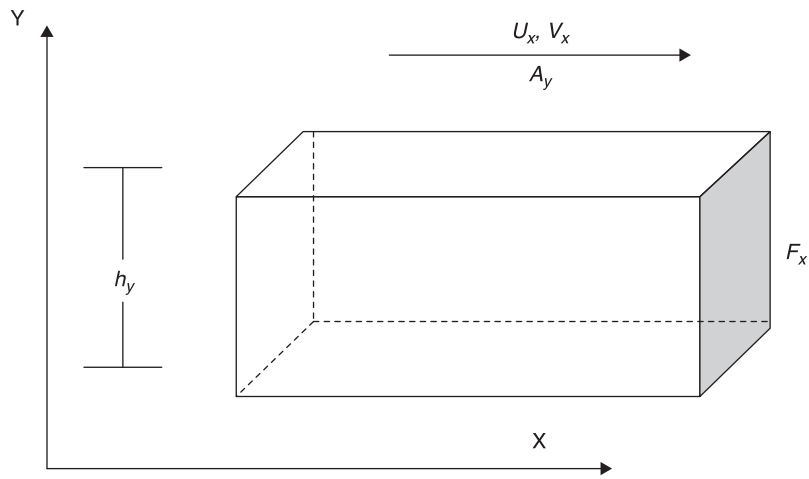

3.1 Simple shear between parallel plates.

where:

$$\dot{\gamma} = \frac{d\gamma}{dt} = \frac{dV_x}{dy} = \frac{V_x}{h_y} \qquad [3.6]$$

and η is the fluid viscosity, which has dimensions of Ft/L^2 with corresponding units of $kgm^{-1}s^{-1}$, or Pa s.

Most common fluids of simple structure are Newtonian, such as water, air, oil, etc.

3.2.2 Laminar flow

It is an empirical fact that a fluid flowing in a small tube or at low velocity does so by the mechanism of laminar flow, also called viscous, or streamline, flow. The layers of fluid slide over each other with no macroscopic mixing, and the velocity in macroscopic steady flow is constant at any point. At higher velocities flow becomes turbulent; there is mixing by eddy motion between the layers, and even in overall steady flow the velocity at a point fluctuates about some mean value.

If different sizes of circular pipe and different fluids are used, it is found that laminar flow generally exists when the dimensionless ratio ($du\rho/\mu$) is less than 2100, and turbulent flow occurs when the ratio is greater than about 4000, with a transition region in between.[5] This ratio is called the Reynolds number, *Re*:

$$Re = \frac{du\rho}{\mu} \qquad [3.7]$$

where d is the pipe diameter, u is the velocity of the flow, ρ is the density of the fluid and μ is the viscosity of the fluid.

The physical significance of the Reynolds number can be appreciated better if it is rearranged as:

$$Re = \frac{du\rho}{\mu} = \frac{\rho u^2}{\mu \frac{u}{d}} \qquad [3.8]$$

The numerator is the flux of 'inertial' momentum carried by the fluid along the tube in the axial direction. The denominator is proportional to the viscous shear stress in the tube, which is equivalent to the flux of 'viscous' momentum normal to the flow direction, i.e. in the radial direction. Thus, the Reynolds number is a ratio of the momentum flux due to inertia (in the flow direction) to the momentum flux due to viscous stresses (in the radial direction).

Since viscous forces are a manifestation of intermolecular attractive forces, they are stabilising, whereas inertial forces tend to pull the fluid elements apart and are destabilising. It is thus quite logical that stable (laminar) flow should occur at low Reynolds numbers where viscous forces dominate, whereas unstable (turbulent) flow occurs at high Reynolds numbers where inertial forces dominate.

Also, laminar flows are dominated by viscosity and are independent of the fluid density, whereas fully turbulent flows are dominated by the fluid density and are essentially independent of the fluid viscosity at high turbulence levels. For fluids flowing near solid boundaries (e.g. inside conduits) viscous forces dominate in the immediate vicinity of the boundary, whereas for turbulent flows (high Reynolds numbers) inertial forces dominate in the region far from the boundary.

Here we consider both the laminar and turbulent flow of Newtonian fluid in pipes (before the boundary of yarn assembly), and the laminar fluid in porous media.

3.2.3 Momentum balance

The conservation of momentum principle is a common approach to a system composed of an arbitrary (differential) cubical volume within any flow field. By accounting for convection of momentum throughout the surface, all possible stress components on any and all surfaces, and any other forces (e.g. gravity), a general microscopic form of momentum equation can be derived, as shown in Eq. 3.9, which is valid at all points within any fluid.

$$\rho\left(\frac{\partial u}{\partial t} + u \cdot \nabla u\right) = -\nabla p + \nabla \cdot \vec{\tau} + \rho g \qquad [3.9]$$

where ρ is the fluid density, u the velocity field, p the pressure, and g denotes gravity. When coupled with appropriate equations relating the shear stress components ($\vec{\tau}$) to the velocity components, the result is a set of differential equations which can be solved (in principle) with the appropriate boundary conditions for the velocity components as a function of time and space. In laminar flows, the shear stress components depend only on the velocity gradients through an appropriate rheological constitutive equation. For example, for Newtonian fluids, the constitutive equation, generalised from the one-dimensional form, is:

$$\vec{\tau} = \eta[(\nabla u) + (\nabla u)^T] \qquad [3.10]$$

where η is the viscosity of the fluid. When these are used to eliminate the stress components from the momentum equation, the result is called the Navier–Stokes equations.[4]

$$\rho\frac{\partial u}{\partial t} - \nabla \cdot \eta(\nabla u + (\nabla u)^T) + \rho(u \cdot \nabla)u + \nabla p = F \qquad [3.11]$$

These equations apply to the laminar flow of any Newtonian fluid in any system and are the starting point for the detailed solution of many fluid flow problems. However, the number of flow problems for which analytical solutions are possible is rather limited, so that numerical computer techniques are required for many problems of practical interest.

The Navier–Stokes equations are supposed to describe all types of Newtonian incompressible flow, including turbulent flow. However, modelling of turbulent flow with the Navier–Stokes equations is impractical in most engineering applications, since it requires that even the smallest eddies are resolved. To resolve these eddies, the number of nodes required becomes very large. In addition, the flow does not become stationary, since the eddies seem to move randomly within the flow. These types of time-dependent simulations are very demanding in terms of the number of operations and memory required, and they are too large to be handled by most computers. It is therefore necessary to use simplified models for the modelling of turbulent flow.

3.3 Flows in porous media

The dynamics of fluids in porous media have been the subject of numerous theoretical and experimental studies because of their importance for engineering and environmental applications. In package dyeing, the dye liquor or air must be distributed evenly within a package and also between one package and another. This means that the fluid must flow at the same rate throughout the porous spaces of the fibrous assembly. This section briefly discusses the main features of porous media, the permeability of porous media and fluid flow patterns in yarn packages.

3.3.1 Description of porous media

A porous medium can be defined as a solid, or collection of solid bodies, with sufficient open space in or around the solids to enable a fluid to pass through or around them.

There are various conceptual ways of describing a porous medium. One concept is a continuous solid with holes in it. Such a medium is referred to as consolidated, and the holes may be unconnected (impermeable) or connected (permeable). Another concept is a collection of solid particles in a packed bed, where the fluid can pass through the voids between the particles, which is referred to as unconsolidated. Both of these concepts have been used as the basis for developing the equations which describe fluid flow behaviour.[5]

One of the key properties of a porous medium is the porosity, ε, which is defined according to Eq. 3.12.

$$\varepsilon = \frac{Total\ vol. - Solids\ vol.}{Total\ volume} = 1 - \frac{A_{solid}}{A} = \frac{A_{voids}}{A} \qquad [3.12]$$

where A_{solid} is the area of the solid phase in a cross-section of area A. The porosity value ε macroscopically characterises the effective pore volume of the medium, as it is directly related to the size of the pores relative to the matrix.

The definition of velocities in porous media is important. The velocity of approach to the system is termed the superficial velocity (V_s) of the fluid, shown in Eq. 3.13:

$$V_s = \frac{Q}{A} \qquad [3.13]$$

and the actual velocity within the pores or voids (interstitial velocity V_i) is described by Eq. 3.14:

$$V_i = \frac{Q}{\varepsilon A} = \frac{V_s}{\varepsilon} \qquad [3.14]$$

where Q is flow rate (m^3/s).

Since the fluid in a porous medium follows a tortuous path through channels of varying size, one method of describing the flow behaviour in the pores is to consider the flow path as a 'non-circular conduit'. This requires an appropriate definition of the hydraulic diameter D_h, as shown in Eq. 3.15:

$$D_h = 4\frac{Flow\ volume}{Wetted\ surface\ area} = \frac{4 \times \varepsilon \times (Bed\ volume)}{(No.\ particles)(Surface\ area\ /\ Particle)} \qquad [3.15]$$

where:

$$No.\ particles = \frac{(Bed\ volume)(Fraction\ of\ solids\ in\ bed)}{Volume\ /\ Particle} = \frac{Bed\ volume(1-\varepsilon)}{Volume\ /\ Particle} \qquad [3.16]$$

Substitution of Eq. (3.16) into Eq. (3.15) leads to:

$$D_h = 4\left(\frac{\varepsilon}{1-\varepsilon}\right)\left(\frac{1}{a_s}\right) \qquad [3.17]$$

where a_s = (particle surface area)/(particle volume). If the particles are spherical, with diameter d, then $a_s = 6/d$. Thus for a medium composed of uniform spherical particles, the relationship can be shown as:

$$D_h = \frac{2d\varepsilon}{3(1-\varepsilon)} \qquad [3.18]$$

The hydraulic diameter and the superficial velocity can be introduced into the definition of the porous medium Reynolds number to give Eq. 3.19:

$$N_{\mathrm{Re}} = \frac{D_h V_i \rho}{\mu} = \frac{2d\varepsilon}{3(1-\varepsilon)}\frac{V_s}{\varepsilon}\rho = \frac{2dV_s\rho}{3(1-\varepsilon)\mu} \qquad [3.19]$$

Usually the numerical constant (2/3) is dropped and a porous medium Reynolds number is defined without this numerical factor:

$$N_{\mathrm{Re}PM} = \frac{dV_s\rho}{(1-\varepsilon)\mu} \qquad [3.20]$$

When $N_{\mathrm{Re}PM} < 10$, the flow can be considered as laminar flow.

In the field of textile finishing and cleaning processes, the fibrous assembly, in the form of yarn or fabric, can be treated as a kind of porous medium. Denton[6] studied the flow pattern of the flow in package dyeing by plotting flow rate against pressure drop for three packages of different densities for air flow and for dye liquor flow, and observed that these were substantially linear over the practical range. He concluded that the flow within the package is laminar. This conclusion is based on the momentum balance equation in porous media.

3.3.2 Momentum balance equation in porous media

The analysis given here is concerned with the movement of fluids through porous media; the equation describing motion (momentum balance) is thus of central importance. Following the original work of Henry Darcy, mathematical descriptions of liquid flow in porous media are based on Darcy's law.[4] This law states that the volumetric flow rate Q of liquid through a specimen of porous material is proportional to the hydrostatic pressure difference Δp across the specimen, inversely proportional to the length L of the specimen, and proportional to the cross-sectional area A. Darcy's law is expressed simply as:

$$Q = k_D A \frac{\Delta p}{L} \qquad [3.21]$$

where the constant of proportionality k_D defined by Eq. 3.21 is the Darcy permeability of the material.

The quantity Q/A has dimension LT^{-1} and is called the Darcy velocity u. Therefore, the general three-dimensional equation for Darcy's law is written as:

$$u = -\frac{k}{\eta}\nabla p \qquad [3.22]$$

In the equation, $k = k_D\eta$ denotes the permeability of the porous media, η the fluid viscosity, p is the pressure and u represents the superficial flow velocity of the fluid. The permeability, k, taken as a constant, is an intrinsic property of the porous medium. The velocity in Darcy's law, u, is actually a mean velocity over the cross-section. Hence, the velocity profile of Darcy flow in a porous medium has a flat shape in the flow direction, indicating a constant velocity.

Although Darcy's law was first established empirically, it has been subsequently derived rigorously from the Navier–Stokes equation. While the Navier–Stokes equation is capable of describing flow in detailed geometries at the pore scale,

Darcy's law averages the flow over a representative volume. The application of Darcy's law is the standard approach to characterising single-phase fluid flow in microscopically disordered and macroscopically homogeneous porous media.[7,8]

Fluid flow in practical dyeing processes, including package dyeing, is assumed to be streamline in nature and is often described by Darcy's law.[6,9–11]

Despite the fact that there is no theoretical evidence to prove this behaviour, researchers claim that model predictions generally show good agreement with experimental data.

In most package dyeing machinery the dye liquor is pumped through the tube and the yarn assembly of the package. Since the flow is from the (vertical) tube to the yarn assembly (parallel), it remains unclear whether the global transport of momentum by shear stresses in the fluid is negligible. In addition, yarns are soft and capable of undergoing substantial deformation. The deformation of soft packages with low density, especially at the surface of the package, is more noticeable due to the higher flow rate and flow direction change that occurs at this soft interface. Therefore flow characteristics through this type of porous medium are different from those in a rigid porous medium such as sandstone, where flow is described by Darcy's law. Darcy's law assumes that the only driving force for flow in a porous media is the pressure gradient, and the global transport of momentum by shear stress in the fluid is negligible.

To account for the viscous drag along bounding walls, the Brinkman equation is often used.[12] The Brinkman equation describes the flow in porous media in cases where the transport of momentum by shear stresses in the fluid is not ignored. The model extends to include a term that accounts for the viscous transport in the momentum balance and introduces the velocities in the spatial directions as dependent variables.

$$\nabla p = -\frac{\eta}{k}u + \eta\nabla^2 u \qquad [3.23]$$

where η is fluid viscosity, u is the velocity vector, and p represents pressure. The permeability of the porous structure is denoted k as in Darcy's law.

The term $(-u\eta/k)$ in Eq. 3.23 is the Darcy resistance term, and the term $(\eta\nabla^2 u)$ is the viscous resistance term; the driving force is still considered to be the pressure gradient. When the permeability k is low, the Darcy resistance dominates the Navier–Stokes resistance, and Eq. 3.23 reduces to Darcy's law. Therefore, the Brinkman equation has the advantage of considering both viscous drag along the walls and Darcy effects within the porous medium itself. In addition, because Brinkman's equation has second-order derivatives of u, it can satisfy no-slip conditions at solid surfaces bounding the porous material (e.g. the walls of a packed bed reactor), whereas Darcy's law cannot. In that sense, Brinkman's equation is more exact than Darcy's law.

3.3.3 Permeability

The permeability of a porous medium, defined by Darcy's law,[13] is called Darcy permeability k_D, which has dimensions $M^{-1}L^3T$. However, the permeability so defined depends both on the material and on the fluid. For permeation flows which are geometrically similar (in practice, Newtonian liquids in laminar flow in inert non-swelling media), the Darcy permeability k_D varies inversely with the fluid viscosity η. Therefore, an intrinsic permeability k can be defined, as shown in Eq. 3.24:[4,14]

$$k = k_D \eta \qquad [3.24]$$

in which k is a material property independent of the fluid used to measure it; the unit for the permeability k in SI system is m^2. The variation of k with temperature is controlled mainly by the change of viscosity,[14] so that:

$$\frac{dk}{dT} = -k \frac{d \ln \eta}{dT} \qquad [3.25]$$

The permeability is related to the pore size distribution, since the sizes of entrances, exits and lengths of the pore walls make up the major resistances to flow. The permeability is the single parameter that reflects the conductance of a given structure.

The permeability and porosity are related. For example, if the porosity is zero the permeability is zero. However, the permeability cannot be predicted from the porosity alone, since additional parameters, which contain more information about pore structure, also affect it.

In the laminar flow region, the flow of a fluid through an assembly of yarns has been described by the appropriate form of Darcy's law by several researchers.[6,9–11] Different theories from which the permeability coefficient in this equation may be predicted start from different concepts of the nature of the fluid flow.[15,16]

The capillary theories focus on the spaces or pores in the porous solid, and an analogy is drawn between the tortuous pore system of the solid and the cylindrical pores of an assembly of capillary tubes. The best-known equation of this type is the Kozeny–Carman equation,[9,15] which gives an expression for the permeability coefficient as a function of the porous structure:

$$k = \frac{1}{K_0 S_0^2} \frac{\varepsilon^3}{(1-\varepsilon)^2} \qquad [3.26]$$

where ε is the porosity or voidage of the porous medium, S_0 is the specific surface, or surface area of the material that makes up the porous body in unit volume, and K_0 is a constant, known as the Kozeny constant.

The Kozeny constant is essentially a correction factor that accounts for the tortuosity and orientation of the pore system. For high porosity values, the actual permeability, determined experimentally, is usually lower than that predicted by

the Kozeny–Carman equation, and so high K_0 values are obtained. This can be attributed to a gradual change of the flow mechanism from a capillary flow to one around a swarm of obstacles. In this region of high porosities, drag theories are more useful for calculating the permeability.[15]

Experimental results have shown[17] that the Kozeny–Carman theory holds well when the porosity is less than 0.8 in porous media. For media with higher porosity, however, the Kozeny–Carman equation is not supported by experimental results.[18,19] Denton's work[6] indicated that, since the porosity of yarn packages lies between 0.1 and 0.7, the Kozeny–Carman equation can be used in investigations of package dyeing processes.

Denton further related the permeability of porous media of general shape to the specific permeability K_s by an equation involving a shape factor S, thus:

$$\frac{Q}{\Delta P} = K_s \frac{S}{\mu} \qquad [3.27]$$

He presented a relationship for calculating the value of the shape factor for cylindrical cheese packages, as shown in Eq. 3.28.

$$S = \frac{2\pi h}{\ln \frac{r_o}{r_i}} \qquad [3.28]$$

where h is the height of the package, and r_i and r_o are the inner and outer radii of the package, respectively. If the permeability of the cheese package were measured, its specific permeability could be calculated, and the effects of package density, winding tension and yarn properties could be compared.

The above discussion provides a means of evaluating permeability of a porous medium experimentally by measuring the pressure drop and the flow rate in systems where these measurements are possible. In package dyeing processes, the flow velocity of fluid through the porous spaces of the package is usually so small and the flow passages so narrow that a laminar flow may be assumed to prevail. The permeability of cross-wound packages may then be deduced by theoretical relationships based on Darcy's law and the Kozeny–Carman equation.

Generally, as permeability decreases, increasing pressure drops are required across a package in order to maintain a desired flow rate.[19] The density differences in a yarn package result in permeability variations, which directly affect flow behaviour within the package. The correlation between package density and permeability was discussed by Denton,[6] who addressed this correlation for cotton yarn packages. Porosity–permeability correlations for other types of fibrous porous media are also available from the literature.[4,5,20] Consideration of these works is beyond the scope of the material presented here.

In order to use a numerical model to predict flow behaviour with real yarn packages, which are typically anisotropic, some means of predicting the package permeability distribution is required. In general, this parameter will be a complex

function of factors such as yarn type, package characteristics including local non-uniformity, and flow magnitude and direction. For simplicity, here, it is assumed that the package density is uniform, and the permeability does not vary with position in the package.

3.4 Convective mass transfer in fluid system

There are different descriptions of diffusion convection and dispersion among different workers and in different fields, which often cause confusion. Thus, to model the mass transfer in real systems a clear definition should first be provided.

3.4.1 Convective dispersion

While the flow of a fluid through a packed bed at a given velocity, v, is a common situation in practice, the description of the problem is quite complicated even in a one-dimensional space with fluids of uniform properties. This is due to the fact that mixing takes place both longitudinally (in the direction of flow) and transversely (perpendicular to the flow). Suppose at $t = 0$ a 'dot' of traced fluid (such as dye) of concentration c_0, rather than over the entire face, is injected. This situation is schematically shown in Fig. 3.2. As the dot moves from left (face 1) to right (face 2) with the flow, it will spread in the direction of flow and perpendicular to the flow. At face 2 the dot is transformed into an ellipse with concentration varying across it.[4]

There are several methods to obtain partial differential equations describing the concentration behaviour of the mixed zone as a function of time and position, to model the phenomenon shown in Fig. 3.2.

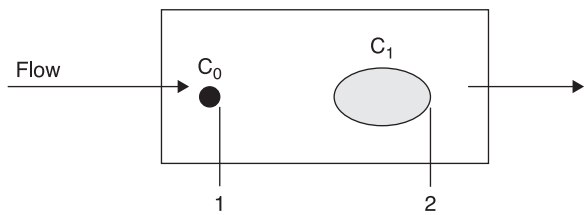

3.2 Convective dispersion.

There are three different phenomena involved in this process:

- Diffusion, a random process due to molecular motion, which is flow velocity independent; hence, diffusion makes the dot at face 1 spread in a circular shape at face 2.
- Dispersion, occurring in flow in which layers of different velocity exist, which is flow velocity dependent, and therefore makes the shape elliptical at face 2. A higher flow velocity will cause a flatter ellipse shape at face 2.

- Convection, the movement of molecules due to the flow, which makes the tracer move from face 1 to face 2.

Diffusion

The most fundamental process in dispersion is molecular *diffusion*, which is a special case of dispersion when the velocity of the fluid is zero.[13] Molecules in the liquid state are not stationary, even if the bulk fluid velocity is zero, because the molecules are in continuous motion. The flux due to the random molecular motion is given by Eq. 3.29:[21]

$$j_{dif} = -D_{dif} \frac{\partial c}{\partial x} \qquad [3.29]$$

where D_{dif} is diffusion coefficient, c is the concentration of diffusant and x represents the distance. If the direction after each collision is random, then the mean square distance travelled is proportional to time and the proportionality constant is the molecular diffusitivity. In mathematical terms, this is known as Fick's second law (after the German physical chemist Fick), and is shown in Eq. 3.30:

$$\frac{\partial c}{\partial t} = D_{dif} \frac{\partial^2 c}{\partial x^2} \qquad [3.30]$$

that is, the change in concentration over time, at a given point, is proportional to the slope of the concentration gradient, with movement from regions of high to low concentration. This law is simply a mathematical description of the macroscopic consequence of random motion.

Dispersion

Dispersion occurs in any kind of flow in which layers of different velocity exist. It is a process of distributing or spreading out of concentration profiles due to mechanisms in which the flux is proportional to the concentration gradient.[22]

$$j_{dis} = -D_{dis} \frac{\partial c}{\partial x} \qquad [3.31]$$

where D_{dis} is the dispersion coefficient, which is flow velocity dependent, c denotes the concentration of chemicals and x is the distance. In the context of this discussion, the term 'dispersion' means the process of distributing or spreading out of concentration profiles due to mechanisms in which the flux is proportional to the concentration gradient. It does not relate to the particle size distribution of dyes or pigments, which is another commonly used meaning in coloration technology.

It is important to note that dispersion is a process in which the mass of the species is conserved. The species mass conservation equation includes a term with the divergence of the flux of the species. If the flux depends on the concentration gradient, then the conservation equation will have second-order spatial derivatives of concentration. Thus, dispersion will add second-order spatial derivatives of concentration (or saturation) to the conservation equation.

$$\frac{\partial c}{\partial t} = D_{dis} \frac{\partial^2 c}{\partial x^2} \qquad [3.32]$$

In this model, similarity to Fick's Law of diffusion is used, whereby a dispersion coefficient, D_{dis}, is defined and employed to present the macroscopic transport of material instead of Fick's molecular diffusion coefficient.

Some published studies relate to the measurement and calculation of longitudinal and lateral dispersion coefficients in packed beds of various materials.[23–25] The effect of dispersion coefficients on physical and operational properties, such as particle size distribution, column length, fluid velocity, etc., have also been investigated.[26,27]

Convection

Convection is the process in which chemicals are transported due to bulk movement of the fluid, and is assumed to be the fastest form of chemical transport in liquor. The flux due to the bulk flow is:

$$J_c = vc \qquad [3.33]$$

where v is the average velocity of the bulk flow. As a result, the concentration decreases in the direction of fluid movement.

$$\frac{\partial c}{\partial t} = -v \frac{\partial c}{\partial x} \qquad [3.34]$$

These three phenomena of diffusion, dispersion and convection are assumed to be additive and independent.[27] The presence of the cross-flow does not bias the probability that the molecule will take a diffusive step to the right or the left; it just adds something to that step. Therefore, the total flux of dissolved solute:

$$\begin{aligned} J &= j_c + j_{dis} + j_{dif} \\ &= vc - D_{dif} \frac{\partial c}{\partial x} - D_{dis} \frac{\partial c}{\partial x} \end{aligned} \qquad [3.35]$$

or, by combining the last two terms:

$$J = vc - D \frac{\partial c}{\partial x} \qquad [3.36]$$

where D in this equation is mathematically similar to diffusion, but it is greater than what would be observed by diffusion alone. It is called the dispersion coefficient,

but it should be emphasised that it includes both convective and diffusive mechanisms. It is also known as the diffusive–dispersive coefficient. If the dispersion is seen to increase with velocity, it is often given as a composite term: $D_{dis} = \alpha v$, where α is the dispersivity, which is a fundamental property of a system.

It should be noted that the difference between D_{dif} and D_{dis} is that D_{dif} is not expected to change with velocity, while D_{dis} changes with fluid velocity. The general form of D is:

$$D = D_{dif} + \alpha v \qquad [3.37]$$

Kramers and Albreda[28] applied the mixing cell model for studying the frequency response of continuous flow in a packed tube by combining the convection/diffusion equations to obtain:

$$\frac{\partial c}{\partial t} + v\frac{\partial c}{\partial x} = D\frac{\partial^2 c}{\partial x^2} + s \qquad [3.38]$$

where s represents all the source and sink terms that occur in the real environment.

3.4.2 Dispersion with adsorption in porous media

When a dye solution crosses a yarn package, it is a process of chemical transport in a porous medium. Assuming the package density is uniform and the porosity ε of the package is constant, Eq. 3.38 can be written as:

$$\varepsilon\frac{\partial c}{\partial t} = D\frac{\partial^2 c}{\partial x^2} - v\frac{\partial c}{\partial x} + s \qquad [3.39]$$

The movement of various chemicals during miscible flow in a porous medium, with dispersion and adsorption, is of interest in many fields, such as chemical engineering, petroleum engineering, hydrology and soil physics. This can be regarded as a problem in dispersion, in which some of the dispersing substance becomes immobilised as dispersion proceeds, or as a problem in chemical kinetics, in which the rate of reaction depends on the rate of supply of one of the reactants by dispersion. Thus, diffusion may take place within the pores of a solid body which can absorb some of the diffusing substance, or through an immobile product resulting from the attraction of the diffusing molecules to fixed sites within the medium.

When dispersion is accompanied by absorption, Eq. 3.39 for a dispersion model in one dimension has to be modified by addition of a rate term[4] as shown in Eq. 3.40.

$$\varepsilon\frac{\partial c}{\partial t} + v\frac{\partial c}{\partial x} = \frac{\partial}{\partial x}D\frac{\partial c}{\partial x} + r(c,t) \qquad [3.40]$$

The term $r(c,t)$ can express a homogeneous reaction in the liquid, adsorption–desorption on the medium, or a heterogeneous reaction within the medium.

Consider a one-dimensional flow, where the displacing fluid has the same properties as the displaced fluid, and both fluids are miscible. The displacing fluid contains a solute, such as a dye, that can be adsorbed and desorbed on and off the medium, such as a textile fibre assembly. If F is the amount of adsorbate on the absorbent (chemical on the medium or dye on the textiles) per unit volume, then Eq. 3.40 is written in one dimension as:[4,29–32]

$$\frac{\partial c}{\partial t} = \frac{\partial}{\partial x} D \frac{\partial c}{\partial x} - v_x \frac{\partial c}{\partial x} - \frac{1}{\varepsilon} \frac{\partial F}{\partial t} \qquad [3.41a]$$

where ε is the porosity of the medium, and v_x is the interstitial velocity of flow within the porous medium.

In a one-dimensional process, and for a concentration-independent dispersion coefficient, the general form of Eq. 3.41a becomes:

$$\frac{\partial c}{\partial t} = D_i \frac{\partial^2 c}{\partial x^2} - V_i \frac{\partial c}{\partial x} - \lambda_i \frac{\partial c_F}{\partial t} \qquad [3.41b]$$

where the coefficients D_i, V_i and λ_i specify the amount of dispersive, convective and adsorptive characteristics of the system, respectively.

The above equations, based on the conservation of mass for chemical transport, yield the convection-dispersion-sorption equation CDSE (Eq. 3.41 and its variations), which is widely used in industrial applications,[33] including dyeing. Many researchers call the term ($D\ \partial^2 c/\partial x^2$) in Eq. 3.41b either dispersion or diffusion, and D is usually treated as a constant. In the context of this analysis, dispersion is used to describe this phenomenon, and the diffusion is considered a special case of dispersion when the velocity of the fluid is zero.

3.4.3 Dispersion in laminar flow: Taylor dispersion

Taylor[34] examined the case of injection of a small quantity of ink into a tube in which water flows at a constant rate. He measured the dispersion by measuring the absorption, by the ink, of light shining through the tube. He concluded that the symmetry came about through an interaction between convection (the mass movement, with a parabolic velocity profile) and diffusion. He also noted that the dispersion due to (convection + diffusion) was less than that due to convection alone (although it could be more than that due to diffusion alone). In other words, a random process (diffusion) decreases the total randomness (dispersion) of the system.

The key to Taylor's analysis is that diffusion has the net result that molecules do not stay in one streamline (the path that would be followed by an individual molecule in the absence of diffusion) forever. Molecules near the wall (velocity = 0) will diffuse towards the centre, and those at the centre will diffuse towards the wall. This reduces the spread of solute that would have resulted if there had been convection only.[35] In Taylor's words, 'The time necessary for appreciable effects

to appear, owing to convective transport, is long compared with the "time of decay" during which radial variations of concentration are reduced to a fraction of their initial value through the action of molecular diffusion.'

In textile dyeing, the fibre assembly is usually considered as a porous medium, within which it is assumed that:

- some streamlines are longer than others, due to a distribution of tortuosity, and
- some streamlines flow faster than others, due to differences in pore size.

These two conditions can be combined by the concept of travel time. Thus, Taylor's comment becomes relevant: dispersion will appear diffusion-like if there is sufficient (diffusive) mixing between short and long travel time pathways. If there is insufficient mixing, dispersion will be primarily due to convection and probably will not look diffusive.

3.4.4 Dispersion model

Based on the above discussion, we can conclude three common mathematical descriptions of dispersion in dyeing.

CDE (Convection-Dispersion Equation) model, also known as the ADE (Advection-Dispersion Equation)

This model is simply a mathematical statement of Taylor's observations. If the centre of mass of the solute travels at the same speed as the mean water flux, and the spreading is normal, then the concentration of solute at a point changes over time as:

$$\frac{\partial c}{\partial t} + v\frac{\partial c}{\partial x} = D\frac{\partial^2 c}{\partial x^2} \qquad [3.42]$$

When spreading is diffusion-like, the width of the solute 'plume' increases proportionately to the square root of time: this is a signature of a diffusive process. Conceptually the CDE is similar enough to Taylor's tube that it can be thought of as just flow in a single tube.

STM (stream-tube model)

This is like the case of a fast flow in Taylor's tube: there is not enough time for diffusive exchange between streamlines, so it is considered that each streamline acts independently. If the velocity distribution is known, the dispersion can be predicted. In this case the centre of mass of the solute still moves at the same velocity as the mean water flux, but the dispersion increases linearly with time, rather than with the square root of time. This indicates that the process is not diffusive. Conceptually it can be seen as flow in several parallel tubes of different diameters.

MIM (Mobile–Immobile Model)

This situation exists when the flow takes place through porous media, while the solute diffuses into and out of the aggregates. Such a model is commonly used to describe solute movement through textiles. This model supposes that water flows through some fraction of the total porosity, the mobile region, and not through the rest, the immobile region. The diffusive exchange between the mobile and immobile regions has the net effect of slowing down the solute movement. So solute does not move at the same velocity as the water, but it scales in the same way: velocity is linear with distance. The concept of the retardation factor ε can thus be introduced. If the solute moves more slowly than water, it is retarded (slowed down), and such a factor can be incorporated into the CDE:

$$\varepsilon \frac{\partial c}{\partial t} = D \frac{\partial^2 c}{\partial x^2} - v \frac{\partial c}{\partial x} - s \qquad [3.43]$$

The dye transport in the dyeing process is almost invariably treated by one of the above models or their variations. A general review of the relevant literature is presented in the next section.

3.5 Dye transfer in dyeing

Several researchers have defined various models for the dyeing process. Some workers have focused on the on-line control of the dyeing process, for which a number of simplifying factors must be used to keep the model as simple as possible. Other workers concentrated on a comprehensive investigation into the effect of various process parameters on dyeing.

Models of particular interest are those that are able to relate the conditions within the dyebath and the material being dyed to the distribution of dye within the material during and at the end of the dyeing process. The models for batchwise dyeing may be divided into two types:[36]

- Detailed mathematical models: in these models a comprehensive investigation into the effect of various dyeing parameters, including both bulk and dispersive fluid flow, is carried out. These parameters are then related to the physico-chemical laws of the dyeing process. Therefore complex differential equations are derived. Major simplifications to the model would be required in order to solve these equations explicitly, and therefore numerical solutions are used.
- Reduced mathematical models: these models can be subdivided into two major groups:
  - Models that are based on the physico-chemical laws that describe the dyeing process, and introduce explicit mathematical equations, but which have a restricted description of the flow of the dye liquor around the machine and within the package. These models are generally used to determine dyeing conditions likely to produce a given desired exhaustion profile.

– Models that simulate dyeing conditions in which no dye migration occurs, and fluid flow takes place only by a bulk mechanism. These models are based upon explicit mathematical equations that allow determination of levelness within a package for a 'worst case' dyeing scenario. Since a number of simplifying factors are used in the model, the equations defined by these models are generally simpler.

3.5.1 The work of McGregor

McGregor[37] was probably the first to suggest that a two-dimensional convective diffusion equation could be used to express the rate of change of concentration in a solution as the sum of contributions from the diffusion of solute and from the motion of elements of the solution from one point to another. He used a convective diffusion equation in vector notation:

$$\frac{\partial c}{\partial t} + (v \cdot grad)c = D\nabla^2 c \qquad [3.44]$$

where c is the concentration of dye in solution, t is the time, D is the aqueous diffusion coefficient (or dispersion coefficient as defined in Section 3.3) and v is a vector representing the velocity of fluid motion.

McGregor followed Levich's[38] approach to solve the problem of convective diffusion to a flat plate immersed in a steady flow of solution (of concentration c_0) at a mainstream velocity v_0 by considering only a two-dimensional model. In this model the y co-ordinate is normal to the surface and the x co-ordinate is parallel to it and in the direction of flow, the origin of the co-ordinate system being located at the leading edge of the plate. He assumed that $\partial^2 c/\partial x^2 << \partial^2 c/\partial y^2$, i.e. that diffusion occurs predominantly towards or away from the surface along the y-axis, so Eq. 3.44 takes a much simpler form. In addition, he further assumed a steady state of convective diffusion ($\partial c/\partial t = 0$); therefore:

$$D\frac{\partial^2 c}{\partial y^2} = v_x \frac{\partial c}{\partial x} + v_y \frac{\partial c}{\partial y} \qquad [3.45]$$

The maximum possible flux of solute to the surface, or the maximum possible rate of dyeing, is given by the solution of Eq. 3.45 for the boundary condition:

$$c \to c_0 \text{ as } y \to \infty$$

$$c = 0 \text{ at } y = 0 \qquad [3.46]$$

However, as McGregor indicated,[37] a solution cannot be obtained until the behaviour of v_x and v_y is known. This presupposes that the hydrodynamic equations of motion of the fluid have already been solved, or that a particular form of the solution has been assumed.

His work further involved the solution of the Navier–Stokes equations. In the convective diffusion problem outlined above, Levich was able to show that

Eq. 3.11 can be simplified and solved, since, in steady-state flow, the quantities $\partial v_x/\partial t$ and $\partial v_y/\partial t$ are zero, also $\partial^2 v_x/\partial x^2 << \partial^2 v_y/\partial y^2$, and the external forces are ignored. Thus, Eq. 3.11 for the x direction can be reduced to:

$$v_x \frac{\partial v_x}{\partial x} + v_y \frac{\partial v_x}{\partial y} = -\frac{1}{\rho}\frac{\partial p}{\partial x} + \mu \frac{\partial^2 v_x}{\partial y^2} \quad [3.47]$$

and the continuity equation becomes:

$$\frac{\partial v_x}{\partial x} + \frac{\partial v_y}{\partial y} = 0 \quad [3.48]$$

with the following boundary conditions:

$$v_x = v_y = 0 \text{ at } y = 0$$
$$v_x \rightarrow v_0 \text{ as } y \rightarrow \infty \quad [3.49]$$

Levich solved this set of equations to give expressions for v_x and v_y, which can be substituted in Eq. 3.45, and the convective diffusion problem as a whole is then solved.

McGregor's work showed the full complexity of some of the problems inherent in rigorously predicting the effect of rate of flow on rate of dyeing. The diffusional boundary layer model outlined in his paper is as simple and useful a treatment of the problem as can be found.

3.5.2 The work of Hoffman and Mueller

Hoffman and Mueller[39] developed a simple mathematical model that includes a uniform flow through a package and Fickian diffusion of a dye within the fibre. The distribution of a dye within the package and the degree of levelness are calculated under a simplified condition. In their study, authors used the mass conservation principle within the package, which connects the convection of the dye by the liquor flow and its diffusion into the fibre. This was written in the following form:

$$\left(1 - \frac{s_p}{s_F}\right)\frac{\partial C_L}{\partial t} = -q\frac{\partial C_L(x,t)}{\partial x} - s_p \frac{\partial M_F}{\partial t} \quad [3.50]$$

where C_L is the volume concentration in the dye liquor at time t at the plane x inside the package, M_F is the mass of the dye taken up per mass of the fibre, at time t and plane x, s_p is package density, s_F is fibre density, and q represents the volume of flow per time and area of the package.

The diffusion of dye from the surface into the interior of the fibres follows Fick's second equation applied to radial diffusion into a homogeneous circular cylinder, as follows:

$$\frac{\partial C_F(r,x,t)}{\partial t} = D(t)\left[\frac{\partial^2 C_F}{\partial r^2} + \frac{1}{r}\frac{\partial C_F}{\partial r}\right] \quad [3.51]$$

The mass of the dye taken up by unit mass of the fibres at time t and position x is given by the following equation:

$$M_F(x,t) = \frac{2}{r_F^2 \rho_F}\int_0^{r_F} C_F(r,X,t)\, rdr \quad [3.52]$$

To solve Eq. 3.50, the authors further assumed that there is a linear adsorption relation between C_L and C_F (concentration of dye on fibres):

$$C_F(r_F,x,t) = kC_L(x,t) \quad [3.53]$$

The authors solved this set of equations with the appropriate initial and boundary conditions for constant dyeing conditions, and uniform liquor flow without reversal. The Laplace transformation method was used for the solution, and the transformed equations were solved explicitly.

The results were presented in a number of graphs, which showed the distribution of dye at various times, over the entire thickness of the package, and also over the entire radius of an individual fibre at different locations in the package. Thus, the dyeing process could be clearly analysed in the light of the results obtained by the simulation of the model.

It can be seen that, although the work of Hoffmann and Mueller was based on a sound approach describing the dye distribution at every position in the system dynamically, some assumptions, such as uniformity of liquor flow, linearity of adsorption relationship, and ignoring the dispersion term during the dye transfer, etc., were quite restrictive, and these limited the validity of their model over a wide range.

3.5.3 The work of Nobbs and Ren

Nobbs and Ren[40,41] developed a model to quantify the total deposition error of dyeing. Their mathematical model employed a convective dispersion equation that described the mass balance between the dye in the liquor and that on the fibre at a given time and position within the package.

$$\xi\frac{\partial C(r,t)}{\partial t} = D\frac{\partial^2 C(r,t)}{\partial r^2} - \frac{F}{2\pi rL}\frac{\partial C(r,t)}{\partial r} - (1-\xi)\frac{\partial M(r,t)}{\partial t} \quad [3.54]$$

where $C(r, t)$ and $M(r, t)$ are the concentration of dye in liquor and on the fibre at a distance r from the centre of the package at time t respectively, L is the height and ξ is the voidage of the packed bed (package), F is the volumetric flow rate, and D is the dispersion coefficient for the movement of liquor in the packed bed.

Ren[41] and Ilett[42] discussed the effect of dispersive flow in package dyeing. Dispersive flow is considered to reduce the concentration gradient of dye liquor flowing through the package, resulting in a more even distribution of dye in the

liquor within the package. Since they intended to develop a worst case dyeing model, they neglected the effect of dispersive flow on the grounds that the results due to their model would represent a more uneven distribution of dye than would occur in practice.

In addition, they assumed that the rate of adsorption of dye follows first-order kinetics, and the constant of proportionality may change with time.

$$\left(\frac{1-\xi}{\xi}\right)\frac{\partial M(r,t)}{\partial t} = K(t)C(r,t) \qquad [3.55]$$

Therefore, Eq. 3.54 was simplified to:

$$\frac{\partial C(r,t)}{\partial t} = -\frac{F}{2\pi rL\xi}\frac{\partial C(r,t)}{\partial r} - K(t)C(r,t) \qquad [3.56]$$

$K(t)$ was assumed by the authors to be a function of time and independent of the local dye concentrations C and F. It was acknowledged that this assumption may not be strictly true in real situations, but they believed that this would be a good approximation in the specific case of acrylic yarns dyed with cationic dyes.

Nobbs *et al.* continued work on optimising the dyeing process as a whole, including control of other variables such as flow rate, flow reversal and controlled addition of dyes and auxiliaries.[43,44] This approach required the control algorithms to be extremely flexible, and to react to the current situation rather than simply following a pre-set cycle.

3.5.4 The work of Burley and Wai

Burley and Wai[45] presented a model to describe the dye transfer in a package dyeing system. The mechanisms of dispersion, convection, absorption and desorption of dye to and from the packed bed of fibres were included. The governing equations describing the distribution of dye in the packed bed consist of a pair of differential equations:

$$\varepsilon\left(\frac{\partial C}{\partial T} + U\frac{\partial C}{\partial X} - D\frac{\partial^2 C}{\partial X^2}\right) = (1-\varepsilon)\frac{\partial Q}{\partial T} \qquad [3.57]$$

$$(1-\varepsilon)\frac{\partial Q}{\partial T} = \varepsilon k_a(Q_M - Q)C - (1-\varepsilon)k_d Q \qquad [3.58]$$

where C and Q are the concentration of dye in liquor and on the fibre respectively, ε is the voidage of the packed bed, U is the bulk velocity and D is the dispersion coefficient for the movement of liquor in the packed bed. Equation 3.57 is derived from a mass balance of dye at any point in the packed bed, taking into account the processes of bulk flow, axial dispersion and removal of dye from the liquor. They assumed that the process is isothermal, in agreement with industry practices, and that the flow is uniform and axial.

Equation (3.58) quantifies the processes of absorption and desorption at the fibre surface with k_a and k_d the absorption and desorption coefficients, and Q_M a maximum saturation value of the fibre. This equation leads to the Langmuir absorption isotherm in the steady state.

At the bed inlet and outlet a mass balance of dye gives the boundary conditions defined by Danckwerts.

$$U(C - C_{in}) = DC_X \text{ at } X = 0 \quad [3.59]$$

$$U(C - C_{out}) = DC_X \text{ at } X = 1 \quad [3.60]$$

In the derivation of these equations the authors assumed that the volume of liquor was conserved as it passed into, through and out of the bed. C_{in} and C_{out} are the values of the liquor concentration just before entry into and just after exit from the packed bed.

Burley *et al.* solved the above set of equations by finite difference techniques and presented the results in the form of a number of graphs representing the variations in the concentration of dye at various points in the dyeing machine with time. Attempts were made to show the effects of a number of machine design and operating conditions on the outcome of the dyeing.

The model of Burley *et al.* is comprehensive in terms of the number of operational situations which it considered. The systematic approach with which it deals with the engineering analysis of some practical complications is recognised, but the model was designed to accommodate various dye adsorption kinetics, such as those associated with linear partition or Freundlich isotherm. Also, the interstitial fluid velocity U in Eqs 3.13 and 3.41 was not defined.

Vosoughi[32] continued the work of Burley and Wai, and further developed the model to describe the diffusion of dye into the fibre interior. These equations were solved numerically using appropriate boundary conditions to result in dimensionless relationships for both axial and radial flows.

3.5.5 The work of Telegin

Telegin[46] emphasised that, to simulate the mass transfer in dyeing, the equations developed must be supplemented with an equation for convective transfer in the package:

$$\frac{\partial C}{\partial t} + \frac{1-\varepsilon}{\varepsilon}\frac{\partial A}{\partial t} = -\frac{1}{X_0 + X}\frac{\partial}{\partial X}[(X_0 + X)UC] \quad [3.61]$$

$$U = \frac{U_0 X_0}{X_0 + X} \quad [3.62]$$

where U is the liquor flow speed at any point along X, and C and A are the concentration of dye in liquor and on the fibre, respectively. It should be noted that they also ignored the dispersion component.

Although these workers recognised that convection plays a crucial role in dye transfer in a fluid system, they failed to define the flow velocity within free channel and yarn assembly during the dyeing for use in a sound mathematical form. To investigate the convective mass transfer to the textile materials, a mathematical description of convective mass transfer in the process of solution flow around single fibre and through a layer of fibres was proposed by Telegin,[47] who modelled an individual cylindrical fibre with transverse liquid flow with the dissolved dye. The process of stationary diffusion near the surface of a cylinder in the case of a thin boundary layer was described by Eq. 3.63, which is in polar co-ordinates:

$$V_r \frac{\partial C}{\partial r} + \frac{D}{r}\frac{\partial}{\partial r}\left(r\frac{\partial C}{\partial r}\right) + \frac{V_\theta}{r}\frac{\partial C}{\partial \theta} = 0 \qquad [3.63]$$

For the boundary conditions:

$$C(R,\theta) = C_0,\ C(\infty,\theta) = C_s,\ C(r,0) = C(r,\pi) = C_s \qquad [3.64]$$

The components V_r and V_θ were estimated as the solution of the stationary Navier–Stokes equations for liquid flow around a single fibre.[39] The author then used what they claimed was Oseen's approximation to describe the velocity field components V_r and V_θ, as well as the hydrodynamic pressure P:

$$V_r = \frac{\partial \varphi}{\partial r} + \frac{v}{U}\frac{\partial \chi}{\partial r} - \chi\cos\theta \qquad [3.65]$$

$$V_\theta = \frac{1}{r}\frac{\partial \varphi}{\partial \theta} + \frac{v}{Ur}\frac{\partial \chi}{\partial \theta} + \chi\sin\theta \qquad [3.66]$$

$$P = -\rho U\frac{\partial \varphi}{\partial r}\cos\theta \qquad [3.67]$$

where the functions φ and χ were estimated according to Eqs 3.68 and 3.69:

$$\varphi = \mathrm{A}_0 \ln r + \mathrm{A}_1\frac{\cos\theta}{r} + \mathrm{A}_2\frac{\cos 2\theta}{r^2} + \ldots \qquad [3.68]$$

$$\chi = -U + \exp\left(\frac{Ur}{2v}\cos\theta\right)\left[\mathrm{B}_0 K_0\left(\frac{Ur}{2v}\right) + \mathrm{B}_1\frac{\partial}{\partial x}K_0\left(\frac{Ur}{2v}\right) + \mathrm{B}_2\frac{\partial^2}{\partial x^2}\left(\frac{Ur}{2v}\right) + \ldots\right] \qquad [3.69]$$

in which A_0, A_1, . . ., B_0, B_1, . . . are constants which must be satisfied at the boundary conditions:

$$V_r(R,\ \theta) = V_\theta(R,\ \theta) = 0 \qquad [3.70]$$

$$P(R,\theta) = 2\mu\frac{\partial V_r(R,\theta)}{\partial r} \qquad [3.71]$$

For further calculations, Telegin considered it necessary to describe in a more simple way the liquid motion near the surface of a cylinder. He followed Protodiakonov's method, using the properties of the function K_0 for small arguments, and, making necessary transformations using Eqs 3.65–3.67 and taking into account Eqs 3.68–3.71, he obtained the following expressions:

$$V_r = \frac{U\cos\theta}{\gamma - 2\ln(Re)}\left[-1 + 2\ln\left(\frac{r}{R}\right) + \left(\frac{R}{r}\right)^2\right] \quad [3.72]$$

$$V_\theta = \frac{U\sin\theta}{\gamma - 2\ln(Re)}\left[-1 - 2\ln\left(\frac{r}{R}\right) + \left(\frac{R}{r}\right)^2\right] \quad [3.73]$$

where $\gamma = 1 - 2C + 2\ln 4 \approx 2.61816$, $C \approx 0.5772$ (Euler's constant).

The work of Telegin *et al.* made real progress on the influence of the convective factor in the convective dispersion equation by defining the flow velocity using a sound mathematical basis. However, since the authors attempted to obtain the result using analytical methods, an exact solution of problem 3.63 to a solid surface could be obtained only where the solution flows at a steady rate past an object of simple geometrical shape.

3.5.6 The work of Shannon *et al.*

Shannon *et al.*[11] developed a flow model which, using a finite difference method, predicts pressure and velocity profiles based on user-defined package geometry, permeability profile and fluid properties. The flow model was obtained by combining the continuity equation for fluid flow in a porous medium:

$$\varepsilon\frac{\partial p}{\partial t} = -(\nabla\rho v_0) \quad [3.74]$$

and Darcy's law:

$$v_0 = -\frac{k}{\mu}(\nabla p - \rho g) \quad [3.75]$$

where v_0 is the superficial fluid velocity, ρ is fluid density, μ is fluid viscosity, ε represents yarn package porosity, k is yarn package permeability, p is pressure, g denotes body force and t is time.

The authors further defined the quantity in parentheses on the right-hand side of Eq. 3.75 as follows:

$$p = \nabla p - \rho g \quad [3.76]$$

then they combined Eqs 3.74–3.76 to obtain:

$$\varepsilon\frac{\partial p}{\partial t} = \nabla\left(\frac{\rho k}{\mu}\nabla p\right) \quad [3.77]$$

For cylindrical geometry (axisymmetric) and steady, incompressible flow, Eq. 3.77 may be further simplified to yield:

$$\frac{1}{r}\frac{\partial}{\partial r}\left(rk_r(r,z)\frac{\partial p(r,z)}{\partial r}\right)+\frac{\partial}{\partial z}\left(k_r(r,z)\frac{\partial p(r,z)}{\partial z}\right)=0 \quad [3.78]$$

where $k_r(r,z)$ and $k_z(r,z)$ are permeabilities in the radial and axial directions, respectively, that vary with position in the package. For an isotropic package, k_r and k_z are equal and independent of position on the package. In this case, Eq. 3.78 reduces to Laplace's equation:

$$\frac{1}{r}\frac{\partial}{\partial r}\left(r\frac{\partial p(r,z)}{\partial r}\right)+\frac{\partial^2 p(r,z)}{\partial z^2}=0 \quad [3.79]$$

This equation may be solved using separation of variables, subject to the following boundary conditions for flow through a yarn package:[11]

$$p(r=r_i,z)=p_i \quad [3.80]$$

$$p(r=r_o,z)=p_o \quad [3.81]$$

$$p(r>r_i,z=0)=p_o \quad [3.82]$$

$$p(r>r_i,z=h)=p_o \quad [3.83]$$

where r_i and r_o are package inner and outer radius, respectively, h is package height, and p_i and p_o are total pressures inside and outside the package.

The solution was accomplished using finite difference techniques. The resulting model allows the user to specify upstream and downstream pressures, package geometry (inner radius, outer radius and height), radial and axial permeabilities, and fluid viscosity. Variable radial and axial permeabilities are assigned in order to simulate package density effects.

The work of Shannon *et al.* is valuable for the investigation of the influence of package geometry and permeability on flow properties within the package. However, they did not consider flow properties before approaching the surface of the package, which, if significant, can affect the flow behaviour in the system.

3.5.7 The work of Scharf *et al.* and Karst *et al.*

Scharf *et al.*[10] employed the flow momentum equation to describe the flow velocity in relation to location and time, as well as the pressure of a fluid in relation to its physical properties (kinematic viscosity, density) for the given initial and boundary conditions. The conservation of momentum for incompressible fluids is described by the Navier–Stokes equation:

$$\rho\left(\frac{\partial v}{\partial t}+(v\nabla)v\right)=\vec{k}-\nabla p+\mu\Delta v \quad [3.84]$$

where p is the static pressure, v is the velocity, μ is dynamic viscosity, ρ is density and k contains the external body forces, which the authors considered as the frictional forces of the porous medium represented by the yarn bobbin.

They further assumed that the flow through the yarn bobbins is laminar and the pressure drop is proportional to velocity. Therefore, turbulence and turbulent viscosity were ignored. The porous media model to describe the yarn bobbins in the calculations was then reduced to Darcy's law. The pressure drop in each of the three coordinates (x, y, z) within the porous region is given by:

$$\vec{k} = \frac{u}{\alpha} v \qquad [3.85]$$

where α is permeability obtained from experimental differential pressure measurements in the dyeing vessel, μ is the viscosity of the liquor and v is the velocity component in the x, y, z direction.

Together with the continuity equation, they form a system of equations that have to be solved considering the proper initial and boundary conditions. The simulation results provided information on the static pressure and velocity distribution in every part of the dyeing vessel.

Karst *et al.*[48] used computational fluid dynamics (CFD) to model dye liquor flow in beam and package dyeing and to determine how certain parameters affect liquor flow through the fibrous assemblies.

It should be noted that, among the above-mentioned models, the works of Hoffman and Mueller, Nobbs and Ren, Burley and Wai, and Vosoughi concentrate on the dye transport through the package during the dyeing, while the works of Shannon *et al.*, Scharf *et al.* and Karst *et al.* focused on the investigation of the flow properties within the package. McGregor and Telegin considered the flow properties in their convective dispersion model, however, with some limitations. These models are further examined in Chapter 4.

3.6 References

1. Burley R., Wai P.C., McGuire G.R. (1987), 'Process Engineering Approach to Dyeing Machinery—A Study of Package Dyeing Machine Dynamics', *Chem. Eng. Res. Des.*, **65**, 505–13.
2. Sposito, G., Gupta, V.K., Bhattacharya, R.N., 'Foundational theories of solute transport in porous media: A critical review' in G.F. Pinder (ed.) (1983), *Flow through Porous Media*, CML Publishing, Ltd, Southampton, England, pp. 76–85.
3. Bear J. (1972), *Dynamics of Fluids In Porous Media*, American Elsevier, New York.
4. Greenkorn R.A. (1983), *Flow Phenomena in Porous Media: Fundamentals and Applications in Petroleum, Water and Food Production*, Marcel Dekker Inc., New York.
5. Darby R. (1996), *Chemical Engineering Fluid Mechanics*, Marcel Dekker, Inc., New York.
6. Denton M. (1964), 'The Permeability of Cross-Wound Cotton Yarn Packages' *Journal of the Textile Institute*, **55**, T228–T242.

7. Adler P. (1992), *Porous Media: Geometry and Transport*, Butterworth-Heinemann, Stoneham MA.
8. Sahimi M. (1995), *Flow and Transport in Porous Media and Fractured Rock*, VCH, Boston.
9. McGregor R. (1965), 'The Effect of Rate of Flow on Rate of Dyeing II–The Mechanism of Fluid Flow through Textiles and its Significance in Dyeing' *Journal of the Society of Dyers and Colourists*, **81**, 429–38.
10. Scharf S., Cleve E., Bach E., Schollmeyer E., Naderwitz P. (2002), 'Three-Dimensional Flow Calculation in a Textile Dyeing Process' *Textile Research Journal*, **72**, 9, 783–8.
11. Shannon B., Hendrix W., Smith B., Montero G. (2000), 'Modeling of supercritical fluid flow through a yarn package' *Journal of Supercritical Fluids*, **19**, 1, 87–99.
12. Brinkman, H.C. (1947), 'The Calculation of the Viscous Force Exerted by a Flowing Fluid on a Dense Swarm of Particles' *Appl. Sci. Res.*, **A1**, 27–34.
13. www.owlnet.rice.edu/~ceng671/CHAP2.pdf, date accessed April 13 2014.
14. www.cmse.ed.ac.uk/MSE3/Topics/MSE-permeability.pdf, date accessed April 13 2014.
15. Van Den Brekel L.D.M and De Jong E.J. (1989), 'Hydrodynamics in Packed Textile Beds' *Textile Research Journal*, **59**, 433–40.
16. Kim A.S., Stolzenbach K.D. (2002), 'The Permeability of Synthetic Fractal Aggregates with Realistic Three-Dimensional Structure' *Journal of Colloid and Interface Science*, **253**, 2, 315–28.
17. Fowler J.S., Hertel K.L. (1940), 'Flow of a Gas through Porous Media' *J. Appl. Phys.*, **11**, 496–502.
18. Lord E. (1955), 'Air Flow through Plugs of Textile Fibres Part 1—General Flow Relations' *Journal of Textile Institute*, **46**, T191–T213.
19. Fretland W. (1997), 'Controlling Fiber and Flow in Yarn Dyeing' *Am. Dyestuff Reporter*, **86**, 9, 42–46.
20. Higdon J.J.L., Ford G.D. (1996), 'Permeability of Three Dimensional Models of Fibrous Porous Media' *J. Fluid Mech.*, **308**, 341–61.
21. Crank J. (1975), *The Mathematics of Diffusion*, 2nd edn, Clarendon Press.
22. Burley R., Flower J. (1991), 'Dynamic Behaviour of Dyeing Machinery and Computer Simulation—Some Examples' *Journal of the Society of Dyers and Colourists*, **107**, 434–8.
23. Kushalkar K.B, Pangarkar V.G. (1990), 'Liquid Holdup and Dispersion in Packed Columns' *Chem. Eng. Science*, **45**, 759–63.
24. P. Legentilhomme, J. Legrand, J. Comiti. (1989), 'Axial dispersion in electrolyte flow through anisotropic packed beds' *Journal of Applied Electrochemistry*, **19**, 2, 263–70.
25. Van Swaaij W.P.M., Charpentier J.C., Villermaux J. (1969), 'Residence Time Distribution in the Liquid Phase of Trickle-Flow Process' *Chemical Engineering Science*, **24**, 1083–95.
26. Han N.W, Bhakta J. (1985), 'Longitudinal and lateral dispersion in packed beds: Effect of column length and particle size distribution' *AICHE J*, **31**, 277–88.
27. http://lawr.ucdavis.edu/classes/ssc107/SSC107Syllabus/chapter6-01.pdf, date accessed 13 April 2014.
28. Kramers H., Albreda G. (1953), 'Frequency response analysis of continuous flow systems' *Chem. Eng. Science*, **2**, 173–81.
29. Sherman W.R. (1964), 'The Movement of a Soluble Material during the Washing of a Bed of Packed Solids' *AIChE Journal*, **10**, 855–60.

30. Wai P.C. (1984), 'Dynamic Behaviour of a Reactive Packed Bed Adsorption System' PhD Thesis, Heriot-Watt University, UK.
31. Ma, Z., Guiochon, G. (1991), 'Application of Orthogonal Collocation on Finite Elements in the Simulation of Non-Linear Chromatography' *Comput. Chem. Engng*, **15**, 6, Pergamon, 415–26.
32. Vosoughi M. (1993), 'Numerical Simulation of Packed Bed Adsorption Applied to a Package Dyeing Machine' PhD Thesis, Heriot Watt University, UK.
33. http://wwwbrr.cr.usgs.gov/projects/GWC_coupled/phreeqc/html/final-20.html, date accessed 13 April 2014.
34. Taylor G.I. (1953), 'Dispersion of Soluble Matter in Solvent Flowing Slowly Through a Tube' *Proc. Roy. Soc.*, CCXIX 186.
35. Cusserler E.L. (1997), *Diffusion: Mass Transfer in Fluid Systems*, Cambridge University Press, Cambridge, UK.
36. Shamey M.R. (1997), 'The Computer Control of Continuous Addition Dyeing of Cotton with Reactive Dyes', PhD Thesis, Leeds University, UK.
37. McGregor R., Peters R.H. (1965), 'The Effect of Rate of Flow on Rate of Dyeing I – The Diffusional Boundary Layer in Dyeing' *Journal of the Society of Dyers and Colourists*, **81**, 393–400.
38. Levich V.G. (1962), *Physicochemical Hydrodynamics*, Prentice-Hall Inc.
39. Hoffmann F., Mueller P.F. (1979), 'Model Calculations on Levelness in Package Dyeing' *Journal of the Society of Dyers and Colourists*, **95**, 5, 178–86.
40. Nobbs J., Ren J. (1984), Proceedings of the13th IFATCC Conference, London.
41. Ren, J. (1985), 'A Thesis on the Development of a Mathematical Model of the Batch Dyeing Process and its Application to the Simulation and Computer Control of a Dyeing Machine' PhD Thesis, Dept. of Colour Chemistry, Leeds University.
42. Ilett S. (1990), 'Investigation of the Package Dyeing Process Using a Fixed Bed Reactor as a Model System' PhD thesis, Leeds University, UK.
43. Nobbs, J.H. (1991), 'Control Parameters in Dyeing Machinery Operation' *Journal of the Society of Dyers and Colourists*, **107**, 430–3.
44. Flower J., Burley R., Nobbs J. (1994), 'New Control Strategies for Batch Dyeing Operations Using Mathematical Modelling and Simulation' *Journal of the Society of Dyers and Colourists*, **110**, 167–9.
45. Burley R., Wai P.C., McGuire G.R. (1985), 'Numerical Simulation of an Axial Flow Package Dyeing Machine' *Appl. Math. Modelling*, **9**, 1, 33–9.
46. Telegin F.Yu., Shormanov A.V., Melnikov B.N. (1997), 'Description of Kinetic Regularities of the Dyeing Process by the Use of Sorption Curve Moments' in: Moryganov, A.P., editor, *Textile Chemistry – Theory, Technology, Equipment*, Nova Sci. Publishers, Inc., Commack, New York, pp. 87–115.
47. Telegin F.Yu. (1998), 'Convective mass transfer in liquid treatment processes' *Journal of the Society of Dyers and Colourists*, **114**, 49–55.
48. Karst D., Yang Y., Rapp W.A. (2003), 'Modeling Dye Liquor Flow in Fabric Beam Dyeing and Yarn Package Dyeing', *Proceeding of Industry Simulation Conference*, Valencia, Spain, 457–61.

4

Developing theoretical models of dyeing

DOI: 10.1533/9780857097583.82

Abstract: Chapter 4 develops theoretical models to simulate the dyeing process, starting from brief critical conclusions based on convective dispersion and fluid mechanics models as well as those that describe both the dye transfer and flow phenomena during dyeing. Using the theoretical concepts discussed in the previous chapters, the system is described by a set of partial differential equations. Models examined include Darcy, Navier–Stokes and Brinkman equations. The boundary conditions and initial conditions are also defined and discussed. The solutions of the model show the dynamic behaviour of the system under given conditions of flow rate and given dyeing parameters.

Key words: convective dispersion, fluid mechanics, package dyeing geometry, modelling fluid flow in dyeing, Darcy's law, Navier–Stokes equations.

4.1 Introduction

In the previous chapter a number of mathematical descriptions of the dyeing process, developed by different workers, were presented. The solution of the model equations can produce results in the form of a distribution of dye throughout the system at any time during the dyeing process, which provides useful insight into the package dyeing operation. These models can be classified into three categories:

- Models based on convective dispersion: these only describe dye transfer during dyeing. These include the works of Hoffman and Mueller,[1] Nobbs and Ren,[2–3] Burley and Wai[4–5] and Vosoughi.[6]
- Models based on fluid mechanics: these only describe the flow phenomena during dyeing. These include the works of Shannon *et al.*,[7] Scharf *et al.*[8] and Karst *et al.*[9]
- Models which describe both the dye transfer and flow phenomena during dyeing. The works of McGregor[10] and Telegin[11] could be placed in this category.

4.1.1 Models based on convective dispersion

The model of Hoffmann and Mueller[1] related a number of dyeing parameters with dyeing quality. They assumed a uniform liquor flow through a package, and Fickian diffusion of dye within the fibres. The distribution of a dye within the package and the degree of unlevelness were calculated for constant dyeing conditions of temperature, pH and electrolyte concentration. However, the model

was restricted to a constant rate of liquor flow. They also ignored the dispersion factor, and only considered a linear adsorption relationship between the concentration of dye in liquor and on the fibres.

The work of Nobbs and Ren,[2] unlike that of Hoffmann and Mueller, does not produce solutions which provide the concentration of dye at any positions in the package at any time. It gives a relationship between a number of variables and the unlevelness of dyeing. The control scheme developed and described subsequently by the authors was aimed at achievement of any of the three exhaustion profiles – linear, exponential or quadratic – by on-line measurement of the dye bath conditions and manipulation of the temperature.

The work of Burley *et al.*[4–5] and Vosoughi[6] treats a number of significant operational conditions such as flow reversal, time delays, and addition (and withdrawal) of dye liquor during the process, in a comprehensive analysis based on sound chemical engineering principles, which is classified as the MIM approach in Section 3.3. It is also supported by robust numerical techniques for treatment of complicated mathematical problems. The simulation model, however, lacks the analysis of various stages of dye absorption, the variable boundary condition due to the variable concentration of dye in liquor, and the variable dispersion coefficient due to the variable dyeing conditions.

One major shortcoming of these models is that the flow property during dyeing is not defined in a sound mathematical form, since, for both the STM and MIM approaches, an exact solution of the problem of convective diffusion to a solid surface first requires the solution of the hydrodynamic equations of motion of the fluid for boundary conditions appropriate to the mainstream velocity of flow and the shape of the package. Another limitation of their work is that those workers did not consider situations like variable boundary conditions and variable dispersion coefficients, which are quite common situations in dyeing practice, in their numerical simulations.

4.1.2 Models based on fluid mechanics

The work of Shannon *et al.*[7] can be used to investigate the influence of package geometry and permeability on flow property within the package, since it can be used to predict pressure and velocity profiles based on user-defined package geometry, permeability profile and fluid properties. However, the model, which was obtained by combining the continuity equation for fluid flow in a porous medium and Darcy's law, only considered the system within the package range. It did not consider the flow before approaching the surface of the package, which, if significant, can affect the flow behaviour in the system due to the definition of the boundary conditions.

Scharf *et al.*,[8] based on the Navier–Stokes equations, simulated turbulent incompressible liquids during the dyeing process. They assumed the flow through bobbins to be linear and described the yarn package using a porosity model. The

simulation results provided information on the static pressure and velocity distribution at every part of the dyeing vessel. However, due to the restricted assumptions used in this model, including direct treatment of the frictional force of the porous medium represented by the yarn bobbin as the external body force in Navier–Stokes equations, it may only be used for a narrow range of dyeing situations.

The work of Karst *et al.*[9] employed computational fluid dynamics (CFD) to model dye liquor flow during beam dyeing and package dyeing and to determine how certain parameters affect liquor flow through the packages. The CFD approach makes it possible to accommodate some complicated subject shapes, three-dimensional analysis and variable parameters.

The work of these three groups focused on the description of flow behaviour during dyeing, based on fluid mechanics. Their work provided useful information to investigate dye transport during dyeing. However, their system geometries were comparatively simple, since they only modelled the flow in porous media (textile assembly). The flow behaviour in the open channel (tube) was not considered, which caused difficulty in defining boundary conditions.

4.1.3 Models based on convective dispersion and fluid mechanics

McGregor's work[10] tried to contain the flow factor into the convective dispersion of dye in dyeing. He was probably the first to realise that the solution of the hydrodynamic equation of motion of the fluid was required in order to investigate the convective dispersion of dye during dyeing. This solution specified the velocity of the fluid at any point and at any time. It is then necessary to substitute the appropriate values for the local fluid velocities in the convective dispersion equation, which must be solved for boundary conditions related to the shape of the obstacle, the mainstream concentration of solute or dye, and the adsorption conditions at the solid surface. However, as he stated, this is a very difficult procedure even for steady flow past obstacles of simple shape. He only showed the full complexity of some of the problems inherent in accurately predicting the effect of the rate of flow on rate of dyeing. In addition, since he employed a CDE (see Section 3.3) approach to model the convective dispersion of dye, his work in this aspect can only be used to model the dispersion of dye in the liquor, rather than through the package.

Telegin's group[11] carried out a considerable amount of work on convective dispersion of solute in dyeing. Apart from initial work in 1997, which used the CDE approach, a simplified model of dye transfer, which is similar to McGregor's work but employing the MIM approach[12] to model the dye transport within the liquor, was used. The model was accompanied by a sound mathematical description of flow based on fluid mechanics. However, his work can only give a description of convective mass transfer from the solution flow to the fibre surface

during dyeing, without considering the adsorption factor. The limitation of his analytical method makes his work only suitable to linear situations and simple system geometries.

It can be seen from the above-mentioned work that, in order to investigate the dynamic behaviour of a package dyeing system, a more comprehensive model, which characterises the mass transfer, with a sound mathematical description for flow based on fluid mechanics, is desirable. A study of dye transport in liquor and porous media, and adsorption by fibres, combined with a clear description of flow properties in both tube and package, is a much more complicated topic, and is the main task in the present work. The mathematical model which will be developed in this chapter is intended to give a much more complete description of the package dyeing process and consideration of the situations which are of more relevance to the present practical problems in package dyeing analysis, design and control.

4.2 System description and basic assumptions

4.2.1 System description

In Chapter 2, typical package dyeing machines were described. In the present chapter a mathematical model of the operation of a pilot scale package dyeing machine is developed.

To allow flexibility, the machine has been designed as three separate units:[13]

- The kier (main tank). This is the part of the machine that contains the wound package of fibres that are to be dyed.
- Flow control and reversal module. This section of the machine consists of a pump, a throttle valve and a four-way flow reversal valve.
- Mixing (stock) tank. Prior to commencement of the dyeing cycle the dye liquor is made up in the mixing tank. This tank also acts as an expansion tank during the heating of the dye liquor.

The above parts are connected together in the configuration shown in Fig. 4.1. The kier is designed to hold two packages, one above the other, on a central spindle. Dyes (and additives) may all be added to the bath at the start of the dyeing process, or they may be partially or totally added after the start of the liquor circulation according to various dosing schemes represented by input flow rates expressed by different functions of time. In the latter case, a relatively small container referred to as the ‘addition tank’ is used, which contains a concentrated solution of dyes and is connected to the main bath through an addition valve. Dye liquor may also be withdrawn from the system by opening a drain valve at any time during the operation.

The rate of circulation of the liquor through the system can be measured, and it may be changed by altering the speed of the pump. The temperature inside the machine can be changed by a heating system with adjustable power input, and by cooling water, which can be passed through coils installed in the system. The

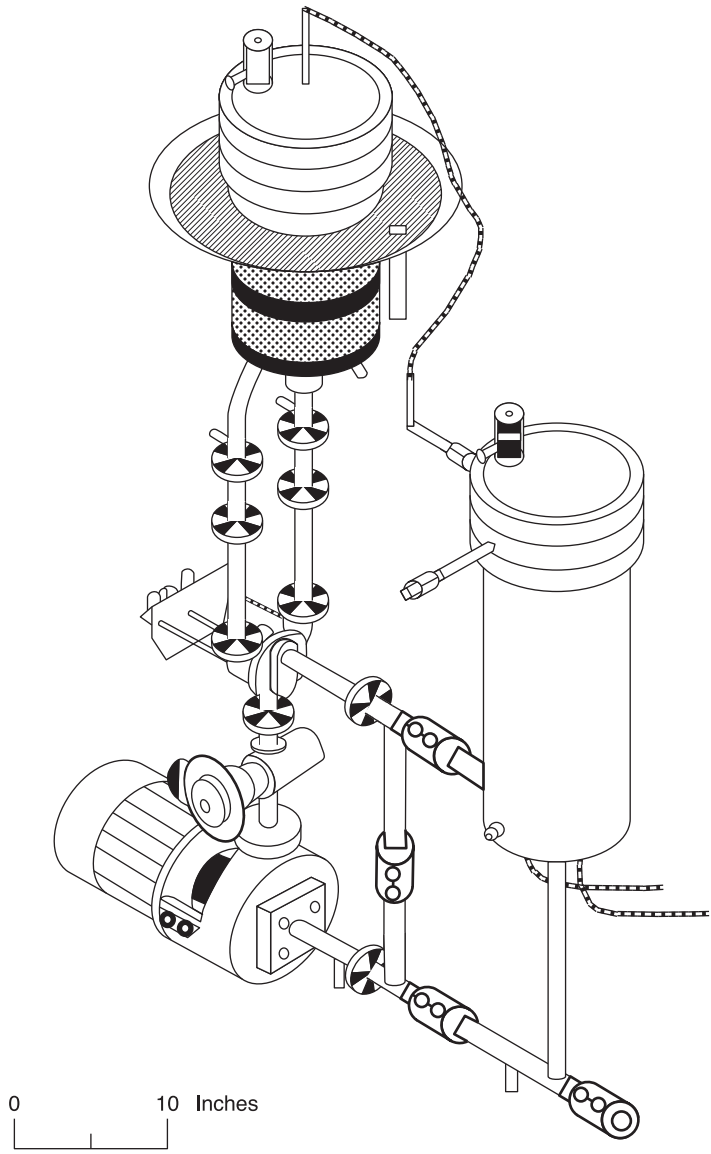

4.1 Pilot-scale batch dyeing machine.

machine is also equipped with a programmable temperature control system which can produce pre-scheduled time/temperature programmes. Flow of liquor through the package may be radial, as shown in Fig. 4.2, where only in-to-out flow is indicated. Pipe work joins the kier and mixing tank. Additional details regarding the control procedure and strategy are given in Chapter 5.

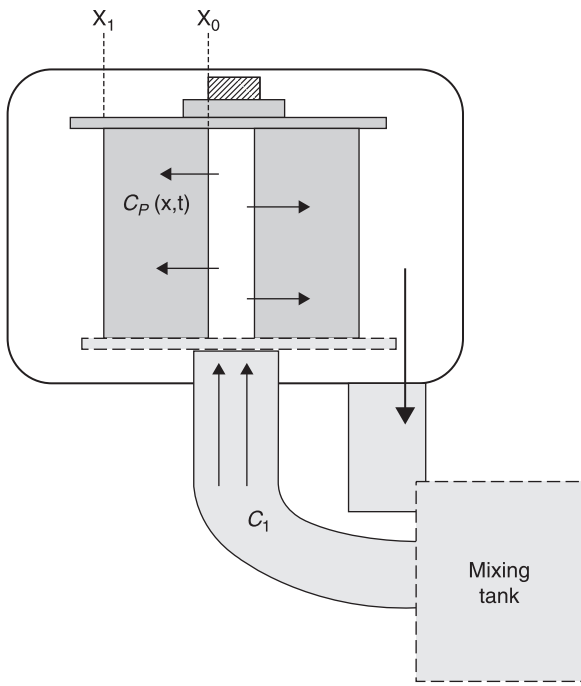

4.2 Flow cycle in package dyeing machine.

During dyeing, the dye liquor is pumped through the tube and the yarn assembly of the package, which consists of a three-dimensional shape with the interstitial space filled with the dye liquor. It is in the packed bed of the fibrous mass that adsorption of dyes takes place.

4.2.2 Basic assumptions

The process of mathematical modelling is one area in which assumptions have always been recognised as playing a key role. To investigate the dyeing process quantitatively, some basic conditions may be assumed, as described below:

1. The packages are uniformly wound so that the package density and porosity are the same throughout a package, as well as among packages.
2. The density and porosity of the packages remain constant during the dyeing process.
3. The dye liquor is considered an incompressible fluid; therefore, the density of dye liquor is constant at isothermal conditions.
4. The dye liquor is assumed to be a Newtonian fluid; thus, the viscosity is constant under isothermal conditions.

5. The dye liquor is well stirred during the dyeing process, so that the concentration of dye across the entrance of the package throughout the liquor can be taken to be uniform.
6. The transport of dye liquor along the packed bed fibrous assembly is represented by an MIM model. Thus, the supply of dye from the dye bath to the surface of the fibres at any position in the package is considered to consist of additive effects of two types of transport phenomena: convective flow and dispersive flow through porous media.
7. The dye concentration at the surface of the fibre is related to the dye concentration in the liquor within the package (local dyebath concentration) according to the sorption isotherm of the dyeing equilibrium.
8. The dye adsorption and any chemical reactions with fibres occur very rapidly in comparison to the diffusion process; thus, local equilibrium can be assumed to exist between the free and immobilized components of the diffusing substance.
9. The temperature within the entire dyebath, i.e. packages and dye liquor, is uniform at all times.

The basic assumptions made are more realistic than these of Hoffman *et al.*,[1] Burley,[5] Wai[4] and Vosoughi,[6] although some may still not be strictly correct. Assumptions 1 and 2 are simplified conditions of the real situation, since packages may not be completely uniformly wound, and also the density and the porosity of the package may be changed during the dyeing process due to the liquor flow and temperature. However, consideration of the changes in the density and porosity of the package during the dyeing would require a more comprehensive study of the effects of such variations, and are not included here.

Assumptions 3 and 4 are reasonable and widely accepted in practice. Assumption 5 is also realistic, particularly for the pilot-scale package dyeing machine considered, as the circulating action of the pump is generally known to provide effective mixing of the free liquor in the machine.

An important assumption, however, is assumption 6, since it separates convection and dispersion. Assumptions 7 and 8 aim to further incorporate the adsorption factor into the model. According to the theory and practice, these assumptions are reasonable. These basic assumptions, and special definitions for some individual cases, provide a basis for mathematical modelling of the dyeing process.

4.2.3 System geometry definition

For the package dyeing machine described above, a clear definition of the system geometry is demonstrated in Fig. 4.3. The dye liquor is assumed to circulate through the package during the dyeing, the direction of the flow being perpendicular to the yarn layers in the package. Figure 4.4 shows a simplified two-dimensional system geometry.

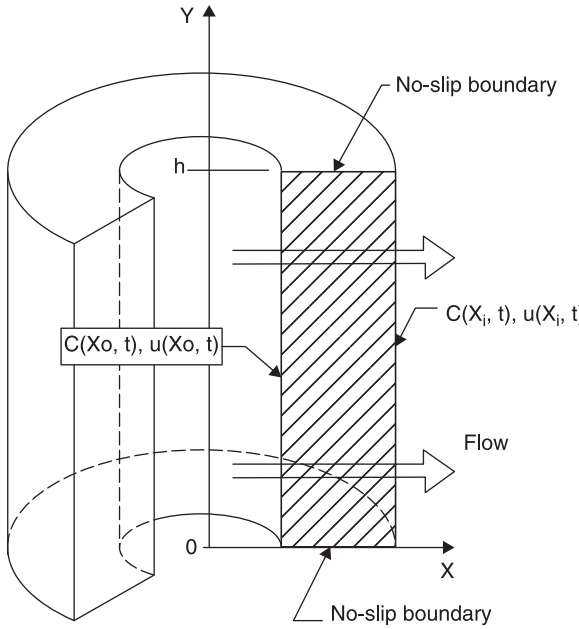

4.3 Flow through the package.

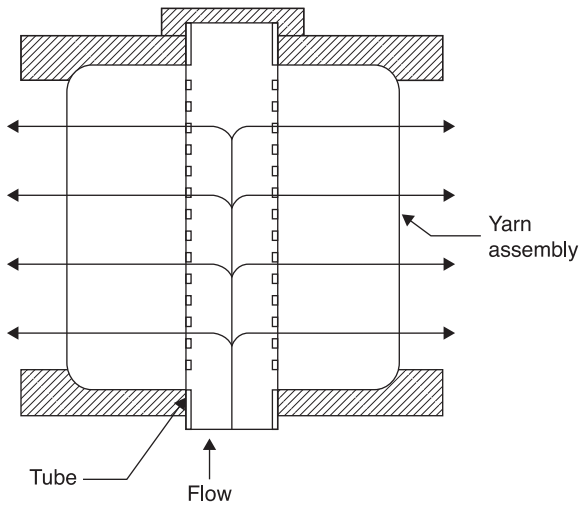

4.4 Flow through the package in two dimensions.

To simplify calculations, it is assumed that the process for both mass transfer and flow behaviour is the same for both sides along the symmetric axis. Therefore, the system geometry can be further simplified to that shown in Fig. 4.5. Only the left side of the symmetric axis line is considered as the system geometry described here.

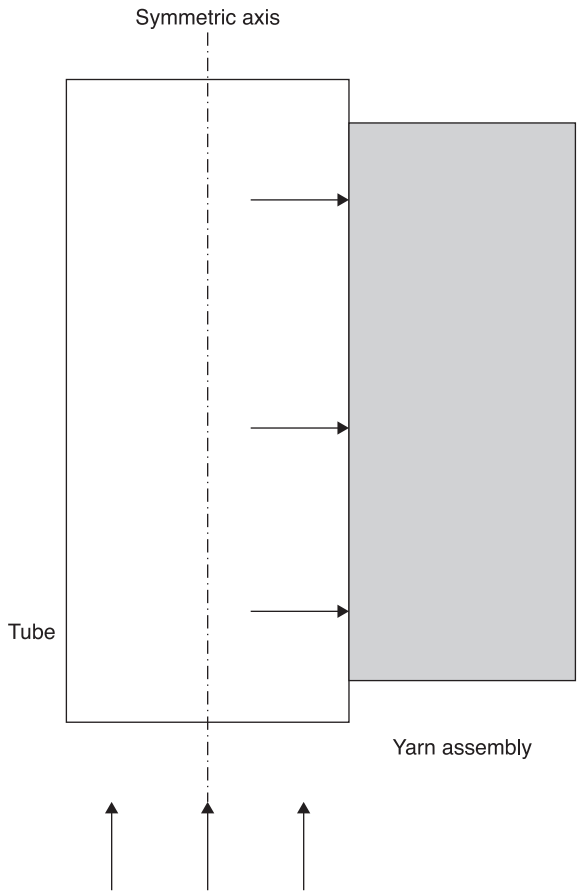

4.5 Geometry of the system in two dimensions.

4.3 Development of mathematical model

Based on the system geometry defined in the previous section, a differential control volume of system may be illustrated, as shown in Fig. 4.6.

In this figure, $J_{x,\,in}$ and $J_{x,\,out}$ are the dye flux at the inflow and outflow faces in the x-direction, respectively, and ε is porosity of the package, which is defined by Eq. 3.12 and here by Eq. 4.1.

$$\varepsilon = \frac{Total\ vol. - Vol.solids}{Total\ volume} = 1 - \frac{A_{solid}}{A} = \frac{A_{voids}}{A} \qquad [4.1]$$

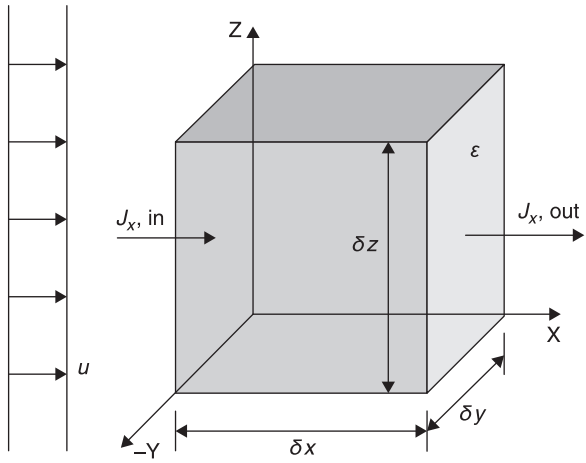

4.6 Differential control volume of system.

4.3.1 Derivation of differential equation of dye transfer with sorption in package dyeing

The derivation of the dye transfer equation within the package relies on the principle of superposition: convection and dispersion can be added together if they are linearly independent. From the previous chapter, dispersion was shown to be a random process due to molecular motion. Due to dispersion, each molecule in time δt will move either one step to the left or one step to the right (i.e. $\pm \delta x$). Due to convection, each molecule will also move $u\delta t$ in the cross-flow direction. These processes are clearly additive and independent; the presence of the cross-flow does not bias the probability that the molecule will take a diffusive step to the right or the left; it just adds something to that step. The net movement of the molecule is $u\delta t \pm \delta x$, and, thus, the total flux in the x-direction J_x, including the convective transport and the dispersion term, must be:

$$J_x = uC + q_x \qquad [4.2]$$

Combining with Eq. 3.36 gives:

$$J_x = uC - D\frac{\partial C}{\partial x} \qquad [4.3]$$

When considering a mass balance as a component of a multi-component system, the overall mass balance can be shown as in Eq. 4.4[14]:

$$\begin{matrix} \textit{Rate of Accumulation} \\ \textit{of Total Mass} \end{matrix} = \begin{matrix} \textit{Rate of Total} \\ \textit{Mass In} \end{matrix} - \begin{matrix} \textit{Rate of Total} \\ \textit{Mass Out} \end{matrix} \qquad [4.4]$$

The flux law shown in Eq. 4.3 and the mass conservation law shown in Eq. 4.4 can now be used, together with a differential control volume (*CV*) depicted in Fig. 4.6, to derive the dye transfer equation. For the left side of Eq. 4.4 this is shown in Eq. 4.5:

Rate of Accumulation of Total Dye within the CV

$$= \textit{Rate of Accumulation of Total Dye in Liquor within the CV} \quad [4.5]$$

$$+ \textit{Rate of Accumulation of Total Dye on Fibres within the CV}$$

where:

Rate of Accumulation of Total Dye in Liquor within the CV over δt

$$= \frac{\delta M_p}{\delta t} \quad [4.6]$$

and:

Rate of Accumulation of Total Dye on fibres within the CV over δt

$$= \frac{\delta M_f}{\delta t} \quad [4.7]$$

where δM_p is the amount of dye in the liquor within the *CV* over the time δt and δM_f is the amount of dye on the fibres within the *CV* over the time δt. If C_p is defined as the concentration of dye in the liquor within the *CV*, C_f is the concentration of dye on the fibre within the *CV*, and *V* is the volume of the *CV*, then:

$$M_p = C_p \varepsilon V = C_p \varepsilon \delta x \delta y \delta z \quad [4.8]$$

$$M_f = C_f (1 - \varepsilon)\, V = C_f (1 - \varepsilon) \delta x \delta y \delta z \quad [4.9]$$

Therefore, the left side of Eq. 4.4 becomes:

$$\frac{\delta M_p}{\delta t} + \frac{\delta M_f}{\delta t} = \varepsilon \frac{\delta C_p}{\delta t} \delta x \delta y \delta z + (1 - \varepsilon) \frac{\delta C_f}{\delta t} \delta x \delta y \delta z \quad [4.10]$$

The convective dispersive mass fluxes in and out of the *CV*, based on Eq. 4.3, for the x-direction can be shown as:

$$J_{x,\,in} = uC_p - D \frac{\partial C_p}{\partial x}\bigg|_1 \quad [4.11]$$

$$J_{x,\,out} = uC_p - D \frac{\partial C_p}{\partial x}\bigg|_2 \quad [4.12]$$

where the locations 1 and 2 are the inflow and outflow faces in Fig. 4.6. To obtain total mass flux, J_x is multiplied by the *CV* surface area $A = \delta y \delta z$. Thus, the net flux (the right side of Eq. 4.4) in the x-direction is:

$$J_{x,\,in} - J_{x,\,out} = \left(uC_p - D\frac{\partial C_p}{\partial x} \right)\Bigg|_1 \delta y \delta z - \left(uC_p - D\frac{\partial C_p}{\partial x} \right)\Bigg|_2 \delta y \delta z \qquad [4.13]$$

To continue, it is necessary to find a method to evaluate $J_{x,\,out}$ or J_x at point 2. To do this, a linear Taylor series expansion can be used. The general form of a Taylor series expansion is shown in Eq. 4.14:[15]

$$f(x) = f(x_0) + \frac{\partial f}{\partial x}\Bigg|_{x_0} \delta x + HOTs \qquad [4.14]$$

where HOTs stands for higher-order terms. Substituting $J_{x,\,out}$ for *f(x)* in the Taylor series expansion yields:

$$uC_p\Big|_2 = uC_p\Big|_1 + \frac{\partial (uC_p)}{\partial x}\Bigg|_1 \delta x + HOTs \qquad [4.15]$$

$$D\frac{\partial C_p}{\partial x}\Bigg|_2 = D\frac{\partial C_p}{\partial x}\Bigg|_1 + \frac{\partial}{\partial x}\left(D\frac{\partial C_p}{\partial x} \right)\Bigg|_1 \delta x + HOTs \qquad [4.16]$$

For a linear Taylor series expansion, the HOTs are ignored. Substituting 4.15 and 4.16 into the net flux Eq. 4.13, and dropping the subscript 1, gives:

$$uC_p\Big|_1 - uC_p\Big|_2 = -\frac{\partial (uC_p)}{\partial x}\delta x \qquad [4.17]$$

and:

$$-D\frac{\partial C_p}{\partial x}\Bigg|_1 + D\frac{\partial C_p}{\partial x}\Bigg|_2 = \frac{\partial}{\partial x}\left(D\frac{\partial C_p}{\partial x} \right)\delta x \qquad [4.18]$$

Thus, the net flux for the x-direction is:

$$-\frac{\partial (uC_p)}{\partial x}\delta x \delta y \delta z + \frac{\partial}{\partial x}\left(D\frac{\partial C_p}{\partial x} \right)\delta x \delta y \delta z \qquad [4.19]$$

For the y- and z-directions the process is similar, but with v and w for the velocity components, giving:

$$-\frac{\partial (vC_p)}{\partial y}\delta x \delta y \delta z + \frac{\partial}{\partial y}\left(D\frac{\partial C_p}{\partial y} \right)\delta x \delta y \delta z \qquad [4.20]$$

$$-\frac{\partial (wC_p)}{\partial z}\delta x \delta y \delta z + \frac{\partial}{\partial z}\left(D\frac{\partial C_p}{\partial z} \right)\delta x \delta y \delta z \qquad [4.21]$$

Substituting 4.10, 4.19–4.21 into Eq. 4.4, and letting δt, δx, δy, and $\delta z \rightarrow 0$, results in:

$$\varepsilon \frac{\partial C_p}{\partial t} + (1-\varepsilon)\frac{\partial C_f}{\partial t} = -\frac{\partial (uC_p)}{\partial x} + \frac{\partial}{\partial x}\left(D\frac{\partial C_p}{\partial x}\right)$$

$$-\frac{\partial (vC_p)}{\partial y} + \frac{\partial}{\partial y}\left(D\frac{\partial C_p}{\partial y}\right) - \frac{\partial (wC_p)}{\partial z} + \frac{\partial}{\partial z}\left(D\frac{\partial C_p}{\partial z}\right) \qquad [4.22]$$

or in vector notation:

$$\varepsilon \frac{\partial C_p}{\partial t} + (1-\varepsilon)\frac{\partial C_f}{\partial t} = -\nabla \cdot (UC_p) + \nabla \cdot (D\nabla C_p) \qquad [4.23]$$

where the cross-flow velocity $U=(u, v, w)$. Equation 4.22 (or 4.23) is then combined with the function describing the relationship between C_p and C_f, to give Eq. 4.24.

$$\frac{dC_f}{dt} = K_a C^a (1 - bC_f) - K_d C_f \qquad [4.24]$$

$$f = \frac{KC^a}{1 + bKC^a} \qquad [4.25]$$

$$C_f = \frac{KC_p}{1 + KC_p} \qquad [4.26]$$

where a and b are constants, and $K = K_a/K_d$ is the adsorption coefficient.

In order to solve Eq. 4.23, proper boundary conditions have to be defined. According to the system description and geometry of the package, demonstrated in Fig. 4.3, the convective flow is probably very large compared with diffusion in the flow direction, and the dye transport by diffusion may be negligible in this direction at the inflow face. Providing the main transport of dyes into the package takes place by convection, the flux at the inlet for the boundary conditions is:

$$J \cdot n = U\, C_1 \cdot n \qquad [4.27]$$

where C_1 is the concentration of dye in liquor at time t, and n is the unit normal vector. Equation 4.27 implies that (in the x-direction):

$$uC_p(0,t) - D\frac{\partial C_p}{\partial x} = uC_1 \qquad [4.28]$$

Also, it is reasonable to assume that the gradients at the exit face are small, so that:

$$\frac{\partial C_p(l,t)}{\partial x} = 0 \qquad [4.29]$$

At all other boundaries, insulating conditions are assumed:

$$J \cdot n = 0 \qquad [4.30]$$

Practically, this implies that the concentration gradients across these boundaries are zero, since the convective term vanishes.

Furthermore, the concentration is 0 at $t = 0$, which gives the initial condition:

$$C_p(x, 0) = 0 \qquad [4.31]$$

An overall description of the variation of fluid and solid phase concentration at a given time and position is therefore derived. Simultaneous solutions to these equations will give the actual dynamic behaviour of a packed bed dyeing machine in terms of fluid and solid phase concentration for given time and position throughout the package.

It must be noted that, since this is a three-dimensional model, it is convenient to use finite element method analysis to investigate the dynamic behaviour of the systems with any different package geometry, or any flow direction, by defining the exact package geometry, and appropriate boundary conditions. The details are discussed in the following chapter.

4.3.2 Modelling of fluid flow within the package

To calculate Eq. 4.23, the flow velocity distribution within the package $U(u, v, w)$ must be defined. This involves the fluid motion equation in porous media. As discussed in Chapter 3, Darcy's law and Brinkman equation can be used to characterise the flow behaviour within the package.

To simplify the definition of the system boundary conditions, boundary index is used, as shown in Fig. 4.7.

Flow in the porous domain (yarn assembly) can be described using Darcy's law:

$$u_1 = -\frac{k}{\eta} \nabla p_1 \qquad [4.32]$$

$$\nabla \cdot u_1 = 0 \qquad [4.33]$$

where k is the permeability of the porous medium, η the fluid viscosity, p_1 the pressure, and u_1 the velocity vector in the porous medium (yarn assembly).

It is assumed that the fluid does not cross the outer boundaries 7 and 8, shown in Fig. 4.7. The velocity vector at the boundaries is set to zero, which corresponds to a no-slip condition:

$$u = 0 \qquad [4.34]$$

For boundary 5, a specific flow perpendicular to the boundary is given by Eq. 4.35:

$$-\frac{k}{\eta} \nabla p_1 \cdot n = u \qquad [4.35]$$

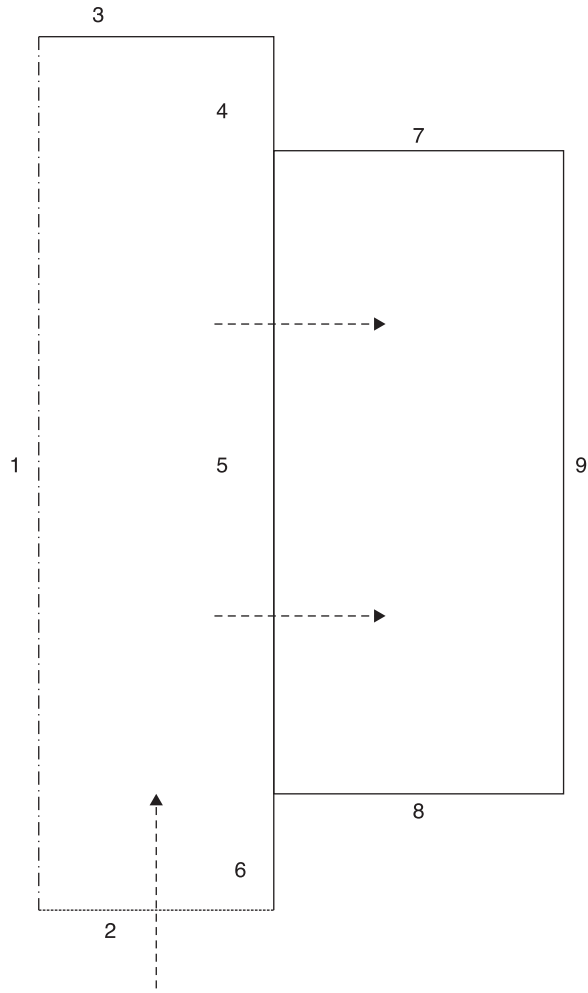

4.7 Boundary index of the system.

where u is the velocity in the x-direction, which is a dependent variable that needs to be defined at free liquor phase.

In order to investigate the influence of shear stresses on the flow property in a yarn assembly, the Brinkman equations are used to model flow in a porous medium, as shown in Eqs 4.36 and 4.37.

$$u_2 = -\frac{k}{\eta}\nabla p_2 + \eta\nabla^2 u_2 \qquad [4.36]$$

$$\nabla \cdot u_2 = 0 \qquad [4.37]$$

Boundary 5 conditions for Eqs 4.36 and 4.37 are given as:

$$u_2 = u,\ v_2 = v \qquad [4.38]$$

where u and v are the velocity in the x-direction and y-direction, respectively. They are dependent variables, which need to be defined at free liquor phase.

It should be noted that in Eq. 4.38 the velocity in both x and y-directions is considered based on the Brinkman equation approach.

For boundary 9, the pressure is set to zero and the straight-out conditions, which set the velocity components in the tangential direction, t, are used.

$$u \cdot t = 0 \qquad [4.39]$$

$$p = 0 \qquad [4.40]$$

A condition for the value of the pressure is defined for boundary 9:

$$p_1 = p_0 \qquad [4.41]$$

It can be seen that u, v and p are actually the fluid flow velocities and the pressure at the face between the package tube and yarn assembly, demonstrated in Fig. 4.5.

The solution for Eqs 4.32 and 4.36 cannot be obtained until the values of u, v and p are known. This presupposes that the hydrodynamic equations of motion of the fluid are already solved, or that a particular form of the solution is assumed. Therefore, a clear description of flow behaviour before the entrance of the yarn assembly (i.e. liquor in the tube) is required.

4.3.3 Modelling of fluid flow in the tube

To model the flow behaviour of free liquor (liquor within the tube), the Navier–Stokes equation is employed to describe the flow velocity and pressure distributions within the tube of the package (see Fig. 4.5).

The general form of the Navier–Stokes equation was discussed in a previous chapter. In vector notation, it can be shown as in Eq. 4.42:

$$\rho \frac{\partial u}{\partial t} - \nabla \cdot \eta(\nabla u + (\nabla u)^T) + \rho(u \cdot \nabla)u + \nabla p = F \qquad [4.42]$$

where η is the dynamic viscosity, ρ is the density, u is the velocity field, p is the pressure and F is a volume force field such as gravity. It should be noted that this formulation allows for variations in viscosity. For many fluids, the shear viscosity, η, depends significantly on the temperature, and when appreciable temperature differences exist in the flow field it is necessary to regard η as a function of position. However, it is assumed that the dye liquor in practical dyeing machines is well stirred and the differences in temperature are small enough for η to be taken as uniform over the fluid, in which case Eq. 4.42 becomes:

$$\rho \frac{\partial u}{\partial t} - \eta \nabla^2 u + \rho(u \cdot \nabla)u + \nabla p = F \qquad [4.43]$$

In addition, it is assumed that the density of the dye liquor is almost constant, which is referred to as incompressible fluid flow. The mass conservation equation is then reduced to:

$$\frac{\partial u}{\partial x}+\frac{\partial v}{\partial y}+\frac{\partial w}{\partial z}=0 \qquad [4.44]$$

In package dyeing, the dye liquor is pumped through the tube and the yarn assembly of the package, which consists of a three-dimensional shape with the interstitial space filled with the dye liquor. Therefore, it is a reasonable assumption that, within the package tube, the influence of an external volume force field such as gravity is ignored. Therefore, for steady-state flow it can be said that:

$$-\eta\nabla^2 u+\rho(u\cdot\nabla)u+\nabla p=0 \qquad [4.45]$$

$$\nabla\cdot u=0 \qquad [4.46]$$

This is simply a particular form of the equation of state for the fluid. Thus, for an incompressible fluid (the case of the dye liquor), provided that adequate boundary conditions are known, Eq. 4.45 and 46 are sufficient for the determination of U (u, v, w) and p within the package tube.

The boundary condition for boundary 1 (shown in Fig. 4.3) is set to the symmetry condition, which states that there are no velocity components perpendicular to this boundary, i.e.:

$$u\cdot n=0 \qquad [4.47]$$

It is assumed that the fluid does not cross the outer boundaries 3, 4 and 6. The velocity vector at the boundaries is also set to zero, which corresponds to a no-slip condition:

$$u=0 \qquad [4.48]$$

The velocity vector at boundary 2, as an inflow boundary, the velocity field of the fluid, is specified:

$$u\cdot n=(u_0, v_0) \qquad [4.49]$$

Since the flow is only in the y-direction, the inflow velocity on boundary 2 can be set to v_0, and the velocity in the x-direction set to 0.

The conditions for boundary 5, to couple Darcy's law (or the Brinkman equation) and the value of the pressure, are defined by setting:

$$p=p_1 \qquad [4.50]$$

where p_1 (or p_2) is one of the dependent variables in Darcy's law (or the Brinkman equation).

The equations governing the dye transfer, which contain the factor of convection, diffusion and sorption, combined with the description of flow in both free liquor

(dye liquor within the package tube) and porous media (yarn package), establish a complete mathematical model for package machinery. The solutions of the model give the dynamic behaviour of the system under given conditions of flow rate and given dyeing parameters. The results are mainly shown in graphical form, illustrating the variations of dye concentration on fibre with time and position for a given flow.

4.4 References

1. Hoffmann F., Mueller P.F. (1979), 'Model Calculations on Levelness in Package Dyeing' *Journal of the Society of Dyers and Colourists*, **95**, 5, 178–86.
2. Nobbs J.H., Ren J. (1984), Proceedings of the 13th IFATCC Conference, London, UK.
3. Ren J. (1985), 'A Thesis on the Development of a Mathematical Model of the Batch Dyeing Process and its Application to the Simulation and Computer Control of a Dyeing Machine' PhD Thesis, Dept. of Colour Chemistry, Leeds University.
4. Wai P.P.C. (1984), 'Dynamic Behaviour of a Reactive Packed Bed Adsorption System' PhD Thesis, Heriot-Watt University, UK.
5. Burley R., Wai P.C., McGuire G.R. (1985), 'Numerical Simulation of an Axial Flow Package Dyeing Machine' *Appl. Math. Modelling*, **9**, 1, 33–9.
6. Vosoughi M., 'Numerical Simulation of Packed Bed Adsorption Applied to a Package Dyeing Machine' PhD Thesis, Heriot-Watt University, UK.
7. Shannon B., Hendrix W., Smith B., Montero G. (2000), 'Modeling of Supercritical Fluid Flow through a Yarn Package' *Journal of Supercritical Fluids*, **19**, 1, 87–99.
8. Scharf S., Cleve E., Bach E., Schollmeyer E., Naderwitz P. (2002), 'Three-Dimensional Flow Calculation in a Textile Dyeing Process' *Textile Research Journal*, **72**, 9, 783–8.
9. Karst D., Yang Y., Rapp W.A. (2003), 'Modeling Dye Liquor Flow in Fabric Beam Dyeing and Yarn Package Dyeing', *Proceeding of Industry Simulation Conference*, Valencia, Spain, 457–61.
10. McGregor R. (1965), 'The Effect of Rate of Flow on Rate of Dyeing II – The Mechanism of Fluid Flow through Textiles and its Significance in Dyeing' *Journal of the Society of Dyers and Colourists*, **81**, 429–38.
11. Telegin F.Yu., Shormanov A.V., Melnikov B.N. (1997), 'Description of Kinetic Regularities of the Dyeing Process by the Use of Sorption Curve Moments' in: Moryganov, A.P., editor, *Textile Chemistry – Theory, Technology, Equipment*, Nova Sci. Publishers, Inc., Commack, New York, pp. 87–115.
12. Telegin F.Y. (1998), 'Convective Mass Transfer in Liquid Treatment Processes' *Journal of the Society of Dyers and Colourists*, **114**, 49–55.
13. Ridgway A. (1991), *Pilot-Scale Package Dyeing Machine – an Overview*, Department of Colour Chemistry and Dyeing, University of Leeds.
14. Ramirez W. (1997), *Computational Methods for Process Simulation*, 2nd edn, Reed Educational & Professional Publishing Ltd.
15. Stroud K. (1987), *Engineering Mathematics*, 3rd edn, Macmillan Education Ltd.

5

Solving dynamic equations in dye transport

DOI: 10.1533/9780857097583.100

Abstract: Chapter 5 provides an examination of the numerical solutions of the dyeing models that can be applied to different conditions. Numerical simulation of the system involves the use of Matlab software to solve systems of highly non-linear simultaneous coupled partial differential equations. The finite difference and finite element methods are introduced. The partition of the fibrous assembly geometry into small units of a simple shape, or mesh, is examined. Polygonal shapes used to define the element are briefly described. The defined geometries, boundary conditions, and mesh of the system enable solutions to the equations of flow or mass transfer models.

Key words: finite difference methods (FDM), finite element methods (FEM), mass transfer equations, numerical solutions, fibrous assembly mesh.

5.1 Introduction

The set of mathematical equations presented in Chapter 4 can be solved in a specific region with a set of boundary conditions for a desired variable. Such models can be used to predict the flow property during the dyeing, and the change of dye distributions throughout the package due to the change of dyeing conditions, to help in the design of optimised dyeing applications. The models can also be used to study the factors affecting the dye uptake and obtain a better understanding of the process behaviour and mechanisms. Using such models it would be possible to simulate and study testing conditions which are difficult to duplicate in the laboratory or in practice.

Computational simulations are playing an increasing role in the design and investigation of technical systems and are used in a wide range of applications. The simulation results can help the user to improve process quality, shorten development times and reduce cost of process optimisation. In particular, the effects of design modifications can be seen immediately by simulation during the development process, rather than only after a series of costly trial and error measurements.[1]

5.2 Numerical methods

To obtain the solutions of the equations involved, the analytical methods and solutions are restricted to simple geometries and to constant dispersion properties. In other words, they apply strictly to linear forms of the dispersion equations and the boundary conditions.[2] This can be a severe limitation, since the dye transfer during the dyeing is often markedly non-linear.

The solution of mathematical equations which more closely model experimental and practical situations is possible by the methods of numerical analysis. During the past half-century, the growth in power and availability of digital computers has led to an increasing use of realistic mathematical models in science and engineering. Numerical analysis of increasing sophistication has been needed to solve these more detailed mathematical models of the world.

The formal academic area of numerical analysis ranges from quite theoretical mathematical studies to computer science issues.[3] Recently, considerable developments have taken place in the subject of numerical analysis and in the construction of efficient computer programs to obtain numerical solutions. A detailed account of numerical analysis is beyond the scope of this book.

Simulating the dyeing process response of a circulating dye fluid can be accomplished by solving a set of partial differential equations. In many chemical engineering problems, the most realistic numerical simulations to date are those obtained by finite difference methods and finite element methods. These are described briefly in the following sections.

5.2.1 Finite difference methods

Finite Difference Method (FDM) is one of the methods used to solve differential equations that are difficult or impossible to solve analytically. The underlying formula is:

$$\frac{\partial p}{\partial x} = \lim_{\Delta x \to 0} \frac{p(x) - p(x - \Delta x)}{\Delta x} \qquad [5.1]$$

One can use the above equation to discretise a partial difference equation (PDE) and implement a numerical method to solve the PDE. For example, if it is required to calculate numerical solutions of the convection-dispersion-sorption equation (CDSE, see Eq. 3.41b, also shown below):

$$\frac{\partial c}{\partial t} = D_i \frac{\partial^2 c}{\partial x^2} - V_i \frac{\partial c}{\partial x} - \lambda_i \frac{\partial c_F}{\partial t} \qquad [5.2]$$

where the column efficiency is infinite (i.e. with D_i zero and $c_F = f_i(c_1, c_2, \ldots)$), the equation can be replaced by the finite difference equation (Eq. 5.3):

$$\frac{c_j^{n+1} - c_j^n}{\Delta t} + V_i \frac{c_j^n - c_{j-1}^n}{\Delta x} + \lambda_i \frac{c_{Fj}^{n+1} - c_{Fj}^n}{\Delta t} = 0 \qquad [5.3]$$

where n and j are the time and space indices, respectively, and Δt and Δx are the time and space increments. For this transformation, the solution domain is considered as an unbounded rectangular area of size $0 \le x \le 1$ and $t \ge 0$, as shown in Fig. 5.1.

The FDM is a very versatile modelling technique, which is comparatively easy for users to understand and implement. The FDM is a time-domain technique,

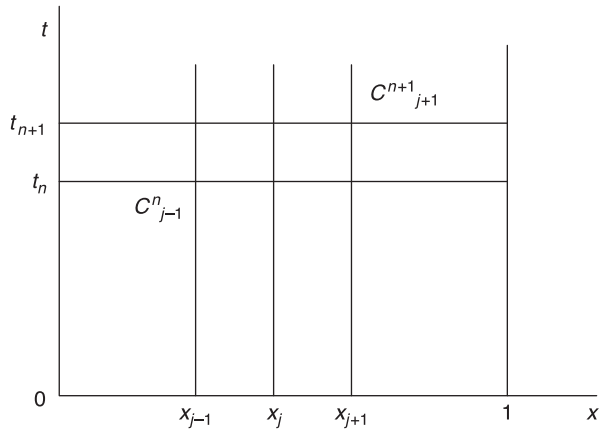

5.1 Mesh points for numerical solution using FDM.

which can find the concentration of dye everywhere in the computational domain at a given time frame.

Burley *et al.*,[4] Wai[5] and Vosoughi[6] solved their convective dye transfer model equations by the FDM and presented the results in the form of a number of graphs representing the variations in the concentration of dye at various points in the dyeing machine with time. Shannon *et al.*[7] used the finite difference method to obtain the solution of their flow model equations, which predicts pressure and velocity profiles based on user-defined package geometry, permeability profile and fluid properties. The FDM works well for their problems, which are two-dimensional models with simplified system geometries. For three dimensional models, non-linear situations and awkward geometries, however, the considerable increase in computational labour calls for simulation attempts based on more efficient methods.

5.2.2 Finite element methods

The Finite Element Method (FEM) is a numerical technique that gives approximate solutions to differential equations that model problems arising in physics and engineering.[8] As in simple finite difference schemes, the finite element method requires a problem defined in geometrical space (or domain) to be subdivided into a finite number of smaller regions (a mesh). In finite differences, the mesh consists of rows and columns of orthogonal lines (see Fig. 5.1); in finite elements, each subdivision is unique and need not be orthogonal. For example, triangles or quadrilaterals can be used in two dimensions (as shown in Fig. 5.2), and tetrahedrons or hexahedrons in three dimensions (see Fig. 5.3). Over each finite element, the unknown variables (e.g. concentration, velocity, etc.) are

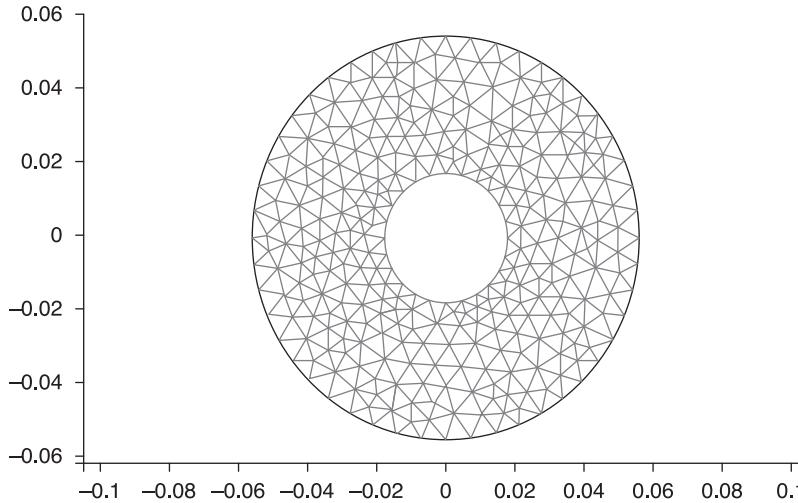

5.2 Mesh of yarn package for numerical solution using FEM in two dimensions.

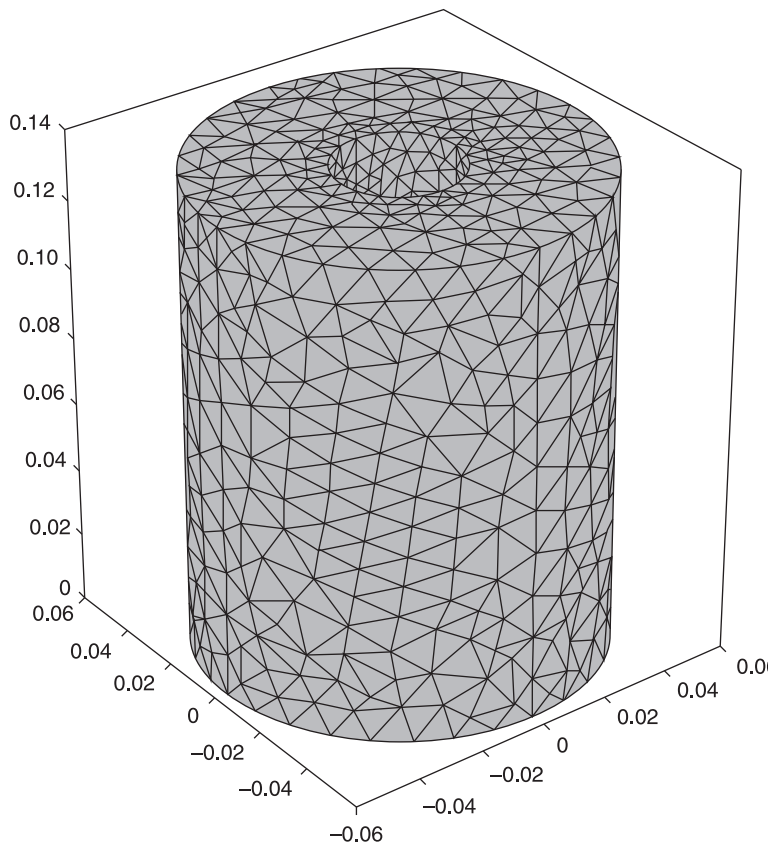

5.3 Mesh of a yarn package for numerical solution using FEM in three dimensions.

approximated using known functions; these functions can be linear or higher-order polynomial expansions that depend on the geometrical locations (nodes) used to define the finite element shape.

In contrast to finite difference procedures, the governing equations in the finite element method are integrated over each finite element and the solution summed ('assembled') over the entire problem domain. As a consequence of these operations, a set of finite linear equations is obtained in terms of a set of unknown parameters over each element. Solution of these equations is achieved using linear algebra techniques. Liggett and Liu[9] summarised the advantages of finite elements as follows:

- FEM is easier to conform to the physical geometry, whereas with finite differences the geometry is usually 'adjusted' to fit the grid spacing.
- The boundary conditions are easier to apply for geometrical reasons.
- It is easier to use variable grid spacing, whereby small elements are used in regions of interest or rapidly changing flow and large elements are used in regions of little interest or slowly changing flow.
- It is easier to write universal programs that apply to any geometry and a large number of physically different situations without having to change the code for each individual case.

The FEM, however, like any other method, has its weaknesses, which mainly include:

- The data input of the grid is time-consuming, although grid generation programs may substantially shorten this process.
- Computational times are long, especially for complex problems and three-dimensional problems.
- The analyst must find an element size such that the governing PDE is satisfactorily approximated everywhere.

The work described here uses the finite element method for its ability to efficiently resolve the non-linear phenomena with non-uniform grid mesh, the ease with which it handles variable boundary conditions, concentration-dependent coefficient, and its firm theoretical foundation. Although a complete 3-D FEM model is established, considering the computational capability of the present system, a 2-D FEM model is mainly used to do simulations. Based on this work, a 3-D FEM model simulation is quite straightforward. The following aspects are discussed in further detail:

- The developed FEM model, including numerical discrimination schemes, is employed with appropriate meshing to simulate and consider flow phenomena in the system.
- A complete FEM simulation system, including variable boundary conditions, is developed, and the non-linear mass transfer is incorporated.

5.2.3 MATLAB software

MATLAB is an integrated technical computing environment that combines numeric computation, advanced visualisation and a high-level programming language.[10] MATLAB was originally developed to be a matrix laboratory (MATrix LABoratory). Its capabilities have expanded greatly in recent years, and it is today among the leading tools for engineering computation. Because MATLAB commands are similar to the way engineering concepts are expressed in mathematics, writing computer programs in MATLAB is quicker than writing computer code in languages such as C/C^{++}. Also, MATLAB provides excellent graphics capability that is easy to use.

The MATLAB software consists of a basic package of mathematical routines as well as optional toolboxes that cover specific engineering application areas such as process control, optimisation, signal processing and symbolic mathematics. It also has a toolbox that makes available many of the Numerical Algorithms Group (NAG) routines. These routines are some of the best implementations of numerical methods that are currently available.[11] MATLAB offers a convenient computing environment for the solution of process simulation problems, and is used here.

5.3 Summary of the model equations

Flow property and mass transfer during dyeing may be described by a set of equations that are outlined as follows.

5.3.1 Flow equations

The flow of free liquor in the tube can be described by Eqs 4.45 and 4.46, summarised here:

$$-\eta\nabla^2 u + \rho(u\cdot\nabla)u + \nabla p = 0 \qquad [5.4]$$

$$\nabla\cdot u = 0 \qquad [5.5]$$

where η is the dynamic viscosity, ρ is the density, u denotes the velocity field and p is the pressure.

The flow of liquor through the porous package can be characterised by Darcy's law (Eqs 4.32 and 4.33) and Brinkman's equation (Eqs 4.36 and 4.37). These are also summarised as follows:

$$u_1 = -\frac{k}{\eta}\nabla p_1 \qquad [5.6]$$

$$\nabla\cdot u_1 = 0 \qquad [5.7]$$

$$u_2 = -\frac{k}{\eta}\nabla p_2 + \eta\nabla^2 u_2 \qquad [5.8]$$

$$\nabla \cdot u_2 = 0 \qquad [5.9]$$

where p_1, p_2, and u_1, u_2 are the pressure and the velocity vectors, when the flow in the porous package is described by Darcy's law and the Brinkman equation, respectively; k is the permeability of the porous package, and η represents the fluid viscosity.

5.3.2 Mass transfer equations

Differential mass balance of dye, considering both convective flow and dispersive flow of dye in the liquor, as well as the absorption by the fibres, results in the following equation:

$$\varepsilon \frac{\partial C_p}{\partial t} + (1-\varepsilon)\frac{\partial C_f}{\partial t} = -\nabla \cdot (UC_p) + \nabla \cdot (D \nabla C_p) \qquad [5.10]$$

The relationship between dye concentration at the surface of a fibre and in the liquor in contact with that point in the package at any time may generally be expressed by:

$$\frac{dC_f}{dt} = K_1 C^a (1 - bC_f) - K_2 C_f \qquad [5.11]$$

$$C_f = \frac{KC^a}{1 + bKC^a} \qquad [5.12]$$

where C_p, C_f are the concentrations of dye in liquor and on the fibres at time t, respectively, U is the flow velocity vector within the package, D is the dispersion coefficient, ε is the package porosity, K_1 is the adsorption rate constant, K_2 is the desorption rate constant, a, b are constants, and K $(=K_1/K_2)$ is the adsorption coefficient.

5.4 Numerical solutions of equations

5.4.1 Parameters used in simulation

The parameters listed in Table 5.1 were used to simulate the dyeing processes.

5.4.2 Fluid model equations

The coupling of free media flow with porous media flow is a common application in the field of chemical engineering. The most common way to deal with free and porous media flow in a system is to couple Darcy's law, which does not account for viscous effects, with the Navier–Stokes equations. However, depending on the pore size distribution of the porous media and the fluid properties, it is not always appropriate to neglect viscous effects. The Brinkman

Table 5.1 General parameter values used in simulation

Parameter	Value	Reference for estimation
Package		4.1
Inside radius	0.018 m	
Outside radius	0.056 m	
Height	0.136 m	
Porosity	0.5	
Permeability	$3.8e^{-11}$ m^2	3.9, 3.11
Dye liquor		
Density (30 °C)	996 kgm^{-3}	3.6
Viscosity (30 °C)	$7.98e^{-4}$ $N{\cdot}s/m^2$	3.6
Flow rate	20–60 l/kg.min	3.19

equations account for momentum transport through viscous effects and through pressure gradients in porous media and could be considered an extension of Darcy's Law.[12]

The flow of dye liquor in an open channel (tube) and in a porous package was coupled here in an attempt to demonstrate the combined features of flow within the system. The flow is described by the Navier–Stokes equation in the free region, and the Darcy's law and Brinkman equations in the porous region.

System geometry

The system studied in the flow model is a 2-D cross-section of the tube with a layer attached to the porous yarn package (see Figs 4.5 and 5.4). The flow enters the tube with a uniform velocity profile over the simulation time.

Boundary conditions

The modelled domain and the notations for the boundary conditions are shown in Fig. 5.4.

The boundary conditions for the Navier–Stokes equations are as follows:

$u \cdot n = 0$	symmetrical boundary
$u \cdot n = u_0$	inlet
$u = 0$	no slip
$p = p_1$	N-S/Darcy boundary
$p = p_2$	N-S/Brinkman boundary

The pressure at the outlet is set to zero, as reference. The expression for the pressure at the boundary between the channel and the porous domain states that the pressure is continuous across this interface.

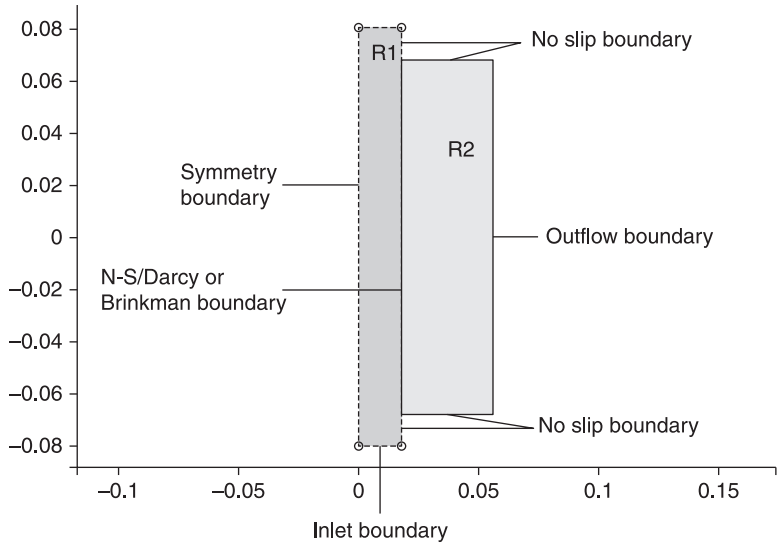

5.4 The modelled domain and the notations for the boundary conditions in flow model.

The corresponding boundary conditions for Darcy's law are:

$u_1 = 0$	no slip
$u_1 \cdot t = 0$	outlet
$p_1 = 0$	outlet
$u_1 = u$	N-S/Darcy boundary

The corresponding boundary conditions for the Brinkman equations are:

$u_2 = 0$	no slip
$u_2 \cdot t = 0$	outlet
$p_2 = 0$	outlet
$u_2 = u$	N-S/Brinkman boundary

These conditions imply that the components of the velocity vector are continuous through the interface between the channel and the porous domain.

Mesh

The starting point for the finite element method is a mesh that is a partition of the geometry into small units of a simple shape. In a two-dimensional domain, the physical (or problem) domain is subdivided into sub-regions, or elements. Many polygonal shapes can be used to define the elements. The simplest geometric structure that easily accommodates irregular surfaces is the triangle, and it is one of the most popular element shapes used today.

The selected element of choice here is a triangle consisting of three vertex nodes. Knowing where to optimally place and size the elements is more an art than a science. In general, one places more elements in those regions of the physical domain where functions are expected to change rapidly. Elements that are equilateral in shape are more accurate than long, narrow triangular elements. This is a consequence of the fact that the error $e(x)$ in a finite element approximation behaves like:[8]

$$|e(x)| \leq ch^{n+1}$$

where c is a constant, n is the order of interpolation polynomial and h is the distance between nodes. Mesh generation may take several 'trials' before a suitable mesh is obtained. Solutions of non-linear equations, particularly those dominated by flow and convection, may require several remeshings before an appropriate solution is obtained.

In order to resolve the velocity profile close to the interface between the open channel and the porous domain, a finer mesh is required at this boundary. The final mesh result is illustrated in Fig. 5.5 and Table 5.2.

5.4.3 Mass transfer model equations

For the numerical solution of the mass transfer model equations using the finite element method, the system must first be clearly defined. The finite element method is based on the numerical approximation of the dependent variables at a specific nodal location, where a set of simultaneous linear algebraic equations is produced that can be solved either directly or iteratively.

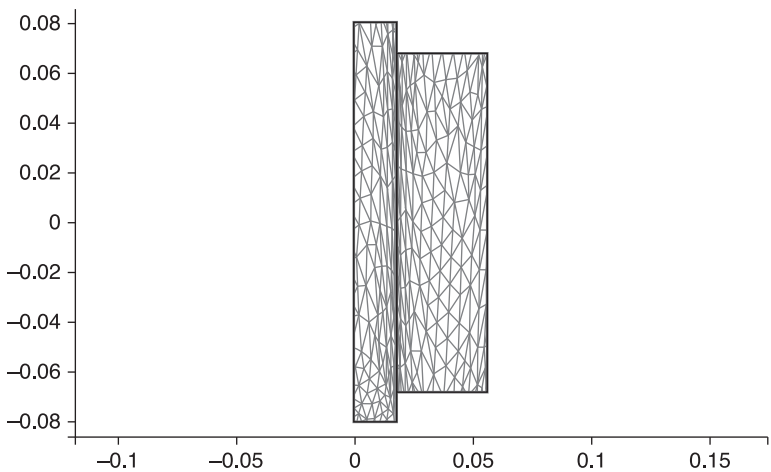

5.5 Mesh for flow model system.

Table 5.2 Statistics of mesh for flow model

Extended mesh	
Number of degrees of freedom	9108
Base mesh	
Number of nodes	976
Number of boundary elements	155
Number of elements	1886
Maximum element area: $5.10744e^{-005}$ for element	260
Minimum element area: $4.52643e^{-007}$ for element	1854
Iterative tolerance	$1e^{-6}$

System geometry

Two shapes of geometries are involved for the mass transfer model. One is a rectangle, which is the cross-section of the package in the axis direction, shown in Fig. 4.5, and the other is a circular shape, which is the cross-section of the package in the radius direction, shown in Fig. 5.2. For the rectangular geometry, since it was assumed that the package properties between layers in axis direction of package are the same, the mass transfer model equations can be solved in one dimension with time. This method greatly reduces calculation time.

Boundary conditions

In porous packages, or for dispersion-driven membrane processes, which are not subjected to pressure variations, it is often possible to neglect the convective component of the flux vector. This simplifies the flux expression by limiting it to transport by dispersion.

The equations below represent the boundary conditions involved in the mass transfer model equations.

$$J_x \cdot n = v(C - C_1) \qquad [5.13]$$

$$J_x \cdot n = 0 \qquad [5.14]$$

$$J_x \cdot n = f_0(t) \qquad [5.15]$$

The first expression (shown in Eq. 5.13) sets a flux at the boundary. The condition requires that the flow conditions and concentration in the bulk outside the boundary are known. Equation 5.14 represents an impervious boundary and states that the flux is zero across this boundary. Equation 5.15 states that the flux through a boundary is given by an arbitrary function f_0. This condition can be used to model the integration dyeing, or stepwise addition and fixation of dye, where the boundary represents the surface of a package and f_0 is the expression for dosing.

Mesh

Figures 5.6 and 5.7 show the mesh results for both shapes of geometry for the mass transfer model. The details of the meshes are given in Tables 5.3 and 5.4.

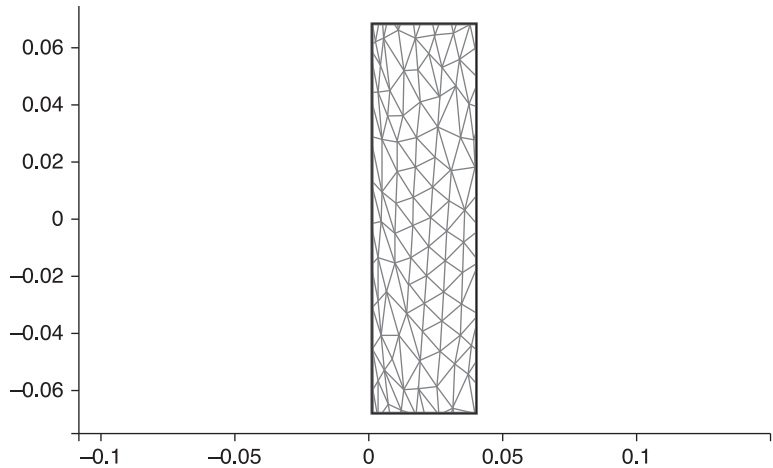

5.6 Mesh for mass transfer model (rectangle geometry).

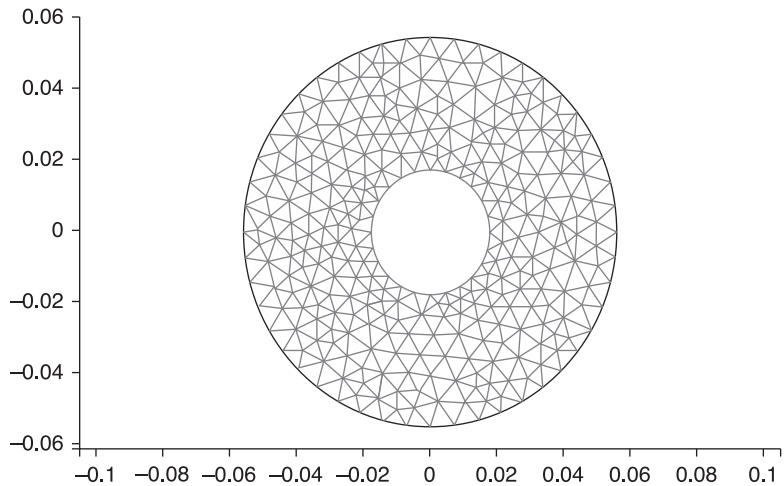

5.7 Mesh for mass transfer model (circular geometry).

Table 5.3 Statistics of mesh for mass transfer model (rectangle geometry)

Extended mesh	
Number of degrees of freedom	493
Base mesh	
Number of nodes	134
Number of boundary elements	40
Number of elements	226
Maximum element area: $4.18872e^{-005}$ for element	85
Minimum element area: $9.07971e^{-006}$ for element	210
Iterative tolerance	$1e^{-6}$

Table 5.4 Statistics of mesh for mass transfer model (circular geometry)

Extended mesh	
Number of degrees of freedom	3216
Base mesh	
Number of nodes	424
Number of boundary elements	88
Number of elements	760
Maximum element area: $2.96813e^{-005}$ for element	272
Minimum element area: $1.84878e^{-006}$ for element	702
Iterative tolerance	$1e^{-6}$

Based on the above defined geometry, boundary conditions and mesh of the system, the equations of flow model and mass transfer model can be solved.

5.5 References

1. Ramirez W. (1997), *Computational Methods for Process Simulation*, 2nd edn, Reed Educational & Professional Publishing Ltd.
2. Levich V. (1962), *Physicochemical Hydrodynamics*, Prentice-Hall, Inc.
3. Van Hentenryck P., Michel L., Deville Y. (1997), *Numerica A Modeling Language for Global Optimization*, The MIT Press.
4. Burley R., Wai P.C., McGuire G.R. (1985), 'Numerical simulation of an axial flow package dyeing machine' *Appl. Math. Modelling*, **9**, 1, 33–9.
5. Wai P.P.C. (1984), 'Dynamic behaviour of a reactive packed bed adsorption system' PhD Thesis, Heriot-Watt University, UK.
6. Vosoughi M. (1993), "Numerical simulation of packed bed adsorption applied to a package dyeing machine" PhD Thesis, Heriot Watt University, UK.
7. Shannon B., Hendrix W., Smith B., Montero G. (2000), 'Modeling of supercritical fluid flow through a yarn package' *Journal of Supercritical Fluids*, **19**, 1, 87–99.
8. Pepper D., Heinrich J. (1992), *The Finite Element Method*, Hemisphere Publishing Corporation.

9. Liggett J., Liu P. (1983), *The Boundary Integral Equation Method for Porous Media Flow*, George Allen & Unwin Ltd.
10. http://www.mathworks.com, accessed 9 April 2014.
11. Zhang Z., Yang Z. (1997), *Master Matlab*, Beijing Air and Space University Press (in Chinese).
12. Bear J. (1972), *Dynamics of Fluids In Porous Media*, American Elsevier, New York.

6

Simulation of the dyeing process

DOI: 10.1533/9780857097583.114

Abstract: The results of the simulation of the package dyeing process based on various models are presented. Darcy's law assumes that the only driving force for flow in a porous medium is the pressure gradient, and the global transport of momentum by shear stress in the fluid is negligible. Brinkman's equations extend Darcy's law to include the viscous transport in the momentum balance and the velocities in the spatial directions as dependent variables. These models, also including the effect of flow velocity and direction, package permeability and dye dosing profiles on dye distribution, are described and their validity examined.

Key words: dynamic mass transfer in dyeing, convection factors, flow velocity integration dyeing.

6.1 Introduction

Based on the model equations derived in Chapter 4, and numerical methods introduced in Chapter 5, the results of computer simulation of dyeings of textile packages are presented and discussed in this chapter. The results are mainly presented in graphical forms.

6.2 Fluid flow behaviour in dyeing

As discussed in Chapter 3, the fluid dynamic behaviours of process liquor flow in a yarn package affect the levelness of the resulting dyed packages. Thus, understanding flow through a yarn package is vital to achieving level treatments in wet processes.

6.2.1 The effect of shear stresses on global transport of momentum in the fluid

Fluid flow in practical dyeing processes, including package dyeing, is assumed to be streamline in nature and is often described by Darcy's law. Despite the fact that there is no theoretical evidence to prove this behaviour, researchers claim that model predictions generally show good agreement with experimental data.

In most package dyeing machinery the dye liquor is pumped through the tube and the yarn assembly of the package, which consists of a three-dimensional shape with the interstitial space filled with the dye liquor (as schematically shown in Fig. 4.2). The flow is from the (vertical) tube to the yarn assembly (parallel). It

remains unclear whether the global transport of momentum by shear stresses in the fluid is negligible. Darcy's law assumes that the only driving force for flow in a porous medium is the pressure gradient, and the global transport of momentum by shear stress in the fluid is negligible. To investigate the dyeing process, it is important to obtain a better understanding of flow through the yarn package, and the influence of shear stress on flow property.

Plate I (see colour section between pages 116 and 117) shows the flow velocity distribution in both tube and yarn assembly, where the flow in porous media (yarn package) is described by Darcy's law. The colour and the length of the white arrow denote the magnitude of the velocity; the white arrows indicate the velocity direction. A velocity direction change across the interface between the tube and yarn assembly is evident. The velocities here are defined for x and y directions in a two-dimensional model. However, based on the assumptions used in Darcy's law, which simply ignore the influence of the shear stress, Equation 4.35 is used to define the boundary.

Figure 6.1 demonstrates the velocity distribution across the cross-section of the tube and yarn assembly (see Plate I, line y = 0). The resulting graph shows that the velocity is not continuous across the interface between the tube and yarn assembly. This indicates that a considerable change in the velocity of flow suddenly occurs in a region comparatively close to the surface of the yarns.

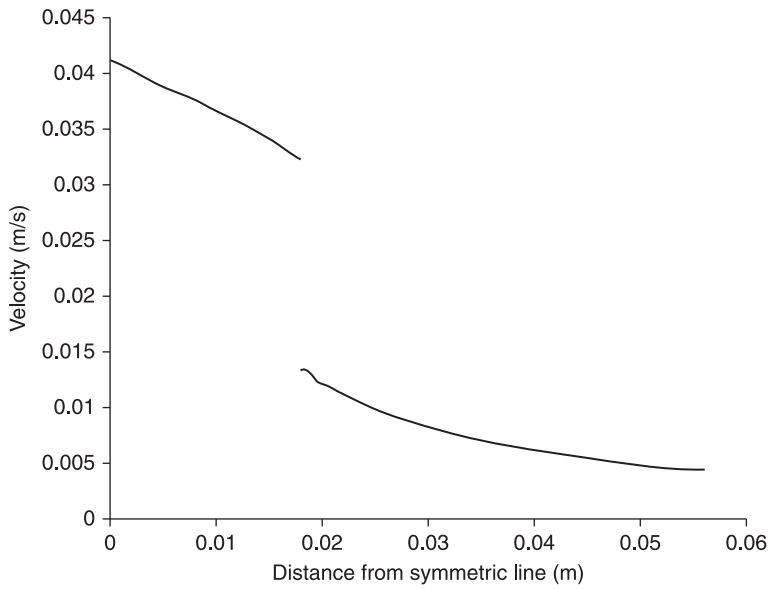

6.1 The distribution of flow velocity in the cross-section (see Plate I, line y = 0) of tube and yarn bobbin, where the flow in the porous medium is described by Darcy's law.

To investigate the influence of shear stress on the flow behaviour throughout the package, Eqs 4.36 and 4.37, combined with proper boundary conditions as defined by Eqs 4.38–4.41, can be solved using Brinkman's approach for fluid in porous media.

It can be seen from Plate II that the velocity in both magnitude and direction has a similar distribution to that shown in Plate I, when introducing the same inflow rate (0.1 m/s) as the simulation in Plate I. The detail of the velocity profile can be seen in Fig. 6.2.

Figure 6.2 shows that the velocity is almost continuous across the interface between the tube and yarn assembly, with a sharp decrease just before the surface of the porous package. In addition, the velocity distribution in the tube phase is fluctuating, indicating different flow features, which is probably closer to reality compared with that shown in Fig. 6.1. However, the velocity distribution in yarn assembly phase is almost the same as specified in Fig. 6.1.

This is an important observation, indicating that, using the conditions employed in the simulation, the shear stress has a very weak influence on flow properties within the yarn assembly. It is shown that the use of Darcy's law to define the flow of dyeing liquor across the yarn package is quite reasonable. This also indicates that the flow rate within the yarns is quite low. Since, in practice, in a package dyeing machine the boundaries 3, 4, 6, 7 and 8 do not strictly follow the no-slip

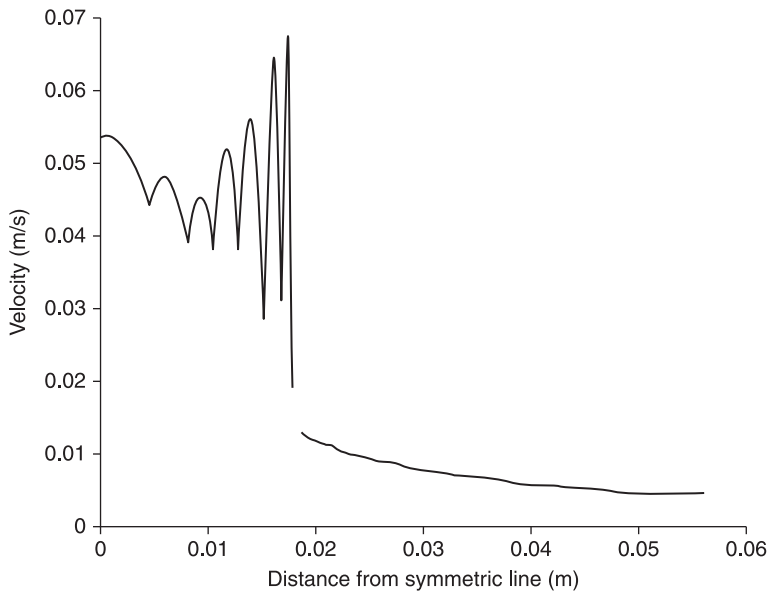

6.2 The distribution of flow velocity in the cross-section (see Plate I, line y = 0) of tube and yarn bobbin, where the porous medium is described by Brinkman's equation.

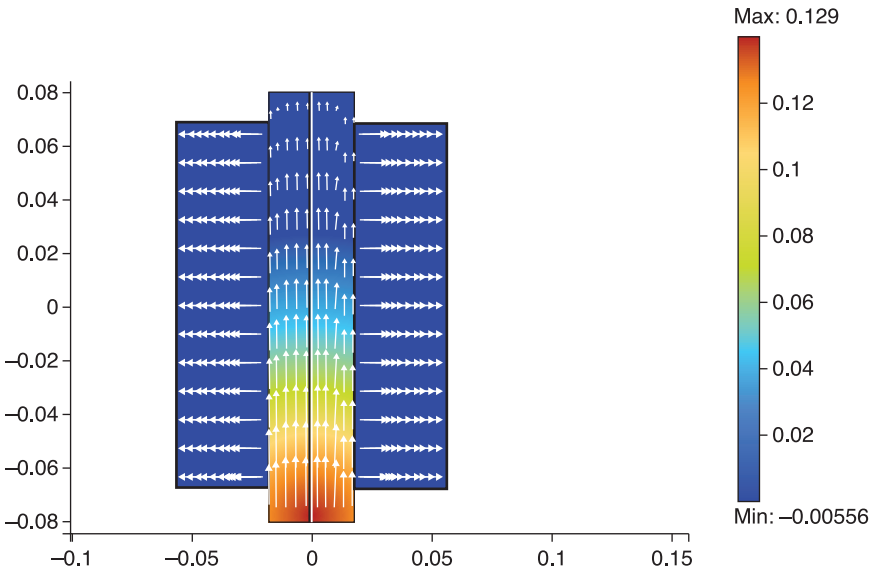

Plate I (Chapter 6) The distribution of flow velocity in tube and yarn bobbin, where the flow in porous media is described by Darcy's law.

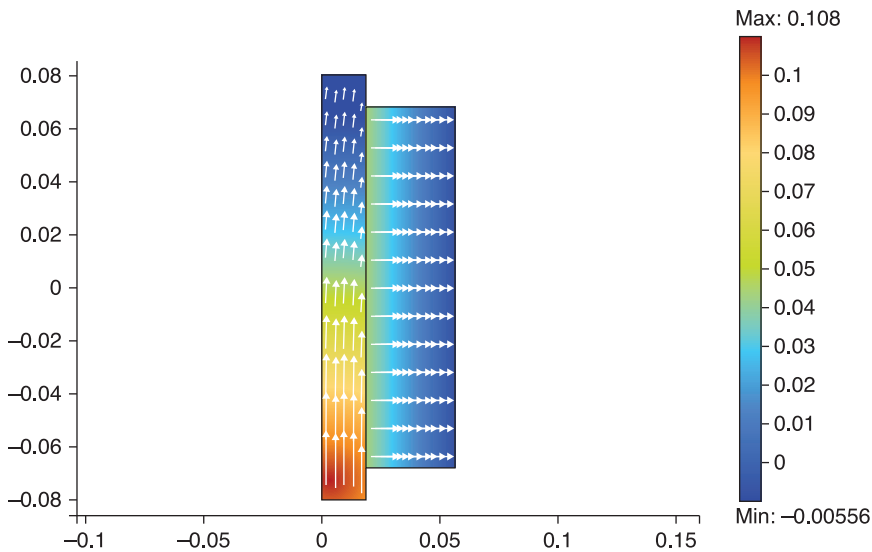

Plate II (Chapter 6) The distribution of flow velocity in tube and yarn bobbin, where the flow in porous media is described by Brinkman's equation.

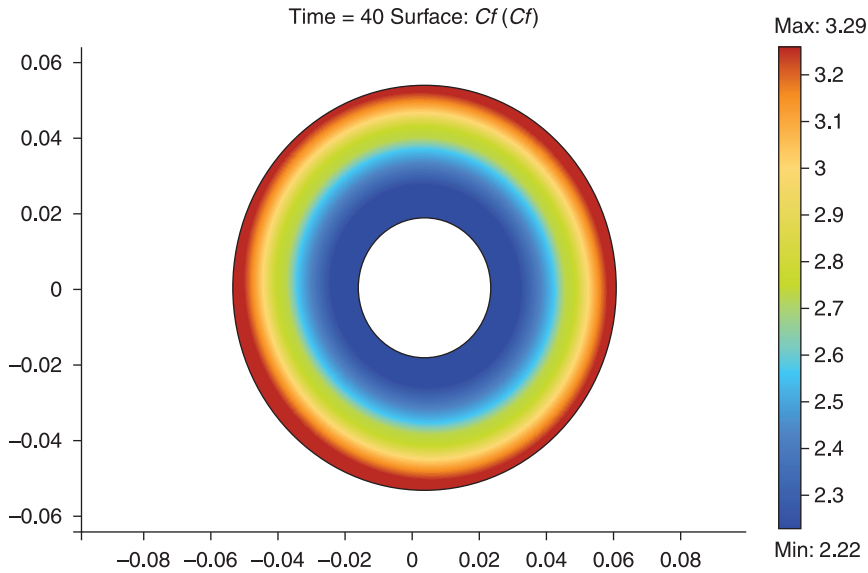

Plate III (Chapter 6) Dye distribution for the out-to-in flow direction.

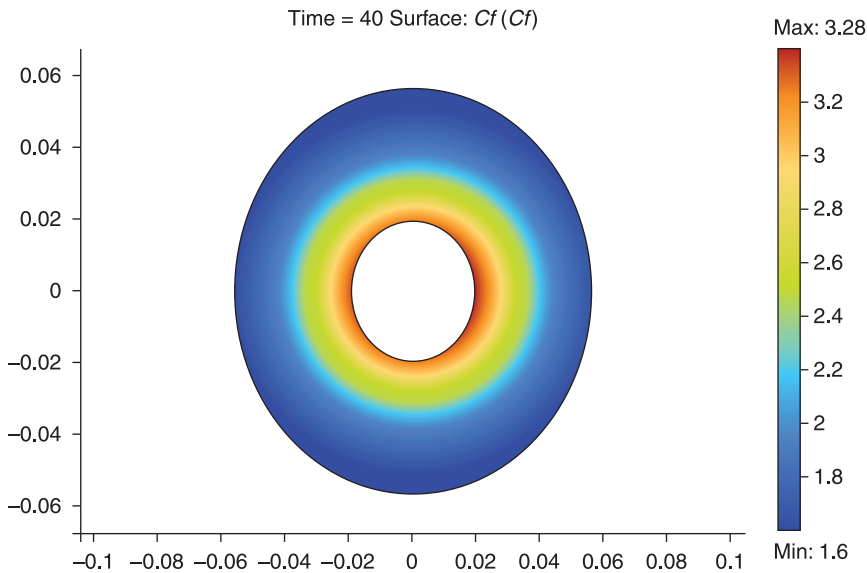

Plate IV (Chapter 6) Dye distribution for the in-to-out flow direction.

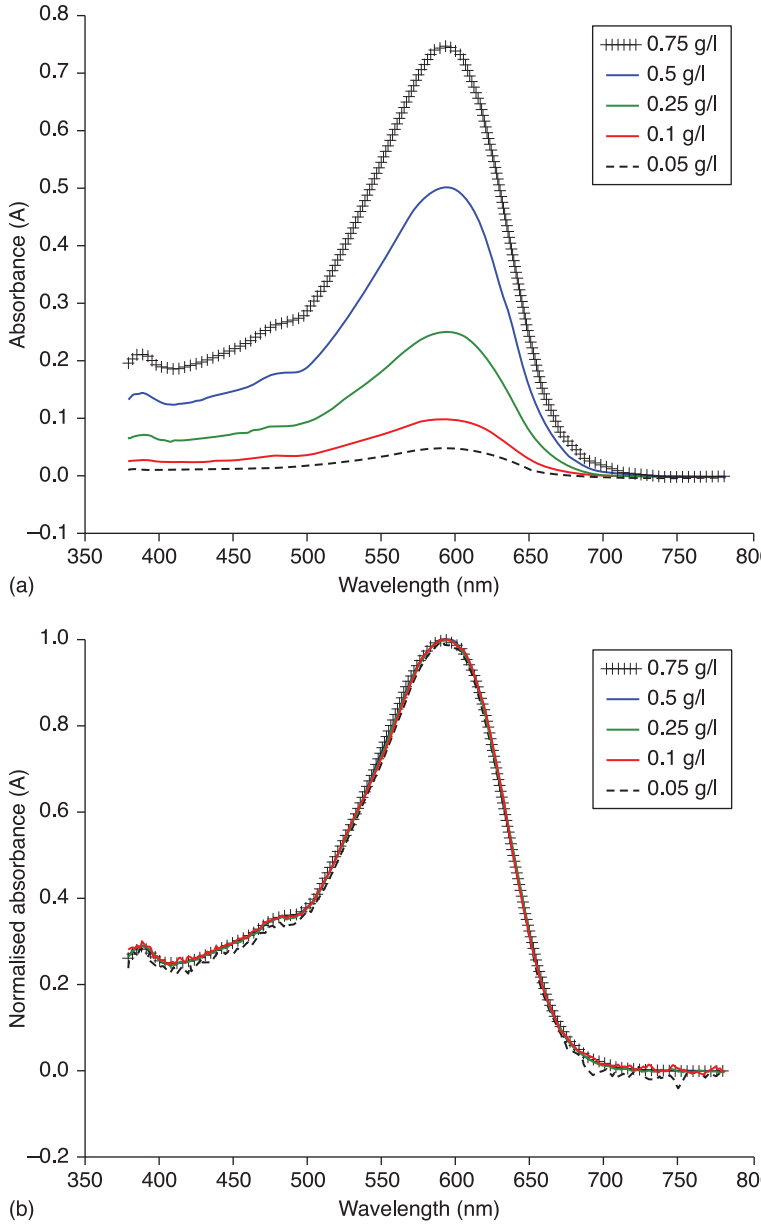

Plate V (Chapter 8) Actual and normalised spectra of Remazol Black. (a) Actual dilution spectra. (b) Normalised dilution spectra.

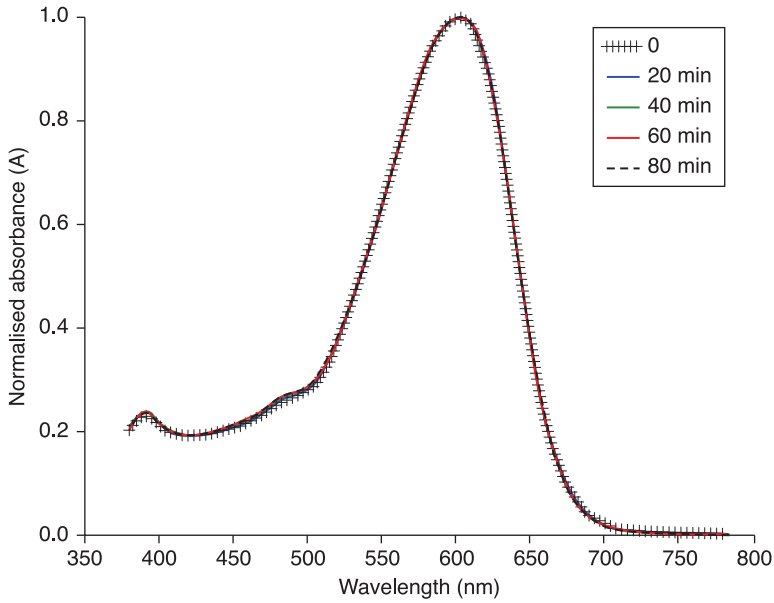

Plate VI (Chapter 8) Normalised spectrum of the dyebath during Reactive Black 109 dyeing.

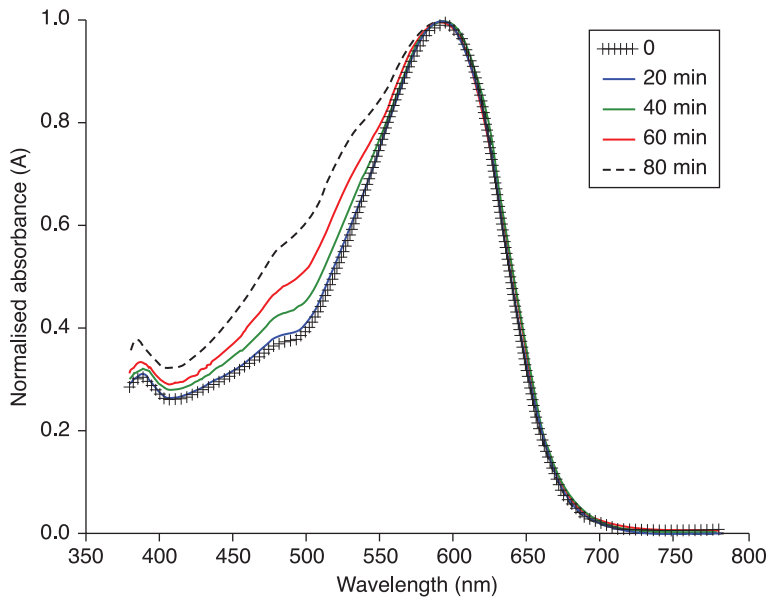

Plate VII (Chapter 8) Spectrum of the dyebath for Remazol Black reactive dyeing. The change in shape is due to spectral morphing.

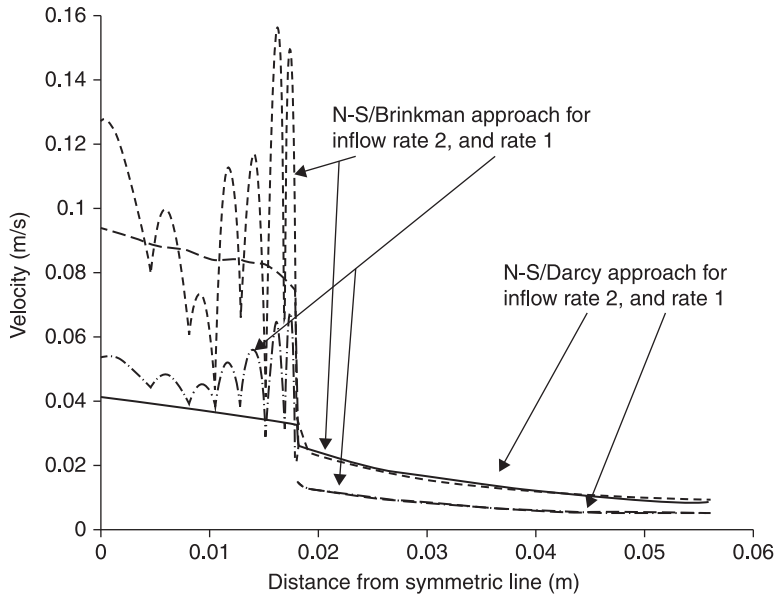

6.3 Comparison of N-S/Brinkman and N-S/Darcy approaches.

condition, this can lead to even lower velocities in the porous media than the results of this simulation suggest. Figure 6.3 further demonstrates the validity of Darcy's law when different flow rates are applied within a selected range.

In Fig. 6.3, the solid line and the dashed line denote the flow velocity at a flow rate of 0.1 m/s and 0.2 m/s, respectively, using N-S/Darcy's approach. The dot-dashed line and dotted line denote the flow velocity at a flow rate of 0.1 m/s and 0.2 m/s, respectively, using N-S/Brinkman's approach. This figure shows that the profile of the dyeing liquor flow within the tube for the N-S/Brinkman approach is fluctuating, while when N-S/Darcy's method is employed it is quite stable for both flow rates. The flow velocity within the yarn assembly, however, at both inflow rates, is almost the same using N-S/Brinkman and N-S/Darcy's approach.

Figure 6.4 uses the same simulation result as that shown in Fig. 6.2, with the fluid flow velocity profiles, where the flow in the porous package is defined by the Brinkman equation, but at different cross-section lines along the package. The solid line is the same as that in Fig. 6.2, i.e. the middle of the package (Plate I, $y=0$), the dotted line is near the top of the package ($y=0.06$) and the dashed line is near the bottom of the package ($y=-0.06$).

It is clear from Fig. 6.4 that, although the velocity profiles within the free liquor (tube) are different from those at different cross-section lines, the velocity profiles within the porous package are almost the same as those at different cross-section lines. This implies that the pressure distributions, rather than the flow velocity

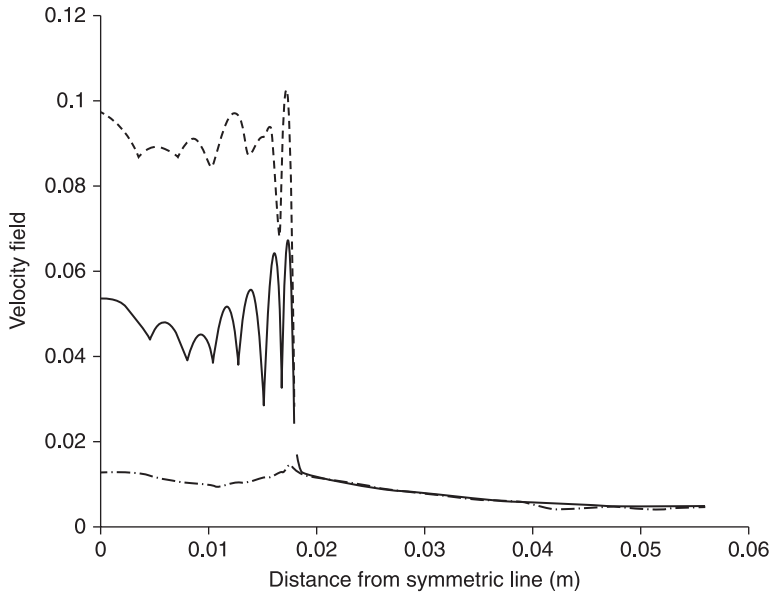

6.4 Velocity profiles in different cross-section lines (see Plate I, y=0.06, 0, and –0.06), where the flow in the porous package is defined by Brinkman's equation.

distributions, within the free liquor dominate the flow velocity distributions within the porous package, although the Brinkman approach accounts for the viscous transport in the momentum balance and introduces the velocities in the spatial directions as dependent variables. This result also proves the validity of Darcy's law to define the flow within the porous package under the conditions of the parameter ranges used in this simulation, since it agrees with the assumption of Darcy's law that the only driving force for flow in a porous medium is the pressure gradient.

The parameters used in the simulation are based on typical practice in package dyeing, i.e. the flow rate is not too high and the permeability of the package is very low. Under such conditions, the numerical simulation results prove that the momentum transport by shear stresses can be ignored; thus, Darcy's law is a reasonable approach to model the flow properties. This result is well known in this field, but here it is demonstrated on the basis of a sound mathematical model.

6.2.2 Effect of flow rate on the fluid flow velocity within the package

In order to consider the effect of convective dispersion of dye during the dyeing on levelness, the velocity of the fluid at any point and any time is required.

However, measurement of flow at different parts of porous packages of various shapes is practically impossible. In addition, solving mathematical equations governing fluid flow in porous media of complex shapes is very difficult.

The mathematical model presented in Chapter 4 offers the possibility of describing the flow velocity distribution within the package during the dyeing. Figures 6.5 and 6.6 demonstrate the velocity distribution across the cross-section of the tube and yarn assembly (see Plate I, line y = 0), under different liquor inflow rates, where the flow in porous media is described by Darcy's law and Brinkman's equation, respectively.

In Figs 6.5 and 6.6, the solid lines denote the flow velocity at a flow rate of 0.1 m/s, while the dot/dashed lines denote the flow velocity at a flow rate of 0.2 m/s. These figures show that, for both the Darcy's law and Brinkman equation approaches for defining the flow behaviour within the porous package, the higher the inflow rate provided, the higher velocity is gained in the yarn assembly, but a less even distribution of the flow velocity across the package will be obtained. In addition, a higher flow rate causes a more fluctuating flow in the tube, subsequently increasing the influence of shear stress on flow properties, which is probably one of the reasons explaining the initial strike.

In practice, the flow velocity within the yarn assembly can be increased by increasing the inflow rate (see Fig. 4.7, boundary 2). However, since a higher flow

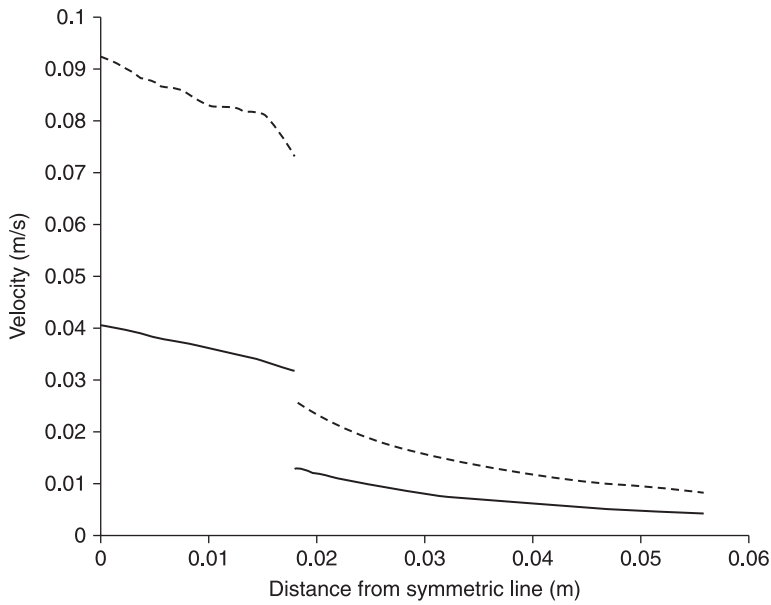

6.5 Fluid velocity distributions across the cross-section of the tube and yarn assembly (see Plate I, line y = 0), under different liquor inflow rates, where the flow in porous media is described by Darcy's law.

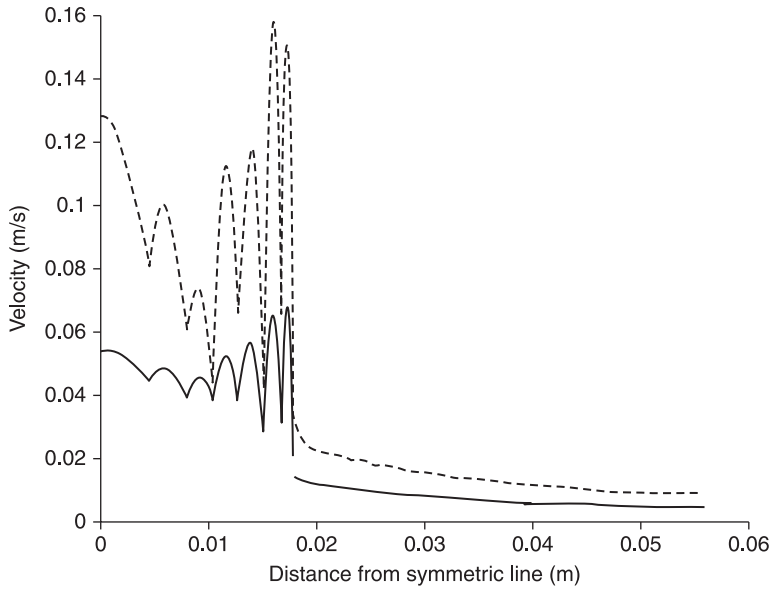

6.6 The velocity distribution across the cross-section of the tube and yarn assembly (see Plate I, line y = 0), under different liquor inflow rates, where the flow in porous media is described by Brinkman's equation.

rate will lead to an uneven distribution of flow velocity through the yarn assembly, and an even distribution of flow velocity is important to achieve a level dyeing, a high flow rate is not used.

The velocity distributions across the different cross-sections of the tube and yarn assembly (see Plate I, line $y \neq 0$) may have different features, while having similar velocity profiles within the porous package.

6.2.3 Relationship between the flow rate and liquor pressure

The flow model presented in this work can not only output the profile for velocity of the flow within the yarn package; it can also output the profiles for pressure throughout the package directly. The measurement of flow velocity in different parts of porous packages is practically not possible, while the measurement of pressures inside and outside the package is quite convenient. In order to validate the numerical flow model results, the relationship between the flow rate and liquor pressure throughout the system is required.

Figures 6.7 and 6.8 demonstrate the pressure distribution across the cross-section of the tube and yarn assembly (Plate I, line y = 0), under the liquor inflow rates of 0.1 m/s and 0.2 m/s, where the flow in porous media is described by

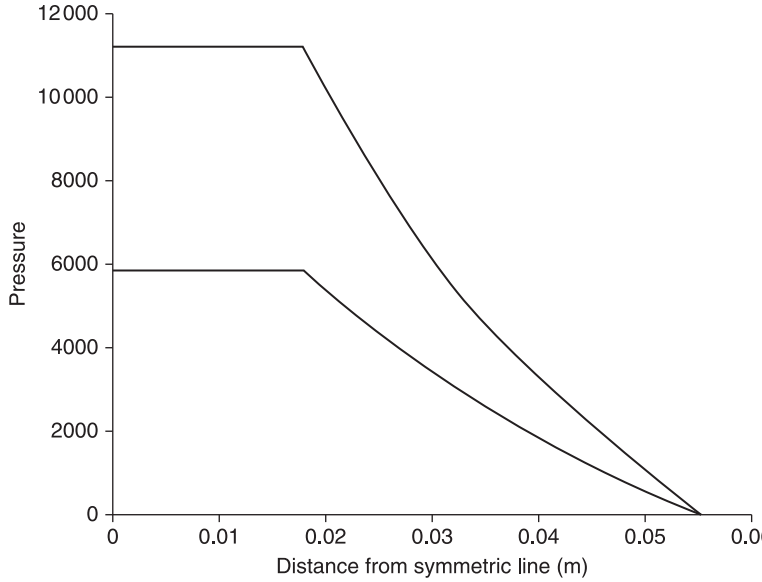

6.7 The pressure distribution across the cross-section of the tube and yarn assembly (see Plate I, line y=0), under different liquor inflow rates, where the flow in porous media is described by Darcy's law.

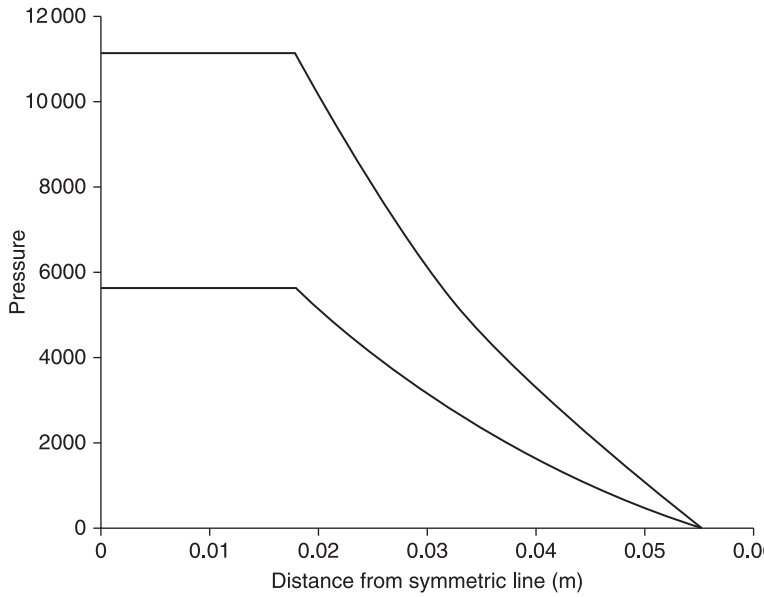

6.8 The pressure distribution across the cross-section of the tube and yarn assembly (see Plate I, line y=0), under different liquor inflow rates, where the flow in porous media is described by Brinkman's equation.

Darcy's law and by the Brinkman equation, respectively. It can be seen that, in both approaches, the pressure profiles within the free liquor (tube) are quite stable and almost constant under the different inflow rates; the pressure profiles within the porous package decrease almost linearly at the different inflow rates.

This simulation result for pressure profiles further demonstrates the validity of Darcy's law for defining fluid flow in a porous package, under the selected range of flow rate and package permeability, which meet the assumptions made for Darcy's law. These results can be also used for the design of package dyeing apparatus, such as the selection of tube materials based on static pressure prediction under different flow rates, and flow meter and pressure sensor selection based on their simulation range.

6.2.4 Effect of package dimension

The effect of package thickness on the flow velocity profile can be seen in Figs 6.9 and 6.10.

In Fig. 6.9, the tube diameters were kept constant; the package thickness was both increased and decreased 20% from the standard package thickness. The solid lines represent the velocity profile when the package thickness is 0.0304 m, while the dashed lines represent the velocity profiles when the package thickness is 0.0456 m. The results show that there is no clear difference in the flow velocity

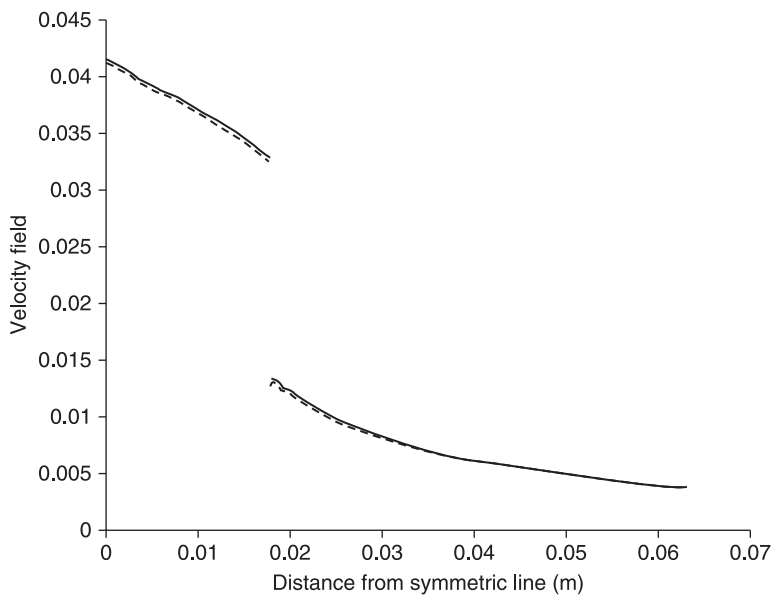

6.9 Flow velocity profiles for different package thicknesses where the inflow rate and tube size are kept constant.

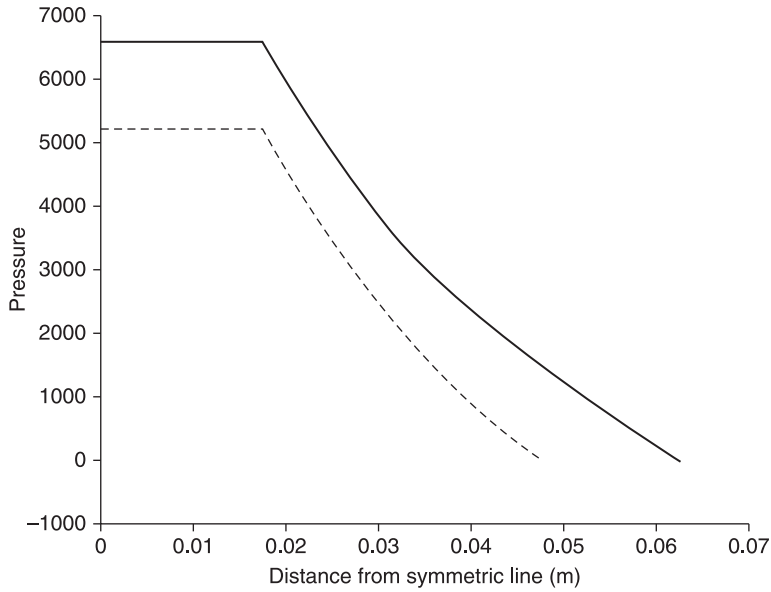

6.10 Pressure profiles for different package thicknesses where the inflow rate and tube size are kept constant.

profiles when the package thickness is changed and the inflow rate and tube diameter remain constant.

This result implies that a slight change in package thickness (for example, 20%) does not affect the flow behaviour in both free liquor (tube) and porous package by changing the pressure drop within the system. This conclusion is demonstrated in Fig. 6.10, which shows the change in pressure within the tube and porous package when changing the thickness of the package. The solid lines represent the pressure profile when the package thickness is 0.0456 m, while the dashed line represents the pressure profiles when the package thickness is 0.0304 m. It can be seen that the pressure within the system will increase with an increase in the package thickness to keep the flow rate through the porous package constant.

Figure 6.11 is the simulation result of the velocity field profile for different tube diameters, while the package thickness is kept constant.

In Fig. 6.11, the package thickness and inflow velocity were kept constant, and different tube diameters were used. The solid line is the same as that in Fig. 6.1, while the dashed line represents the velocity profiles under the same parameters as those used in Fig. 6.1, but with a 20% larger tube diameter. The result shows that a higher velocity field in both the tube and porous package is obtained when the tube diameter is increased. The increase of the velocity field, however, is not directly caused by the increase of the tube size, but by a higher flow rate, to keep

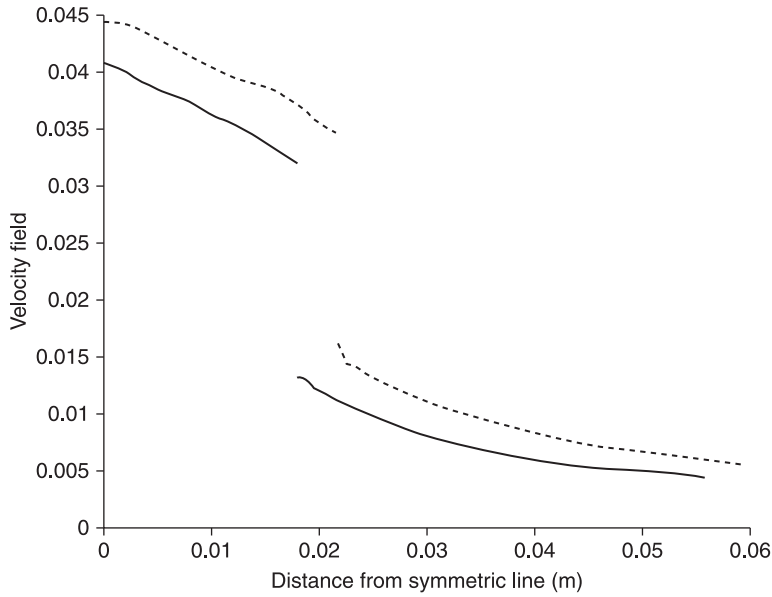

6.11 Flow velocity profiles for different tube diameters.

the inflow velocity constant. This result is consistent with that of Section 6.1.2: i.e. a higher flow rate causes a higher velocity field distribution throughout the package.

6.2.5 Effect of package permeability

Differences in yarn package density result in porosity and permeability variations, which directly affect flow behaviour within the package. Denton addressed this correlation for cotton yarn packages.[1] Porosity–permeability correlations for other types of fibrous porous media are also available from the literature.[2–3]

As has been discussed before, Darcy's law is only valid under the condition of low permeability of the porous package. However, there is no quantitative information (how low the permeability should be) available in the literature. Present work on this aspect aims to find a permeability range in which Darcy's law is valid.

In Fig. 6.12, there are four lines representing the fluid flow velocity field distribution in both free liquor and porous package at the cross-section of $y=0$. The parameters in Table 5.1 are used, but with different permeabilities of the package, i.e. 3.8×10^{-11}, 1×10^{-10}, 3.6×10^{-9} and 3.8×10^{-9} (m^2). The flow within the porous package is defined by Darcy's law.

It can be seen from Fig. 6.12 that the velocity field profiles within the tube (free liquor) and porous package are almost the same for the different package

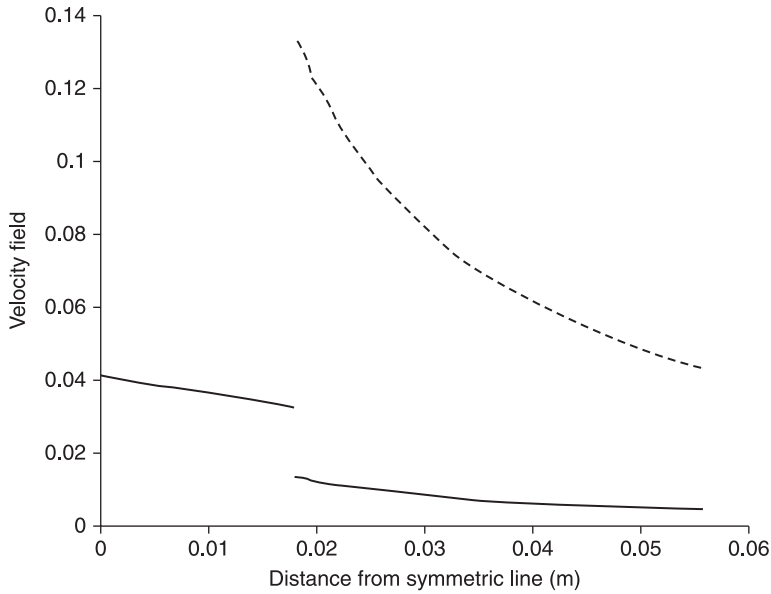

6.12 The velocity field distribution under different package permeability.

permeabilities, if the permeability is less than 3.6×10^{-9}. This is because, if the inflow rate is kept constant, increasing the package permeability will cause a decrease of pressure drop across a package (see Fig. 6.13).

When the package permeability is slightly higher (for example, 3.8×10^{-9}), Fig. 6.13 shows that the velocity field profile within the tube remains the same; however, within the porous package it is dramatically changed (dashed line). In this case the velocity field profile becomes unreasonably larger than it should be, implying that Darcy's law is no longer valid to describe the flow behaviour for packages with very high permeability.

Figure 6.13 demonstrates the pressure profiles when the package permeability changes. The solid line, dash-dotted line, dotted line and dashed line represent the pressure profiles through both tube and porous package at the cross-section of $y = 0$, under different package permeability values: 3.8×10^{-11}, 1×10^{-10}, 3.6×10^{-9} and 3.8×10^{-9} (m^2), respectively. Numeric results show that the pressure drop decreases with increasing package permeability. However, there is an exception when package permeability is 3.8×10^{-9} (dashed line), where the pressure is higher than that when package permeability is 3.6×10^{-9} (dotted line). This behaviour further shows that for the current simulation Darcy's law becomes invalid when the package permeability is high (e.g. 3.8×10^{-9}).

It should be noted that the value of the fluid flow pressure at each side of the package can be measured, and the measurements can be easily used to verify the

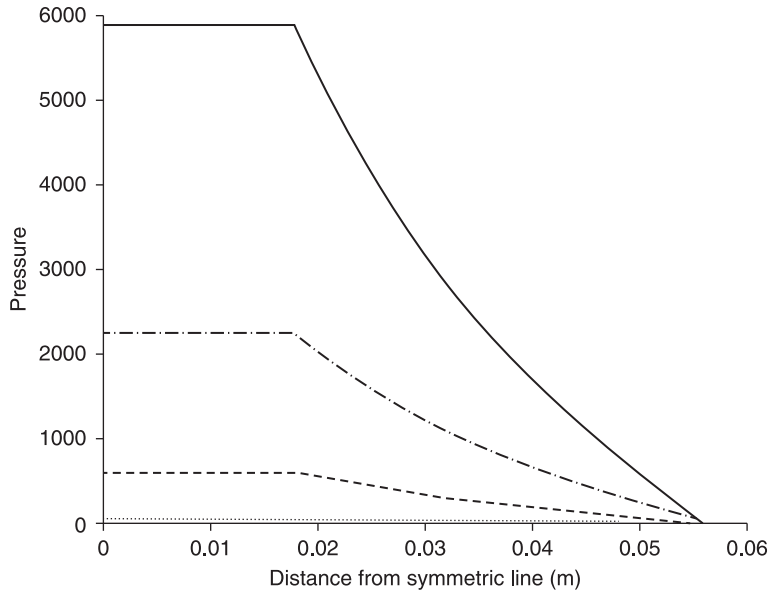

6.13 Pressure profiles under different package permeability.

model. For example, numerical simulation showed that when the package permeability is 3.6×10^{-9} the general trend (i.e. the pressure drop is decreased with an increase in package permeability) is valid, but pressures less than 100 Pa may not be realistic in practice, which implies that Darcy's law in practice may be valid in a smaller package permeability range than those implied in the numerical simulation.

Figure 6.14 compares the difference in flow velocity distribution through the package when the package permeability is 3.8×10^{-9} and the flow in the porous package is described by Darcy's law (the dashed line) and Brinkman's equation (solid line). The dashed line shows the same result as the previous two, that when the package permeability is higher than 3.8×10^{-9} Darcy's law is not valid to describe the flow in the porous package. The solid line shows, however, that Brinkman's equation is still valid to define the flow through the porous package, since the flow velocity profile (solid line) through both free liquor (tube) and porous package is still in a reasonable range.

The simulation results demonstrate that Brinkman's equations extend Darcy's law to include a term that accounts for the viscous transport in the momentum balance and introduce the velocities in the spatial directions as dependent variables. This approach seems to be more robust than Darcy's law, since it is valid over a wider range of flow rates, and for different permeabilities of the porous media.

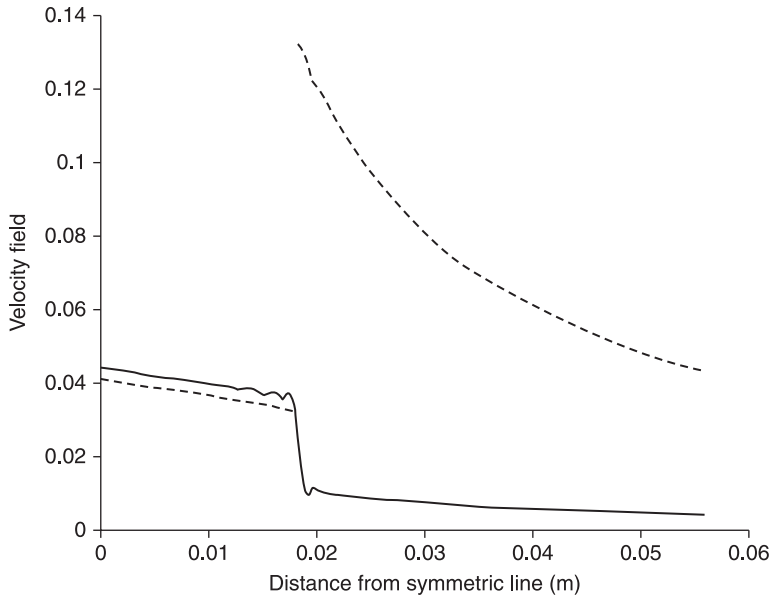

6.14 Demonstration of the validity of Darcy's law in porous media.

6.2.6 Effect of the liquor temperature

The liquor viscosity and density decrease with increasing temperature. Therefore, variations in temperature cause the flow behaviour to vary; thus, both liquor viscosity and density are important parameters in defining the flow properties.

Figure 6.15 illustrates the influence of temperature on flow behaviour. The solid line and dashed line represent the flow velocity profiles through the tube and porous package at 30 °C and 70 °C, respectively. Numerical simulation shows that the higher the temperature, the higher the flow velocity in both free liquor (tube) and porous package. In addition, higher temperatures cause a fluctuating flow in the free liquor stage.

According to the numerical results, the influence of liquor temperature on flow property is quite remarkable, despite the fact that the change of permeability of the porous medium with temperature was not considered. A higher temperature is thus favourable to the fluid flow transport in both free liquor and porous media, as well as the mass transfer in the fluid system.

6.3 Dynamic behaviour of mass transfer in package dyeing

The mass transfer process within porous yarn packages depends on many factors, including sorption (dye/fibre systems, sorption constant), convection (fluid flow

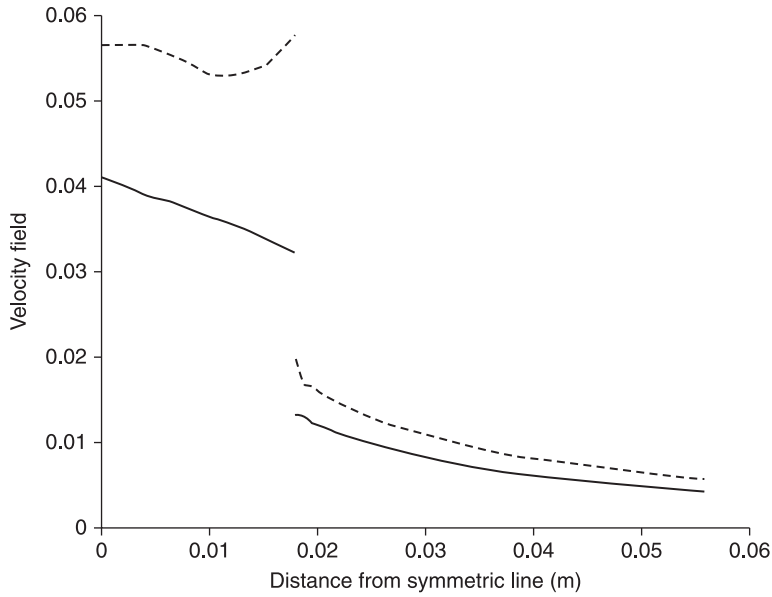

6.15 The influence of temperature on the flow behaviour.

rate and flow direction), dispersion, package parameters (thickness, density/porosity) and others (temperature, etc.). The numerical simulation, based on the model equations derived in Chapter 4, provides a powerful method to investigate the dynamic behaviour of mass transfer in package dyeing under different dyeing conditions.

To evaluate dyeing quality, two aspects of dyeing should be considered: the dye uptake rate on fibres and the levelness of dye distribution throughout the package. The concentration of dye at the end line (flow exit face) of the package (CDEP) with time could be used to represent the rate of dye uptake, if no flow reversal is used during the dyeing. Also, the simulation results give the opportunity to formulate a dimensionless criterion for the prediction of the levelness of dyeing of a cylindrical fibrous package. This criterion is denoted dye distribution factor (DDF), which is the ratio of the lowest to the highest concentration of dye on fibres in the package at the time at which the levelness is examined. When no flow reversal is employed during the dyeing, the DDF is equal to the ratio of the concentration of dye on fibres (Cf) at the end and entrance line of the package, i.e.:

$$\mathrm{DDF} = Cf(l,t)/Cf(0,t)$$

It is reasonable to emphasise that the DDF represents the ratio between the concentration of dye on fibres at the entrance and end line of the package and, consequently, characterises dyeing unlevelness.

The CDEP is an absolute value, which indicates the concentration of dye at the end layer (flow exit face) of the package at time *t*, while the angle between the tangent line of the curve and the time coordinate represents the rate of dye uptake. The DDF, on the other hand, is a relative term. The final values of DDF indicate the degree of levelness at the time *t*, and the curves show the change of the dye distribution throughout the package. Both CDEP and DDF may be used to evaluate the dyeing quality.

6.3.1 Effect of sorption factors on package dyeing

Dyeing behaviour for different adsorption isotherms

As was discussed in Chapter 2, it is assumed that any dyeing system to which the simulation model is applied can be represented by one of the three isotherms (Nernst, Freundlich or Langmuir), or by a combination of them. For example, the dyeing of many synthetic fibres with disperse dyes follows the Nernst isotherm; high concentrations of direct and vat dyes on cellulosic fibres commonly exhibit Freundlich type isotherms; and the levelling acid dyes on protein fibres follow Langmuir isotherms. Employing one of the isothermal relationships makes it possible to simulate any kind of dyeing system with any dye/fibre combinations.

Figures 6.16 and 6.17 demonstrate the dye concentration distributions in liquor and on fibres through the package, for a Nernst type adsorption isotherm. In

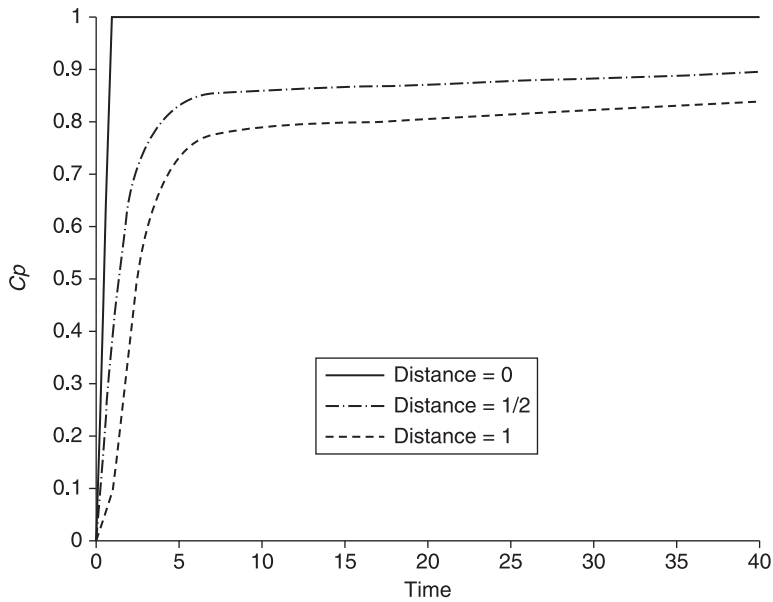

6.16 Concentration of dye in the liquor (*Cp*) at the entrance, middle and exit line of the package against the process time, for a Nernst type adsorption isotherm.

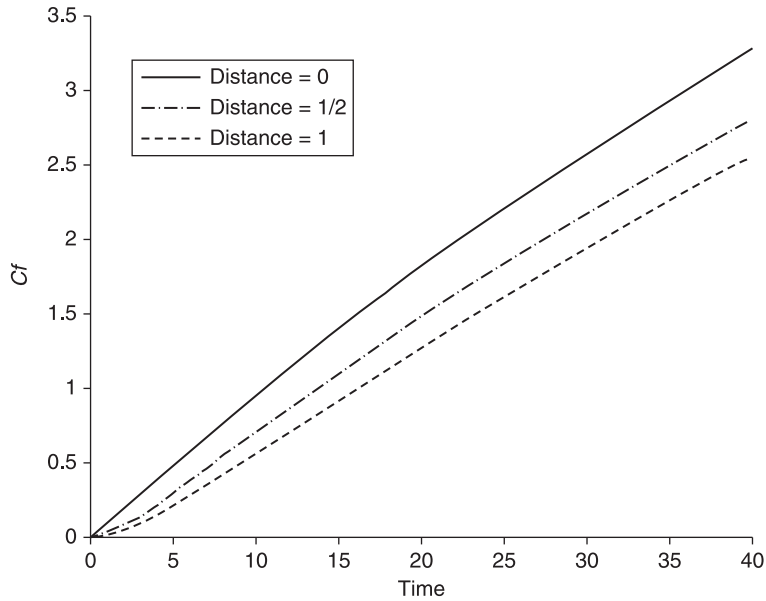

6.17 Concentration of dye on fibres (*Cf*) at the entrance, middle and exit line of the package against the process time, for a Nernst type adsorption isotherm.

Figure 6.16, the solid line represents the concentration of dye in the liquor (*Cp*) at the entrance of the package with time, the dashed-dotted line displays *Cp* at the middle of the package, and the dashed line displays *Cp* at the end of the package, respectively. The simulation results show that the concentration of dye through the package (*Cp*) increases rapidly within a short time (about 5 time units), but further increase at both middle and end line of the package is quite slow. The difference in *Cp* throughout the package decreases slightly until 40 time units, indicating that, under the conditions employed in the simulation, an uneven dye distribution in liquor through the package may develop over a long time period.

Figure 6.17 displays the distribution profiles of the concentration of dye on fibres at the entrance (solid line), middle (dash-dotted line) and end line (dashed line) of the package with time. It can be seen that *Cf* increases almost linearly with time at different layers of the package, but the differences of *Cf* at different layers, which may be used to represent the uniform distribution of the dye across the package, seem to slightly increase with time until 40 time units, indicating an unlevel distribution of dye on fibres through the package under the simulation conditions employed.

From the results shown in Figs 6.16 and 6.17, it can be concluded that, under the current simulation conditions, an uneven dye distribution both in the liquor and on the fibre through the package will exist in the initial stage of dyeing.

Figure 6.18 further demonstrates the distributions of dye concentration on fibres at different times.

Figure 6.18 shows the concentration of dye on fibres (*Cf*) throughout the package at 1, 5, 10, 20, 30 and 40 time units. It can be seen that the concentration of dye on the fibre throughout the package increases with time, but the difference between the *Cf* at entrance and exit line of the package, which could represent the levelness of the dyeing through the package, seems to remain relatively constant with time until 40 time units.

Figures 6.16–6.18 display the simulation results when the adsorption of dyes by fibres follows the Nernst adsorption isotherm. Figures 6.19 and 6.20 present the concentration of dye adsorbed by fibres (*Cf*) throughout the package at 1, 5, 10, 20, 30 and 40 time units, for Freundlich and Langmuir type adsorption isotherms, respectively.

The results shown in Figs 6.18–6.20 demonstrate that, for the dyeing systems with different adsorption isotherms, representing different dye/fibre combinations, dyeing behaviours are different. Systems with Freundlich type adsorption gave the highest *Cf* at 40 time units, indicating a higher dye uptake rate gained during the dyeing. Systems with Nernst type adsorption gave a similar result to that of the Freundlich isotherm, but slightly lower *Cf* at the exit line of the package. This indicates a slightly poorer uniformity in dye distribution through the package.

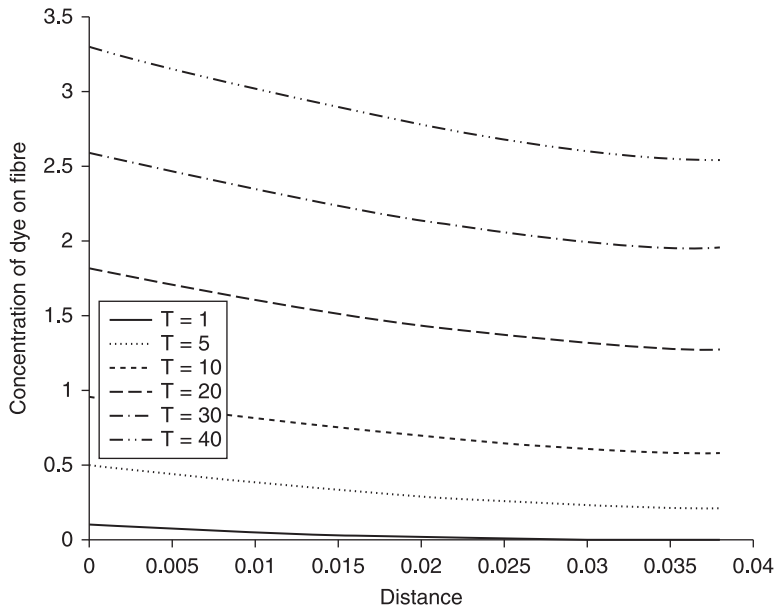

6.18 Concentration of dye on fibres (*Cf*) throughout the package against time, for a Nernst type adsorption isotherm.

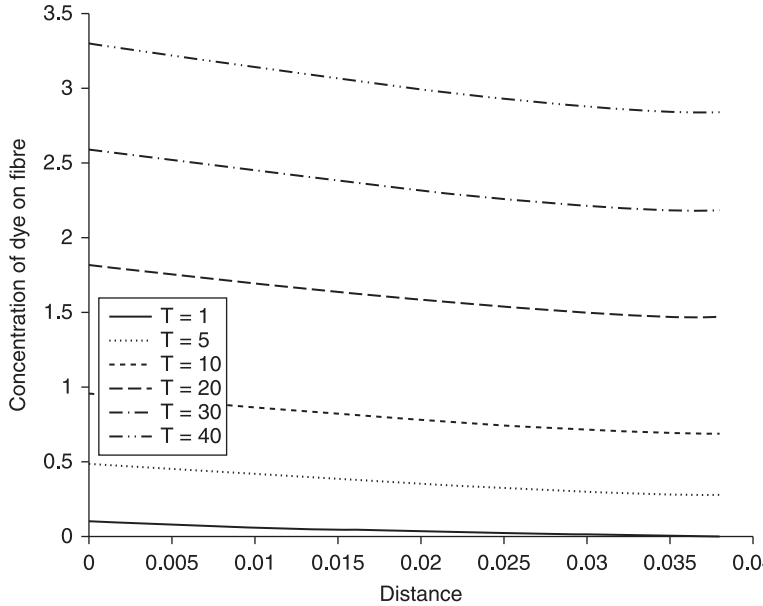

6.19 Cf throughout the package at different times, for a Freundlich type adsorption isotherm.

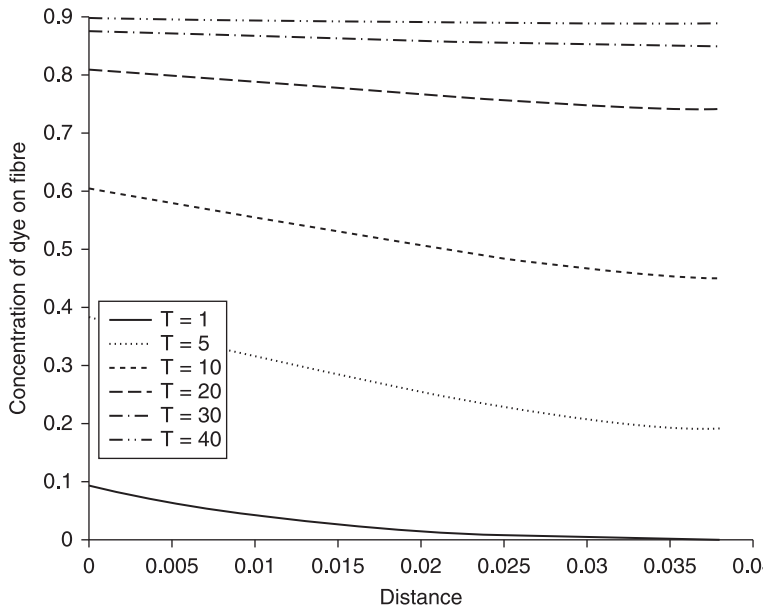

6.20 Cf throughout the package at different times, for a Langmuir type adsorption isotherm.

Systems with Langmuir type adsorption, however, present different behaviour under the same conditions.

It can be seen from Fig. 6.20 that the dyeing system with the Langmuir type adsorption isotherm gained a lower *Cf* at both sides of the package at the same dyeing time (40 time units) compared with the other two dyeing systems, indicating a very slow dye uptake rate obtained. However, the difference in *Cf* between two sides of the package appears very small after a short time (20 time units), which means that a better levelness was obtained than that of the other two dyeing systems.

Figure 6.21 displays the DDF against dyeing time for three different adsorption isotherms. It is clear that, for the three different dyeing systems, the DDF increases rapidly in the first 10 time units, and thereafter increases gradually with time. The dyeing system based on a Langmuir adsorption isotherm shows the best DDF (dash-dotted line) result after about 10 time units, which means that under the simulation conditions the best dye migration through the layers of the package occurs. The result for the dyeing system based on a Nernst adsorption isotherm (solid line), on the other hand, suggests the poorest dye distribution through the package over the simulation time examined. The results for a dyeing system based on a Freundlich adsorption isotherm (dashed line) show that the best dye migration is achieved in the initial stage (with 10 time units) of dyeing, and then the DDF increases slowly over the remaining simulation period.

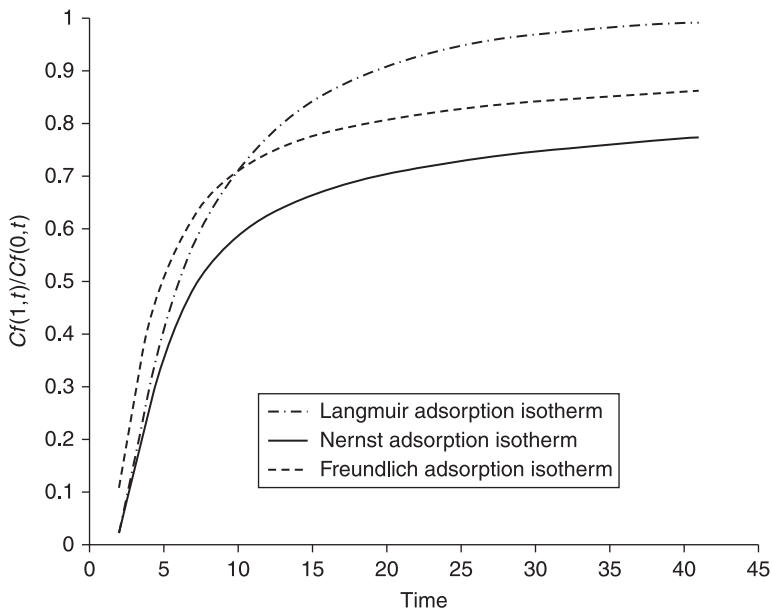

6.21 Comparison of DDF for the different adsorption isotherms.

Adsorption coefficient

An interesting aspect of sorption is the effect of the rate constant of sorption ($k=k1/k2$) on the dyeing process. As mentioned before, $k1$ and $k2$ are the adsorption and desorption rate constants, respectively. Thus, k ($k1/k2$) is the actual adsorption coefficient, which characterises the adsorption properties for different dye/fibre combinations.

In Fig. 6.22, the dashed and solid lines represent the concentration of dye on fibres at the exit line of the package (CDEP), where the adsorption coefficients are 20 and 10, respectively. A higher adsorption coefficient ($k=k1/k2$) leads to a higher dye uptake rate during the initial time of simulation. The levelness of dye distribution across the package is shown in Fig. 6.23.

Figure 6.23 shows that the DDF in both cases increases sharply within 10 time units, but then the increase becomes very slow, indicating that the initial stage of dyeing is crucial for a level dyeing. An interesting result is that dyeing with a higher adsorption coefficient (dashed line) presents a poorer levelness of the dye distribution through the package, compared with dyeing with a lower adsorption coefficient (solid line).

The simulation results indicate that there is a close relationship between the adsorption coefficient and the rate of dye uptake. High values of the adsorption coefficient lead to a short dyeing time and high initial unlevelness of textile

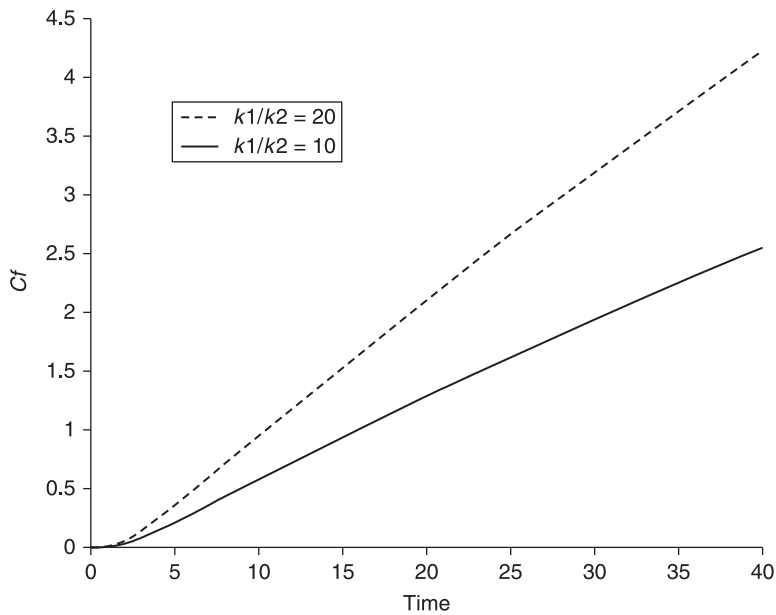

6.22 Concentration of dye on fibres at the exit line of the package with time, according to a Nernst type adsorption isotherm.

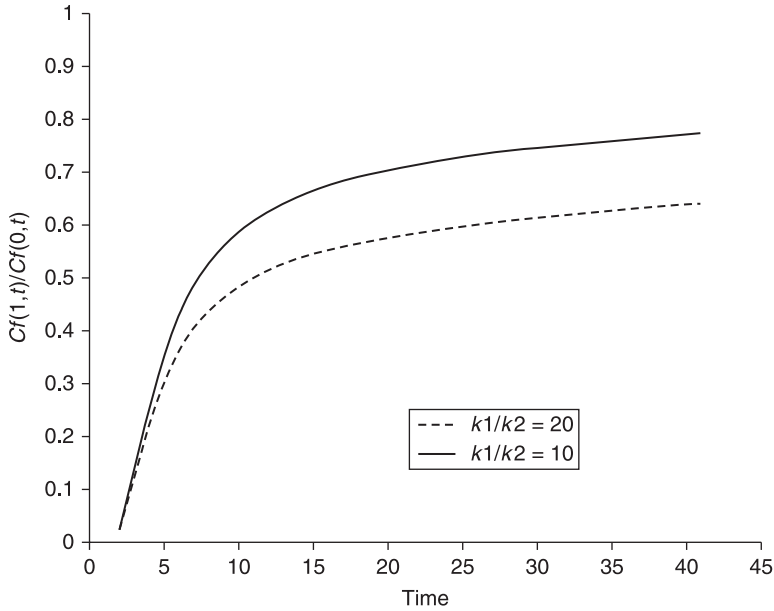

6.23 DDF against time for different adsorption coefficients and a Nernst type adsorption isotherm.

package dyeings. On the contrary, low adsorption coefficient values correspond to a small risk of uneven dyeing, but reduce the rate of dye uptake during the process.

The conclusions above are drawn from Figs. 6.22 and 6.23, for the Nernst type adsorption isotherms. In the case of Freundlich adsorption isotherms, the simulation shows the same trend (see Figs 6.24 and 6.25) in both CDEP and DDF, although the dyeing system with a Freundlich adsorption isotherm seems to give a better dye distribution through the package.

Figures 6.26 and 6.27 show a different behaviour in the case of dyeing systems based on a Langmuir adsorption isotherm. A higher adsorption coefficient causes a higher CDEP, although it increases very slowly and only reaches 0.93 after 40 time units. In addition, in terms of levelness of dye distribution, a higher adsorption coefficient does not cause a lower DDF. On the contrary, a higher adsorption coefficient produces a slightly higher DDF value and results in an increased dye uptake rate without adversely affecting the levelness of dye distribution through the package, when the dye/fibre adsorption is according to the Langmuir isotherm.

Thus far, from the simulation results demonstrated in Figs 6.16–6.27, it can be concluded that dyeings with different adsorption isotherms, representing different dye/fibre combinations, exhibit differences in dye uptake rate and levelness of dye distribution through the package in the initial stage of dyeing. Dyeing systems based on a Freundlich adsorption isotherm exhibit the highest dye uptake rate,

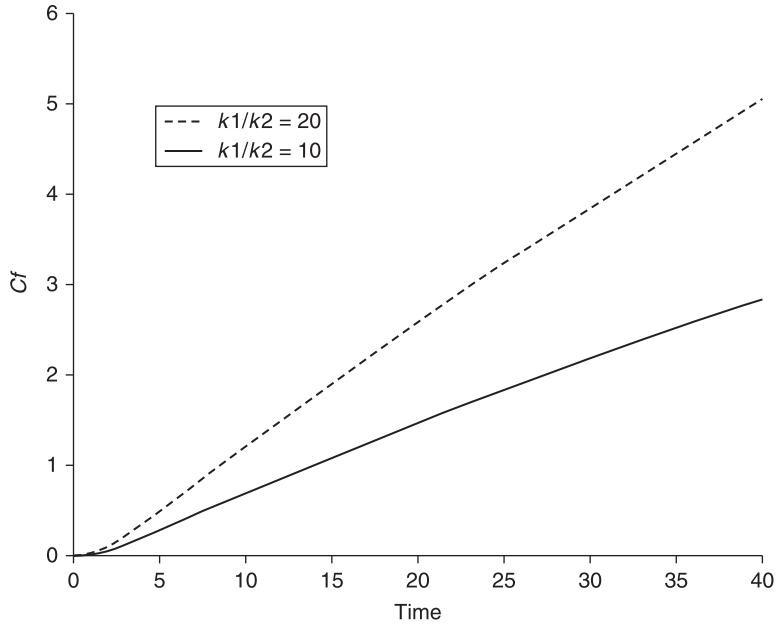

6.24 Concentration of dye on fibres at the exit line of the package with time, for a Freundlich type adsorption isotherm.

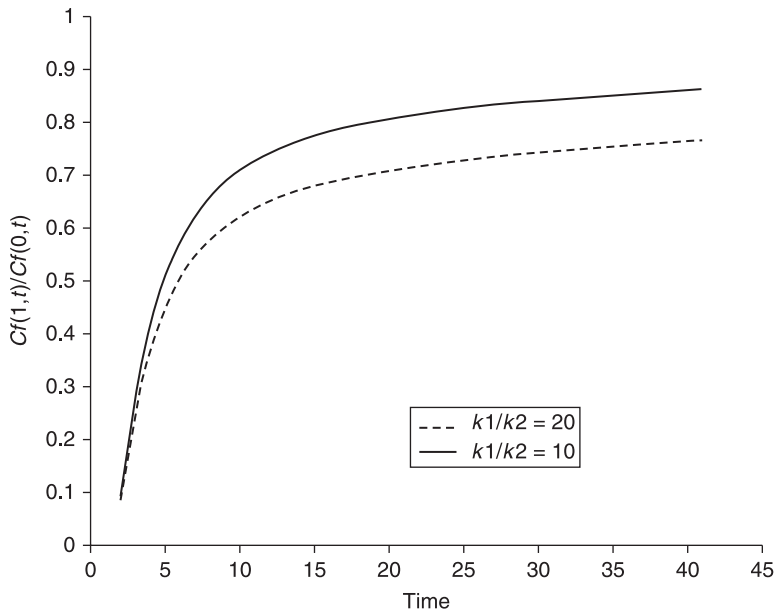

6.25 DDF against time for different adsorption coefficients and a Freundlich type adsorption isotherm.

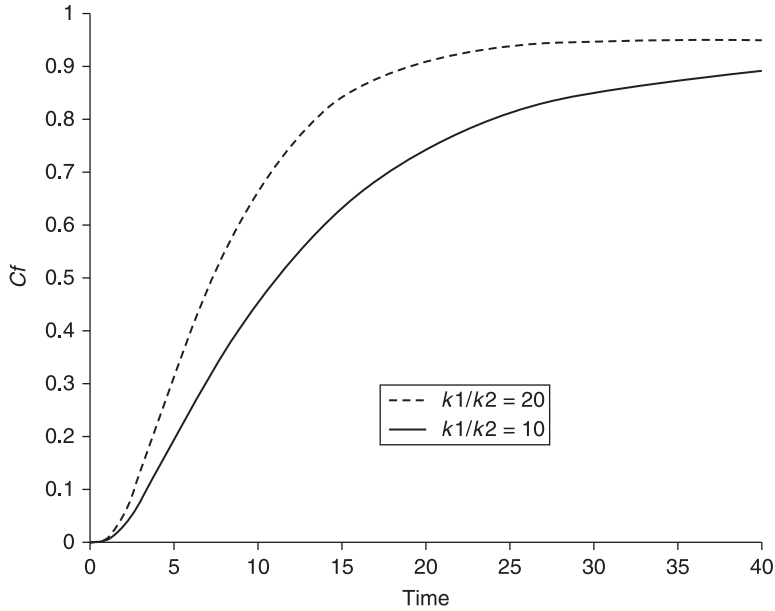

6.26 Concentration of dye on fibres at the exit line of the package with time, according to a Langmuir type adsorption isotherm.

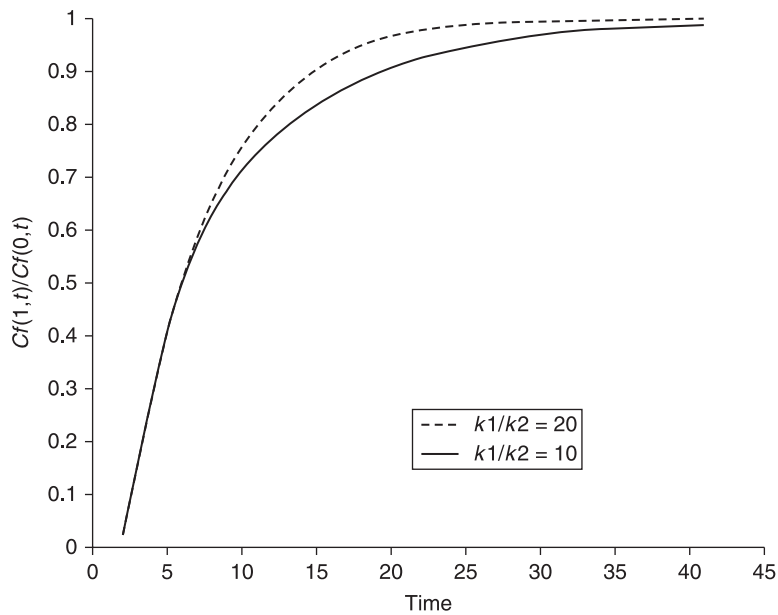

6.27 DDF against time for different adsorption coefficients and a Langmuir type adsorption isotherm.

while those based on a Langmuir adsorption isotherm show the best levelness of dye distribution across the package.

A higher adsorption coefficient in dyeing leads to a higher dye uptake rate, and a poorer levelness of dye distribution through the package, except for systems based on a Langmuir adsorption isotherm. This result is consistent with the observed behaviour of commercial dyeing systems. For example, it is widely known that high affinity dyes result in high equilibrium exhaustion and are difficult to apply uniformly.

To design an on-line control system for practical package dyeing, a simplified form of the model would be crucial. Control strategies based on 'the worst case scenario'[4] usually require the control of key parameters that influence or define the outcome of the process, a good example being the uniformity of dye distribution across the package in the package dyeing process. Since dyeing systems based on the Nernst adsorption exhibit the poorest levelness of dye distribution through the package, the linear adsorption relationship may be used to represent the dyeing system of any dye/fibre combination. This may be considered as a reasonable approach to simplify a general dyeing model, especially since a linear relationship for the dye adsorption is an easier approach to modelling the dyeing process.

6.3.2 Effect of convection factors

Flow rate

It is well established that the rate of dyeing in practice is markedly dependent on the efficiency with which the dye liquor is circulated through the material being dyed. The velocity of liquor flow in package dyeing plays a rather special role in dyeing, since it also determines the nature of the distribution of dye throughout the porous yarn package during the dyeing.

In practical dyeing, the normal flow rate range may be between 20 and 60 l/min. kg, which is equivalent to a rate of about 0.1–0.2 m/s at the inflow face of the package tube of the package machine. According to the simulation results from the previous section, the flow rate within the porous package may be considered to be in the range of 0.01–0.02 m/s.

Figure 6.28 displays the concentration of dye on fibres at the flow exit face of the package against time, where the flow velocity within the package is 0 (dotted line), 0.01 (solid line) and 0.02 (m/s) (dash-dotted line), respectively. The adsorption relationship follows the Nernst isotherm. The simulation result shows that the difference in flow rate does not affect the dye uptake significantly. For example, when the flow velocity within the package is increased by 100%, i.e. from 0.01 to 0.02 m/s, the CDEP at time 40 only increases by 10%, i.e. from 2.5 to 2.75. When $V = 0$, however, the difference in dye uptake is quite large, compared with that of flow velocity in the normal range. Figure 6.29 further demonstrates the effect of convection factor on dyeing in terms of DDF.

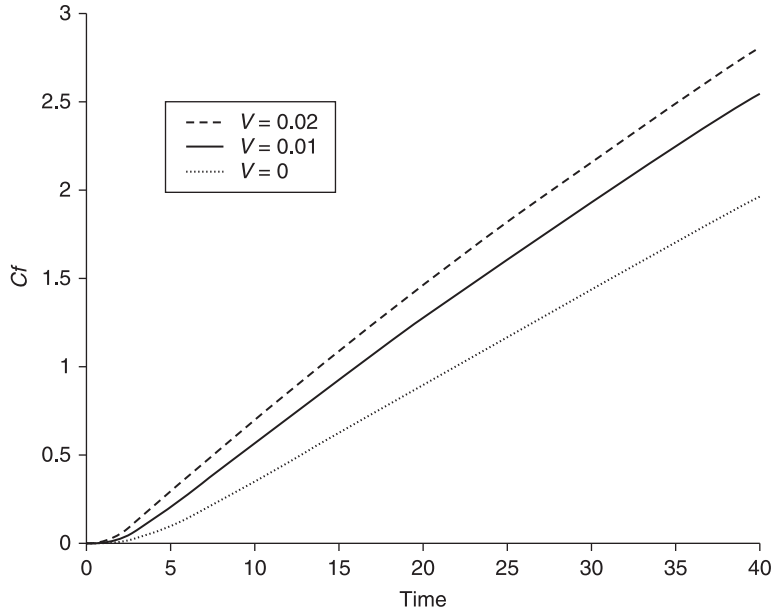

6.28 Concentration of dye on fibres at the flow exit face of the package, where the flow velocity within the package is 0, 0.01 and 0.02 (m/s), respectively.

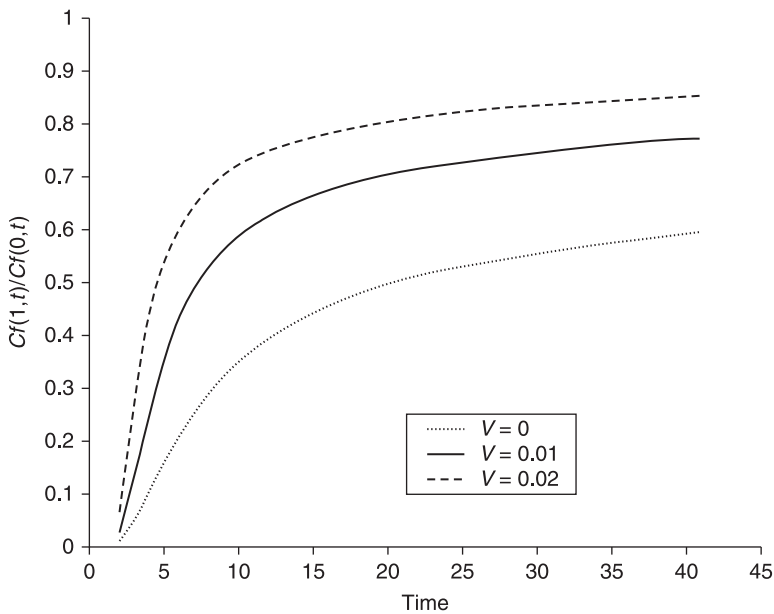

6.29 Levelness of dye distribution through the package, where the flow velocity within the package is 0, 0.01 and 0.02 (m/s), respectively.

In Fig. 6.29, the dotted, solid and dashed lines represent the DDF against time, where the flow velocities within the package are 0, 0.01 and 0.02, respectively. The results show that the levelness of dye distribution through the package improves with an increase in flow velocity within the package. The increase in DDF in the first 10 time units for 0.01 and 0.02 m/s flow velocities is rapid, and it then gradually rises to 0.78 and 0.86, respectively. This means that a 100% increase in flow velocity causes a 10.2% increase in DDF. This result implies that at sufficiently high flow rates (within the normal practical range) the levelness of dyeing will not be significantly affected by a change in flow rate.

When the flow velocity is zero, a convection factor is not considered in dyeing. In this case the DDF reaches approximately 0.6 at the end of the simulation time. The difference in DDF for cases with and without convection, for velocities in the practical range, is as high as 30%–43%. This result, as well as that shown in Fig. 6.29, suggests that the convection factor should not be ignored when modelling the dyeing process.

Figures 6.28 and 6.29 only present the results where the adsorption relationship follows the Nernst isotherm. Dyeings where the adsorption relationships follow the other two isotherms show a similar trend as shown in Figs 6.28 and 6.29, although for dyeing with Langmuir adsorption both CDEP and DDF seem to change even less with a change in flow rate. This implies that, under this condition, flow rate does not affect the dyeing too much. More simulation results on this aspect can be seen in Appendix B.

Flow direction

Flow direction during the dyeing is believed to be another important factor affecting the dyeing process. Due to the adsorption of dye by fibres, when the dye liquor flows past the porous package, the rate of adsorption will be affected; it will be greater at the entrance of the package than that at the exit point of the package.

Plates III and IV illustrate the distribution of dye concentration on fibres within the package for both flow directions, i.e. out-to-in and in-to-out. The difference in dye transfer between the two flow direction patterns is clear. It should be noted that under the same conditions the DDF at time 40 for the out-to-in flow direction is 0.67, while for the in-to-out direction it is only 0.49.

The simulation results indicate that the out-to-in flow direction is favoured for the dye migration across the package compared with that of the in-to-out direction. This may be due to the geometry of the package. When liquor flows in the out-to-in direction through the package, it encounters a much larger contact area affecting the adsorption of dye by fibres, compared with the opposite direction.

6.3.3 Effect of dispersion factors

Dispersion coefficient

In the mass transfer model, the dispersion factor is assumed to reduce the concentration gradient of dye liquor flowing through the package, resulting in a more even distribution of dye in the liquor within the package. Reported investigations of the influence of dispersion factor on dyeing rate, however, are very rare. Burley *et al.*[5] and Vosoughi[6] included a dispersion coefficient to describe the dispersive transport of dye in their model of textile dyeing processes in formal mathematical equations; however, the significance of the inclusion of this parameter on the outcome of dyeing was not clarified.

Figures 6.30 and 6.31 present the simulation results of both CDEP and DDF against time, where the dispersion coefficients are 1.25×10^{-4}, 1.25×10^{-5} and 0 (no adsorption term), respectively.

Figure 6.30 shows that an increase in dispersion coefficient hardly changes the rate of dye uptake on fibres after a very short time (5 time units), although it increases the value of CDEP somewhat during the process. The effect is minor, since a tenfold increase in dispersion coefficient only causes an increase of

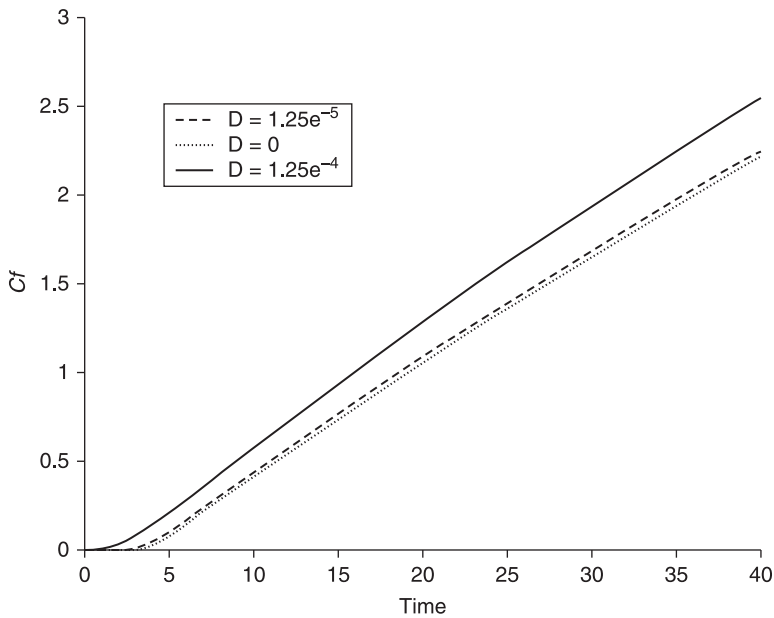

6.30 Concentration of dye on fibres at the exit line of the package against time, using different dispersion coefficients and a Nernst type adsorption isotherm.

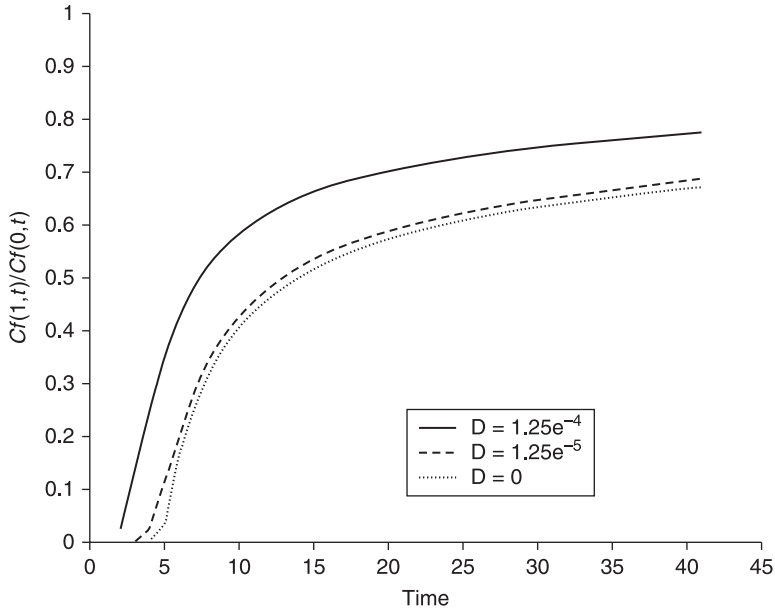

6.31 DDF against time for different dispersion coefficients and a Nernst type adsorption isotherm.

13.4% in CDEP. When the dispersion coefficient is zero, i.e. when the dispersion term is ignored in the system, the final CDEP value is only slightly less than that when the dispersion coefficient is 1.25×10^{-5}. This simulation result implies that the dispersion term does not play an important role in terms of dye uptake rate.

Figure 6.31 shows that the effect of dispersion coefficient on the levelness of dye distribution across the package is similar to that of the dye uptake rate, i.e. the DDF rises as the dispersion coefficient is increased. This is consistent with the well-accepted assumption that increased uniformity in distribution of dye in the liquor within the package is achieved by reducing the concentration gradient of dye liquor flowing through the package.

For dyeing systems based on the Freundlich and Langmuir adsorption isotherm types, similar results are obtained for both CDEP and DDF, further demonstrating that a higher dispersion coefficient leads to a higher dye uptake and a better levelness of dye distribution across the package, though the effect seems to be minor.

These results also theoretically suggest that the dispersion term is favourable for dye uptake and levelness, compared with the results obtained from the dyeing when the dispersion term is ignored.

6.3.4 Effect of package factors

Package thickness

Package thickness, or the distance which dye liquor must penetrate in the direction of liquor flow, is an important variable which should be considered when modelling the dyeing process. The solid and dashed lines in Fig. 6.32 represent the CDEP with time, where the thicknesses of the package are 0.038 and 0.046 m, respectively. The results indicate that the influence of package thickness on the rate of dye uptake is significant, since a 21% increase in package thickness leads to an 8% decrease in CDEP at 40 time units. Figure 6.33 further demonstrates the effect of package thickness on dyeing in terms of DDF. The solid and dashed lines represent the DDF against time, where the package thicknesses are 0.038 and 0.046 m, respectively. It can be seen that a 21% increase in package thickness leads to a decrease in DDF as high as 10% over the simulation time, indicating that a thicker package will cause a clear worsening of levelness of dyeing. The effect of package thickness on dyeing of fibres following other types of adsorption isotherms seems to be similar to that discussed earlier, as shown in Figs 6.32 and 6.33.

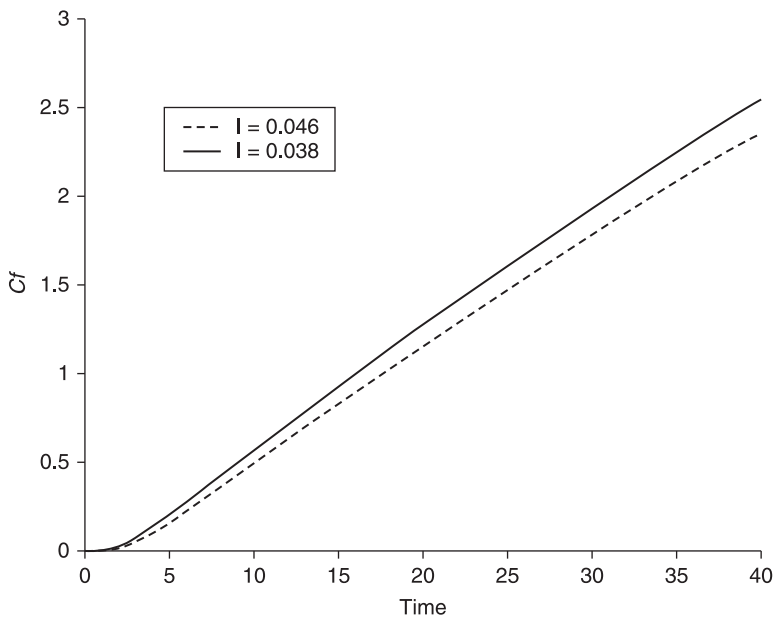

6.32 CDEP against time for different package thicknesses and a Nernst type adsorption isotherm.

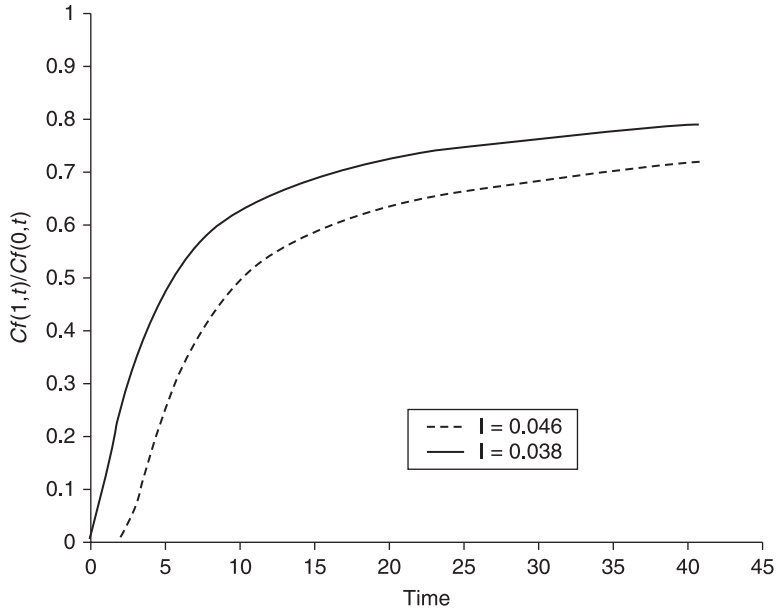

6.33 DDF against time for different package thicknesses and a Nernst type adsorption isotherm.

Package porosity

As mentioned earlier, the package density and porosity are closely related. A high package density results in a package of low porosity. In practice, the normal package porosity range is between 0.3 and 0.5, although in some cases it could be between 0.1 and 0.7. Figures 6.34 and 6.35 present the effect of package porosity on dyeing when the porosities of the package are 0.5 and 0.3.

In Fig. 6.34, the solid and dashed lines represent the concentration of dye on fibres at the exit line of the package at time t, when the porosity of the package is 0.5 and 0.3, respectively. Simulation results reveal that the package porosity strongly affects the dye uptake during the dyeing, as a 40% decrease (from 0.5 to 0.3) in package porosity causes a 23.1% decrease in CDEP at simulation time 40.

Figure 6.35 shows that the effect of package porosity on levelness of dye distribution across the package is also significant. For example, when the porosity of the package decreases by 40%, e.g. from 0.5 to 0.3, the DDF decreases by 23%, i.e. from 0.78 to 0.6.

Thus, according to the simulation results, both package thickness and porosity are important variables, which strongly affect the dyeing process. The effect of package thickness and porosity on dyeing for the other two types of adsorption isotherm is similar.

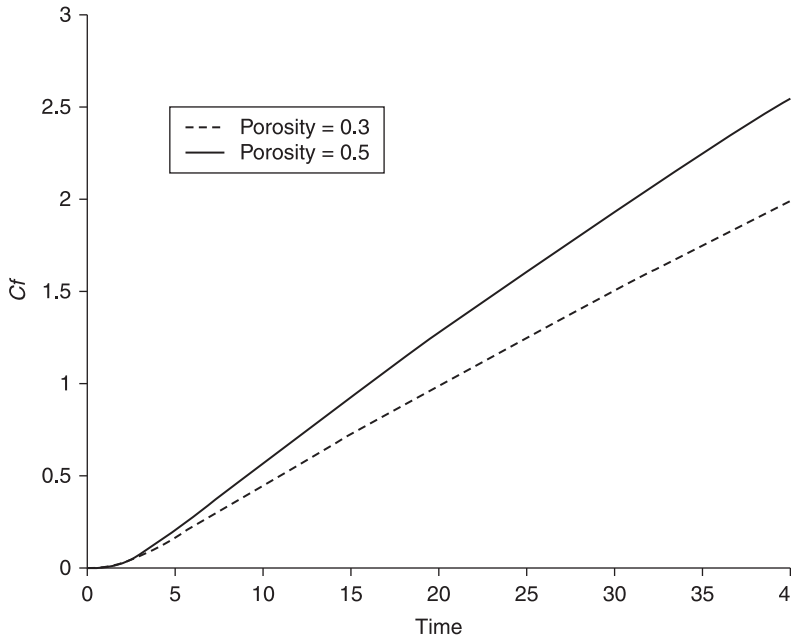

6.34 CDEP against time for different package porosities, based on a Nernst adsorption isotherm.

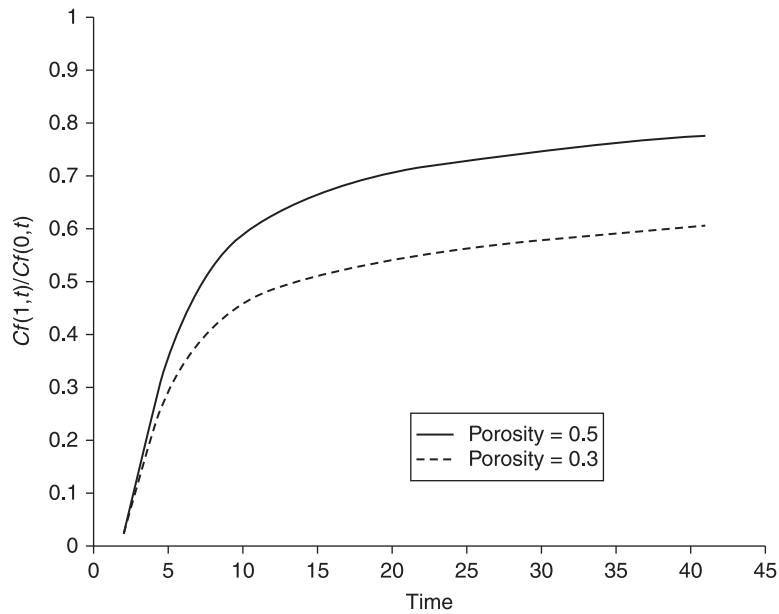

6.35 DDF against time for different package porosities, based on a Nernst adsorption isotherm.

To simplify the model, researchers in this field usually consider the yarn to be uniformly wound throughout the package, and thus constant porosity is assumed in these mass transfer models. In practice, however, the yarn may be wound tightly at the inner layers and more loosely at the outer layers of the package, or vice versa. Current analysis assumes that the porosity is a function of the distance, i.e.:

$$\varepsilon = f(x) \qquad [6.1]$$

In the case of a linear relation between ε and x, Eq. 6.1 becomes:

$$\varepsilon = m + nx \qquad [6.2]$$

where ε is the porosity of package, x is distance from the entrance face of the package in the flow direction, m, and n is a constant. Clearly the relation between ε and x may follow other types of functions, but these are not considered here.

Figure 6.36 illustrates the influence of porosity change across the package layers on dye transfer behaviour. Dotted and dashed curves represent the CDEP when the package porosity linearly decreases from 0.5 to 0.462, and increases from 0.5 to 0.538 (or the package density increases and decreases) with distance

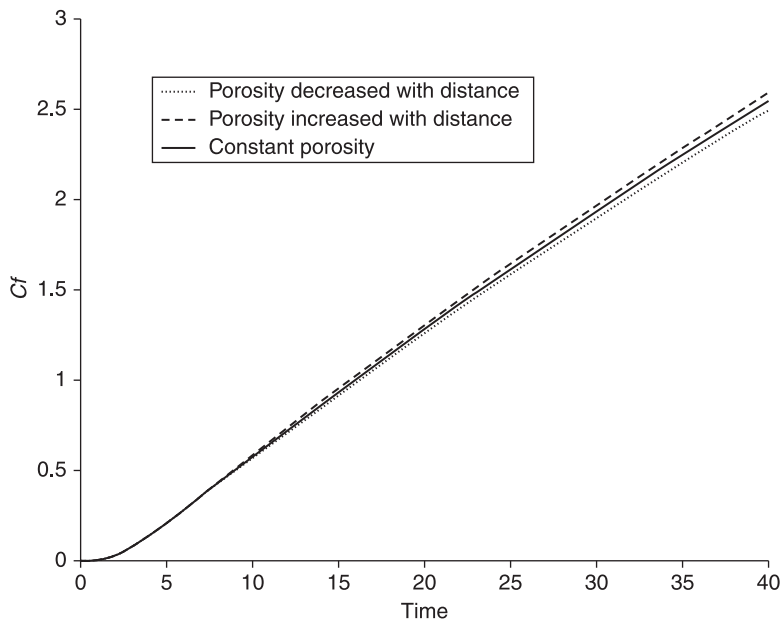

6.36 CDEP against time where the porosity of the package changes linearly with distance from the entrance of the package in the flow direction.

across the package in the flow direction, respectively. Solid line shows the CDEP where the package porosity (or density) is kept constant.

The simulation result shows that variations in package porosity have little effect on dye uptake. However, dyeings in which the porosity increases with the distance in the flow direction present a slightly better dye uptake feature, while dyeings in which the porosity decreases with the distance in the flow direction present a slightly poorer dye uptake feature.

The effect of the variation in porosity of the package on DDF is similar to that on CDEP, according to Fig. 6.37. Dyeings in which the porosity of the package increases linearly with distance in the flow direction exhibit the best DDF (dashed line), while dyeings in which the porosity of the package decreases linearly with distance in the flow direction show the poorest DDF (dotted line), but the difference is minor.

6.3.5 Comparison of dyeing behaviour for different dosing profiles

During the dyeing, the concentration of dye in the mixing tank (C_1) can be controlled by dosing the appropriate quantity of dye into the system. If C_1 is a function of time, it causes a variable boundary condition at the entrance line of the

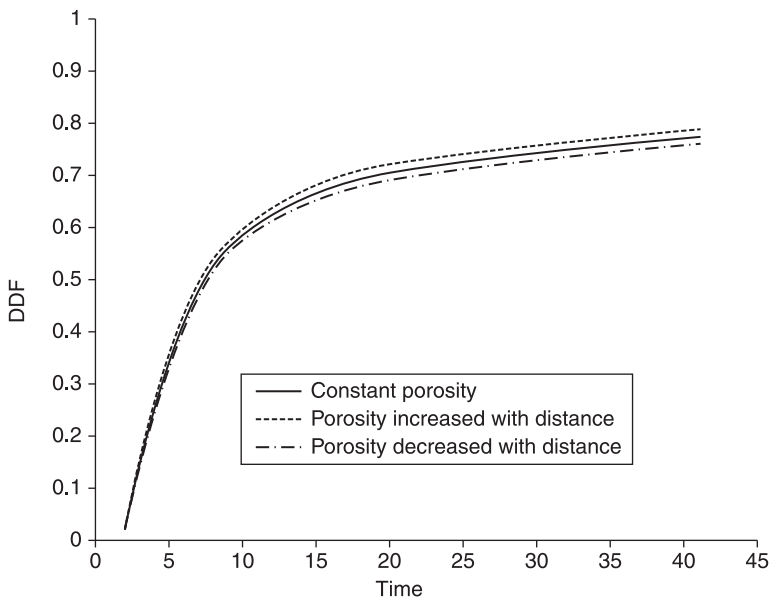

6.37 DDF against time where the porosity of the package changes linearly with distance from the entrance of the package in the flow direction.

package (in the flow direction). Under this condition, the solution of the model can be used to evaluate different dye dosing profiles. This could be used to demonstrate a suitable control strategy for the dyeing process.

Three types of dosing profiles are examined in the simulations discussed here, which can be expressed as functions of dyeing time as shown in Eqs 6.3–6.5.

$$\text{Linear: } C_1 = C_{ini} + a \times t \quad [6.3]$$

$$\text{Exponential: } C_1 = C_{ini} + 1 - exp((-t-b)/d) \quad [6.4]$$

$$\text{Quadratic: } C_1 = C_{ini} + (t/e)^2 \quad [6.5]$$

where C_1 is the concentration of dye in the mixing tank at time t, C_{ini} is the initial concentration of dye in the mixing tank, and a, b, d, e are constants, which determine the shape of the curves.

Figure 6.38 shows three dosing profiles for a zero initial concentration of dye in the mixing tank and a dosing time of 40. The solid, dotted and dashed lines represent linear, exponential and quadratic dosing profiles, respectively.

The graph of DDF against the dyeing time for the three dosing profiles, in Fig. 6.39, shows that the trends of the DDF against the dyeing time are similar. For all three dosing methods, the DDF increases rapidly only in the first 15 time units of the dyeing process and then gradually increases over the dosing time,

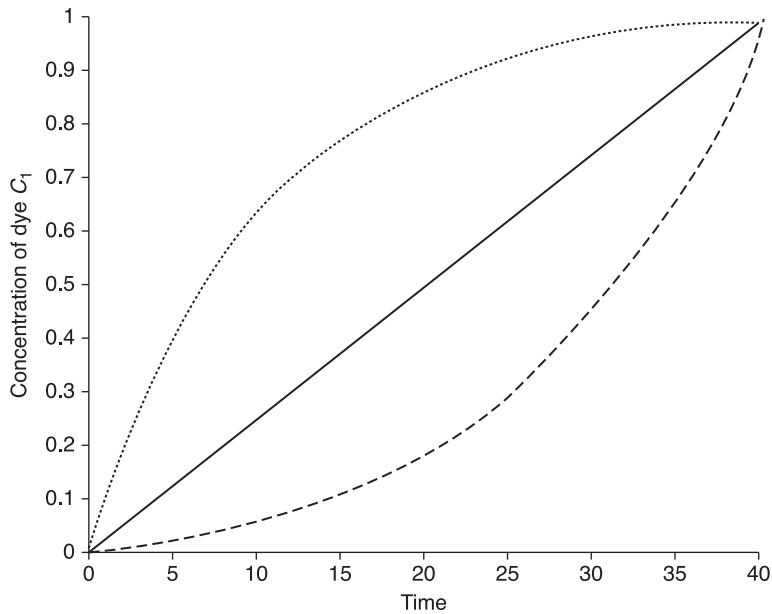

6.38 Linear (solid line), exponential (dotted line) and quadratic (dashed line) dosing profiles.

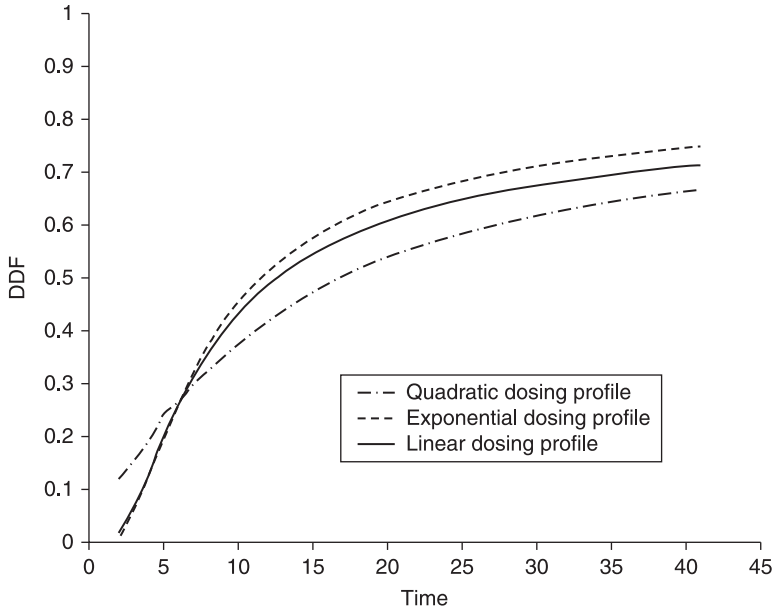

6.39 Effect of various dosing profiles on levelness of dye distribution through the package for a Nernst adsorption isotherm.

reaching final values of 0.67, 0.71 and 0.74, respectively. This indicates that, for the dosing algorithms employed, a fast dye migration throughout the package can only be achieved within a short period of time after the start of dosing, and then the dosage has a small impact on dye distribution; therefore the control of levelness may depend on other factors such as temperature, pH, etc.

A comparison of the distribution factors after 40 time units indicates that the quadratic profile (dotted and dashed line) gives a better DDF value during the first 6 time units of dosing, and then the rate of DDF decreases over the dosing time for all profiles. On completion of dosing, the exponential dye injection profile (dashed line) produces a better dye distribution (0.74) across the package, compared with the linear and quadratic dosing methods, which only achieve 0.71 and 0.67, respectively. Although using different dosing methods results in different degrees of uniformity, the difference in DDF between the dosing methods is less than 5%.

Simulation results indicate that in the case of integration dyeing, in which dyes and auxiliaries are continuously dosed into the dyebath over a period of time, the quadratic dosing method will be the preferred method during the initial stage of dyeing, since the rate of dye injection starts slowly. After 7 time units the rate increase may be too rapid for a level distribution of dye (as shown in Fig. 6.36, dashed line), and an exponential dosing method may be the preferred method

since it shows a better DDF result. This may be caused by a gradual decrease of dosing rate (Fig. 6.37, dotted line). Therefore, the ideal dosing profile may be based on gradually increasing the dosing rate (quadratic) and then employing a gradually decreasing dosing rate (exponential). However, since the difference in DDF for different dosing profiles is not remarkable (less than 5% in this case), a linear dosing profile could be a reasonable approach for use in integration dyeing due to its simplicity in practice. A similar conclusion can be drawn from the simulation results for the other two types of adsorption relationships.

6.4 Conclusions from simulation results

The following conclusions may be drawn from simulation results of dye liquor flow properties during the dyeing process:

- Brinkman equations extend Darcy's law to include a term that accounts for the viscous transport in the momentum balance and introduce the velocities in the spatial directions as dependent variables. This approach is more robust than using Darcy's law alone, since it can be applied in a wider range of flow rates and porous package permeabilities.
- The flow rate of dye liquor through the package is not typically high, and, since the permeability of the package is typically low, the momentum transport by shear stresses can be ignored. Thus, using Darcy's law is a reasonable approach to model the flow properties.
- The higher the rate of liquor flow entering the package, the higher the velocity of liquor within the yarn assembly. The uniform distribution of the velocity across the package, however, may be compromised at higher liquor flow velocities within the package. If we assume that an even distribution of flow velocity within the package is directly related to the results of a uniform dyeing, it can be inferred that employing a high flow rate is not necessarily beneficial in practice.
- A high liquor flow rate will cause a more fluctuating flow in the spindle, which increases the influence of shear stresses on flow properties. This is probably a cause of the initial strike.
- A high flow rate will also cause an increase in pressure within both the tube and the porous package. An increase in pressure could result in package distortion and tunnelling, which can lead to non-uniform dyeing results, and is therefore not desired.
- The flow velocity distributions within the porous yarn assembly are dominated by the pressure rather than the flow velocity distributions within the free liquor circulating in the spindle. This result is obtained using Brinkman equations. It further proves the validity of Darcy's law in characterising the flow within the porous medium, since it agrees with Darcy's assumption that the only driving force for flow in a porous medium is the pressure gradient.

- Slight variations in package thickness (for example, 20%) do not significantly affect flow characteristics in free liquor (tube) and porous yarn package, but will change the pressure gradient within the system.
- For a given flow velocity, increasing the diameter of the tube will result in an increased flow rate. This will cause a larger velocity field in both the tube and the porous package. Therefore, theoretically, within practical limits, larger tube diameters would be preferred because of associated higher flow velocities within the porous package.
- Providing the flow rate entering the package is kept constant, increasing the package permeability will decrease the pressure drop across the package. However, the velocity field profiles within the tube and porous package for varying common package permeabilities would not be significantly different.
- Increasing the temperature of the dyeing liquor will cause a higher flow velocity in both tube and porous package, but it will also result in a fluctuating flow in the free liquor region. The use of high dyeing solution temperatures could facilitate mass transfer and improve fluid flow transport in free liquor as well as the porous medium. Obviously, this would depend on the nature of the dye/fibre combination under study. Other thermodynamic aspects of the dyeing which are affected by temperature are not considered.

The following conclusions may also be drawn from the simulation results based on mass transfer analysis.

6.4.1 Adsorption factor

Dyeing of different dye/fibre combinations can be represented by a number of adsorption isotherms. The analysis of the simulations based on various adsorption isotherms demonstrates distinct rates of dye uptake and levelness of dye distribution in the package during the initial stage of dyeing for various adsorption profiles:

- Based on results, dyeings following a Freundlich adsorption isotherm demonstrate the highest dye uptake rate, while those based on the Langmuir adsorption isotherm exhibit the best levelness of dye distribution throughout the layers of the package. Dyeings represented by the Nernst adsorption isotherm show the poorest levelness of dye distribution across the package.
- Since simulations based on the Nernst adsorption isotherm produce the poorest levelness results, a worst case scenario control strategy based on the Nernst adsorption isotherm could be used to control the dyeing of any dye/fibre combination. This would result in a simplified modelling and control methodology, since the Nernst isotherm represents a linear relationship between control and measurement parameters.
- A higher adsorption coefficient in dyeing will lead to a higher dye uptake rate and a poorer distribution of dye through the package (poor levelness). This,

however, does not hold for the Langmuir adsorption isotherm, in which the use of higher adsorption coefficients favours the increase of dye uptake rate and does not hinder the uniform distribution of dye throughout the package.

6.4.2 Convection factor

The convection term plays an important role in mass transfer balance:

- For a normal flow velocity range, the difference in the value of DDF when the convection term is and is not included can be as high as 30–43%. This implies that the convection term should not be ignored in the modelling of the dyeing process.
- The rate of dyeing typically increases by increasing the flow rate. However, in practice, slight variations of the flow rate, when common flow rates are employed, do not affect the rate of dyeing significantly.
- The 'out-to-in' flow direction is favoured for an optimal dye transfer across the package compared with the 'in-to-out' direction. This could be due to an increased surface area on the outer compared with the inner surface of the package, which in turn would increase the contact between dye molecules and the fibres at the outer interface.

6.4.3 Dispersion factor

With regard to the dispersion factor the following conclusions are noteworthy:

- The simulation results prove, theoretically, that the inclusion of the dispersion term in the dyeing model improves the results of the dyeing process in terms of dye uptake and levelness.
- Increasing the size of the dispersion coefficients in simulations resulted in increased dye uptakes and improved degree of dye distribution across the package. However, the recorded difference in simulated results was minimal. Therefore, in order to simplify the dye transfer model it may be reasonable to ignore the dispersion effect.

6.4.4 Package geometry

Package geometry plays a very important role in uniformity of the dyeing process and affects other parameters. Specifically the following points should be noted:

- The thickness of the package significantly affects the outcome of the dyeing process by influencing both CDEP and DDF. For instance, a 21% increase in package thickness decreases DDF by up to 10% over the simulation time. Increasing the radius of the package will adversely affect the levelness of the dyeing process, and a practical compromise should thus be considered.

- Package porosity strongly affects dye uptake during the dyeing process. Decreasing the porosity of the package decreases both the rate of dye uptake and DDF.
- Winding yarn packages with an uneven density can result in interesting dye transfer profiles. For instance, increasing the porosity of the package (reduced density) in the direction of liquor flow, according to a pre-set linear profile corresponding to flow velocity, produces a better DDF value. Conversely, dyeing simulation of packages where porosity is linearly reduced (increased density) in the direction of liquor flow shows poorer DDF values. However, it should be noted that the apparent difference in DDF values is not significant.

6.4.5 Integration dyeing

As already mentioned, a number of different approaches have been employed to introduce the colorants to the fibrous assembly. In the so-called integration dyeing, the effect of influential parameters on the outcome of the dyeing should be carefully considered. The following conclusions should be noted:

- In integration (continuous addition) dyeing, the use of different dosing methods produces different dye transfer profiles; however, the difference in terms of DDF between the dosing methods is less than 5%.
- Simulation results reveal that an ideal dosing profile may entail an initial increase of dye concentration according to a quadratic dosing profile followed by a gradual decrease of the dosing rate according to an exponential profile. However, the DDF values obtained for various dosing profiles are not significantly different, and therefore a simplified control approach based on a linear dosing profile would be recommended for practical applications involving continuous addition dyeings.

6.5 References

1. Denton M.J. (1962), 'The Wetting-Out of Yarn Packages' *J. Text Institute*, **53**, T477–T488.
2. McGregor R. (1965), 'The Effect of Rate of Flow on Rate of Dyeing II–The Mechanism of Fluid Flow through Textiles and its Significance in Dyeing' *Journal of the Society of Dyers and Colourists*, **81**, 429–38.
3. Crank J. (1964), 'The Permeability of Cross-Wound Cotton Yarn Packages' *Journal of the Textile Institute*, **55**, T228.
4. Shamey, M.R. (1997), 'The Computer Control of Continuous Addition Dyeing of Cotton with Reactive Dyes' PhD Thesis, Leeds University, UK.
5. Burley R., Wai P.C., McGuire G.R. (1985), 'Numerical simulation of an axial flow package dyeing machine' *Appl. Math. Modelling*, **9**, 1, 33–9.
6. Vosoughi M. (1993), 'Numerical simulation of packed bed adsorption applied to a package dyeing machine' PhD Thesis, Heriot-Watt University, UK.

7

Principles of control in dyeing processes

DOI: 10.1533/9780857097583.154

Abstract: Many dyeing processes consist of repetition of certain procedures or sequences of events that can be modelled and thus controlled. The first part of Chapter 7 introduces the main types of control strategies. The mathematical methods of controlling different dyeing parameters are then explained. Specifically, pH measurement, the effect of various parameters on pH and the development of pH control strategies are examined. The performance of different control strategies on the outcome of dyeing, using a pilot package dyeing machine, is also briefly investigated. The control of the dyeing process according to pre-set exhaustion and other profiles is also described.

Key words: control algorithms, discontinuous control modes, continuous control modes, composite control modes, analog and digital processing, pH measurement and control, dyeing control.

7.1 Introduction

Computer systems directly involved in production can be broken down into two areas of monitoring and control. In most cases both functions are performed by the same system; however, the primary purpose of a control system is generally considered to be the determination and control of the conditions and parameters that can be controlled.

In a broad sense, various processes have been controlled in the textile industry for several decades. However, the use of complete feedback control systems has been generally confined to specific parts of machinery, such as the temperature of fluids in dyeing and finishing processes.[1]

The greatest activity over the last decades in the computerisation of wet processing has been in the field of batch dyeing. This is likely to be due to the fact that batch dyeings typically consist of repetition of certain 'procedures' or step-by-step sequences of events.

An early review of developments in control engineering by Mylroi[2] demonstrated that the use of PID control methods (proportional, integral and derivative; explained later) for the operation of valves will result in an optimum control procedure. Dyebath conditions can now be controlled to produce given profiles. Several authors have reviewed the developments in this domain, as can be found elsewhere.[3–7]

The first part of this chapter introduces the main types of control strategies that are generally employed in various systems. Next, mathematical means of establishing control in the dyeing system are explained. The performance of a simulated dyeing process based on a specific control strategy is also briefly

examined as an example, and, finally, some results from practical dyeings based on the use of these models are reviewed.

In order to test the performance of a given mathematical model, the time–temperature profile or conventional dyeing may first be studied as a reference system. In a set profile a dyeing system can be used for monitoring where a constant temperature rise to the boil, or a set temperature, may be applied and the performance of the machine monitored. The controlled exhaustion profiles can then be analysed in the context of results from set profiles. The desired rate of exhaustion can be calculated based on a change in the set temperature. This method uses a control system known as a feed-forward algorithm. The performance of the control system based on a simulation program and the use of various exhaustion profiles for the dyeing of textile fibres, as well as the merits and shortcomings of each method, are also briefly discussed.

7.2 Introduction to process control

The primary objective of process control is to cause some controlled variable to remain at or near to some desired specific value.[8] When variables are dynamic, a corrective action must be continually provided to keep the variables in agreement. This is the case in the control of various parameters in textile dyeing, including pH, temperature, fluid flow/direction, multiple injections of chemical auxiliaries and dyes, and, of course, the concentration of dye in the dye liquor.

The term 'regulation' defines the operation of value maintenance. Therefore, it can be said that process control regulates a dynamic variable. This is of great importance, since the values of the process cycle in some cases should remain exactly at or near a fixed pre-set value. For instance, pH control in some textile coloration processes can be crucial, and an unsuitable value may adversely affect the quality of the product or may even result in the destruction of the fabric.

In general, measurement refers to the conversion of some variable into analogous electrical or pneumatic information. The controller in a control loop requires two values: measured representation of the dynamic variable and a representation of the desired value of that variable, the latter being referred to as the setpoint. Therefore, the control process consists of a comparison between these two values and an action is required to bring the measured value to the setpoint value.

The error signal is the difference between the measured value C_M and desired value C_{SP}, as shown in Eq. 7.1:

$$E = C_M - C_{SP} \qquad [7.1]$$

A schematic view of the process cycle is represented in Fig. 7.1.

Generally, a setpoint C_{SP} is expressed with some allowable deviation C about the nominal value. The greater the allowable deviation, the easier the system is to control; however, this value cannot be smaller than the inherent system error. This

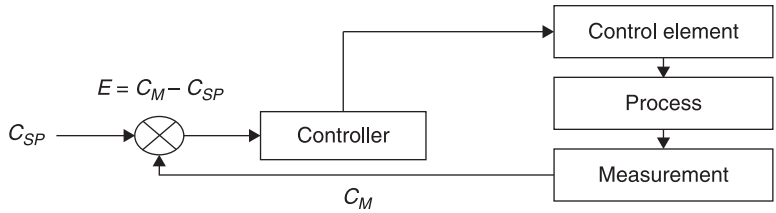

7.1 Schematic representation of the control loop.

may vary for different controlled parameters and the level of accuracy required. Figure 7.2 represents the signal flow in a feedback control system.

The setpoint might be changed during a process control, producing a new value. The control process must be able to bring the dynamic variable to this new value. The approach to the setpoint can be cyclic or damped. In the former system a number of oscillations may occur before the value is stabilised to the setpoint; however, in the latter system the dynamic variable value never overshoots the setpoint or performs oscillations, but approaches the setpoint on an asymptotic-like curve, as shown in Fig. 7.3.

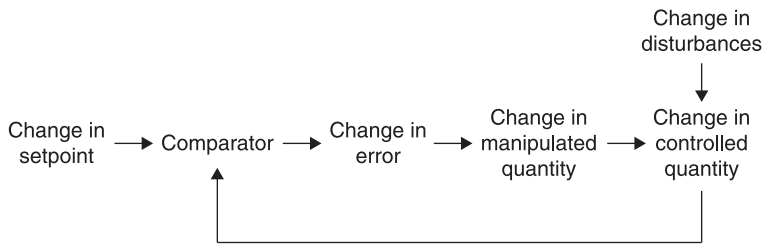

7.2 Signal flow in a feedback control system (from Grady and Mock[1]).

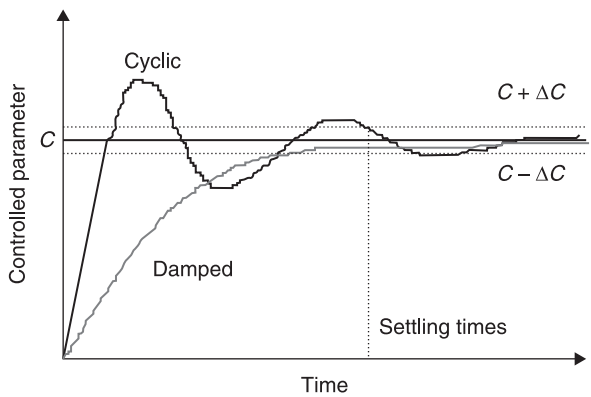

7.3 Comparison of cyclic and damped control methods.

The settling time is the minimum time required to bring the dynamic variable back to within allowable error limits.[9] In some cases, this can be a very small time lag; in others, it may be a few seconds. An example of the latter case is the settling time required for the measurement of pH in a dyebath after an injection of either acid or alkali. In a typical pH control program a few seconds may be allowed for settling time before values are reported to the computer. The insertion or retraction of the pH probe may be carried out by sending an electrical signal to a pneumatic valve. Heaters and the cooler coil may be switched ON or OFF by using simple electrical information, and pumps used for the injection of chemicals may be controlled analogously.

During the monitoring stage the system is normally programmed to produce periodic reports at the end of, usually, time intervals. The information gathered is then analysed to evaluate the performance of the system.

7.3 Control algorithms

7.3.1 Discontinuous controller modes

Two-position mode or the on-off control

This is an example of a discontinuous mode; it is the simplest and the cheapest. In this method of control, power is simply switched on or off depending on the conditions of the system. Although an analytic equation cannot be written, this mode can be represented by logic statements, as shown in Eq. 7.2. For example, if the temperature is lower than the setpoint the heaters are switched on, and if the temperature is equal to or higher than the setpoint the heaters are switched off.

$$P = \begin{cases} 100\% & E_P > 0 \\ 0\% & E_P < 0 \end{cases} \qquad [7.2]$$

where P represents the controller output as percentage of full scale and E_P is the error as percentage of range from setpoint.

A representation of this control method can be found in Fig. 7.4.

Generally the two-position control mode is best applied to large-scale systems with slow process rates. This method leads to the oscillation of the variable about the setpoint, and therefore, in cases where overshooting cannot be allowed, the on-off method cannot be used. This method is used in the control of many home appliances, such as the oven control.

Multi-position mode

This mode of control is based on the extension of the two-position mode by the inclusion of several intermediates for the setting of the controller output. This mode is represented by Eq. 7.3.

$$P = P_i \qquad E_P > |E_i| \qquad [7.3]$$

P_i represents pre-set output values and E_i is the set error value for $i = 1, \ldots, n$. The most common example is the three-position controller, where:

$$P = \begin{cases} 100\% & E_P > E_1 \\ 50\% & -E_1 < E_P < E_1 \\ 0\% & E_P < -E_1 \end{cases} \qquad [7.4]$$

Figure 7.5 illustrates this model graphically. This mode of control usually requires a more complicated final control element because it must have more than two settings.

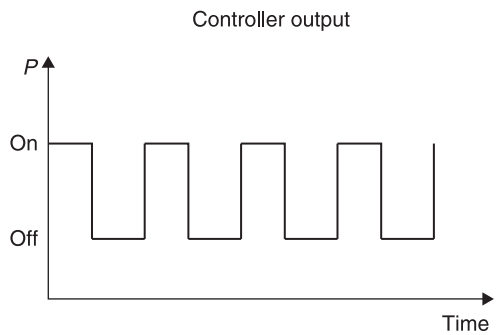

7.4 On-off control method (adopted from Johnson[8]).

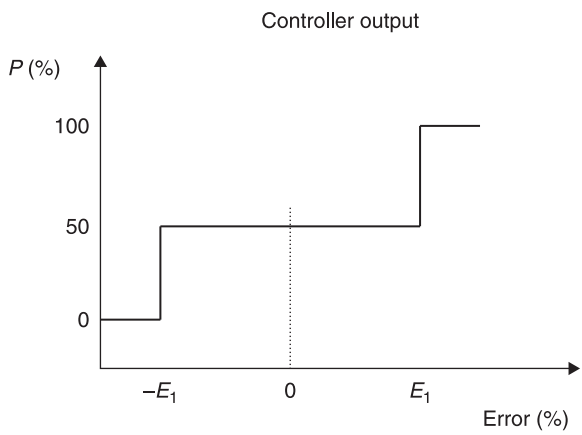

7.5 Three-position controller action (adapted from Johnson[8]).

7.3.2 Continuous controller modes

Proportional control

In a two-position control mode the output has a value of either 100% or 0%, depending on the error being greater or less than the specified value. In a multi-position mode, the number of divisions of the controller output is increased. In a proportional control mode, a smooth linear relationship exists between the output and the error. Therefore, a one-to-one correspondence exists between each value of the controller output and the error. This mode can be represented as shown in Eq. 7.5.

$$P = K_P E_P + P_0 \qquad [7.5]$$

where P_0 is the controller output with no error (%) and K_P is the proportional constant between error and controller output.

In this mode of control, the controller applies high power to the heater if the temperature is well below the setpoint, and the applied power decreases as the temperature approaches the setpoint. Proportional control is also referred to as stepless control, since it avoids the sharp changes inherent in a discontinuous control mode. This mode of control can be represented as shown in Fig. 7.6.

The proportionality constant determines the proportional band. One of the important characteristics of proportional control is that it produces a permanent residual error in the operating point of the controlled variable when a change in system conditions occurs. This error is referred to as offset. This error limits the use of proportional control to processes with moderate to small process lag times, where large changes in conditions are unlikely to happen.

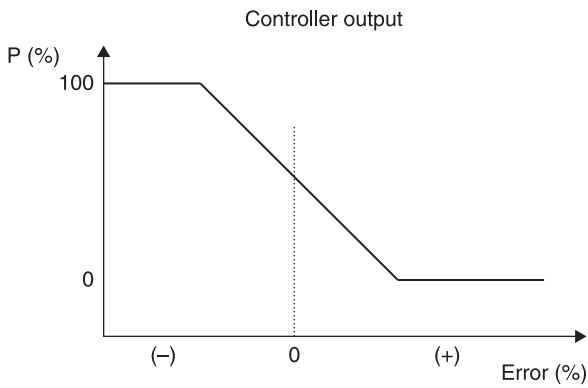

7.6 Schematic representation of proportional mode of control (adapted from Johnson[8]).

Integral control

In this mode of control, the rate of change in controller output depends on the size of the error (see Fig. 7.7). This mode is often referred to as reset action. Analytically, the integral control mode can be represented as shown in Eq. 7.6.

$$\frac{dP}{dt} - K_I \cdot E_P \qquad [7.6]$$

where dP/dt is the rate of controller output change and K_I is the constant relating the rate to the error. The integration of Eq. 7.6 results in obtaining the actual form of controller output at any time, as shown in Eq. 7.7.

$$P = K_I \int_0^t E_P dt + P(0) \qquad [7.7]$$

where $P(0)$ is the controller output at time $t = 0$.

In this mode of control, the value of the output P depends on the history of errors from when observation started at $t = 0$. For a fixed error, the different K_I values produce different values of P as a function of time. Faster rates provided by larger values of K_I thus cause a much greater controller output at a particular time after the error is generated. The relationship between the output values and the error for two different values of K_I is illustrated in Fig. 7.8.

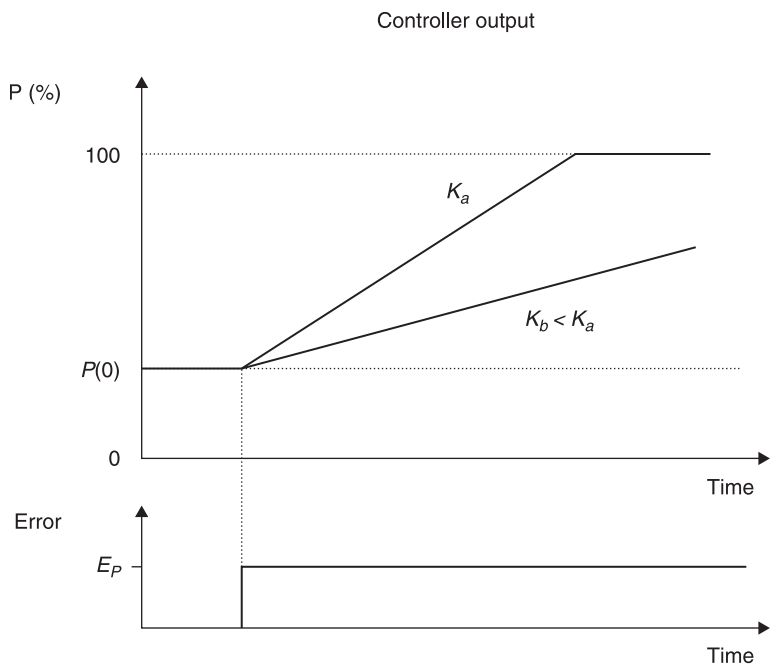

7.7 Integral mode of control (adapted from Johnson[8]).

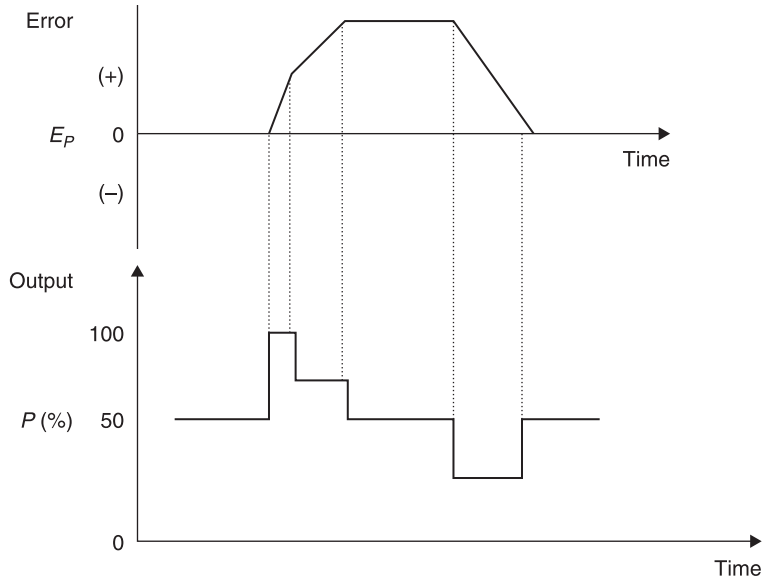

7.8 Schematic representation of the derivative control mode (adapted from Johnson[8]).

In the integral mode, the value of output initially changes very rapidly, but as the error decreases the rate of change of output also decreases. Typically the integral mode is not used alone, the exception being for systems with small process lags.

Derivative control

In this mode, the controller output depends on the rate of change of error. This method of control is also referred to as rate or anticipatory control. The output in this mode of control has no value when the error is either zero or constant, and therefore this mode cannot be used alone. This mode can be expressed by Eq. 7.8.

$$P = K_D \frac{dE_P}{dt} \qquad [7.8]$$

where K_D is the derivative gain constant and dE_P/dt is the rate of change of error. In this mode, for a given rate of error change there is a unique value of controller output. This mode of control is illustrated in Fig. 7.8.

7.3.3 Composite control modes

In most industrial cases a combination of the control methods previously defined is needed to fit given specific requirements. In the following sections these methods are explained.

Proportional-integral control (PI)

This mode of control is a result of the combination of the proportional and integral methods, and can be represented by Eq. 7.9.

$$P = K_P E_P + K_P K_I \int_0^t E_P dt + P_I(0) \qquad [7.9]$$

where $P_I(0)$ is the integral term value at $t = 0$.

The main advantage of this mode is that the integral mode eliminates the inherent offset value while maintaining the proportionality between the error and the output value. The integral feature allows the error to be zero after a load change and effectively provides a reset of the zero error output after the load change.

Because of the nature of this control mode, it can be used in systems where frequent or large load changes occur. However, because of the integration time, the process should have relatively slow changes in load to prevent oscillations induced by the integral overshoot. Another disadvantage of this mode of control is the introduction of a considerable overshoot of the error and output during the startup of a batch process. Figure 7.9 illustrates the PI control mode.

Proportional-derivative control (PD)

In this mode of control, a serial combination of proportional and derivative control modes is used. This mode has many industrial applications, and can be represented as shown in Eq. 7.10.

$$P = K_P E_P + K_P K_D \frac{dE_P}{dt} + P_0 \qquad [7.10]$$

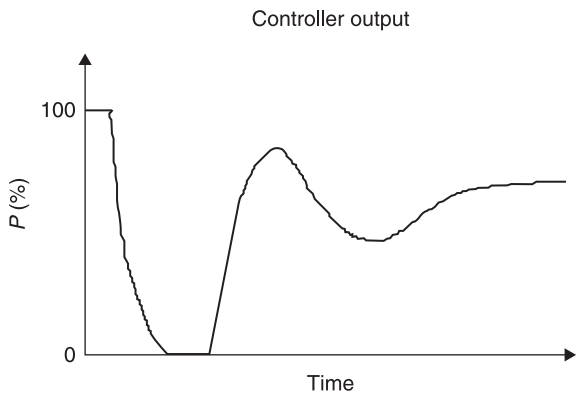

7.9 Schematic representation of a PI control (adapted from Johnson[8]).

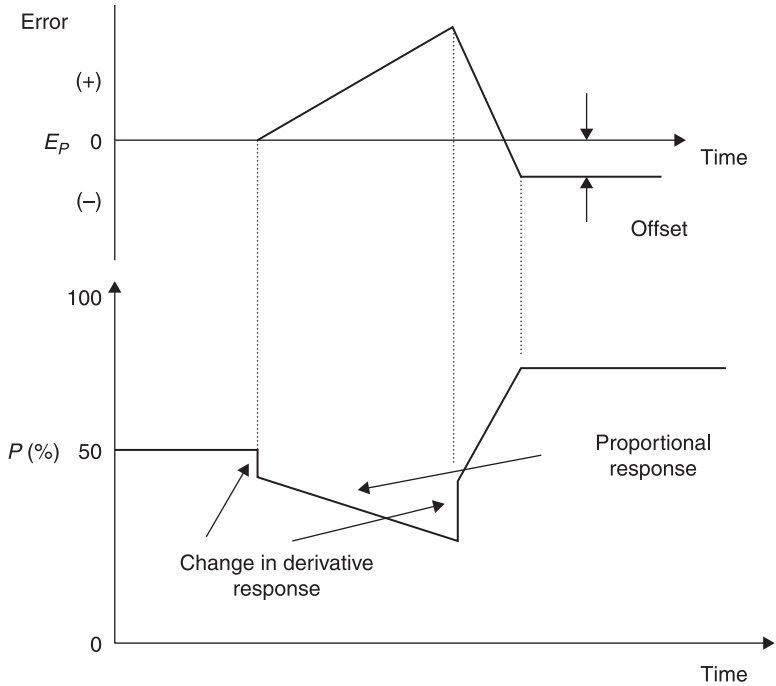

7.10 Schematic representation of the PD control (adopted from Johnson[8]).

The offset generated by the proportional feature of the control mode cannot be eliminated; however, rapid load changes can be handled as long as the offset generated is at an acceptable level. This mode is illustrated in Fig. 7.10.

Proportional-integral derivative control (PID)

The three-mode or PID control is one of the most powerful but complex modes of operation. This mode is a combination of proportional, integral and derivative control modes and thus enjoys the advantages of each of these control systems. The PID mode can be represented by Eq. 7.11.

$$P = K_P E_P + K_P K_I \int_0^t E_P \, dt + K_P K_D \frac{dE_P}{dt} + P_I(0) \qquad [7.11]$$

The integral feature eliminates the offset while the derivative mode provides a fast response. PID controllers are, however, difficult to tune. PID controllers are expensive, but they provide the best control system if properly tuned. A schematic representation of this mode of control can be seen in Fig. 7.11.

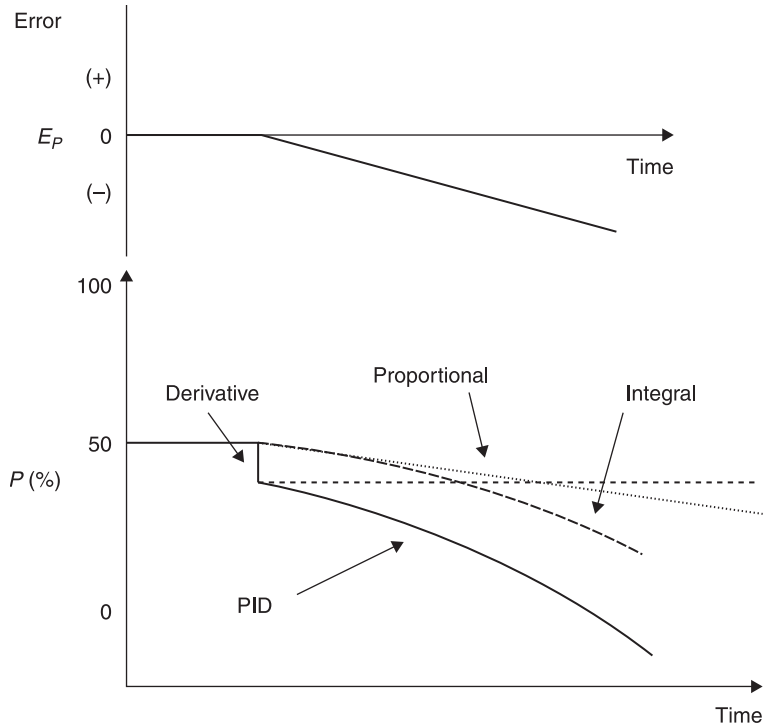

7.11 Representation of PID control mode (adopted from Johnson[8]).

7.4 Analog and digital processing

In an analog process, the variable is represented by a proportional electrical signal. This signal is an analog of the variable. The measured values are sent back to the control system with analog signals. For instance, a means of analog control can be used to control the rate of dosage of chemicals with a metering pump. Analog control in general requires careful attention.

In digital processing, however, all information carried in the process control loop is encoded into a signal that is binary in nature. The electrical signals are represented by a binary 0, also denoted by L, corresponding to 0 volts or a binary 1, denoted by H, corresponding to about 5 volts. Heaters, the cooler coil and the pH probe are examples of elements that may be controlled with digital signals.

The value of the dynamic variable is represented as some encoding of the binary levels. Information in a digitally encoded system can be transmitted through the control loop by two methods: the parallel transmission mode and the serial transmission mode. In the former method a separate wire is required for each binary digit in the word, whereas in the latter method a time sequence of pulses over a single wire transmits the whole word.

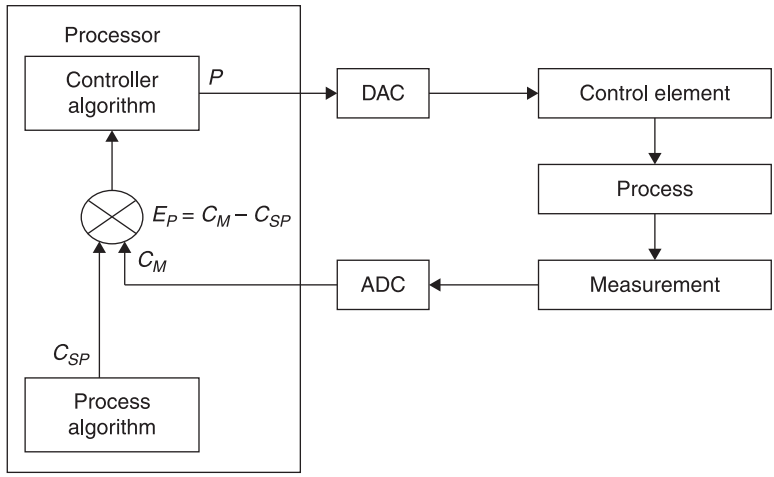

7.12 Process control loop using a computer.

The analog to digital converter (ADC) encodes an analog input. These instruments are designed for a specific range of signal inputs. The digital to analog converter (DAC) provides the reverse action. The schematic diagram of the process cycle including ADC and DAC can be seen in Fig. 7.12.

7.5 Practical application in a pilot-scale operation

To provide a practical example, the general specifications of a pilot-scale package dyeing machine and means of controlling various elements are given in the following sections. Table 7.1 provides general specifications of the machine. Table 7.2 gives a description of digital connections of various instruments to the interface unit. Table 7.3 provides a list of analog connections of various instruments to the interface unit.

Table 7.1 General specifications of a pilot-scale package dyeing vessel

Manufacturer	Longclose Ltd
Total volume with a package inside	16.8±0.1 l
Volume without the package	20±0.1 l
Total power of heaters	11 000 W
Temperature rise rate to 70 °C at room temperature	4.5±0.1 °C/min
Temperature rise rate to 100 °C at 70 °C	3.75±0.01 °C/min
Temperature rise rate to 140 °C at 100 °C	2.8±0.1 °C/min
Equilibrium temperature	38±1 °C
Maximum temperature	140±1 °C
Air cooling power	0.35±0.01 °C/min
Cooling rate at 100 °C to 50 °C	2.25±0.01 °C/min
Cooling rate at 50 °C to 38 °C	0.75±0.01 °C/min

(*Continued Overleaf*)

Table 7.1 Continued

Fluid flow rate range with package inside	0–60 ± 1 l/min
Fluid flow rate range without package	0–78 ± 1 l/min
pH measurement range	0–14.0 ± 0.1
Maximum pressure tested on the original machine	30 lbs/in^2(5.5 kg/cm^2)
Dye concentration measurement range	0–1000 ± 1 ppm
Maximum number of packages	1

Table 7.2 Examples of digital connections for various instruments to an interface unit

BIT No	PORT A		PORT B
0	Small band heater	1.5 kW	Spool valve, fill tank
1	Small band heater	1.5 kW	Spool valve, drain tank
2	Large band heater	3.0 kW	Spool valve, flow reversal
3	Rod heater	2.5 kW	Spool valve, main ventilator
4	Rod heater	2.5 kW	Spool valve, kier ventilator
5	pH probe insert/retract		Spool valve
6	Dosing pump #1		Dosing pump #3
7	Cooling water coil	5.5 kW	Dosing pump #2

Table 7.3 Examples of analog connections of various instruments to an interface unit

BIT No.	Analog INPUT	Analog OUTPUT
0	pH meter	Current to pressure converter
1	Temperature, kier top	Dosing pump #4
2	Temperature, kier base	Conductivity meter
3	Temperature, mixing tank	Not in use
4	Conductivity probe	Not in use
5	Pressure meter #1	Not in use
6	Pressure meter #2	Not in use
7	Flow meter	Not in use

7.5.1 Temperature control and measurement

This process can be divided into two parts: temperature measurement and temperature control. The former may consist of a number of resistance probes (e.g. Platinum100 or similar) that can be located at the bottom and top of the main kier and in the bottom of the mixing tank. These provide a representative temperature of the whole system; however, when necessary their position can be

changed. These probes may be connected to the interface unit analogously, e.g. through terminals 1–3. A connection can also be made to a digital display unit.

Heating may be provided by several band heaters. In the example pilot machine described, the total heat output is 11 kW. Various configurations may be used to achieve the desired output, including two 1.5 kW and one 3 kW heater around the main kier and two 2.5 kW rod heaters in the base of the mixing tank. A control panel may be provided for the manual control of these units. However, heaters could also be controlled via interface. Table 7.2 shows that the interface in this case includes eight TTL-level outputs, i.e. BITs 0 to 7. BITs 0 to 4 are connected to the heaters. In this implementation, single precision integers can be used to store the status of the heaters.

Cooling may be carried out by means of circulating cold water in a coil located around the mixing tank. The coil could also be operated automatically through a digital connection to the interface, in this case BIT 7 of PORT A. Control algorithms of the temperature control are described in more detail later.

A PID system may be used for the control of the heating/cooling. The heat capacity of the heaters and the effect of the main circulating pump should be taken into account and the cooling rate of the machine should also be calculated. The response time of the system should also be measured. As indicated, the system described here is capable of controlling temperature in the dyeing vessel to ± 0.2 °C.

7.5.2 Flow control and measurement

Various types of flow meters are available that are used to determine fluid flow rates in a vessel. An example is an electromagnetic device which allows in-pipe measurement with minimum flow obstruction. Flow reversal can be carried out by using throttle valves that are operated manually or digitally, e.g. BIT 2 of PORT B. Flow measurement readings were taken directly from the instrument display. This could also be logged by the control computer through an analog connection to BIT 7 of Analog INPUT. Figure 7.13 is a photograph of the flow meter used in this study.

A bypass pipe connection may be used to isolate the mixing tank from the rest of the dyeing vessel; in this way low liquor ratios can also be established. The fluid flow loop through the pipes, however, can be controlled by means of pneumatic valves that direct the fluid from inside to outside, or vice versa, of yarn packages. This may be done with the aid of a four-way valve located at the base of the kier. A ventilator valve may be used to direct the liquid in the top of the kier to the mixing tank, and once the kier is full this valve is shut off. Valves may be controlled manually via a control box or via connections to the interface, which in the example in Table 7.2 are BITs 0–5 of PORT B. All pneumatically operated ball valves on the machine may be fitted with double-acting actuators. The actuators may be controlled by solenoid/spring spool valves (e.g. 5/2). The term 5/2 denotes a valve with five ports and two positions.

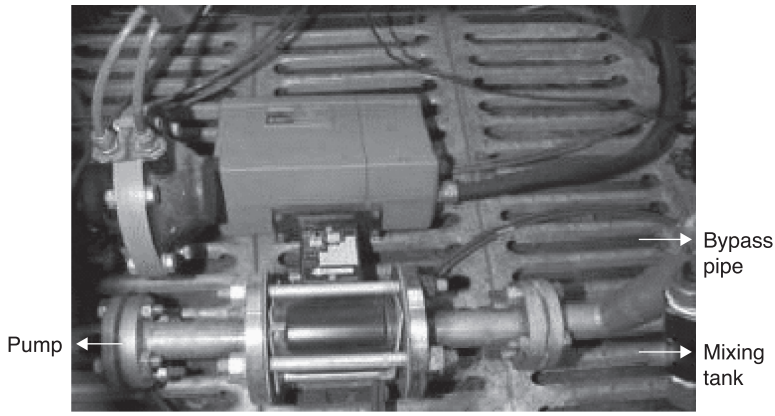

7.13 An electromagnetic flow meter attached to a pilot package dyeing machine.

Spool valves are connected so that the safest position is set; this means that, for instance, the pressure relief valves are connected so that they open if solenoid failure occurs.

7.5.3 Pressure sensors

Pressure sensors may be mounted to report the pressure drop across the package in the event of pressure dyeing, for example in the entry and exit points of the kier. Sensors may also be equipped with displays. Readings may be obtained via analog connections; e.g. BITs 5 and 6 in Table 7.3. The pressure sensors could also be used to measure the flow properties of the package by means of measuring the pressure drop across the package. It is important to note that, due to safety regulations, the dyeing vessel must be suitably checked before any attempts at pressure dyeing are carried out.

7.5.4 Chemical dosing control

Several pumps may be connected to the dyeing vessel to provide liquid delivery (e.g. dyes and auxiliaries) to the bath during the dyeing process without disrupting the overall process. The amount of delivery by pumps can be controlled according to their variable stroke length. The stroke rate per minute can also be adjusted so that the rate of liquid delivery as well as its volume per stroke can be altered. Pumps can be controlled with an analog or digital signal. If the OUTPUT signal from the interface is a voltage signal and the connection requires a current signal, a circuit would be needed to provide the necessary transformation for the running action of the pump. In the case of an analog connection, e.g. BIT 1 of Analog

OUTPUT in Table 7.3, the control program can adjust the rate of liquid delivery according to the requirements of the dyeing bath.

The point of delivery of the pumps should be at a considerable distance from the main circulating pump, since the suction effect of the main pump can seriously affect the metering performance of the dosing pumps.

7.5.5 Dye concentration measurement

A number of methods are currently available to analyse the concentration of dye in the dyebath. In one example, a stainless steel reflectance cell can be mounted to the main section of the pipeline to allow semi-continuous measurements to be taken. The back of the cell may be curved and highly polished to allow a multi-path length reflection, needed for a wide range of possible dye concentrations in the liquor. The front of the cell may house a quartz window to allow visual observation of the liquor during the dyeing process. However, if a cell with a quartz window is used, the cell must be kept clean, as any deposit on its surface would adversely affect the luminance values and therefore the measured concentration of dye.

A variety of measurement heads may be connected onto the cell to obtain readings, and a series of readings should be taken to ensure accuracy. The processed data may include spectral reflectance for each colorant, as well as their L*a*b* and XYZ values. The measuring head must be routinely calibrated, according to instrument type and specifications, to reduce instrumental drift and to minimise error. Readings may be triggered by the software while monitoring the dyeing process at short intervals, e.g. once per minute. The process of measurement and feedback takes only a few seconds in total.

7.5.6 pH measurement and control

A pH meter is often incorporated in modern dyeing vessels to determine changes in pH during the dyeing process. Since control of pH is critical in many applications, this section addresses the process in more detail. The methods for reducing the consumption of chemicals and energy in the dyeing industry are based on:

- regulation of the equilibria and the equilibrium repartition of the dyeing system
- recycling of the rinsing baths.

Processors are used to achieve these energy savings by controlling and lowering the dyeing temperature, and reducing migration time as well as reuse of the dyebath liquor. Saving dyestuff by increasing bath exhaustion and by lowering the consumption of auxiliaries such as levelling and retarding agents is another aspect of increased control. The reutilisation of dyebaths by optimising control also results in water savings and the reduction of environmental pollution.

Level dyeing can be achieved by either controlling the rate of exhaustion or redistributing initially un-evenly absorbed dye by means of migration. The latter is a very energy-intensive process.[10]

The rate of exhaustion is usually controlled by adjustment of the dyebath temperature. In some cases it is also possible to control exhaustion by using a constant or nearly constant temperature, while affecting the composition of the dyebath by addition of salt, acid, alkali or other chemicals. pH influences the 'exhaustion at equilibrium', and the higher this value, the higher is the rate of dyeing at that moment. The value of the initial exhaustion (strike) in a pH-controlled process must be selected in such a way that the initial unlevelness is no more than can be rapidly corrected by the migration of the dye.

The addition of salt, acid, base or other appropriate chemicals to change the ion activity and control equilibrium (exhaustion) can be done continuously in response to a pre-set program, or, through conductivity and pH measurements, by closed-loop feedback control.

The following analysis methods can be used in conjunction with systems that regulate pH in a dyebath:[11]

- titro-processing
- spectrophotometric multi-component analysis
- three-dimensional chromatography.

Titration of a strong base with a strong acid can result in a reusable dyebath, which saves energy and time. This requires a closed-loop control system. However, using weak acids or bases such as acetic acid, NH_4OH and so on produces buffers and a build-up of buffers. So the reuse of such dyebaths necessitates exact knowledge of the chemical composition of the dyebath.

In the dyeing of cellulosic substrates with reactive dyes, or protein and polyamide fibres with acid dyes, to name but a few cases, pH regulation is necessary. Controlled metering of such products as acids, auxiliaries and dyes offers improved reproducibility and levelness, together with reduced labour requirements; machine down-times are also reduced for the same reason.

The term pH is based on p, for power, and H, representing the element of hydrogen. Therefore, pH means the hydrogen ion exponent and pH is a measure of acidity of a solution. The well-known definition of pH can be shown as:

$$\mathrm{pH} = -\log 10\ [\mathrm{H}^+] \qquad [7.12]$$

However, the exact relationship is a measure of the activity of hydrogen ion, and this is shown in Eq. 7.13.

$$\mathrm{pH} = -\log 10\ \alpha_{\mathrm{H}^+} \text{ or } \alpha_{\mathrm{H}^+} = 10^{-\mathrm{pH}} \qquad [7.13]$$

The activity is the effective concentration of the hydrogen ion in the solution. This activity can be related to the concentration of hydrogen ion in terms of its molality (C_{H^+}) and the activity coefficient (f_{H^+}), in other words:[12]

$$\alpha_{H^+} = f_{H^+} C_{H^+} \quad [7.14]$$

In case of dilute solutions, where the ionic strength is low, the activity coefficient is considered to be nearly unity, and therefore the concentration of the hydrogen ion equals its activity. In other words, the difference between the actual and effective concentrations of hydrogen ion becomes progressively less important when moving towards a more dilute solution in which ionic interaction is reduced.

It should be mentioned that the concentration of hydronium ion, instead of hydrogen ion, is considered when referring to pH measurements. This is because hydrogen ion is normally in its solvated form, as shown below.

$$H^+ + H_2O \rightleftharpoons H_3O^+$$

The complexing of hydrogen ion with water affects its activity; however, other more subtle factors are also involved in the correlation of activity and concentration. These factors include temperature T, the ionic strength u, the dielectric constant ε, the ion charge Z_i, the size of the ion in angstrom (Å) and the density of the solvent d. These are specific characteristics of the solution measured.

Two main factors affect the characteristics of the solution, which should be taken into account when relating the activity of the hydrogen ion to its concentration. The first factor is known as the salt effect, expressed as $f^x_{H^+}$. For the hydrogen ion, this effect can be expressed by Eq. 7.15:[13]

$$\log f^x_{H^+} = \frac{-0.5u^{1/2}}{1 + 3u^{1/2}}$$
$$u = \frac{1}{2} \sum C_m Z_i^2 \quad [7.15]$$

where u is the ionic strength, which is defined in Eq. 7.16.

$$u = \frac{1}{2} \sum C_m Z_i^2 \quad [7.16]$$

This is one half of the sum of the square of the charge of ionic species times molality. The exact relationship between the activity coefficient and ionic strength can be expressed by the Debye–Hückel model, shown in Eq. 7.17:[14]

$$\log f^x_{H^+} = \frac{aZ_i^2 I^{1/2}}{1 + b\mathring{A} I^{1/2}} \quad [7.17]$$

In this relationship I is the ionic strength, a and b are the temperature-dependent constants known as Debye-Hückel constants, Z_i is the valence of the ion (i) and $\mathring{A}$ is the ion-size parameter in angstroms.

Table 7.4 shows the approximate effect of salt on activity of hydrogen ion, where monovalent anion and hydrogen ion are considered to reduce Z to 1.[15]

Table 7.4 shows that the activity is decreased when the salt concentration is increased, and therefore the pH value of solutions with the same hydrogen ion concentration will differ if the ionic strength of the solutions varies.

Table 7.4 Approximate salt effects

Molality of salt	0.001	0.005	0.010	0.050	0.100
Activity coefficients	0.964	0.935	0.915	0.857	0.829

The second effect is the medium effect. The medium in which the pH values are measured also influences the activity of the ions. This is designated as $f^{m}_{H^+}$, which reflects the electrostatic and chemical interactions between the ion and the solvent.[16] This is beyond the scope of the current chapter. Therefore, when defining pH, aqueous samples are normally implied. The glass electrode measurement of the activity is mainly influenced by ionic strength, the temperature and the solvent.[17] This is shown in Eq. 7.18.

$$\alpha_H = f^{x}_{H^+} f^{m}_{H^+} C_m \qquad [7.18]$$

Because of these variables, the conditions under which the pH values are measured should be stated. Since temperature, ionic strength and other conditions influence the activity of the hydrogen ion, the pH value of any given sample would not be known automatically if one or more of these conditions were changed. Therefore, when establishing the pH control method for a dyeing system, the variation of hydrogen ion activity should be studied under different conditions (temperature, salt, additions, etc.) if these are to be changed throughout the process. A typical example of this is the activity of hydrogen ion for two buffer solutions under different temperatures, as shown in Table 7.5.

In order to provide an effective and convenient means of representing pH, a pH scale has been established. The range of this scale is based on the dissociation constant for water, K_w. K_w is the activity of the hydrogen ion times that of the hydroxide ion, i.e.:

$$K_w = \alpha_{H^+}\, \alpha_{\mathrm{OH}-} \qquad [7.19]$$

The concentrations of hydrogen ion and hydroxide ion in pure water at 25 °C are equal to 10^{-7} M. The dissociation constant of water, however, changes with a change in temperature. This is shown in Table 7.6.

Tables 7.5 and 7.6 illustrate that the same solutions will have different pH values if the temperature is changed. It has to be mentioned that temperature has little effect on the pH values of acidic solutions.

The measurement of pH is normally carried out electrochemically with a glass electrode and by using the Nernst equation (Eq. 7.20). As can be seen, this equation is also temperature dependent.

$$E = E^{0'} - 0.198\, T_k\, \mathrm{pH} \qquad [7.20]$$

where E is the observed potential, $E^{0'}$ is the stable fixed potential including reference internal potential and T_k is the temperature in Kelvin. Therefore, if

Table 7.5 Activity of hydrogen ion under different temperatures[15]

Solution	Temperature (°C)		
	25	0	60
Neutral			
(H^+)	10.00^{-7}	3.30×10^{-8}	3.10×10^{-7}
(OH^-)	10.00^{-7}	3.30×10^{-8}	3.10×10^{-7}
pH	7.00	7.47	6.51
Basic			
(H^+)	10.00^{-14}	1.14×10^{-15}	9.60×10^{-14}
(OH^-)	10.00^{0}	10.00^{0}	10.00^{0}
pH	14.00	14.94	13.02

Source: Westcott.[15]

temperature is changed during the measurement, the glass electrode should be at thermal equilibrium with the solution to obtain stabilised pH readings.

The full form of the Nernst equation is:[17,18]

$$E = E_0 + 2.3\ \mathrm{R}T/F \log a_{H^+} \qquad [7.21]$$

where E is the measured potential, R is the universal gas constant, E_0 is the standard potential, F is the Faraday constant, T is the temperature in Kelvin, and a_{H^+} is the H^+ activity of the solution being measured.

Replacing the value of 2.3 RT/F with a constant S, it can be said:

$$E = E_0 - \mathrm{S\ pH} \qquad [7.22]$$

Table 7.6 The effect of temperature on the dissociation factor of water

Temperature (°C)	–log K_w	K_w
0	14.943	1.13×10^{-15}
5	14.733	1.85×10^{-15}
10	14.535	2.92×10^{-15}
15	14.347	4.50×10^{-15}
20	14.167	6.81×10^{-15}
25	13.996	1.01×10^{-14}
30	13.833	1.47×10^{-14}
35	13.680	2.09×10^{-14}
40	13.535	2.90×10^{-14}
45	13.396	4.02×10^{-14}
50	13.262	5.47×10^{-14}
55	13.137	7.30×10^{-14}
60	13.017	9.60×10^{-14}

Source: Britton.[19]

and therefore the difference between the potentials of the glass and reference electrodes is a function of the pH of the solution being measured.

$$\mathrm{pH} = (E_0 - E)/\mathrm{S} \text{ at a fixed temperature.} \quad [7.23]$$

S is known as the slope of the electrodes.

The temperature change also influences the resistance of the glass membrane in the electrode. This value doubles for every 7 °C decrease in temperature; therefore, it is normally recommended to use a low-resistance glass electrode for low-temperature measurements. However, this will inhibit the measurement in a full pH range; it is normally limited to the pH of 0–11.

Despite the above, unfortunately there is not a defined relationship between temperature and pH variation. However, it might be empirically possible to approximate a general quadratic relationship, as shown in Eq. 7.24:

$$\mathrm{pH}_T = \mathrm{pH}_0 + \mathrm{B}T + \mathrm{C}T^2 \quad [7.24]$$

The values of B and C depend on the solution used. pH_T and pH_0 represent pH at any temperature T and pH at 0 °C, respectively.

If a temperature compensation method is used in measuring pH values of a solution at a temperature different from that of the standardised temperature, the correct pH value at any given temperature can be calculated using Eq. 7.25.[15]

$$\mathrm{pH}_S = 7 - (7 - \mathrm{pH}_T)T_S/T \quad [7.25]$$

T_S and T are the temperatures of the standardisation and the sample in Kelvin; pH_S and pH_T refer to the correct pH value and the observed pH value, respectively, at temperature T. In order to verify the effectiveness of this corrective approach, a series of buffer solutions of different types should be prepared and the variation of pH with temperature should be recorded with laboratory-grade pH meters. Figure 7.14 shows the relationship for the buffer solutions, where the continuous lines are according to Eq. 7.24.

This relationship is empirical, and therefore the constants for various solutions should be known before any attempt is made to use it in a control system. However, as can be seen, the variation of pH, except at extreme pH ranges, e.g. calcium hydroxide, is typically small, and therefore it might be possible to ignore this effect providing it is sufficiently compensated for in the control algorithm.

Figure 7.15 shows the effect of temperature on pH variation for different concentrations of sodium bicarbonate, similar to those used in the dyeing of cellulosic substrates. However, for practical purposes, changes in pH due to temperature over the dyeing range, with a magnitude of about 0.5 pH units, may be considered negligible.

Another issue to consider is the thermo-volumetric relationship of the solution. Table 7.7 shows the relationship between temperature and volume of a sodium carbonate solution under controlled experimental conditions. The coefficient of volume expansion for liquids is the ratio of the change in volume per degree to the

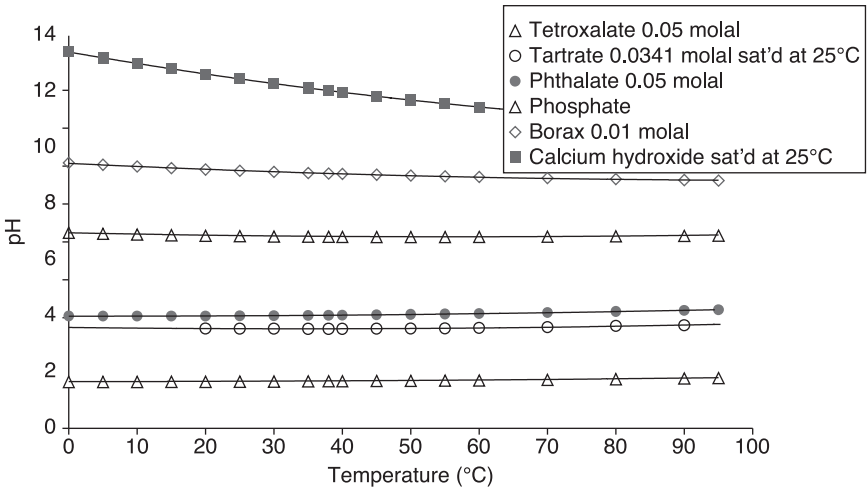

7.14 pH values of different buffer solutions at temperature 0–95 °C.

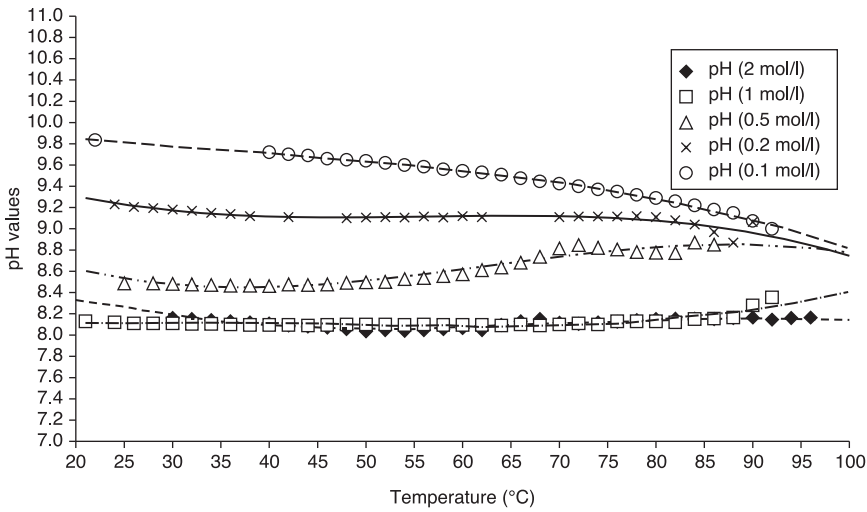

7.15 The effect of temperature on pH values of sodium bicarbonate solutions.

Table 7.7 Empirical results of thermo-volumetric expansion of sodium carbonate (±0.02 ml over a range of 19–97 °C)

Change in T/°C	0	20	34	40	56	72	75	76	78
Change in vol/ml	0.00	0.02	0.03	0.04	0.06	0.07	0.08	0.08	0.08

volume at 0 °C.[20] The value of the coefficient varies with temperature according to Eq. 7.26.

$$V_T = V_0 (1 + \alpha t + \beta t^2 + \gamma t^3) \quad [7.26]$$

where α, β, γ are empirically determined coefficients, and V_T and V_0 refer to volume at temperatures T and 0 Celsius respectively.

It is important to note that, in experimental work involving glassware, correction factors for the expansion of the vessel itself should also be considered. The corrections in volume of the solution as a result of the expansion can be found elsewhere.[15] The coefficients of expansion of glasses used for volumetric instruments are generally considered to vary from 0.000023 to 0.000028.[21]

A similar method to determine the thermo-volumetric relationship of solutions involves the use of a pyknometer, glassware designed for the measurement of density. The cap of the pyknometer includes a capillary which allows the liquid to expand. The liquid can be heated up and then the glass cap including the excess solution is dried. The pyknometer is then weighed. The difference in weight of samples provides a means of determining the volumetric expansion of the solution.

7.5.7 Sodium ion error

Sodium ions can penetrate into the silicon/oxygen network of the glass electrode and cause a potential response error. Table 7.8 shows the correction for sodium ion error. *K* is the selectivity coefficient that relates the ion-exchange equilibrium of the sodium ion compared with that of the hydrogen ion, and S is the Nernst factor, equal to 2.3 R*T*/nF (R and F are constants, n is the charge on the ion,

Table 7.8 Sodium ion correction for glass electrodes

	Glass type	
	0–11	0–14
25 °C		
0.1 M Na^+		
pH 11	0.05	–
pH 12	0.15	0.01
pH 13	0.45	0.03
pH 14	1.00	0.10
1.0 M Na^+		
pH 11	0.15	0.01
pH 12	0.40	0.03
pH 13	1.00	0.10
pH 14		0.30

Source: Westcott.[15]

including sign, T is the temperature in Kelvin). K is a temperature-dependent constant for ion-exchange equilibrium between sodium and hydrogen in the glass and in solution. This effect can be related to the predicted potential by the Nernst equation.

$$E = E^{0'} + \mathrm{S} \log (\alpha_{H^+} + K\, \alpha_{Na^+}) \qquad [7.27]$$

In experimental work involving addition of sodium chloride, in various concentrations, to a series of dye liquors containing different amounts of sodium carbonate under isothermal conditions, while measuring the pH of the solution, the relationship depicted in Fig. 7.16 was observed. As can be noted, an increase in the concentration of salt, for all solutions regardless of initial pH, results in a reduction of pH by up to 0.6 units. The slope of decrease is higher when salt is introduced to the system and becomes flatter beyond sodium chloride concentrations of about 100 gl^{-1}.

In general, the high salt content of some samples can considerably affect pH measurements. This is a result of the ion competition between the ions in the electrode filling solution and those of the sample. This effect is even greater at extremes of pH, since hydrogen and hydroxide ions have such large limiting equivalent conductance values. There are some methods to reduce this effect:

- The use of high-salt buffers, such as those prepared with sea-water.
- The use of a fast-flowing low-resistance junction, such as the sleeve junction.
- The addition of a small quantity of an acid or base to the filling solution increases its compatibility with the solution; this will, however, reduce the stabilisation time.

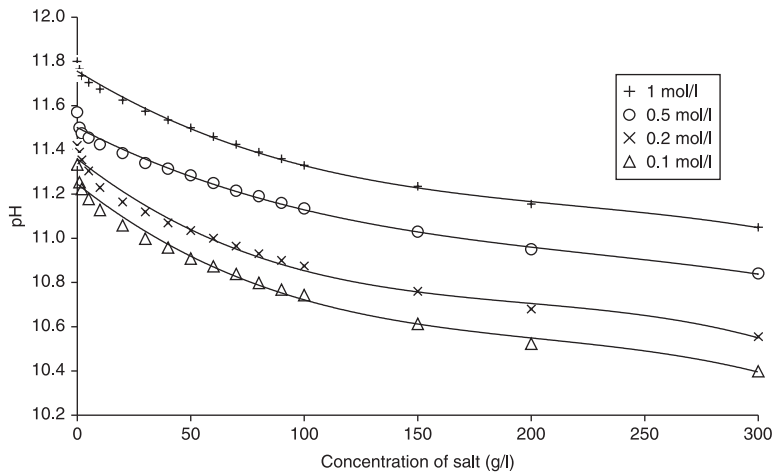

7.16 The effect of the addition of salt on pH readings for sodium carbonate solution.

7.5.8 The effect of the presence of fibre and internal fibre pH

The effective pH within the fibre can vary from that of the circulating liquor. The concentration of any ion in the dye liquor, even those that are non-substantive to the fibre, can be quite different when fibre is present compared with when it is absent. This is explained by the Donnan equilibrium theory and the need to satisfy the requirements of electrical neutrality. The hydrogen ions, although of small molecular size, require significant time to diffuse in or out of, and desorb from, the fibre, thus causing a time lag in achieving a steady pH following a change in the pH of the dye liquor. The presence of fibre in the dyebath further complicates the control of pH in any dynamic system. It has been shown that the internal pH of cellulose affects the fixation stage of reactive dyes[22] and that the internal pH properties of different fibres vary markedly from one to another.[23]

Sumner[22] also showed that the presence of an electrolyte can make a considerable impact on the difference between the internal pH and the pH in the liquor, and that this relationship is different for different fibres. For instance, in the case of cellulose the addition of sodium chloride reduces the difference between the internal and the external pH values, but the internal pH never exceeds that of the dyebath. The difference can be as much as 3 pH units when no electrolyte is present. The presence of 1 mol.l^{-1} of NaCl, however, reduces this difference to about 0.2 pH units. In the presence of anionic dyes, this difference becomes even larger. However, a study of nylon type fibres reveals that, in the absence of dye, the internal and external pH values intersect at the isoelectric point of the fibre. When the fibre carries a positive charge, the internal pH is always higher than that in the dyebath, while after the isoelectric point it is lower than the external pH.

Figure 7.17 demonstrates absorption of sodium hydroxide on cellulose in g/kg of fibre.[24] Experimental results involving the addition of alkali to a dyebath containing a cotton substrate are shown in Fig. 7.18. Results show an initial increase of pH in response to dosing alkali followed by a region of little to no change in pH value. Additional injections of alkali cause the increase of pH value to resume until it reaches its equilibrium for 1 M solution of sodium bicarbonate at around 10.3. This demonstrates that devising a general rule for the inclusion of the internal fibre pH into the control model would be challenging.

7.5.9 Acid error

Acid activity can cause an error in readings. The magnitude of this error is dependent on temperature (weakly), the exposure time and the size of the anions in the solution.

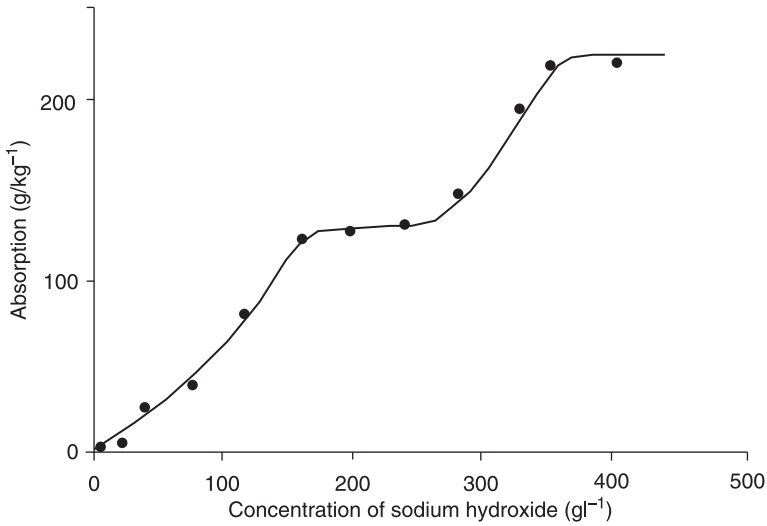

7.17 Apparent absorption of sodium hydroxide by cotton.

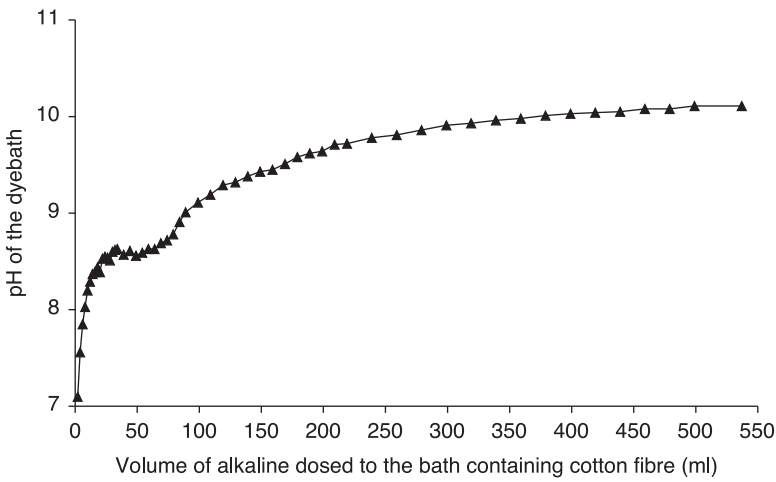

7.18 Observed relationship between dyebath liquor pH and the concentration of alkali.

7.5.10 Other possible sources of error

There are a number of other factors that can cause errors in pH measurements. Table 7.9 illustrates the possible causes of error in pH readings.

Table 7.9 Error sources in pH readings

Difficult samples	Error sources			
	Contamination	Sample resistance	Junction potential	Sample conditions
Non-aqueous oils	×	×	×	
Distilled water	×	×	×	
High salt			×	
Solids (flat, dry)		×	×	×
Viscous slurry	×	×	×	
Extremes of temperature or pressure				×
Strong acid or base			×	×

Each of these errors can be minimised if certain procedures are employed. Contamination of a sample may be reduced by multiple rinses with solvent or purging the sample with an inert gas. High sample resistance can be reduced if a neutral salt is added to the sample. Altering the reference filling solution, using an intermediate electrolyte in an auxiliary salt bridge or changing the type of junction can reduce problems associated with large liquid junction potential. Problems related to sample conditions are potentially numerous, and therefore have to be dealt with according to the type of sample and their characteristics.

The presence of carbon dioxide in the atmosphere is a crucial factor in the pH measurement of some air-sensitive solutions, which should not be underestimated. Sodium carbonate, bicarbonate and disodium phosphate are all sensitive to the presence of CO_2. The presence of carbon dioxide, which may enter a reaction with the ionic species in these solutions, may result in the formation of carbonic acid. In addition, these solutions may act as buffers, and therefore resist dilution. This may be prevented by the introduction into the system of an inert gas such as N_2, which prevents CO_2 from entering any reaction in the system. The quality of water used may also be an influential factor.

7.5.11 Distilled or high-purity water

Distilled or high-purity water has a very low conductivity, such as less than 10 micro-ohms. Therefore samples are likely to show noise caused by high resistance, the unbuffered nature of pure water and also the liquid junction potential. The sample may need a considerable time to stabilise, during which it may absorb carbon dioxide from the atmosphere. In order to reduce these problems the following methods may be used:

- A meter with low bias current capable of handling the high resistance between the inputs may be used.

- A neutral electrolyte can be added; however, this will increase the ionic strength, which in turn will affect the hydrogen ion activity.
- Contamination by carbon dioxide can be reduced by purging the sample with an inert gas such as nitrogen or measuring the sample quickly after exposure to the atmosphere.

It is also important to rinse the electrode thoroughly after standardisation in a buffer solution, since a small amount of buffer can greatly affect the pH value of a high-purity sample.

7.6 pH measurement and control in a dyeing system

A control system can be implemented to measure and monitor the pH change in a typical dyeing cycle. A retractable probe system may be used for pH measurement. The probe can be mounted into a specially designed housing. The insertion and retraction of the probe may be controlled pneumatically, which in turn may be controlled electronically from a signal given by the interface unit.

The pH probe may be connected to a double-screened cable, with the outer screening earthed at the amplifier and the inner screening connected to the reference electrode. The probe may be programmed to be inserted and retracted every minute to allow continuous pH readings to be made. However, the probe may need to remain in the bath for about 10 s each time to establish the equilibrium prior to recording values.

7.6.1 Calibration

Reiterative calibration may be carried out using the following buffer solutions: pH 7 and pH 9.21 for the alkaline range and pH 7 and pH 4.01 for the acid range.

These solutions should be carefully prepared and measured with already calibrated instruments. Buffer solutions prepared from buffer tablets may also be used for comparison to ensure the calibration is carried out properly. The following precautions should be considered:

- If the electrode is dry, it should be placed in an electrolyte solution for a period of 18–24 h.
- For different solution temperatures, sufficient time should be allowed for the pH electrode to establish new conditions.
- In the calibration process, the pH meter mode should be set to ‘Calib’ and the solutions kept at 26 °C.

Figure 7.19 represents the change in the span and zero settings of a typical pH meter in the calibration of buffer solutions over a period of 20 days following the recommended procedure above. It can be seen that, while small variations occurred, the calibration was satisfactory.

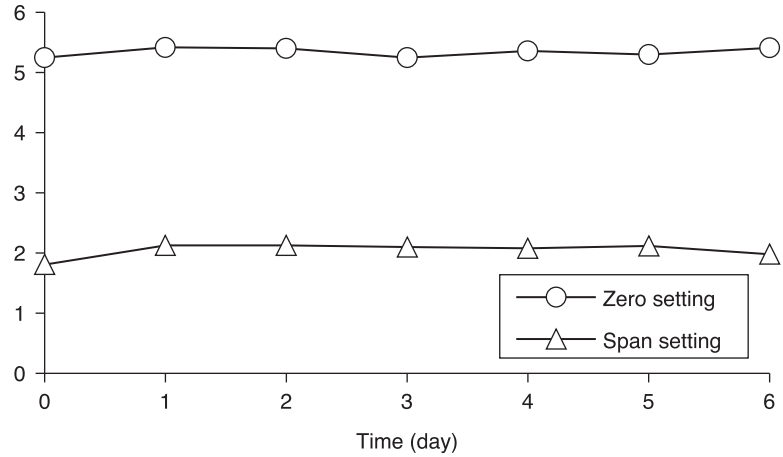

7.19 Span and zero settings of the pH meter over a period of 20 days.

With the probe satisfactorily calibrated, the values recorded by the system should also be calibrated. This can be achieved by plotting signal values against the pH values of different solutions being measured. The next step is to ensure that the values on the pH meter display are calibrated against the logged values.

7.6.2 Measurement of pH values by computer and pH meter

A solution of a known alkali or acid (e.g. 10 g/l NaOH) may be injected isothermally into the circulating liquor of the dyeing machine at 25 °C to eliminate any possible effects of temperature change on the measured values. Readings by the pH meter and the controller are obtained just before the start of the next injection. Injections of known amounts of the reference solution (e.g. 10 ml) may be carried out at 5-min intervals. The values read by the system and pH meter should show a satisfactory agreement to ensure a high level of consistency and accuracy, such as that depicted in Fig. 7.20.

7.6.3 Development of the software for pH control

Two different approaches may be taken to control dyebath pH. The first approach may be based on the specific rate of the inflow of either acid or alkali to the dyebath with spot checks of the pH gradient. In the second method a closed loop control system may be used, in which the addition of chemicals is based on the pH value of the dyebath and the desired pH gradient. Both of these methods are described in greater detail here.

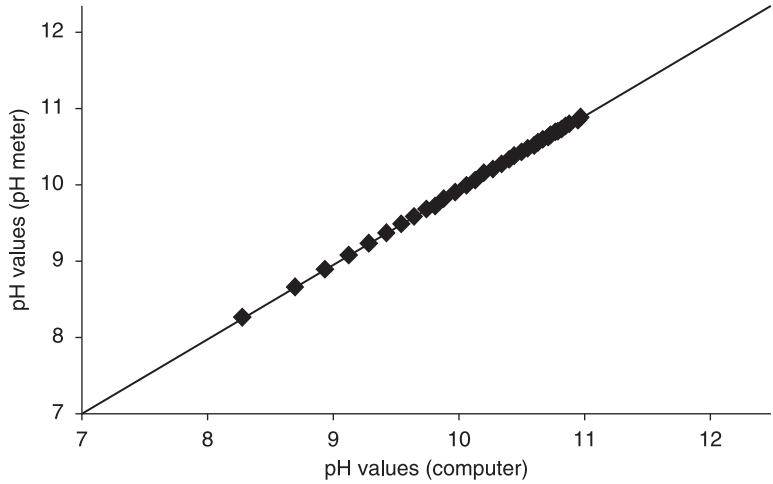

7.20 Calibration of pH meter displayed values against the controller logged values.

7.6.4 Control according to pre-set dosage profiles

The dosage of various solutions according to pre-set profiles is routinely controlled. Several different profiles may be considered, but only three are examined further here: linear, quadratic and exponential.

These profiles may be defined by the following equations, where V is the total volume of the solution to be dosed and V_{dos} is the rate of dosage at any time t. The total volume of the solution that has to be dosed together with the total dosing time determines the constants a, b and c in the pre-set dosing profiles. However, one of the main shortcomings of this system is that these constants need to be known for each profile and each of the various solutions that may be used; therefore, a relatively large database would be required.

Linear profile:

$$V = at \quad [7.28]$$

$$V_{dos} = dV/dt = a \quad [7.29]$$

Quadratic profile:

$$V = a + bt + ct^2 \quad [7.30]$$

$$V_{dos} = dV/dt = b + 2ct \quad [7.31]$$

Exponential profile:

$$V = a\,(e^{bt} - 1) \quad [7.32]$$

$$V_{dos} = dV/dt = abe^{bt} \quad [7.33]$$

Dosage values may be calculated every 20 s for dosage in the following cycle. However, the pH measurement should take place continuously, e.g. once per minute.

Dividing these values by the pump rate would give the dosing time for each cycle:

$$t_p = V_{\text{dos}}/\text{pmprate} \qquad [7.34]$$

where t_p is the dosing time.

Having considered the rate of pH change with the addition of certain chemicals, it should be noted that, if strong solutions are applied, sharp pH gradients will result. On the other hand, the use of dilute solutions will require considerable quantities of the solution to produce a given pH value. For instance, an addition of about 1 ml per litre of a 1:1000 diluted HCl to a neutral bath results in a pH value of 5. The required quantity of the same solution to adjust the pH from 4 to 3 is 90 ml/l. An initial high stroke setting may not be desirable, since a sudden change in the pH could result in unlevelness or dye hydrolysis in the bath. A potential, though not perfect, solution is to employ two different solutions: a strong solution for a pH change at extreme levels and a dilute solution for the adjustment of values towards neutrality. The difficulty involving the initial high sensitivity of the pH change to the amount of solution dosed can also be overcome by controlling the metering pump, varying both the number of seconds per control period that the pump stays on and the rate of pumping during the on period. The control algorithm can determine when small quantities of solution are needed; as the sensitivity of the system is reduced, larger amounts may be injected.

The pumps can be controlled by signals which switch them ON and OFF. The ON time of the pumps is controlled according to the selected profile, which in turn controls the desired volume to be dosed. In order to eliminate the ON/OFF errors of the pumps, any volume which requires a short pumping time, e.g. less than 5 s, can be added to the value of the next cycle.

The temperature of the bath may be compared against the desired temperature at which the dosing should take place. The final desired pH of the bath should also be checked continuously to terminate dosing when this value is achieved. Figure 7.21 illustrates a simple flowchart for this process.

Figures 7.22 and 7.23 show the performance of linear and exponential dosage profiles with a cellulosic yarn package inside the dyeing machine, demonstrating that the control is feasible.

7.6.5 Control according to pre-set pH change profiles

A pH change within the dyebath may be controlled according to one of three profiles: linear, quadratic and exponential with time. This can be shown as:

Linear profile:

$$pH_t = pH_0\left(1-\frac{A}{T}\right)+pH_f\left(\frac{A}{T}\right) \qquad [7.35]$$

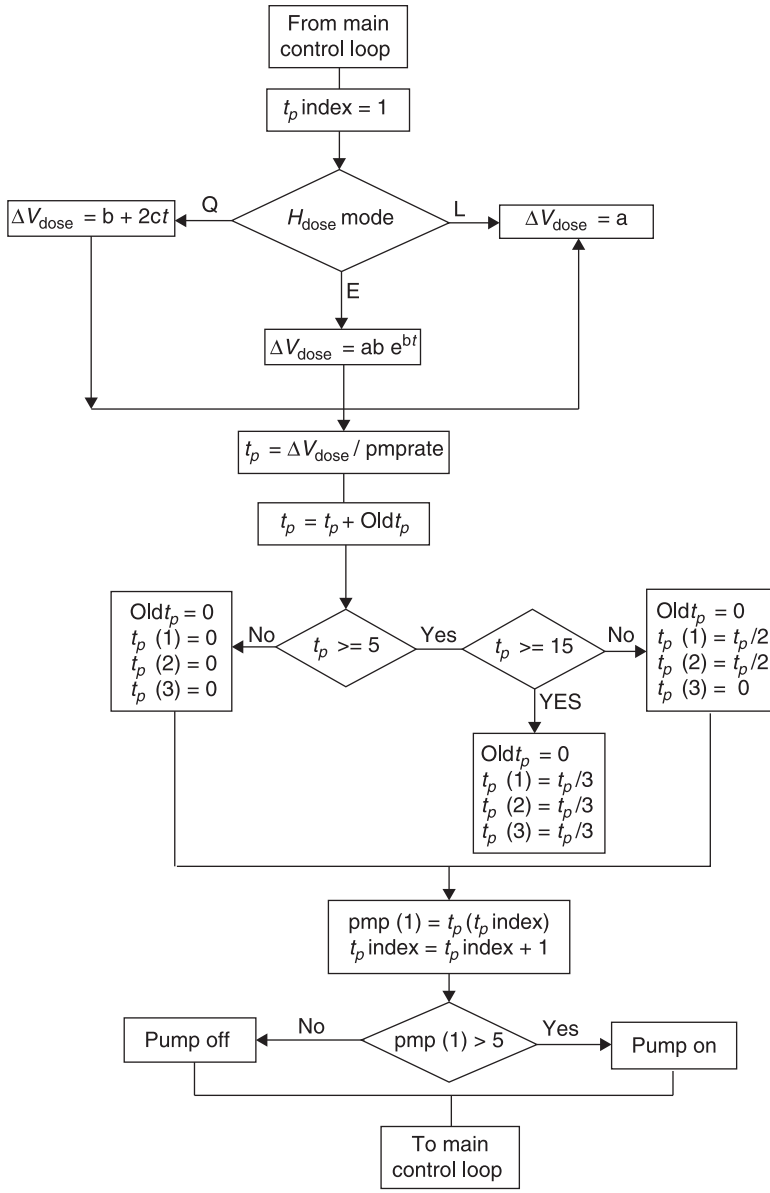

7.21 Flowchart of the program to control dosage according to pre-set profiles.

Quadratic profile:

$$pH_t = pH_0 \left\{ 1 - \frac{\left[1 - \left(\frac{pH_f}{pH_0} \right)^{0.5} \right] A}{T} \right\}^2 \qquad [7.36]$$

Exponential profile:

$$pH_t = pH_0 Exp \left\{ \left[\frac{1}{T} \ln \left(\frac{pH_f}{pH_0} \right) \right] A \right\} \qquad [7.37]$$

The A values are coefficients whose values are determined by the time period over which the change is to be made. pH_t, pH_f and pH_0 refer to pH at any time (t), target pH at the end of the process and pH at the start of the process. T is the total period of time at which the target pH is to be achieved. These profiles are shown in Fig. 7.24.

The pH control sequence involves two major sections: measurement of pH and control of dosing pumps. A simple flowchart for pH measurement is shown in Fig. 7.25.

The effects of the addition of salt, concentration of dye and the dyebath temperature may also be considered in the design of the pH control algorithm. If the desired pH at any given cycle is not achieved, the next cycle's pH value should compensate for this shortcoming. A simple flowchart of this process is given in Fig. 7.26.

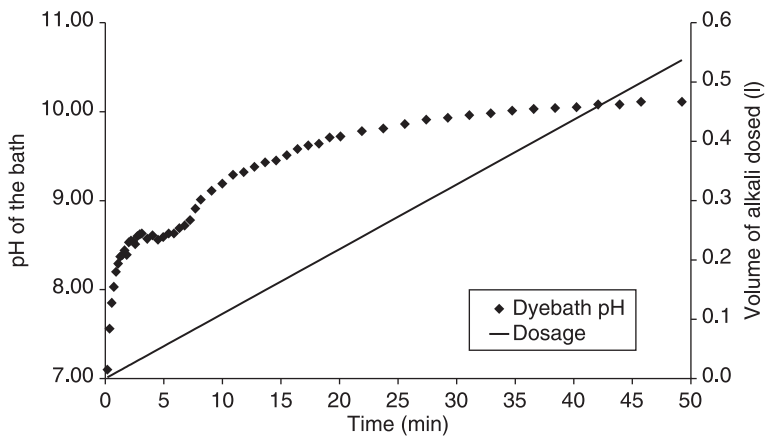

7.22 Linear dosing profile.

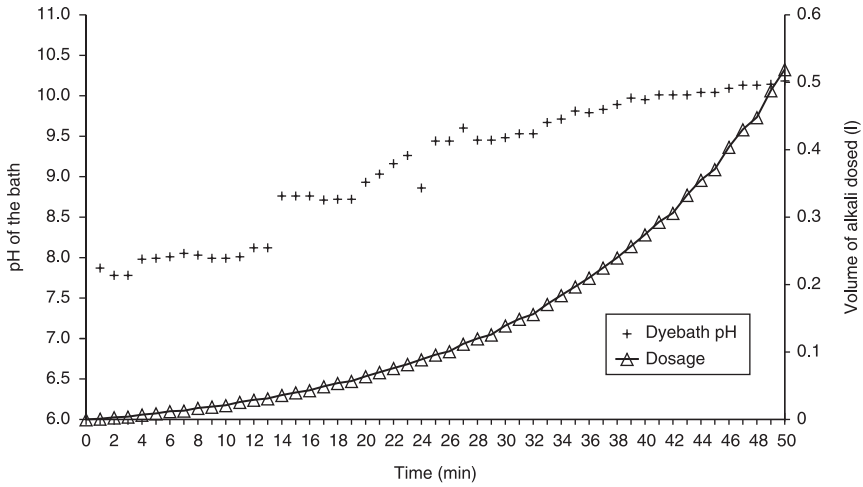

7.23 Exponential dosage control.

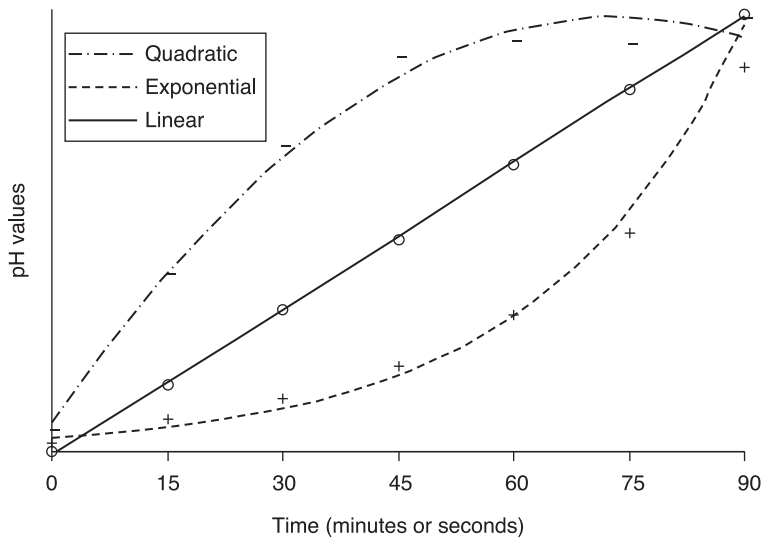

7.24 pH control profiles.

Figure 7.27 demonstrates a flowchart that aims to establish the concentration and type of solution being used as well as the initial and final pH values. The pH control part of the overall control program can take into account the temperature dependence of the dissociation constant of the components in the dyeing liquor. However, it is also possible to reduce the importance of this factor by the careful selection of the materials used.

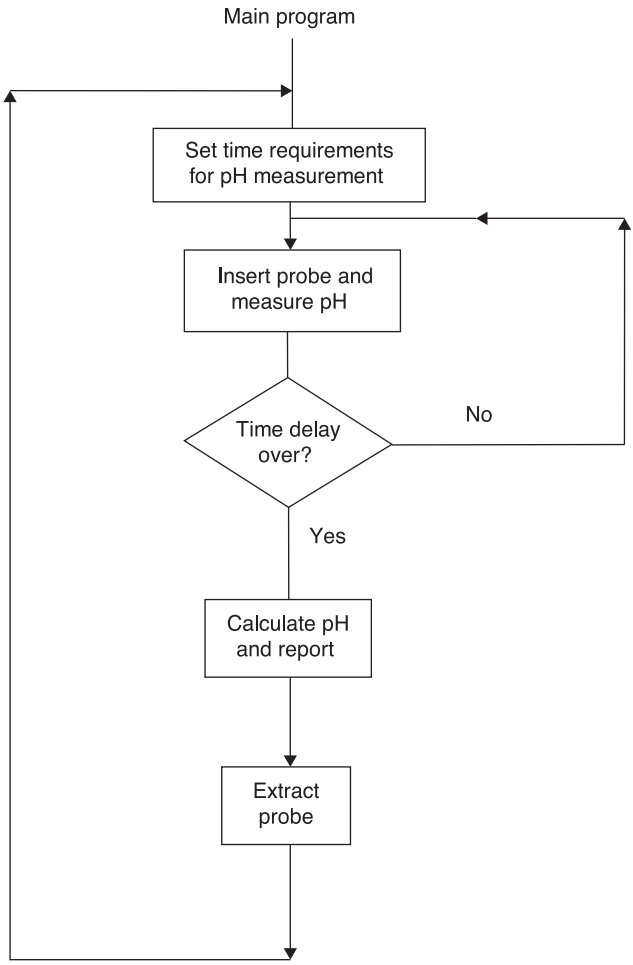

7.25 A simple pH measurement flowchart.

Figures 7.28–7.30 demonstrate the performance of linear, quadratic and exponential control profiles based on the addition of sodium carbonate to the dyebath liquor to adjust pH values. As can be noted, deviations from set values are evident for all profiles based on the use of a single solution at a given strength. As stated previously, the performance of the system can be improved by employing solutions of different ionic strength, though this would increase the complexity of the control algorithm.

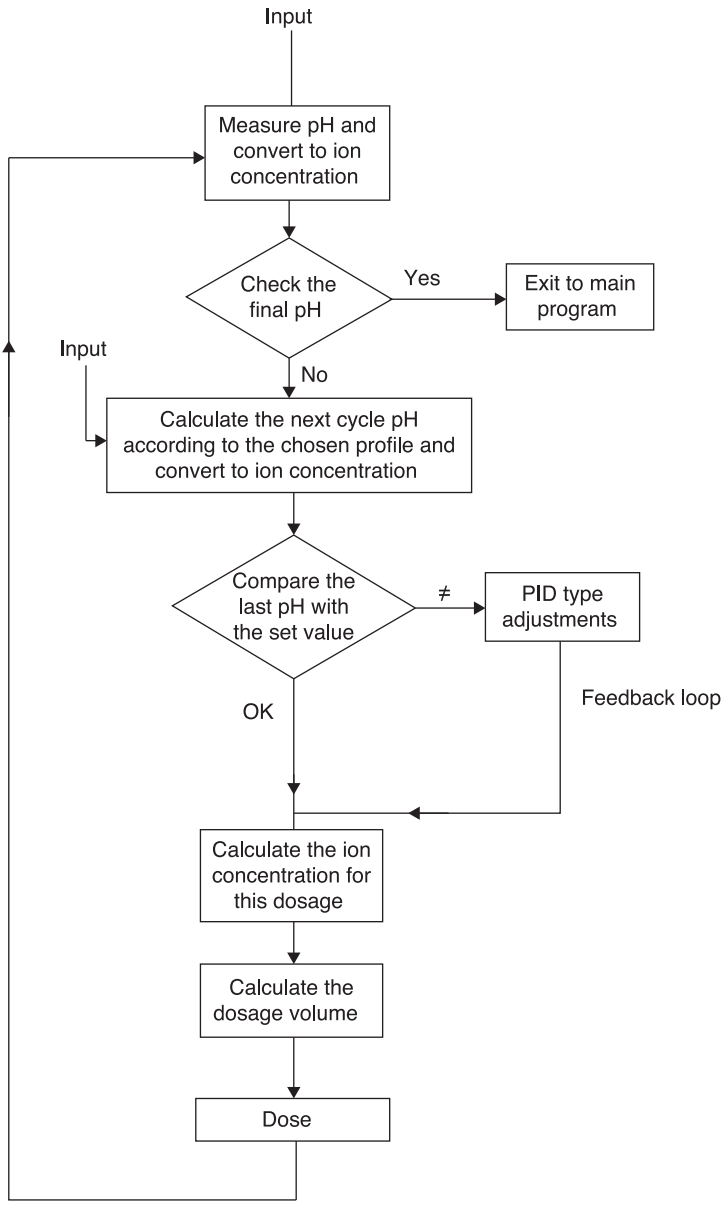

7.26 Main flowchart of the pH change control program.

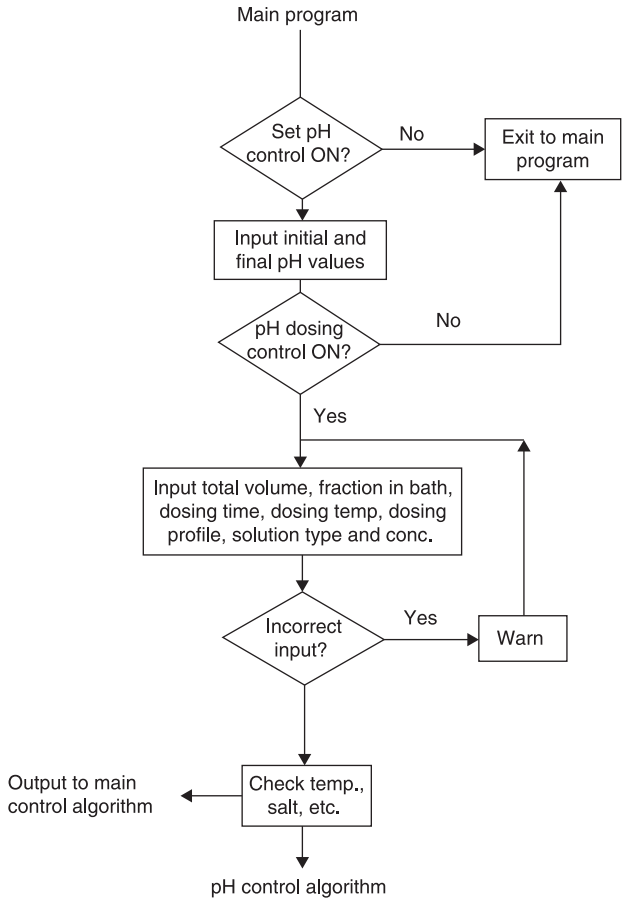

7.27 Input flowchart of the pH change control program.

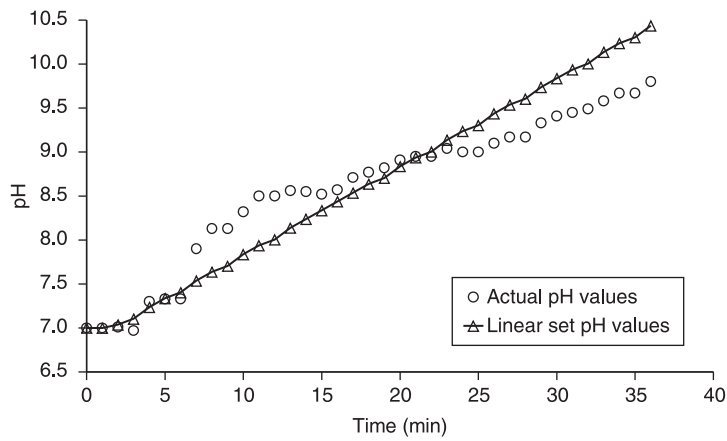

7.28 Set pH against actual pH values for a linear profile based on addition of Na_2CO_3 inside dyeing machine.

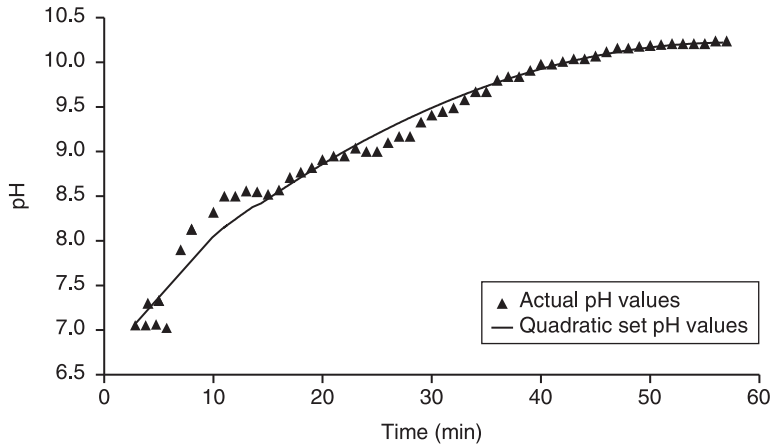

7.29 Comparison of set and actual pH values for a linear profile based on addition of Na_2CO_3 for quadratic control.

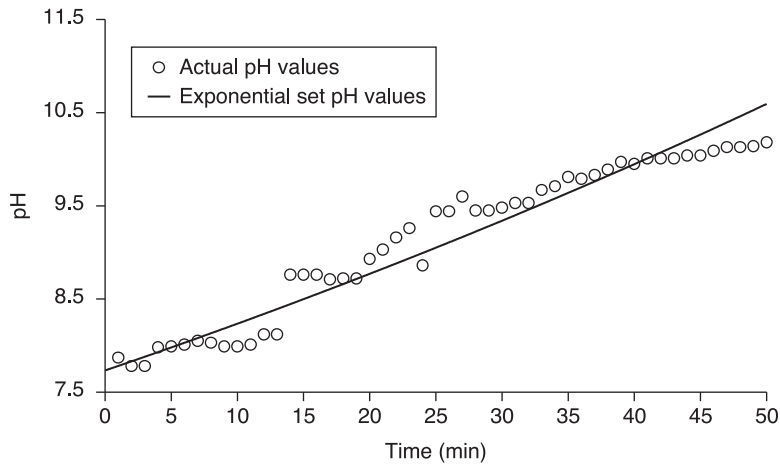

7.30 Comparison of set and actual pH values for an exponential control profile based on addition of Na_2CO_3 to the dyebath liquor.

7.6.6 The relationship between ionic concentration and pH

Although Eq. 7.12, which defines pH, relates the hydrogen ion concentration to pH, it does not provide a means of relating this value to the amount of a material in the solution or the volume of dosing solution of a given concentration needed to produce it. Approximations are required to relate these quantities to pH, as shown in the following section.

Strong acids and alkalis

$$[H^+] = M_0,\ [OH^-] = M_0 \qquad [7.38]$$

where M_0 is the molarity of the original solution defined as shown in Eq. 7.39.

$$M_0 = \frac{\text{Concentration of solution (g/l)}}{\text{Molecular weight} \times \text{Total volume (l)}} \qquad [7.39]$$

Weak acids and bases

$$\left[H^+\right] = \sqrt{M_0 K_a} \qquad \left[OH^-\right] = \sqrt{M_0 K_b} \qquad [7.40]$$

K_a and K_b refer to dissociation constants of acids and bases.

Salt of very weak acid or base

$$\left[H^+\right] = \sqrt{\frac{K_w}{K_a} C} \qquad \left[OH^-\right] = \sqrt{\frac{K_w}{K_b} C} \qquad [7.41]$$

Multi-protonic acids and multi-basic alkalis

A good example of this kind of system is Na_2CO_3, which undergoes the following reactions in water.

$$Na_2CO_3 \rightleftharpoons Na^+ + NaCO_3^- \qquad [7.42]$$

$$NaCO_3^- \rightleftharpoons Na^+ + CO_3^{2-} \qquad [7.43]$$

$$CO_3^{2-} + H_2O \rightleftharpoons HCO_3^- + OH^- \qquad [7.44]$$

$$HCO_3^- + H_2O \rightleftharpoons H_2CO_3 + OH^- \qquad [7.45]$$

If $K_{b2} \ll K_{b1}$ then

$$[OH^-]^2 + K_{b1}[OH^-] - M_0 = 0$$

$$\left[H^+\right] = \frac{-K_{a1}\sqrt{K_{a1}^2 + 4M_0}}{2} \qquad \left[OH^-\right] = \frac{-K_{b1}\sqrt{K_{b1}^2 + 4M_0}}{2} \qquad [7.46]$$

Using these relationships, with appropriate approximations, the volume of the solution that needs to be dosed to produce a given ion concentration in the bath can be calculated. The difference between the calculated pH value and the measured value can then be rectified by the next cycles' calculations. Table 7.10 provides the dissociation constants for some common materials.

Table 7.10 Dissociation constants of some common materials

Name	Formula	K_a	K_b	pK
Hydrochloric acid	HCl	–	–	–
Nitric acid	HNO_3	–	–	–
Formic acid	HCOOH	1.77×10^{-4}	–	3.75
Acetic acid	CH_3COOH	1.76×10^{-5}	–	4.75
Boric acid	$HBO_2\cdot H_2O$	6.00×10^{-6}	–	9.20
Carbonic acid	H_2CO_3	$K_{a1}=3.00\times10^{-7}$	–	6.50
		$K_{a2}=6.00\times10^{-11}$	–	10.20
Phosphoric acid	H_3PO_4	$K_{a1}=9.40\times10^{-3}$	–	–
		$K_{a2}=1.40\times10^{-7}$	–	6.90
		$K_{a3}=2.70\times10^{-12}$	–	11.6
Sodium hydroxide	NaOH	–	–	–
Ammonia	NH_3	–	1.80×10^{-5}	4.70
Calcium hydroxide	$Ca(OH)_2$	–	$K_{b1}=3.74\times10^{-3}$	2.43
			$K_{b2}=4.00\times10^{-2}$	1.40

In conclusion, pH control in the dyebath is influenced by a number of factors, some of which, including the salt content, have a relatively large impact on the measured value. Some of the parameters are rather complicated, and subtle changes may be exerted due to the presence of fibre. Providing relatively small changes in pH can be tolerated (up to 0.5 pH units), it is recommended to consider approximations in various parts of a given control cycle, as this would result in a much simpler control algorithm.

7.6.7 Summary of control strategy

The control strategy discussed above is based on the use of time loops to log data from sensors and control activators based on an appropriate algorithm. In this method the entire dyeing process is divided into short time cycles, e.g. 2 min. Each cycle is then subdivided into smaller loops, e.g. 20 s. The concentration of dye in the liquor is thus measured and reported once every 20 s. In the example given, 5 s may be allowed for the measurement and logging of the data and 15 s for the calculation of the values. The values of the exhaustion based on the concentration of dye in the dye liquor are then updated every 2 min. Temperature readings may be carried out once every second. The change in temperature may be calculated with rolling regression over 40 s. Several consecutive regressions can be performed, each at over 8 s, to calculate the derivative form for the PID temperature control algorithm. A possible PID control of temperature can be based on a 2:1:1 proportion, implying that the importance of the proportional factor is twice that of either the integral or the derivative form. The calculation of the simulated parameters for feed-forward control may be performed once every

Table 7.11 Control algorithm of various parameters

Parameter	Control algorithm
Temperature (T)	PID
pH	Feedback control
Chemical injection	Two-position control, PID
Dye concentration (dosing)	Two-position control
Exhaustion	Feed-forward predictive control
Flow direction	Two-position control
Flow rate	PID

second. The whole cycle is then projected forwards by 2-min steps, each step again being subdivided into smaller loops lasting 20 s. Table 7.11 summarises the methods of control for various parameters throughout this section.

7.7 The feed-forward control strategy

Feed-forward predictive control models are among several that may be used in the control of the dyeing to obtain set pre-defined exhaustion profiles. This is achieved by altering the temperature of the system based on the prediction of exhaustion at any given stage. The model, based on dyeing kinetics, assumes an Arrhenius-type relationship between the exhaustion rate and the temperature.

First, based on experimental work, the concentration derivative (rate of change in the concentration of dye in the dyebath with time) is calculated using rolling linear regression methods. This provides an average value that minimises the random errors that may be associated with single readings.

7.7.1 Calculation of the set exhaustion rate using a set temperature

The aim of developing the dyeing kinetics is to establish an approximate relationship between the rate of exhaustion, the dye liquor concentration and the temperature during the dyeing process. The main feature of such a control program is to predict the dyeing temperature for the next control cycle from the dyebath variables measured during the last control cycle. In order to achieve this, the following information is required:

- the mathematical formula of the exhaustion profile and the value of the control parameter Qi
- the activation energy of dyeing E_a (in most dyeings, activation energy of diffusion)
- for some dye–fibre combinations, the second-order transition temperature range (not always necessary).

The change in the desired exhaustion rate in the model is governed by a change in temperature. In order to calculate the set temperature required for any given exhaustion, the dyeing period is divided into a series of 'control cycles'. Within each cycle it is assumed that the rate of exhaustion has a first-order dependence on the current concentration of dye in the dyebath.

The complete dyeing cycle is divided into N control cycles of period T. At the Jth control cycle the time at which the control cycle starts is t_j; for the previous and following control cycles it is t_{j-1} and t_{j+1}, respectively. The following parameters are then defined:

$C(t_j)$ dye concentration in dyebath at time t_j
$T(t_j)$ temperature of dyebath at time t_j
E_a the activation energy of dyeing
Q the pre-set value of the control parameter.

The first-order assumption defines a rate constant according to Eq. 7.47.

$$K(t) = \frac{1}{c(t)} \cdot \frac{dc(t)}{dt} \qquad [7.47]$$

The control parameter for different exhaustion profiles is then defined as follows[19]:

Linear:

$$Q_1 = -\frac{1}{C_0} \cdot \frac{dC(t)}{dt} \qquad [7.48]$$

Exponential:

$$Q_2 = -\frac{1}{C(t)} \cdot \frac{dC(t)}{dt} \qquad [7.49]$$

Quadratic:

$$Q_3 = -\frac{1}{\sqrt{C_0 \cdot C(t)}} \cdot \frac{dC(t)}{dt} \qquad [7.50]$$

Therefore, a general control parameter for all exhaustion profiles can be expressed as:

$$Q = K(t_j) \cdot C(t_j)^{n/2} \qquad [7.51]$$

where $C(t_j)$ denotes the ratio $C(t_j)/C_0$, and for values of n from 0 to 2 this is an exponential, a quadratic and a linear function, respectively.

In terms of the units used for the practical dyeings, the first-order rate constant is given by Eq. 7.52.

$$\frac{d(cnow)}{dt} = cdrv = -Kave.cnow \qquad [7.52]$$

where *cdrv* is the calculated concentration derivative (ppm/min)

Kave is the first-order rate constant (1/min)
cnow is the current concentration of dye in the dyebath (ppm).

Integration of Eq. 7.47 for the concentration of dye at times t_1 and t_2 results in Eq. 7.48.

$$\ln\left(\frac{c(t_2)}{c(t_1)}\right) = -Kave.(t_2 - t_1) = -Kave.\Delta t \qquad [7.53]$$

where Δt is the length of the control cycle.

The control program assumes that over a short time interval Δt temperature remains constant and then there is an instantaneous temperature jump to the value required to produce an exhaustion rate that gives the value of Q pre-set in the model.

The dye concentration measured at time t (as opposed to the predicted values of dye liquor) is denoted by a dash, i.e. $C'(t)$.

Having measured $C'(t_j)$ and $C'(t_{j-1})$, the quantity $K'(t_j)$, characterised by the actual rate of exhaustion of the liquor, can be determined as:

$$K'(t_j) = -\frac{C'(t_j) - C'(t_{j-1})}{C'(t_j)} \times \frac{1}{t_j - t_{j-1}} \qquad [7.54]$$

and for short time intervals, to a good approximation:

$$K'(t_j) = \left(-\frac{1}{C(t)} \times \frac{dC(t)}{dt}\right)_{t=t_j} \qquad [7.55]$$

From 7.50 and 7.54 and using approximations it follows:

$$C(t_{j+1}) = C'(t_j) \cdot \exp(-K'(t_j) \cdot \Delta t) \qquad [7.56]$$

and since:

$$Q = K(t_{j+1}) \cdot C(t_{j+1})^{n/2} \qquad [7.57]$$

$$K(t_{j+1}) = \frac{Q}{\left[C'(t_j)\exp.(-K'(t_j).\Delta t\right]^{\frac{n}{2}}} \qquad [7.58]$$

It is assumed that over the small temperature and concentration ranges involved in the period t_j to t_{j+1} the Arrhenius equation can be applied to describe the temperature dependence of $K(t_j)$: hence

$$\frac{K(t_{j+1})}{K'(t_j)} = \exp\left(-B.\left(\frac{1}{T(t_{j+1})} - \frac{1}{T'(t_j)}\right)\right) \qquad [7.59]$$

where B is a constant, which for an ideal system would be E_a/R (gas constant). To find the temperature $T(t_{j+1})$, Eqs 7.58 and 7.59 can be equated and rearranged:

$$\frac{1}{T(t_{j+1})} = \frac{1}{T'(t_j)} - \frac{1}{B}\left\{ Ln\left(\frac{Q}{Q'}\right) + \frac{n}{2} \cdot K'(t) \cdot \Delta t \right\} \quad [7.60]$$

where:

$$Q' = K'(t_j)[C'(t_j)]^{\frac{n}{2}} \quad [7.61]$$

The right-hand side of the equation only contains terms that are either set at the start of the dyeing (B, Q, t) or measured quantities (Q', $K'(t_j)$, $T'(t_j)$). The equations can be generalised in form by re-expression without the use of the control parameter Q.

Following Eq. 7.52, the desired concentration *cset* and the desired rate constant *Kset* are determined for the next control cycle.

$$\ln\left(\frac{cset}{cnow}\right) = -Kset.\Delta t \quad [7.62]$$

And from this equation the rate constant can be calculated:

$$-\frac{1}{\Delta t}\ln\left(\frac{cset}{cnow}\right) = Kset \quad [7.63]$$

It was mentioned earlier in this chapter that an Arrhenius type relationship is assumed between the temperature and the rate constant. This is now used to find the temperature *Tset* necessary to produce the given rate constant.

$$Kave = A.\exp\left(\left(\frac{-E_a.}{R}\right).Tave\right) \quad [7.64]$$

where A is the pre-exponential factor or the Arrhenius constant (1/min), E_a is the activation energy of dyeing (J/mol) and R is the ideal gas constant (J/K.mol).

If *Tave* is the current temperature, then:

$$Kset = A.\exp\left(\left(\frac{-E_a.}{R}\right).Tset\right) \quad [7.65]$$

Therefore it can be said that:

$$Kset = Kave.\exp\left(\left(\frac{-E_a.}{R}\right).\left(\frac{1}{Tset} - \frac{1}{Tave}\right)\right) \quad [7.66]$$

Thus:

$$\frac{1}{Tset} = \frac{1}{Tave} - \frac{R}{E_a.}\ln\left(\frac{Kset}{Kave}\right) \quad [7.67]$$

Kset and *Kave* were calculated in terms of dye concentration according to Eq. 7.62. Substituting for these terms in Eq. 7.67 results in Eq. 7.68.

$$\frac{1}{Tset} = \frac{1}{Tave} - \frac{R}{E_a.} \ln\left\{\frac{cnow}{cdrv}.\frac{1}{\Delta t}.\ln\left(\frac{cset}{cnow}\right)\right\} \quad [7.68]$$

Thus it can be seen that the set temperature for the next cycle can be calculated from the current and desired concentrations, the activation energy of the dyeing process and the length of the dyeing.

The rate of temperature rise is calculated from the division of the difference of desired and current temperatures over the control cycle time, i.e.:

$$Trmp = \frac{(Tset - Tave)}{\Delta t} \quad [7.69]$$

In order to control the exhaustion rate, the equations introduced by Nobbs and Ren can be used.[25] These make use of the total elapsed time since the start of the cycle. However, in order to minimise the cumulative errors associated with random deviation of concentration values from the set values, the exhaustion rate can be calculated from the current concentration (or exhaustion). In this method, the consequence of the initial high strikes of some of the profiles at the start of the dyeing is suppressed and the dyeing demonstrates less deviation, since the model restarts at each measured point. Practical determination of the target exhaustion rate takes this into account by replacing c_0 with *cstart*.

As was shown earlier, three exhaustion profiles were used in this model: linear, quadratic and exponential. The general equation defining the exhaustion rate can be shown as:

$$ExhRate = \frac{-dc}{dt}.\frac{1}{c_0} = -\left(\frac{cdrv}{cstart}\right) \quad [7.70]$$

where *ExhRate* is the desired exhaustion rate (fraction/min) and *cstart* is the true starting concentration in ppm. The exhaustion rate for each profile can be calculated as shown below.

Linear profile

This is the simplest form of the exhaustion control, where a constant rate of exhaustion is applied. The concentration at any time *t* is given by:

$$c(t) = -c_0.\left(1 - \frac{t}{td}\right) \quad [7.71]$$

where *td* is the desired exhaustion time in min.

Therefore:

$$\frac{dc(t)}{dt} = -\frac{c_0}{td} \quad \Rightarrow ExhRate = \frac{1}{td} \quad [7.72]$$

Quadratic profile

$$c(t) = -c_0 \cdot \left(1 - \frac{t}{td}\right)^2 \quad \Rightarrow \frac{dc(t)}{dt} = -c_0 \cdot \frac{2}{td} \cdot \sqrt{\left(\frac{c(t)}{c_0}\right)} \qquad [7.73]$$

and the exhaustion rate is:

$$ExhRate = \frac{2}{td}\sqrt{\frac{cnow}{cstart}} \qquad [7.74]$$

As can be seen in this profile, the exhaustion rate is dependent on the total time of dyeing and the current concentration of dye in the dyebath.

Exponential profile

This is defined as shown in Eq. 7.75.

$$c(t) = -c_0 . \exp\left\{\frac{t}{td} . \ln\left(\frac{c(td)}{c_0}\right)\right\} \qquad [7.75]$$

where $c(td)$ is the concentration of dye at time $t = td$ in ppm.

This complicates the model, as the exhaustion time is defined as the time at which 99% exhaustion is attained, since, according to this model, 100% cannot be achieved. Therefore:

$$\frac{c(td)}{c_0} = \frac{1}{100} \qquad [7.76]$$

$$c(t) = -c_0 . \exp\left\{\frac{t}{td} . \ln\left(\frac{1}{100}\right)\right\} \qquad [7.77]$$

thus:

$$\frac{dc(t)}{dt} = \frac{c(t)}{td} . \ln\left(\frac{1}{100}\right) \qquad [7.78]$$

and:

$$ExhRate = \frac{\ln(100)}{td} . \frac{cnow}{cstart} \qquad [7.79]$$

Here, again, the exhaustion rate is dependent upon both the states of progress of the dyeing and the overall time of dyeing. The exhaustion rate is used to calculate the desired concentration at any time t and therefore the rate constant of dyeing. Since the exhaustion is defined as a fraction of the start concentration per minute, the target concentration is calculated by:

$$cnxt = cnow - ExhRate \times cstart \times \Delta t \quad [7.80]$$

where *cnxt* is the target concentration.

7.7.2 Modification of the theoretical model

The model explained in the previous section predicts an increase in unlevelness with decreasing flow rate, as would be expected, the effect being linear with the reciprocal flow rate. It has been shown[26] that, because of the time lags caused by dead pipes, lower rates of fluid flow result in higher unlevelness values than expected. This means that the assumption made in the basic theory about the uniformity of the dye liquor does not hold. The dye–fibre rate constant was previously assumed to be dependent only on the rate of dye absorption and to be constant through the package. In order to modify this theory, a radial dependence to the dye–fibre rate constant of the following form can be used.

$$K(r, t) = K(t) \cdot (1 + \gamma r^n) \quad [7.81]$$

n is initially set as −1, so that:

$$K(r, t) = K(t) \cdot (1 + \gamma/r) \quad [7.82]$$

γ values are set through experimental results.

The control theory assumes that a change in temperature will be immediately achieved. However, in practice this is not the case and a change in temperature is achieved over a period of time. Therefore, the theory is modified to take this issue into account. Gilchrist showed that an increase of 1.5 times the value calculated for set temperature resulted in a better control strategy in the dyeing of acrylic yarn packages.[26] In other words:

$$Knxt = Kave + 1.5\,(Kset - Kave) \quad [7.83]$$

where *Knxt* is the adjusted target rate (1/min).

The other correction is based on the fact that as the current concentration decreases the exhaustion rate will also decrease. Gilchrist also showed that 1-min look-forward times resulted in a good control for exponential and quadratic exhaustion profiles.[26] Therefore, the equations for the desired exhaustion rate can be modified to those shown below.

Linear:

$$ExhRate = \frac{1}{td} \quad [7.84]$$

Quadratic:

$$ExhRate = \frac{2}{td}\sqrt{\frac{cnow}{cstart}} - \frac{2}{td}\sqrt{\frac{cnow}{cstart}} \quad [7.85]$$

Exponential:

$$ExhRate = \frac{\ln(100)}{td} . \frac{cnow}{cstart} . \left[1 - \frac{\ln(100)}{td} \right] \quad [7.86]$$

The final correction to the model is based on adjusting the exhaustion rate at the end of the non-linear exhaustion profiles, when it drops to very low values which would result in the control program trying to cool off the machine. The controller may be adjusted to accommodate a pre-set final ramp rate when the target exhaustion rate drops below 0.2%.

7.7.3 Test of the performance of the model using simulations

Figure 7.31 illustrates a comparison of set exhaustion and exhaustion achieved in a linear exhaustion control profile which shows a very good agreement between the sets. Figures 7.32 and 7.33 illustrate this comparison for a quadratic and exponential control profile, respectively. Again, a good agreement between set and achieved exhaustion values is observed. Therefore, based on simulations of the dyeing process, the model performs satisfactorily in achieving linear, quadratic and exponential profiles.

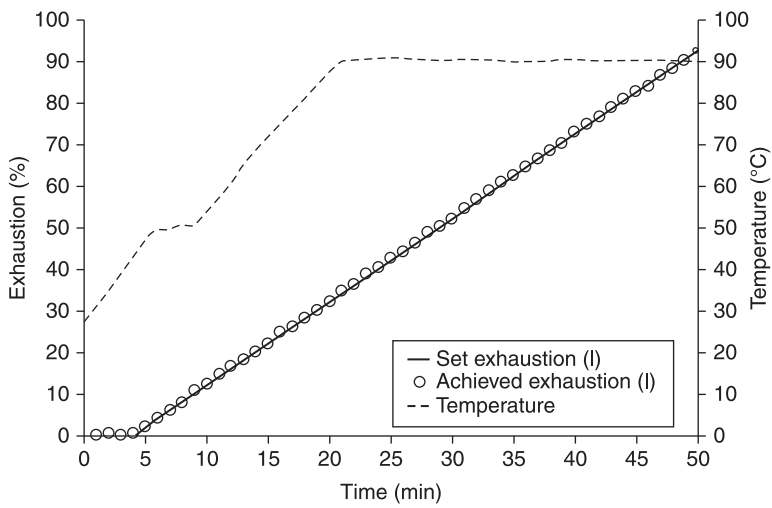

7.31 Simulation results demonstrating a comparison of set and achieved exhaustion values using a linear exhaustion profile.

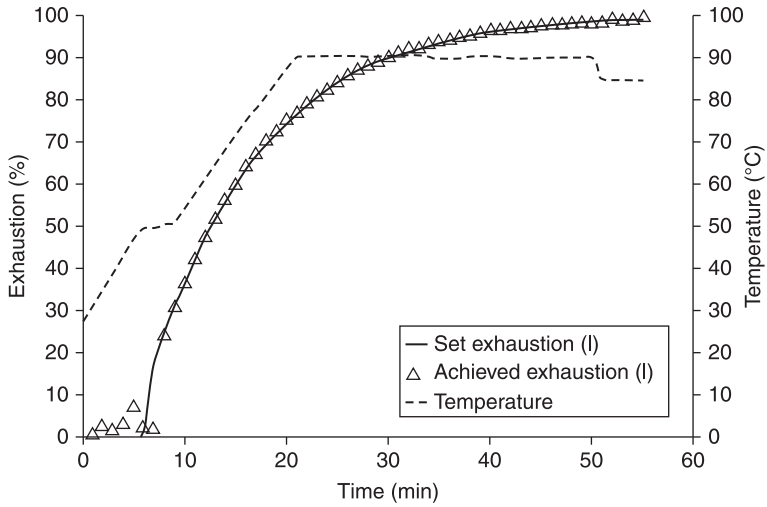

7.32 Simulation results demonstrating a comparison of set and achieved exhaustion values using a quadratic exhaustion profile.

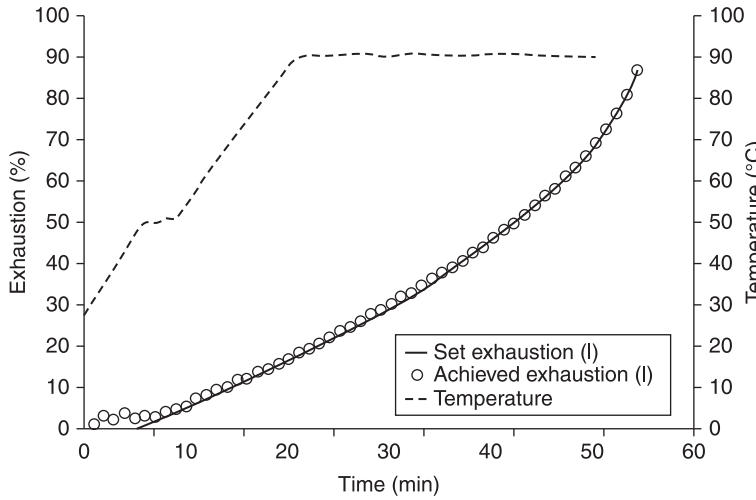

7.33 Simulation results demonstrating a comparison of set and achieved exhaustion values using an exponential control profile.

7.7.4 Assessment of the performance of the model using a dyeing machine

Figure 7.34 illustrates the comparison of measured and predicted dye concentration values in the dyebath based on experimental work. In the example shown, dye

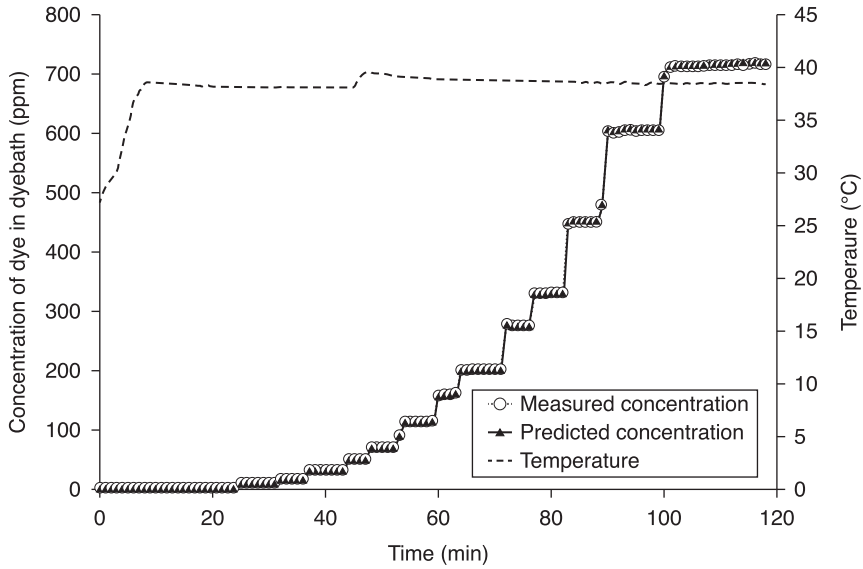

7.34 Comparison of measured and predicted concentration values in a dyebath.

was progressively dosed into the dyebath according to a pre-set profile of dosing, in the absence of a fibre package, and under the following conditions:

Dosing time	80 min
pH	7
Flow rate	50 l/min

The concentration of the dye was changed from 0 to 700 ppm while the temperature was maintained at 38 °C (equilibrium temperature of the dyeing machine). Such comparisons can be used to confirm that the performance of the dye inventory at predicting the amount in the dyebath is satisfactory. Control profiles can also be tested in a similar manner.

The performance of the metering pumps

The addition of dye is used in controlled exhaustion as well as integration dyeing. Therefore, it is important to assess the performance of the metering pumps in dosing calculated quantities of the solution to the dyebath.

To demonstrate the performance of the system, a series of experiments were conducted in which up to 1000 ppm of dye was added to the dyebath at 38 °C according to the linear and exponential profiles over 50 min. The flow rate was adjusted to 50 l/min. Figure 7.35 illustrates the performance of the metering

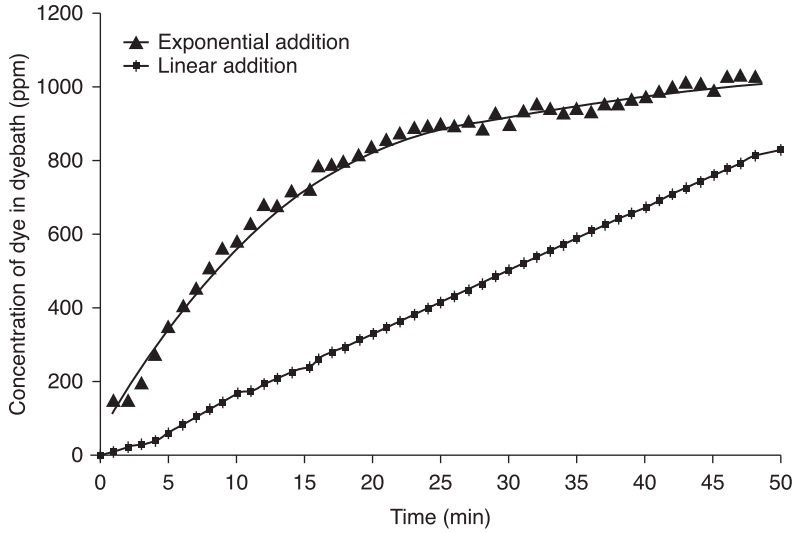

7.35 Testing the performance of the addition pumps based on linear and exponential profiles.

pumps, which was satisfactory. Continuous lines show the target values, and triangles and diamonds show achieved values. Having established this, the control of the dyeing according to pre-set exhaustion and other profiles was investigated. In the following sections a selected group of experimental results representative of each series are explained.

7.7.5 Overall comparison of various control profiles

A close look at the reported exhaustion values at the end of each dyeing profile suggests that complete exhaustion of dye from dyebath is impractical in many cases. Given the number of factors that could affect the outcome of the dyeing process, it is difficult to suggest any one profile as the best profile in terms of overall performance. Various researchers, however, have promoted different exhaustion profile shapes as producing the overall best results compared with the average. However, no conclusive evidence in support of any of the models for use on all fibres has so far been reported.

7.8 Acknowledgement

A software program to control a dyeing machine was written in Quick Basic 4.5 by Dr J.H. Nobbs, in the Department of Colour Chemistry of Leeds University, UK, in the late 1980s. This software incorporated many of the models discussed

here. The work was further developed by a number of researchers, including one of the authors of this book.

7.9 References

1. Grady P.L, Mock G.N. (1983), 'Microprocessors and Minicomputers in the Textile Industry', North Carolina State University.
2. Mylroi, M.G. (1972), *Rev. Prog. Col.*, vol. 3, pp. 33–8.
3. Bialik Z., Park J., Walker D.C. (1979), *Rev. Prog. Col.*, vol. 10, pp. 55–60.
4. Squire D.H. (1974), *American Dyestuff Reporter*, vol. 63, no. 3, pp. 21–5.
5. Anon (1975), *Text. World*, vol. 125, no. 4 pp. 48–59.
6. Anon (Feb. 1981), *Int. Textile. Bull.*, 'Dyeing, Printing, Finishing', p. 155.
7. Bauer K.H., Boxhammer J., Kockett D., Toldrian P. (1979), *Textilveredelung*, vol. 145, no. 5.
8. Johnson C.D. (1988), 'Process Control Instrumentation Technology', 3rd edn, Prentice-Hall Int. Ed., London.
9. Morris N. M. (1991), 'Control Engineering', 4th edn, McGraw-Hill Book Co., London.
10. Carbonell J. (1987), *Am. Dye. Rep.*, vol. 76, no. 3, p. 34.
11. Bettens L., in 'Computers in the world of Textiles', The Textile Institute, Int. Conf., Hong Kong, (1984).
12. Meites L. (1981), 'An Introduction to Chemical Equilibrium and Kinetics', Hungary, Pergamon Press.
13. Bates R.G. (1973), 'Determination of pH, Theory and Practice', 2nd edn, USA.
14. Mac Innes, D.A. (1939), 'The Principles of Electro-Chemistry', Reinhold Publishing Corp, New York.
15. Westcott C. C. (1978), 'pH measurements'.
16. Ricci J.E. (1952), 'Hydrogen Ion Concentration, new concepts in a systematic treatment'.
17. Wilson A. (1970) (ed.) in 'pH meters', Kogan Page, London.
18. Hartley F. R., Burgess C., Alcock R. M. (1980), 'Solution Equilibria', Ellis Horwood Ltd., Chichester.
19. Britton H.T.S. (1955), 'Hydrogen Ions', 4th edn, Vol. 1, Chapman & Hall.
20. Kell G.S. (1975), *Chem. Eng. Data*, vol. 20, no. 1, p. 97.
21. CRC Handbook of Chemistry and Physics, (1980–81), 61st edn, CRC Press.
22. Sumner H.H., Weston C.D. (1963), *Amer. Dye. Rep.*, vol. 42, p. 442.
23. Sumner H.H., in Johnson A. (ed.) (1989), 'The Theory of Coloration of Textiles', S.D.C.
24. Nevell T.P., in Shore J. (ed.) (1995), 'Cellulosic Dyeing', S.D.C.
25. Nobbs J. H., Ren J., 29th Hungarian Textile Conference, Budapest (1985).
26. Gilchrist A. (1995), Ph.D. Thesis, Dept. of Colour Chemistry, University of Leeds.

8

Measurement and control of dyeing

DOI: 10.1533/9780857097583.206

Abstract: The traditional dyeing process is described as a black box, in which the amount of dye on the fabric is not known until the dyeing is completed. Advances in spectrophotometry and computation have enabled an indirect determination of the amount of dye on fabric during the dyeing process based on Beer's law. The principles of a dyebath monitoring technology that allow the analysis and control of the dyeing process are introduced. This measurement technology can aid in troubleshooting root causes in shade reproducibility that can occur from variability in dye strength, the fabric or the dyeing process.

Key words: dye concentration measurement, Beer–Lambert law, real-time monitoring and control, spectral additivity, spectral morphing.

8.1 Introduction

With increasing competition, dye houses are required to meet more exact colour requirements while at the same time reducing the cost of manufacturing. In order to stay competitive, dyers are required to exercise tighter quality control and seek ways to optimise dyeings. This necessitates an understanding of dyes and auxiliaries, substrates and their compatibilities, and parameters that influence the rate and extent of dye uptake by the substrate (Park and Shore, 2007).

The variables that are objectively measured and monitored during a dyeing for quality control purposes have traditionally been limited to time, temperature, pH and conductivity. Measurement of the fabric's reflectance is only utilised in the development of new recipes/procedures and the verification of the dyed fabric shade. During the development of recipes/procedures and the debugging of dyeing problems, dyers continue to rely on indirect information obtained from *ad hoc* trial and error procedures, subjective observations and visual assessments.

Recognising the inherent limitations in attempting to measure the quality of a dyeing without an objective measure of colour, the first prototype systems (Beck *et al.*, 1990; Keaton and Glover, 1985) to monitor the dyebath in real time during a dyeing were developed in the 1990s. However, two main factors limited the adoption of these prototype systems by the industry. The first was the reluctance by machinery manufacturers to incorporate dyebath monitoring and control equipment into new models, as well as the resistance among dyers and dyestuff manufacturers to change the way they analysed the dyeing process. The second factor was technological limitations such as the high cost of spectrophotometers, the low processing speed of computers, and insufficient computer memory restricting the

amount of data that could be manipulated for an accurate determination of dye concentrations.

For example, to determine the dye concentrations of a three-dye combination precisely in real time to an accuracy of two decimal places, it is necessary to use a computer with more than 500 MB of memory. After 2005, computers with these configurations became available at low cost.

With advances in computation and electronics by the mid-2000s, these limitations were overcome. As a result, two research groups, one in England and the other in the US, began adapting dyebath monitoring systems (Dixon and Farrell, 2009; Ferus-Comelo *et al.*, 2005). These systems became the backbone of commercial Right First Time (RFT) dyeing systems in select plants. The historical progress of these technologies was discussed in detail by Smith (Smith, 2007) in his acceptance of the AATCC Olney Award at the 2007 AATCC conference.

8.1.1 The Beer–Lambert law

Although it is self-evident that the main objective of dyeing a fabric is to adhere a colorant onto the fibres in some economically justifiable manner that meets a predetermined set of requirements such as shade, levelness, light fastness or wash fastness, the one parameter that is neither measured nor controlled is the amount of dye on the fabric during the dyeing process. Accurate measurements of dye concentrations on a fabric during a dyeing are quite difficult to perform in real time. This has necessitated performing indirect measurements and calculations of this important quantity. Although it is currently impractical to directly measure the concentration of dye on the fabric, there are analytical techniques for measuring the concentration of dye in a solution. Knowing the concentration of dye in solution and the initial amount of dye, one can determine the liquor ratio, dyebath exhaustion, as well as the concentration of dye on the fabric.

The underlying equation that is a common starting point for most dyebath monitoring systems is the Beer–Lambert (McDonald, 1997) which states that the absorbance A of a solution can be given as:

$$A(\lambda) = l\ \varepsilon\ (\lambda, pH, T, s)\ c \qquad [8.1]$$

where ε is the extinction coefficient (l/g cm), A is absorbance, l is the path length (cm) and c is the dye concentration (g/l). Note that the absorbance and the extinction coefficient are functions of the wavelength λ, the temperature T, the pH, and the salt concentration s, while the path length and the concentration are not.

Although the Beer–Lambert law is somewhat empirical, it has its roots in Kubelka–Munk theory (Kubelka and Munk, 1931), where it is assumed that the medium or solution only absorbs light, and does not scatter it. By measuring the absorbance of the dyebath solution in real time, it then becomes possible to calculate the concentration of the dye or dyes in the solution, and from there calculate the exhaustion of the dye and the concentration of dye on the fabric.

8.2 Real-time measurement of dye concentration

8.2.1 Instrumentation

A typical dyebath monitoring system such as that shown in Fig. 8.1 enables dyers to monitor multiple dye concentrations in the dyebath while simultaneously measuring the temperature, pH and conductivity. Although there are different devices that measure the absorbance of the dyebath and convert these data to concentration or exhaustion, most fall into two main categories: *direct dyebath monitoring* and *indirect dyebath monitoring* systems.

In direct dyebath monitoring systems, a small amount of the dyebath circulates through one or more flow cells, where the dyebath absorbance spectrum is measured by a spectrophotometer. The reason for using more than one flow cell is that large variations in the dye concentration will cause absorbances to be measured that are outside the range of the spectrophotometer. Typically, a spectrophotometer operates in a range of 0.005 to 1.5 absorbance units. One of the

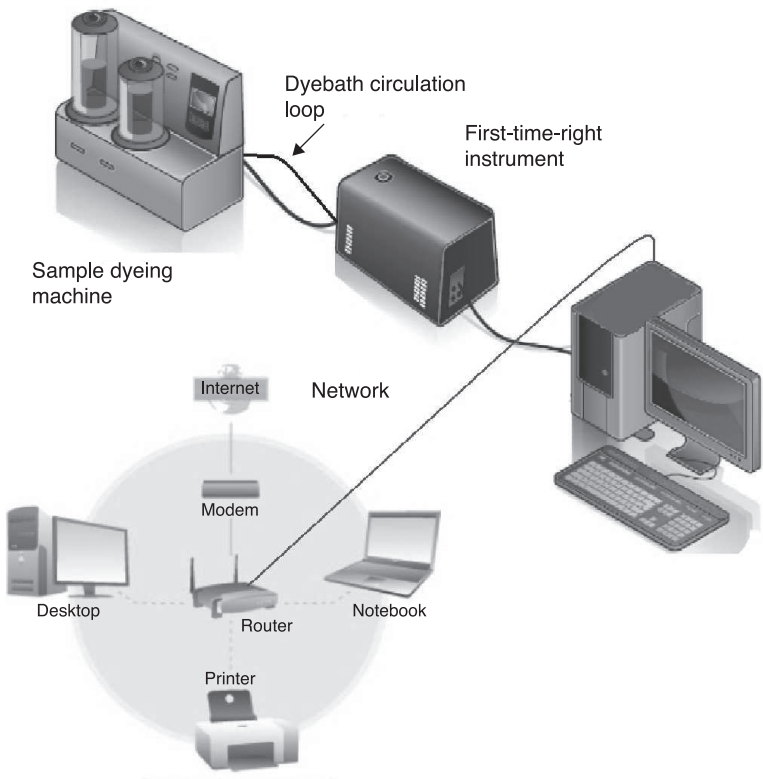

8.1 Indirect dyebath monitoring system.

drawbacks of a direct dyebath monitoring system is that errors in exhaustion readings can occur for non-soluble dyes, dye aggregation, and dyes whose absorbance spectra change with temperature, salt or pH.

The other type of monitoring system is the indirect dyebath monitor, where a small sample of the dyebath is sampled and conditioned in a buffer solution to remove any dependency on temperature, salt or pH. Also, if the dye is insoluble in water, it can be dissolved in the buffer solution. Then the dyebath sample is diluted to a range between 0.005 and 1.5 absorbance units before being read by the spectrophotometer.

These systems determine individual dye concentrations according to the Beer–Lambert law (McDonald, 1997) and the additivity of dye spectra (Johnson, 1989). Some of the existing systems (Dixon and Farrell, 2009) are now capable of measuring dye concentrations of most dye classes, including water-insoluble disperse and indigo dyes or dyes of similar hues.

8.2.2 Calibration of single and multiple dyes

For a single dye, one can establish a relationship between the concentration and the absorbance at a particular wavelength by measuring the absorbances for known concentrations (Johnson, 1989). Figure 8.2 shows absorbance readings at wavelength 606 nm for the Multireactive Blue FN-R at a fixed path length. Note

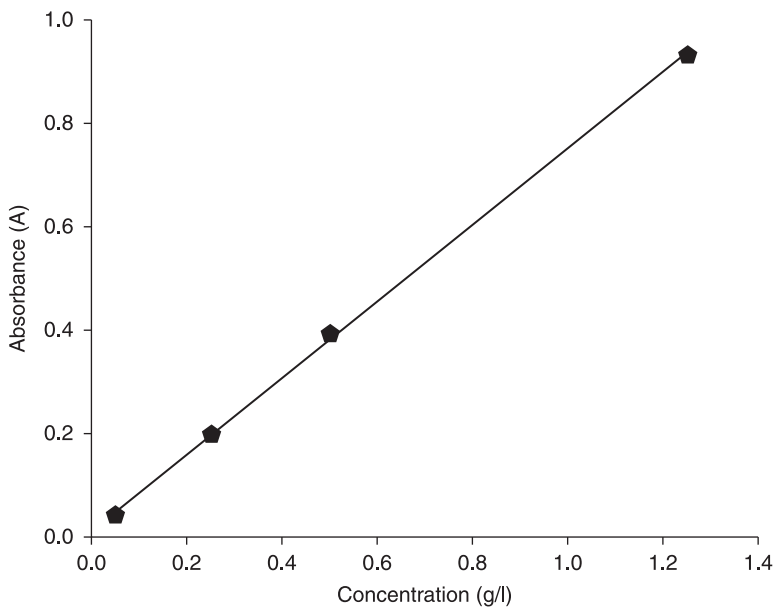

8.2 Absorbance vs concentration of Multireactive Blue FN-R.

that the slope of the line is equal to the product of the molar extinction coefficient and the path length. The molar extinction coefficient is a property of the dye, as given in Eq. 8.1.

While the determination of the concentration for a single dye is relatively easy, an accurate determination of each dye's concentration in a mixture requires the identification of the individual spectral dye components of Eq. 8.2 using a prediction method such as least squares (Berkstresser and Beck, 1993; Lijung, 1987; Saguy *et al.*, 1978, Zamora *et al.*, 1998).

In a dyebath where the dye or dyes are exhausting onto a fabric, the absorbance of the dyebath will change over time. Thus, a more general expression of Eq. 8.1 can be given as:

$$\boldsymbol{A}(t) = \sum_{i=1}^{\#\,dyes} \mathbf{f}_i c_i(t) \qquad [8.2]$$

where $\boldsymbol{A}(t)$ is the absorbance of the dyebath at time t, c_i is the concentration of dye i, and the $\mathbf{f}_i$ are vectors of the spectral components of the individual dyes.

8.2.3 Accuracy, precision and sample rates

Equation 8.2 has the following five basic assumptions:

- Measurements are repeatable. The same input will give the same output.
- The dyes obey the Beer–Lambert law of linear scaling.
- The dyes obey the super-position (spectral additivity) law.
- The $\mathbf{f}_i$ are constant for a given dye (no spectral morphing) (Günay and Jasper, 2010).
- The $\mathbf{f}_i$ are linearly independent.

Violations of these assumptions are the root causes for predictions of concentration to fail using a linear model.

For a single dye, Eq. 8.3 may be used to quantify the error in prediction (Berkstresser and Beck, 1993).

$$\%\text{Error} = \frac{\left(c_{\text{actual}} - c_{\text{predicted}}\right)}{c_{\text{actual}}} \times 100 \qquad [8.3]$$

There are many ways to generalise Eq. 8.3 to the case of multiple dyes. A common approach is to develop a norm or metric. A norm is a function that assigns a non-negative length to all vectors in a vector space. Two common examples are the 1 norm and the 2 norm. The 1 norm is defined as:

$$\%\text{Error}_{\text{1 norm}} = \frac{\sum_i^n \left| \left(c_{i_{\text{actual}}} - c_{i_{\text{predicted}}} \right) \right|}{\sum_i^n c_{i_{\text{actual}}}} \times 100 \qquad [8.4]$$

while the 2 norm or RMS is defined as:

$$\%\text{Error}_{2\ \text{norm}} = \sqrt{\frac{\sum_i^n \left(c_{i_{\text{actual}}} - c_{i_{\text{predicted}}}\right)^2}{\sum_i^n c_{i_{\text{actual}}}^2}} \times 100 \qquad [8.5]$$

It is difficult to quantify which metric is better, or how errors in concentration correspond to errors in perceived colour on a fabric. One reason for this is that dyeing is a dynamic process, where the final shade and levelness depend upon the rate at which the dye was applied onto the fabric, not just the final amount.

Measurement repeatability

It is important that the dye in the solution is uniformly dissolved and that the solution is free of air bubbles and foreign material. Although this may not be achieved all the time, measurement errors may be reduced by increasing the sample concentration or averaging data where possible.

For example, air bubbles change the index of refraction of the water, causing fewer photons to reach the detector. If the bubbles appear during the measurement of the reference, I_0, the absorbance for the whole spectrum is lower; if the bubbles appear while measuring the dye solution, I, the absorbance at all wavelengths will be increased, as seen in Fig. 8.3. A decrease or increase in absorbance for a single dye may result in a decrease or increase, respectively, in the predicted concentration.

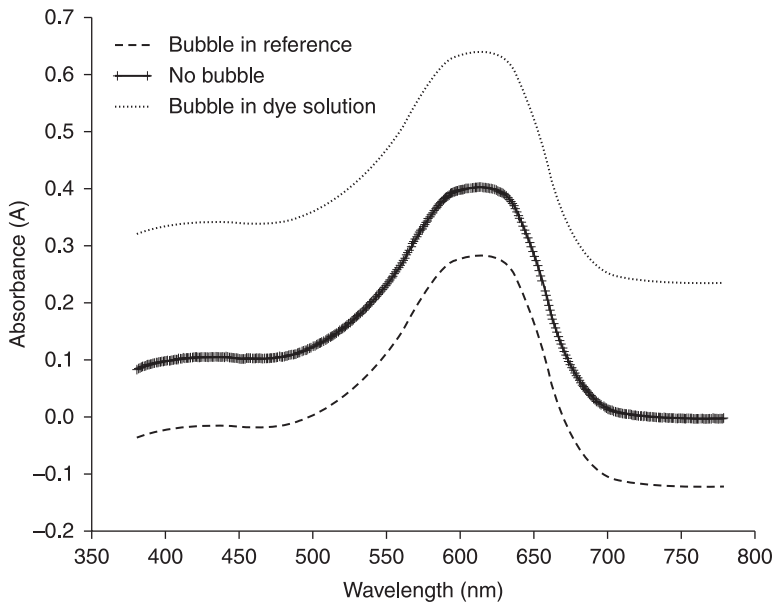

8.3 Shift in absorbance due to imperfections (air bubbles) in the solution.

In addition, attention has to be given to proper cleaning of the instrument between measurements when different classes of dyes are to be measured. It is a well-known fact that basic dyes have a high staining potential. Unless dye residue is completely removed from the instrument, subsequent measurements may produce erroneous results due to contamination.

Application of the Beer–Lambert law

When the path length and colorant are kept constant, the Beer–Lambert law suggests a linear relationship between the absorbance and dye concentration at a given wavelength. Using Eq. 8.1:

$$A = -\log\left(\frac{I}{I_0}\right) = lec \qquad [8.6]$$

$$I = I_0 10^{-lec} \qquad [8.7]$$

where I_0 is the initial light intensity or photon flux entering the flow cell, and I is the light intensity exiting the flow cell. Figure 8.4 shows a plot of the photon count of the light intensity reaching the spectrophotometer that has been transmitted through a medium of coloured solutions of various concentrations. In this example, $I_0 = 23\,000$ counts and the concentration varies from 0 to 2.75 g/l.

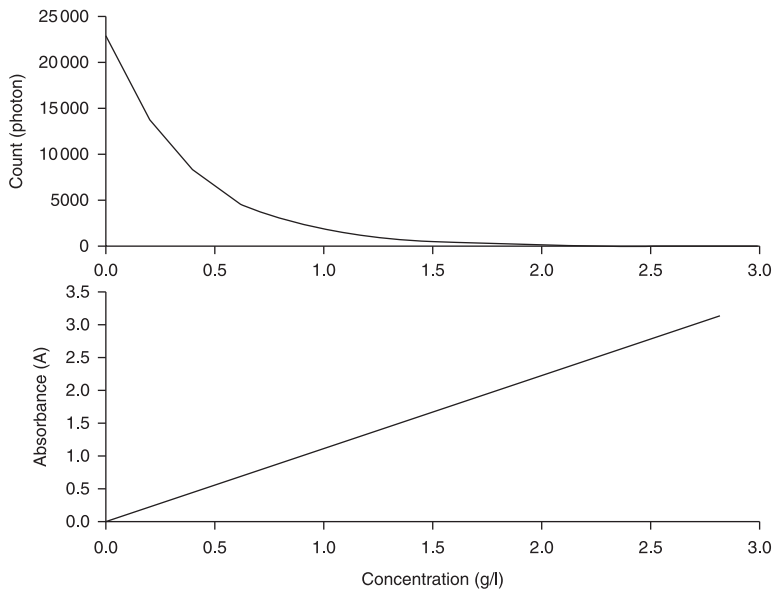

8.4 Relationship between transmittance, absorbance and concentration.

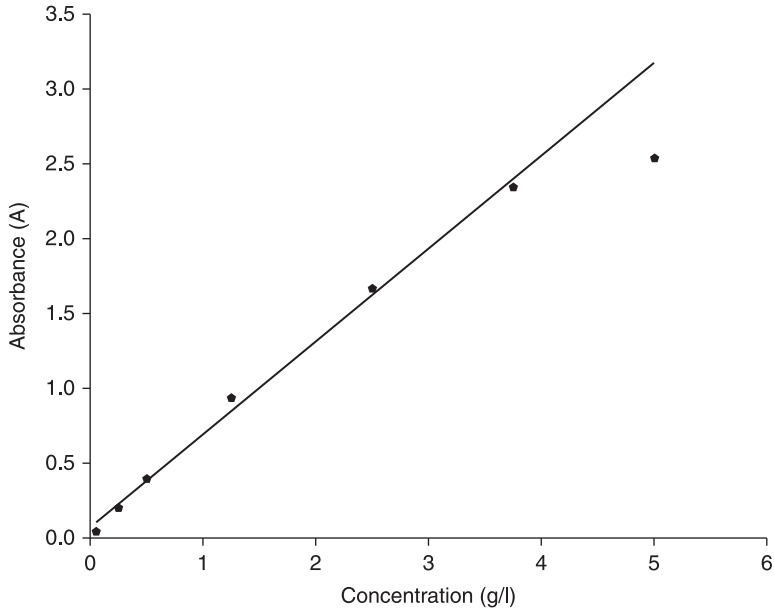

8.5 Violation of the Beer–Lambert law.

Although there is a linear relationship between absorbance and concentration, beyond certain absorbance values an increase in concentration does not result in a proportional measured increase in the absorbance value, as shown in Fig. 8.5. The violation of Beer's law may be attributed to reduced solubility of the dye at high concentrations, dye aggregation causing light scattering in the flow cell, or instrumental errors due to stray light and quantisation errors.

For example, the Ocean Optics USB4000 (OceanOptics, 2008) spectrophotometer has a signal-to-noise ratio of 300:1 at full strength. Its sensitivity is 130 photons per count at 400 nm and 60 photons per count at 600 nm. Figure 8.6 shows a typical transmittance spectrum of the USB4000 with a blue filter installed. Because the instrument is less sensitive below 450 nm (i.e. it takes more photons to cause a change in the charge-coupled device count) and there are fewer photons generated by the source, the total count drops below 5000 at wavelengths below 450 nm. The total error is about 106 counts due to quantisation and dark noise. This corresponds to a detectable limit of 1.6 A at 450 nm and 2.3 A at 565 nm, as shown in Fig. 8.7. Below 400 nm, the spectrophotometer will not be able to accurately detect absorbance changes caused by the increase in solution concentration at absorbance measurements of 1.2 absorbance units. For this particular instrument, it is important that the peak absorbance stays under 1.2 to ensure a linear relationship between absorbance and concentration for dyes that absorb in the 380–500 nm range.

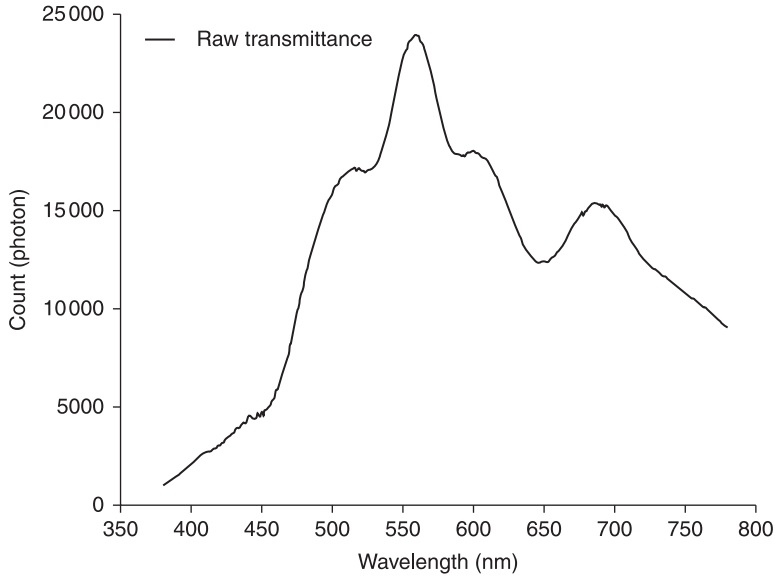

8.6 Raw spectrum of the Ocean Optics USB4000.

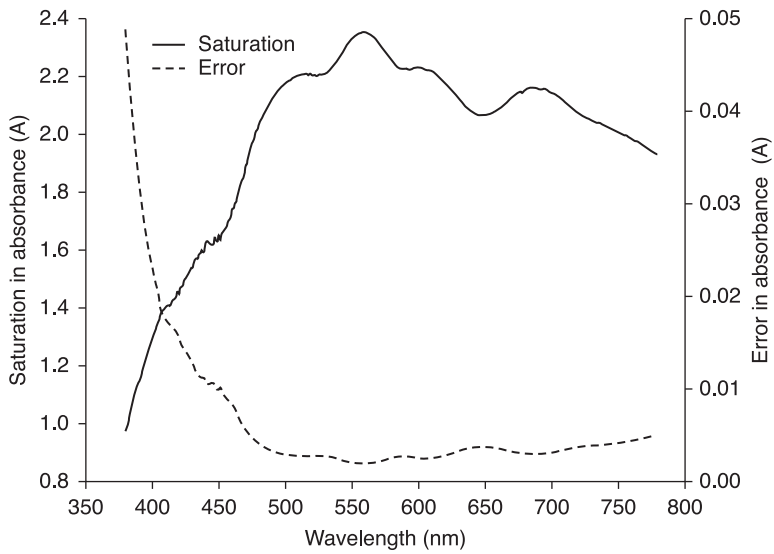

8.7 Raw spectrum sensitivity.

Spectral additivity

When two or more dyes are mixed together, if there is no chemical interaction between them, the sum of the spectra of the individual dyes should equal the spectrum of the mixture. Dyes which have this property obey the law of spectral additivity. A number of investigations with direct and vat dyes in mixtures have shown that this statement is often not valid. Neale and Stringfellow (Neale and Stringfellow, 1943) concluded that for certain direct dyes the spectra of the mixtures in water are not additive. In an aqueous solution, pairs of dyes interact with each other, possibly through the operation of resonance bonds or residual valence forces similar to those which are responsible for anchoring the dye onto the hydroxyl groups of cellulose.

Figure 8.8 shows the absorbance spectra of a Direct 83.1, Direct Blue 85 and Direct Red 89 at concentrations of 2.60 g/l, 1.00 g/l and 0.90 g/l, respectively. When these three dyes are mixed together, the dye interaction between the Direct Blue 85 and the other two dyes shifts the spectrum compared with a spectrum comprised of the linear sum of the absorbance spectra, as shown in Fig. 8.9. Such shifts due to spectral additivity (or super-position) can cause significant errors in concentration predictions using Eq. 8.2.

A pair test of the dye mixture indicated that Direct Blue 85 interacts with both Direct 83.1 and Direct Red 89. However, when these dyes are mixed with Direct Blue 78 in a three-dye mixture, the dye interaction that was observed earlier, as shown in Fig. 8.9, was observed to be less pronounced (see Fig. 8.10).

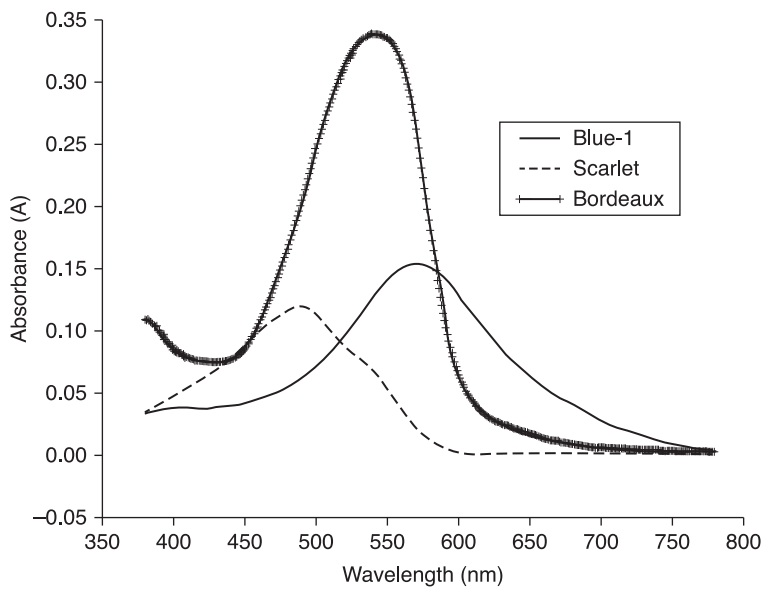

8.8 Absorbance spectra of 3 different direct dyes: Direct Blue 85 (Blue), Direct Red 89 (Scarlet) and Direct Red 83:1 (Bordeaux).

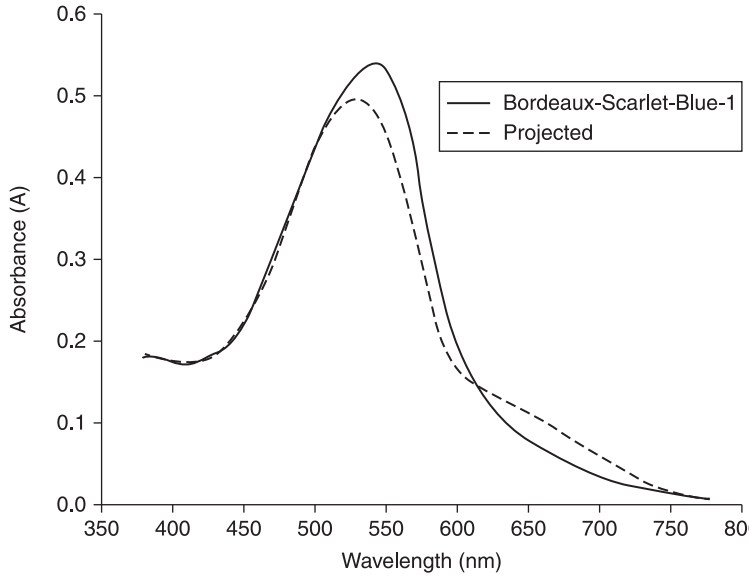

8.9 Combined spectrum of Direct Red 83.1, Direct Blue 85 and Direct Red 89.

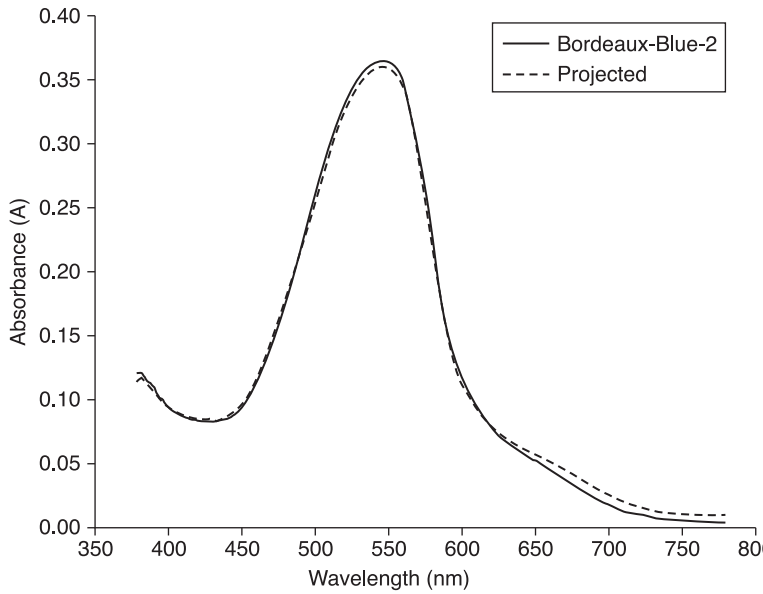

8.10 Combined spectrum of Direct Red 83.1, Direct Blue 78 and Direct Red 89.

Spectral morphing

According to the Beer–Lambert law, when a dye is diluted with water, its absorbance spectrum drops proportionally, as shown in Plate V(a) (see colour plate section between pages 116 and 117). By dividing the absorbance value of each wavelength by the highest absorbance value of the entire spectrum, the individual spectrum curve can be normalised. When these normalised spectra of each dilution are plotted, they overlie almost perfectly, as shown in Plate V(b).

Plate VI shows the normalised spectrum of a commercial Reactive Black 5 at different times during a dyeing. Throughout the dyeing, the shape of the spectrum is mostly preserved. This is expected behaviour in cases where the shading components of the dye are stable and exhaust uniformly. However, commercial dyes are rarely composed of a single dye, but, rather, mixtures which may exhaust at different rates throughout the dyeing process. A normalised plot of the absorbance spectra at different times would show that the shape of the absorbance spectrum has changed or morphed during exhaustion. This phenomenon is called spectral morphing (Günay and Jasper, 2010), and is shown in Plate VII for Reactive Black 5. Spectral morphing is equivalent to changing the spectral component vectors during the dyeing. In this case, there is no longer a one-to-one relationship between concentration and absorbance.

To achieve a stable dyeing, it is important to quantify the homogeneity of the dye and to use these data to predict the performance of the dye in the dyeing. Spectral morphing is an indication that components of a dye are exhausting at different rates, which can lead to levelness and shade matching issues.

Linear independence

To solve for the concentrations in Eq. 8.2, the spectral vectors $\mathbf{f}_i$ must be linearly independent. Linear dependence can occur when two dyes with the same absorbance spectra are mixed together, or when a dye is comprised of a mixture of dyes that occurs in the dyebath. Commercial dyes are rarely comprised of a single dye, so a lack of linear independence between the dye components can cause errors in predicting the concentration of the individual species in a mixture.

As an example, assume that dye W is a mixture of dyes X and Y, and that we are interested in measuring the concentrations of a dye solution comprised of dyes W, Y and Z. Due to the linear dependence between W and Y, it may not be possible to predict concentrations of these individual dyes accurately.

Mathematically, the $\mathbf{f}_i$ are not linearly independent. If Eq. 8.2 is expressed in matrix form:

$$A = Fc \; A \in R^n \; F \in R^{n \times i} \; c \in R^i \qquad [8.8]$$

where n is the number of measured wavelengths and i is the number of dyes in the dyebath, then the relative error in concentration due to a relative error in the absorbance measurement can be given by:

$$\frac{\|\Delta c\|}{\|c\|} \leq \frac{\sigma_{\max}(F)}{\sigma_{\min}(F)} \frac{\|\Delta A\|}{\|A\|} \quad [8.9]$$

where $\sigma_{max}(F)$ is the maximum singular value of F and $\sigma_{min}(F)$ is the minimum singular value. The quotient is known as the condition number of a matrix and is commonly denoted by $\kappa(F)$. Equation 8.9 gives an upper limit on the relative error in concentration due to an error in absorbance.

When the $\mathbf{f}_i$ spectral vectors of the F matrix are linearly independent, the condition number is 1, and increases as the F matrix becomes ill conditioned. In terms of bits of accuracy:

$$\#\text{bits of accuracy in concentration} <= \#\text{bits of accuracy in absorbance} - \log_2 \kappa(F)$$

To calculate the dye concentration to an accuracy of three decimal places requires 10 bits of accuracy. If $\log_2\kappa(F)$ is 2, it will require at least 12 bits of accuracy in the absorbance measurement. This is a fundamental limit in converting spectrophotometric data into concentration, and is a reason why some dye combinations are difficult to predict.

8.3 Data processing and tools to analyse and interpret real-time dye monitoring data

Establishing a standard for quality attributes against which assessments will be made is critical in dyeing quality control.

The quality attributes that have practical importance are:

- concentration
- exhaustion
- temperature
- pH
- conductivity
- strike rate (maximum rate of exhaustion)
- strike temperature (the temperature at which exhaustion accelerates).

Among these attributes, concentration, temperature, pH and conductivity are measured directly, and the exhaustion, maximum rate of exhaustion (strike rate) and the temperature at which the exhaustion accelerates (strike temperature) are derived from these measurements.

Figure 8.11 shows the percentage exhaustion of red, yellow and blue colour dyes on a fabric made of polyester, cotton and wool blended fibres versus time. Ideally, the acid dyes adsorb onto the wool, the direct dyes adsorb onto the cotton, and the disperse dyes adsorb into the polyester fibres. Figure 8.11 shows that,

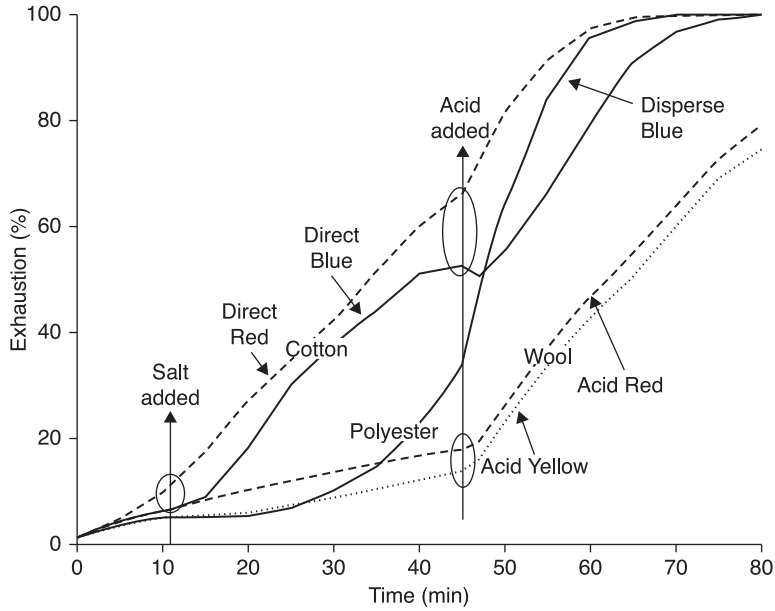

8.11 The monitoring of dye uptake by the fabric for individual dyes during a dyeing cycle.

during the dyeing, the addition of salt triggers the cotton fibres to absorb the direct dyes, the addition of acid triggers wool fibers to absorb acid dyes, and the rise of temperature eventually starts the dyeing of polyester with heat-driven disperse dyeing.

Furthermore, Fig. 8.11 shows that the citric acid also interacts with direct dyes, resulting in the exhaustion of these dyes by the cotton fibres. The capability to capture such detailed information on dyes and their interactions with chemicals, fabric and process variables enables the dyer to develop a quality control methodology for a dyehouse.

In the evaluation of quality attributes one has to be aware of the limitations of the technology, which are discussed by Günay and Jasper (Günay and Jasper, 2010). In addition, note that using equipment for solution and dispersion preparation in conjunction with the low-cost electronic dispensing pipette for dyebath preparation increases confidence in results and improves repeatability of tests.

Figure 8.12 demonstrates the definitions of critical attributes on exhaustion versus time and the rate of exhaustion versus time. For this dyeing, the final exhaustion was about 90%. The strike time occurs around the 16th minute of the dyeing.

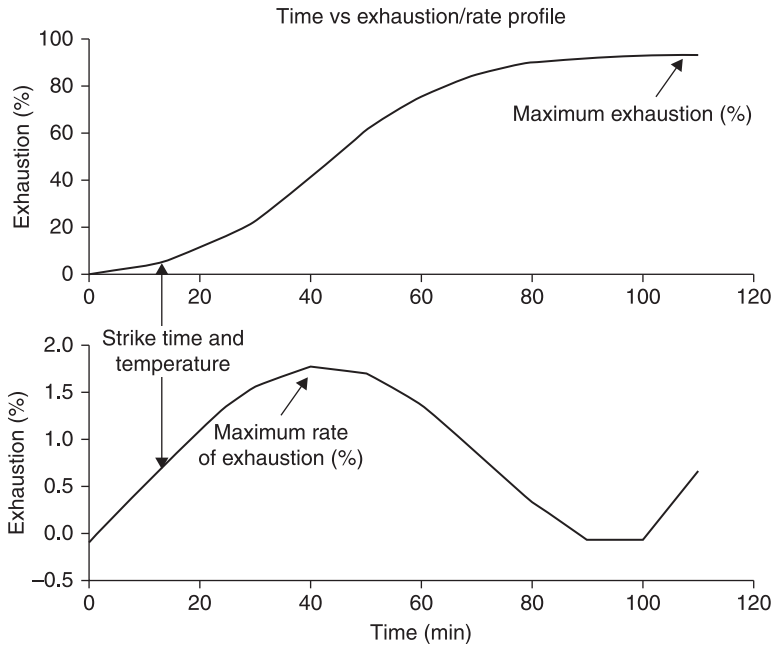

8.12 Display of critical attributes on exhaust profile for a typical dyeing.

8.4 Conclusion

Recent advances in spectrophotometry and instrumentation have enabled dyers to measure the concentration of dyes in the dyebath and indirectly on the fabric as a function of time. Although there are theoretical and practical limitations to this approach, it is none the less a major advancement in monitoring and ultimately controlling the dyeing process. Use of a spectrophotometric approach can aid the dyer in troubleshooting errors in shade and levelness, as well as form the basis for quality control assessment of dyes (dye strength) and fabric (dye uptake). In addition, this approach will enable dyers to optimise dyeing input parameters such as salt, chemicals, dyes, water and energy, which are prerequisites to a lean six sigma approach to dyeing.

8.5 References

1. Beck, K., Madderra, T. and Smith, B. (1990), Real-time data acquisition in batch dyeing, AATCC National Technical Conference and Exhibition.
2. Berkstresser, G. and Beck, K. (1993), Novel approaches for the real-time prediction of dye concentrations in three-dye mixtures, Book of Papers, AATCC International Conference, Montreal, Canada, pp. 108–13.

3. Dixon, W. and Farrell, M. (2009), HueMetrix Dye-It-Right User Instrument Manual, Huemetrix Inc., 617 Hutton St. Raleigh, NC USA.
4. Ferus-Comelo, M., Clark, M. and Parker, S. (2005), Optimisation of the disperse dyeing process using dyebath analysis, *Coloration Technology* **121**(5): 255–7.
5. Günay, M. and Jasper, W. J. (2010), Limitations in predicting dyebath exhaustion using optical spectroscopy, *Coloration Technology* **126**(3): 140–6.
6. Johnson, A. (1989), *The Theory of Coloration of Textiles*, 2nd edn, Woodhead Publishing Limited, UK.
7. Keaton, J. and Glover, B. (1985), A philosophy for dyeing in the next decade, *Journal of the Society of Dyers and Colourists* **101**: 86.
8. Kubelka, P. and Munk, F. (1931), Ein beitrag zur optik der farbanstriche, *Z. Tech. Phys*. **12**: 593–601.
9. Lijung, L. (1987), *System Identification: Theory for the User*, Prentice-Hall, Englewood Cliffs, NJ.
10. McDonald, R. (ed.) (1997), *Colour Physics for Industry*, 2nd edn, Society of Dyers and Colourists, West Yorkshire, England, chapter 1, pp. 33–6.
11. Neale, S. M. and Stringfellow, W. A. (1943), The absorption by cellulose of mixture of direct cotton dyes, *Journal of the Society of Dyers and Colorists* **59**: 241–5.
12. Ocean-Optics (2008), USB4000 Data Sheet, Ocean Optics, 830 Douglas Ave., Dunedin, FL, USA.
13. Park, J. and Shore, J. (2007), Significance of dye research and development for practical dyers, *Coloration Technology* **123**: 209–16.
14. Saguy, I., Mazrahi, S. and Kopelman, I. (1978), Mathematical approach for the determination of dyes concentrations in mixtures, *Journal of Food Science* **43**: 121–4.
15. Smith, C. B. (2007), Dyebath monitoring and control: Past, present, and future, *AATCC Review* **7**(11): 36–41.
16. Zamora, P., Kunz, A., Nagat, N. and Poppi, R. (1998), Spectrophotometric determination of organic dye mixtures by using multivariate calibration, *Talanta* **47**: 77–84.

Index